

**Extracellular ATP Signalling Mechanisms in Mesenchymal Stem
Cells**

Hongsen Peng

Submitted in accordance with the requirements for the degree of
Doctor of Philosophy

The University of Leeds
School of Biomedical Sciences

September, 2014

The candidate confirms that the work submitted is his own and that appropriate credit has been given where reference has been made to the work of others.

This copy has been supplied on the understanding that it is copyright material and that no quotation from the thesis may be published without proper acknowledgement.

Acknowledgements

First and foremost, I would like to give my gratitude to my supervisors, Dr. Lin-Hua Jiang and Dr. Xuebin Yang. My primary supervisor Dr. Lin-Hua Jiang, who is a very talented scientist with extensive knowledge for science, was patient and gave me continuous advice and encouragement during my PhD study. This thesis would not have been finished without his supervision, guidance and selfless support. My co-supervisor Dr. Xuebin Yang, who is such a hard working scientist, gave me thoughtful guidance in stem cells which led me to a broader engineering world. I would like to give a big thanks to Prof. David Beech for providing me with Stim/Orai siRNA and Synta66. I would like to express my appreciation to Dr. Seb Roger for offering me plasmids of P2X purinergic receptors. I would like to thank Dr. Jing Li for her valuable suggestions and continuous help on my research.

I would like to thank the University of Leeds for supporting my study with a Fully-Funded International Research Scholarship.

I would like to thank Mrs Claire Godfrey for giving me teeth for my research. I would also like to thank Dr. Reem El-Gendy for training me with mesenchymal stem cell isolation from dental pulp. I would like to thank Mrs Jackie Hudson for offering me training on Histology. I would like to thank Dr. Gareth Howell for offering me training on confocal laser scanning microscopy and flow cytometry.

I would like to express my appreciation to members in the lab, namely, Dr. Wei Yang, Dr. Jie Zhou, Mr Bin Hou, Prof. Asipu Sivaprasadarao, Dr. Judith, Dr. Christopher John Cockcroft, Dr. Yasser, and Mrs Hon-lin Rong for helping me. I have spent such amazing four years with all of you.

I would like to give my deepest thanks to my dear wife, Dr. Aiqin Liu. There is no word I can find to express how grateful I appreciate her love and support and how very much I love her.

I would like to express my eternal appreciation towards my mother, older sister, brother-in law, and parents-in law. Thank you for having given me so much understanding and support to my research. Thank my lovely baby boy for having brought me so much laughing and happiness since he was born.

Last but not least, thanks to all people who have directly or indirectly helped or supported me in any way throughout my PhD study.

Abstract

Human mesenchymal stem cells (hMSCs) are considered to have promising applications in cell therapy and tissue regeneration. The chemical molecules in the local environments are known to be important in controlling the functions of MSCs. The intrinsic mechanisms activated by such extracellular molecules are not fully understood. ATP is a well-established extracellular signalling molecule and activates two structurally and functionally different subfamilies of purinergic receptors on the cell surface, ATP-gated ion channel P2X receptors and G-protein-coupled P2Y receptors. Activation of the P2Y receptors leads to depletion of intracellular Ca^{2+} store and subsequent activation of the store-operated Ca^{2+} (SOC) channels. ATP is released by MSCs constitutively or in response to stimulation. This study using MSCs isolated from human dental pulp (hDP-MSCs), investigated the effects of extracellular ATP on proliferation, migration, osteogenic and adipogenic differentiation and the underlying signalling mechanisms.

Exposure of hDP-MSC to extracellular ATP up to 300 μM resulted in no effect on cell proliferation as shown in the MTT assays and cell counting. ATP at 30 μM promoted cell migration using the wound healing assays. ATP also inhibited the ALP expression and activity or osteogenesis of hDP-MSCs in basal medium (BM) and osteogenic differentiation medium (ODM), and by contrast increased the number of Oil red O-stained, fat droplet-containing cells or adipogenesis of hDP-MSCs cultured in adipogenic differentiation medium (ADM).

RT-PCR revealed consistent expression of mRNA transcripts for P2X4, P2X6, P2X7, P2Y1, P2Y11 and also the SOC channel components, Orai1, Orai2, Orai3, Stim1 and Stim2. Single cell imaging and FLEXstation experiments in a combination of pharmacological intervention using selective inhibitors or genetic intervention using specific siRNA provide consistent evidence to show functional expression of the P2X7, P2Y1 and P2Y11 receptors and Stim1/Orai SOC channels. For example, ATP-induced Ca^{2+} responses were inhibited by AZ11645373 (a P2X7

antagonist), 2-APB (a SOC channel inhibitor), Synta66 (a SOC channel inhibitor) or siP2X7, siP2Y1, siP2Y11, siOrai1, siOrai2, siOrai3 and siStim1.

Treatment with AZ11645373 or siP2X7 significantly inhibited ATP-induced stimulation of cell migration, but had no effect on ATP-induced inhibition of osteogenesis and stimulation of adipogenesis. Treatment with siP2Y1 or siP2Y11 strongly blocked ATP-induced stimulation of cell migration and adipogenesis, and inhibition of osteogenesis. Finally, treatment with siStim1/siOrai1 attenuated ATP-evoked stimulation of cell migration and inhibition of osteogenesis. ATP-induced increase in adipogenesis was reduced by treatment with 2-APB and siOrai3 but not with siStim1/siOrai1.

In summary, the present study shows that extracellular ATP regulates cell migration via the P2X7, P2Y1 and P2Y11 receptors and Stim1/Orai1 SOC channels, osteogenic differentiation mainly via the P2Y1 and P2Y11 receptors and Stim1/Orai1 SOC channels, and adipogenic differentiation via the P2Y1 and P2Y11 receptor and Orai3 in hDP-MSCs. These findings provide a better understanding of the mechanisms underlying the actions of extracellular ATP on hDP-MSCs and useful information that facilitates developing better applications of hMSCs for regenerative medicines.

Table of Contents

Acknowledgements	iii
Abstract	iv
Table of Contents	vi
List of Tables	xi
List of Figures	xii
List of Abbreviations	xiv
Chapter 1 Introduction	1
1.1 Stem cells	1
1.2 Mesenchymal Stem Cells.....	4
1.2.1 Bone marrow mesenchymal stem cells	7
1.2.2 Adipose tissue mesenchymal stem cells.....	8
1.2.3 Dental pulp mesenchymal stem cells	9
1.3 Extracellular ATP Signalling	12
1.3.1 ATP release, degradation and purinergic signalling	12
1.3.2 P2X receptors	15
1.3.2.1 P2X1 subunit-containing receptors	19
1.3.2.2 P2X2 subunit-containing receptors	21
1.3.2.3 P2X3 subunit-containing receptors	22
1.3.2.4 P2X4 subunit-containing receptors	23
1.3.2.5 P2X5 subunit-containing receptors	24
1.3.2.6 P2X6 subunit-containing receptors	25
1.3.2.7 P2X7 receptor.....	25
1.3.3 P2Y receptors	26
1.3.3.1 P2Y1 receptor.....	30
1.3.3.2 P2Y2 receptor.....	30
1.3.3.3 P2Y4 receptor.....	31
1.3.3.4 P2Y6 receptor.....	32
1.3.3.5 P2Y11 receptor.....	32
1.3.3.6 P2Y12 receptor.....	33
1.3.3.7 P2Y13 receptor.....	34
1.3.3.8 P2Y14 receptor.....	34
1.3.4 Store-operated calcium channels.....	35

1.3.4.1	Distribution and function	39
1.3.4.2	Activation.....	40
1.3.4.3	Inhibition.....	40
1.4	Extracellular ATP-evoked Ca ²⁺ Signalling in Stem Cells	41
1.4.1	Expression and function of the P2X receptors.....	41
1.4.2	Roles of the P2X receptors.....	42
1.4.2.1	Proliferation.....	42
1.4.2.2	Migration.....	43
1.4.2.3	Differentiation.....	43
1.4.3	Expression and function of the P2Y receptors.....	44
1.4.4	Roles of the P2Y receptors.....	47
1.4.4.1	Proliferation.....	47
1.4.4.2	Migration.....	47
1.4.4.3	Differentiation.....	48
1.4.5	Expression and function of the SOC channels.....	48
1.4.6	Roles of the SOC channels.....	49
1.4.6.1	Proliferation.....	49
1.4.6.2	Migration.....	49
1.4.6.3	Differentiation.....	49
1.5	Aim and Objectives.....	51
Chapter 2 Materials and Methods.....		52
2.1	Materials.....	52
2.1.1	General materials	52
2.1.2	Solutions.....	52
2.2	Methods.....	52
2.2.1	Cell isolation and culture	52
2.2.2	Cell subculture	53
2.2.3	Preparation of frozen cells	57
2.2.4	Thawing and restoring frozen cells.....	57
2.2.5	Colony-forming test	57
2.2.6	Flow cytometry	58
2.2.7	Osteogenic differentiation.....	58
2.2.8	ALP staining assay.....	59
2.2.9	DNA content determination	59
2.2.10	ALP activity assay.....	60

2.2.11	Adipogenic differentiation	60
2.2.12	Oil red O staining	61
2.2.13	Chondrogenic differentiation	62
2.2.14	Alcian blue staining for monolayer cells	62
2.2.15	Alcian blue/Sirius red staining for cell pellets	63
2.2.16	Cell proliferation assays	64
2.2.17	Cell migration assays	65
2.2.18	Measurements of the intracellular Ca^{2+} levels	65
2.2.19	Real-time reverse transcription polymerase chain reaction (RT-PCR)	67
2.2.20	Transfection with siRNA	70
2.2.21	Data analysis	70
Chapter 3 Effect of ATP on Cell Proliferation, Migration and Differentiation of Human Dental Pulp Mesenchymal Stem Cells		74
3.1	Introduction	74
3.2	Results	75
3.2.1	Isolation and characterization of cells	75
3.2.1.1	Isolation of cells from human dental pulp	75
3.2.1.2	Formation of colony-forming units	75
3.2.1.3	Expression of MSC positive and negative markers	76
3.2.1.4	Osteogenic, adipogenic and chondrogenic differentiation	80
3.2.2	Effects of extracellular ATP on cell proliferation	81
3.2.3	Effects of extracellular ATP on cell migration	81
3.2.4	Effects of extracellular ATP on osteogenic differentiation	90
3.2.5	Effects of extracellular ATP on adipogenic differentiation	92
3.3	Discussion	94
Chapter 4 Expression of P2 Purinergic Receptors in Human Dental Pulp Mesenchymal Stem Cells		97
4.1	Introduction	97
4.2	Results	98
4.2.1	Ca^{2+} oscillations and ATP-induced Ca^{2+} responses in individual cells	98
4.2.2	RT-PCR analysis of mRNA expression of P2 receptors	100
4.2.3	Effects of PPADS on ATP-induced Ca^{2+} responses	100
4.2.4	Ca^{2+} responses to P2X receptor agonists	105
4.2.5	ATP and BzATP concentration-response relationships	105

4.2.6	Effects of P2X antagonists on ATP-induced Ca ²⁺ responses....	105
4.2.7	Ca ²⁺ responses induced by P2Y receptor agonists.....	106
4.2.8	The role of P2X7 receptor in ATP-induced Ca ²⁺ responses	113
4.2.9	The role of P2Y1 receptor in ATP-induced Ca ²⁺ responses	117
4.2.10	The role of P2Y11 receptor in ATP-induced Ca ²⁺ responses	117
4.3	Discussion	121
Chapter 5 Expression of Stim/Orai SOC Channels in Human Dental Pulp Mesenchymal Stem Cells		126
5.1	Introduction	126
5.2	Results	127
5.2.1	Single cell Ca ²⁺ responses to TG and ATP	127
5.2.2	mRNA expression levels of SOC channel component proteins.....	129
5.3.3	Effects of extracellular Ca ²⁺ on constitutively active Ca ²⁺ -permeable conductance	129
5.3.4	Effects of 2-APB on the constitutively active Ca ²⁺ -permeable conductance	131
5.3.5	Effects of Synta66 on the constitutively active Ca ²⁺ -permeable conductance	131
5.3.6	Ca ²⁺ responses in TG-treated cells.....	134
5.3.7	Effects of 2-APB on TG-induced Ca ²⁺ responses.....	134
5.3.8	Effects of Synta66 on TG-induced Ca ²⁺ responses.....	137
5.3.9	Effects of 2-APB on ATP-induced Ca ²⁺ responses.....	137
5.3.10	Effects of Synta66 on ATP-induced Ca ²⁺ responses.....	137
5.3.11	Effects of reducing Stim and Orai expression using siRNA on ATP-induced Ca ²⁺ responses	138
5.3.12	Effects of co-transfection with siRNA for Stim1 and Orai on ATP-induced Ca ²⁺ responses	149
5.3	Discussion	153
Chapter 6 Roles of P2 Purinergic Receptors and SOC Channels in MSC Migration and Differentiation.....		156
6.1	Introduction	156
6.2	Results	157
6.2.1	The role in hDP-MSK migration.....	157
6.2.1.1	Effects of inhibitors for P2 receptors and SOC channels.....	157
6.2.1.2	Effects of transfection with siRNAs on ATP-induced increase in cell migration.....	158

6.2.2	The role in osteogenic differentiation of hDP-MSCs	165
6.2.2.1	Effects of inhibitors for P2 receptors and SOC channels.....	165
6.2.2.2	Effects of transfection with siRNAs on ATP-induced inhibition of osteogenic differentiation	166
6.2.3	The role in adipogenic differentiation of hDP-MSCs.....	171
6.2.3.1	Effects of inhibitors for P2 receptors and SOC channels.....	171
6.2.3.2	Effects of transfection with siRNAs on osteogenic differentiation.....	174
6.3	Discussion	177
Chapter 7 General Discussion.....		181
7.1	Expression and function of the P2X7 receptor in hDP-MSCs.....	183
7.2	Expression and function of the P2Y1 and P2Y11 receptors in hDP-MSCs	185
7.3	Expression and function of Stim1/Orai SOC channels in hDP-MSCs	186
7.4	Future studies	188
7.5	Conclusion	189
References		191

List of Tables

Table 1.1	Classification of stem cells.	3
Table 1.2	Main distribution, agonists and antagonists of P2X receptors.	17
Table 1.3	Main distribution, agonists and antagonists of P2Y receptors.	28
Table 1.4	Proposed function of ATP-sensitive P2 purinergic receptors in stem cells.	45
Table 2.1	General chemical and reagents used.	54
Table 2.2	Solutions and culture media used in the present study.	56
Table 2.3	Primers used for PCR.	71
Table 2.4	siRNAs used.	73
Table 3.1	Summary of expression of cell surface markers in hDP-MSCs from four donors.	79

List of Figures

Figure 1.1	Differentiation capacities of multipotent MSCs.....	6
Figure 1.2	ATP degradation and the purinergic receptor family.....	14
Figure 1.3	The structural features of Stim1 and Orai1.....	36
Figure 1.4	Store-operated Ca^{2+} entry (SOCE) pathways.....	37
Figure 3.1	Isolation, morphology and colony-forming units of hDP-MSCs.....	77
Figure 3.2	Flow cytometry analysis of expression of cell-surface markers in hDP-MSCs.....	78
Figure 3.3	Differentiation potential of hDP-MSCs.....	83
Figure 3.4	No effect of ATP on hDP-MSC proliferation by XTT assay.....	85
Figure 3.5	No effect of ATP on hDP-MSC proliferation by cell counting.....	87
Figure 3.6	Effects of ATP on hDP-MSC migration by counting cells.....	88
Figure 3.7	Effects of ATP on hDP-MSC migration determined by real-time imaging.....	89
Figure 3.8	Effects of ATP on osteogenic differentiation of hDP-MSCs.....	91
Figure 3.9	Effects of ATP on adipogenic differentiation of hDP-MSCs.....	93
Figure 4.1	Spontaneous and ATP-induced Ca^{2+} responses in single hDP-MSCs.....	99
Figure 4.2	The mRNA expression of P2 receptors in hDP-MSCs.....	102
Figure 4.3	ATP-induced Ca^{2+} responses and inhibition by PPADS.....	104
Figure 4.4	Ca^{2+} responses to P2X receptor agonists in hDP-MSCs.....	107
Figure 4.5	Agonist concentration- Ca^{2+} response relationship curves for ATP and BzATP.....	108
Figure 4.6	No effect of P2X4 receptor antagonist 5-BDBD on ATP-induced Ca^{2+} responses.....	109
Figure 4.7	Inhibition of ATP-induced Ca^{2+} responses by P2X7 receptor antagonist AZ11645373.....	110
Figure 4.8	Ca^{2+} responses to P2Y receptor agonists in hDP-MSCs.....	112
Figure 4.9	Effect of siControl on ATP-induced Ca^{2+} responses in hDP-MSCs.....	114
Figure 4.10	Effects of knocking down the P2X7 expression on Ca^{2+} responses by ATP and BzATP in hDP-MSCs.....	116
Figure 4.11	Effects of knocking down the P2Y1 expression on the Ca^{2+} responses by ADP and ATP in hDP-MSCs.....	119
Figure 4.12	Effects of knocking down the P2Y11 expression on the Ca^{2+} responses by ATP in hDP-MSCs.....	120

Figure 5.1	Single cell Ca²⁺ responses to TG and ATP in hDP-MSCs.....	128
Figure 5.2	The mRNA expression of the SOC channels in hDP-MSCs.	130
Figure 5.3	Characterization of the constitutively active Ca²⁺ conductance.	133
Figure 5.4	The SOC channel-mediated Ca²⁺ responses in hDP-MSCs.	136
Figure 5.5	Effects of 2-APB on ATP-induced Ca²⁺ responses in hDP-MSCs.	140
Figure 5.6	Effects of Synta66 on ATP-induced Ca²⁺ responses in hDP-MSCs.	141
Figure 5.7	Effects of transfection with siControl on Ca²⁺ responses in hDP-MSCs without or with TG treatment.	142
Figure 5.8	Effects of transfection with siRNA on the mRNA expression of Stim and Orai in hDP-MSCs.	143
Figure 5.9	Effects of transfection with siRNA for Orai and Stim on TG-induced Ca²⁺ responses in hDP-MSCs.	146
Figure 5.10	Effects of transfection with siRNA for Orai and Stim on ATP-induced Ca²⁺ responses in hDP-MSCs.....	148
Figure 5.11	Effects of co-transfected with siRNAs for Stim1 and Orai on TG-induced Ca²⁺ responses in hDP-MSCs.	151
Figure 5.12	Effects of co-transfected with siRNAs for Stim1 and Orai on ATP-induced Ca²⁺ responses in hDP-MSCs.....	152
Figure 6.1	Effects of inhibitors on ATP-induced increase in hDP-MSC migration.....	161
Figure 6.2	Effects of transfection with siRNA for P2X7, P2Y1, P2Y11, Stim1 and Orai1 on ATP-induced increase in hDP-MSC migration.	164
Figure 6.3	Effects of inhibitors on osteogenic differentiation in ATP-treated hDP-MSCs.....	168
Figure 6.4	Effects of siRNAs on osteogenic differentiation in ATP-treated hDP-MSCs.....	170
Figure 6.5	Effects of inhibitors on ATP-induced increase in adipogenic differentiation of hDP-MSCs.	173
Figure 6.6	Effects of transfection with siRNA on adipogenic differentiation in ATP-treated hDP-MSCs.....	176
Figure 7.1	Schematic summary of ATP-induced Ca²⁺ signalling mechanism in migration and differentiation of hDP-MSCs.	190

List of Abbreviations

2-APB	2-aminoethyldiphenyl borinate
2D	2-dimensional
2-MeSATP	2-Methylthioadenosine 5'-triphosphate
2-MeSADP	2-methylthio ADP
2-thio-UTP	2-thio-uridine 5'-triphosphate
3D	3-dimensional
$\alpha\beta$ meATP	$\alpha\beta$ -methylene ATP
α -SMA	α -smooth muscle actin
$\beta\gamma$ -meATP	β,γ -methylene ATP
ADM	Adipogenic differentiation medium
ADP	Adenosine 5'-diphosphate
ADSCs	Adipose-derived stem/stromal cells
ALP	Alkaline phosphatase
AMP	Adenosine monophosphate
ASCs	Adult stem cells
AT-MSCs	Adipose tissue mesenchymal stem/stromal cells
ATP	Adenosine 5'-triphosphate
ATP γ S	Adenosine-5'-(γ -thio)-triphosphate
BBG	Brilliant blue G
BM	Cell growth basal medium
BM-MSCs	Bone marrow mesenchymal stem cells
BMP	Bone morphogenetic protein
BzATP	2'-&3'-O-(4-benzoyl-benzoyl)-ATP
cAMP	Cyclic adenosine monophosphate
CPA	Cyclopiazonic acid
CRAC channels	Ca ²⁺ -release-activated Ca ²⁺ channels
CSCs	Cancer stem cells
CTP	Cytidine triphosphate
DAG	1,2-diacylglycerol
DMEM	Dulbecco's modified Eagle's medium
DMSO	Dimethyl sulfoxide

DP-MSCs	Dental pulp mesenchymal stem cells
DPSCs	Dental pulp stem cells
DSPP	Dentin sialophosphoprotein
EDTA	Ethylene diamine tetraacetic acid
ERK	Extracellular signal-regulated kinases
ESCs	Embryonic stem cells
FBS	Foetal bovine serum
FGF-2	Fibroblast growth factor 2
GAG	Glycosaminoglycans
hESCs	Human embryonic stem cells
HSCs	Hematopoietic stem cells
IP ₃	Inositol 1,4,5-triphosphate
IP ₅ I	Di-inosine pentaphosphate;
iPSCs	Induced pluripotent stem cells
GFAP	Glial fibrillary acid protein
GMP	Good manufacturing practices
GTP	Guanosine-5'-triphosphate
LuSCs	Lung stem cells
MAP2	Microtubule-associated proteins 2
MAPK	Mitogen-activated protein kinases
MSCs	Mesenchymal stem/stromal cells
MTT	Methylthiazoltetrazolium
MuSCs	Muscle stem cells
NPCs	Neural progenitor cells
NSCs	Neural stem cells
ODM	Osteogenic differentiation medium
PBS	Phosphate-buffered saline
PIP2	4,5-bisphosphate
PLC	Phospholipase C
PPAR γ 2	Peroxisomal proliferator activated receptor γ 2
RB2	Reactive blue 2
rpm	Rotation per minute
RT-PCR	Reverse-transcription polymerase chain reaction
RUNX2	Runt-related transcription factor 2
SBS	Extracellular Ca ²⁺ -containing solution

SHEDs	Stem cells from human exfoliated deciduous teeth
SOC channels	Store-operated calcium channels
SOCE	Store-operated calcium entry
Stim1	Stromal interaction molecule 1
STRO-1	Stromal-derived factor 1
TG	Thapsigargin
TNP-ATP	2'(3')-O-(2,4,6-trinitrophenyl) ATP
TRP channels	Transient receptor potential channels
TRPC channels	Transient receptor potential canonical channels
UDP	Uridine diphosphate
UDP β S	Uridine 5'-O-thiodiphosphate
UMP	Uridine monophosphate
Up ₃ U	Diuridine triphosphate
Up ₄ U	Diuridine tetraphosphate
UTP	Uridine-5'-triphosphate
UTP γ S	Uridine 5'-O-3-thiotriphosphate
VCAM-1	Vascular cell adhesion molecule 1
VEGF-R2	Vascular endothelial growth factor receptor 2

Chapter 1

Introduction

1.1 Stem cells

Stem cells are defined as undifferentiated cells and have the ability to self-renew and to produce mature progeny cells of a particular tissue through differentiation (Reya, Morrison et al. 2001).

According to their ability or potency of differentiation (also known as potency), stem cells are now commonly classified into totipotent, pluripotent, multipotent and unipotent categories, as shown in Table 1.1 (Wagers and Weissman 2004; Ranganathan and Lakshminarayanan 2012). Totipotent stem cells (for example, zygotes's cells) are able to divide and produce all type of cells in an organism, including extraembryonic tissues (for example, placenta) (Friedlander, Cullinan et al. 2009). Pluripotent stem cells (for example, embryonic stem cells (ESCs) from blastocysts (Thomson, Itskovitz-Eldor et al. 1998) can differentiate into almost any of the three germ layers: endoderm (for example, interior stomach lining, gastrointestinal tract and lung), mesoderm (for example, muscle, bone and blood) or ectoderm (for example, epidermal tissues and nervous system), excluding extraembryonic tissues (Friedlander, Cullinan et al. 2009; Ranganathan and Lakshminarayanan 2012). Multipotent stem cells (for example, mesenchymal stem cells (MSCs)) are able to give rise to cells from a multiple, but more limited number of lineages (Friedlander, Cullinan et al. 2009; Ranganathan and Lakshminarayanan 2012). Unipotent stem cells (for example, skin cells, hepatocytes and precursors) have the capacity to form only one specific type of cells (Wagers and Weissman 2004). As shown in Table 1.1, induced pluripotent stem cells (iPSCs) are created from multipotent stem cells or adult somatic cells (for example, fibroblasts) (Takahashi and Yamanaka 2006; Takahashi, Okita et al. 2007), in the culture by introducing a few defined factors, like Oct3/4, Klf4, Sox2 and c-myc; thus, these cells have similar properties to that of pluripotent stem cells. Furthermore, somatic cell nuclear transfer is a cloning technique by nucleus transfer from an adult somatic cell into a de-nucleated ovum (totipotent) that then divides to form the entire organism. This

method could be used to produce human stem cell lines for therapeutics (Wilmot 2002). Particularly, if taken a tumour as an aberrant organ, tumorigenic cells can be considered as cancer stem cells (CSCs) that undergo aberrant processes similar to the self-renewal and differentiation of normal stem cells (Reya, Morrison et al. 2001).

The pluripotent ESCs and iPSCs are good sources of stem cells for biomedical research and clinical applications (Alvarez, Garcia-Lavandeira et al. 2012; Bai, Desprat et al. 2013). However, the ethical issue concerning isolation of human ESCs (hESCs) from embryos hinders their therapeutic use. Alternatively, although there is no ethical issue about iPSCs as they are directly reprogrammed from adult cells, the potential biological safety issue associated with production of iPSCs could undermine their use for modelling diseases and therapeutic applications (Bai, Desprat et al. 2013). In order to optimize the reprogramming process and ultimately provide medically safe iPSCs, further investigations are required to carefully examine the impact on the genome integrity by all factors, including expression of different reprogramming transcription factors and carryover of non-human genetic materials from the vectors used, reprogramming protocols and early culture/passaging conditions (Bai, Desprat et al. 2013).

Adult stem cells (ASCs) or postnatal stem cells have been extensively researched as a potential cell source for both research and clinical application (Alvarez, Garcia-Lavandeira et al. 2012). ASCs have been identified in a wide range of tissues, such as mesenchymal stem cells (MSCs) (Zapata, Alfaro et al. 2012), hematopoietic stem cells (HSCs) (Kiel, Yilmaz et al. 2005), muscle stem cells (MuSCs) (Cheung, Quach et al. 2012), neural stem cells (NSCs) (Bonaguidi, Wheeler et al. 2011), lung stem cells (LuSCs) (Kajstura, Rota et al. 2011), skin stem cells (bulge) (Fuchs and Horsley 2011), small intestine stem cells (Formeister, Sionas et al. 2009), liver and pancreas stem cells (Burke and Tosh 2012), cardiac stem cells (D'Amario, Fiorini et al. 2011), and pituitary stem cells (Castinetti, Davis et al. 2011).

Table 1.1 Classification of stem cells.

Type of stem cells	Source of stem cells	Differentiation potential/plasticity
Embryonic stem cells	Fertilized Zygote	Totipotent
	Blastocyst-inner cell mass (5-7 day embryo)	Pluripotent
Embryonic germ cells	Gonadal ridge (6-week embryo)	Pluripotent
Fetal tissue stem cells	Primitive cell types of organs and tissues (neural crest stem cells, primitive hematopoietic stem cells, progenitor cells of pancreatic islets, etc.)	Pluripotent/ Multipotent
Adult/postnatal stem cells	Infant: umbilical cord blood/ Wharton jelly	Pluripotent/ Multipotent
	Hematopoietic stem cells	Multipotent
	Epidermal stem cells	
	Mesenchymal stem cells	
	Bone marrow stoma	
	Dental pulp	
	Adipose tissue stem cells	
	Neural stem cells	
	Limbal stem cells	
	Hepatic stem cells	
Induced pluripotent stem cells*	Multipotent stem/progenitor cells subjected to retroviral transcription of embryonic genes	Pluripotent
Somatic cell nuclear transfer*	Adult somatic cells introduced into ovum-therapeutic cloning	Totipotent/Pluripotent

*Product of tissue engineering. Taken from (Ranganathan and Lakshminarayanan 2012)

1.2 Mesenchymal Stem Cells

Mesenchymal stem cells (MSCs), also known as mesenchymal stromal cells, are the most commonly studied adult stem cells. MSCs were initially isolated from bone marrow by Friedenstein in 1970 (Friedenstein, Chailakhjan et al. 1970). MSCs were defined as multipotent stem cells with the capability to differentiate into bone, adipose tissue, and cartilage by Pittenger in 1999 (Pittenger, Mackay et al. 1999). Apart from bone marrow, MSCs can be found in several other tissues and organs, such as adipose tissue (Zuk, Zhu et al. 2001; Zuk, Zhu et al. 2002), dental pulp (Gronthos, Mankani et al. 2000; Gronthos, Brahim et al. 2002), synovial membrane (De Bari, Dell'Accio et al. 2001) and umbilical cord blood (Lee, Kuo et al. 2004).

Due to the absence of specific MSCs markers and the heterogeneity of the MSC populations, the Mesenchymal and Tissue Stem Cell Committee of the International Society for Cellular Therapy (ISCT) proposed three minimal criteria defining human MSCs in 2006 (Dominici, Le Blanc et al. 2006; Wagner and Ho 2007). First, MSCs must have the ability to adhere to the plastic surface when maintained in standard culture conditions (alpha modified minimal essential medium plus 20% fetal bovine serum). Second, MSCs must show strong expression of positive markers CD105 (endoglin), CD90 (Thy-1/Thy-1.1), CD73 (an ecto-5'-nucleotidase), and MSCs must be deficient in expressing negative markers CD45 (a protein tyrosine phosphatase, a common marker for leukocyte and hematopoietic origin), CD34 (a marker for hematopoietic stem cells and endothelial cell lineage), CD14 (monocyte-macrophage differentiation antigen) or CD11b, CD79 α or CD19 and HLA-DR. Finally, MSCs can differentiate *in vitro* into osteogenic, adipogenic, and chondrogenic lineages.

MSCs can be expanded *in vitro* for several passages and can self-renew while maintaining their multi-potency to differentiate into various tissues, as shown in Fig. 1.1 (Jiang, Jahagirdar et al. 2002; Phinney 2007; Bonfield, Nolan Koloze et al. 2010). Furthermore, MSCs have potent immunoregulatory functions (Lee, Lim et al. 2014; Wuchter, Bieback et al. 2014). Due to their regenerative potential and immunoregulatory effect, MSCs can be considered as promising therapeutic

candidates for the treatment of degenerative, inflammatory, and autoimmune diseases (Fernandez Vallone, Romaniuk et al. 2013; Farini, Sitzia et al. 2014; Figliuzzi, Bonandrini et al. 2014; Lee, Lim et al. 2014). Currently, a number (at least 88) of completed clinical trials using *in vitro* expanded MSCs were published in the public clinical trials database (www.clinicaltrials.gov) showing potential applications in cell-based therapies. However, there are still many questions to be taken into account, such as safety (for example, tumor development and metastases), quality control (for example, bacteriological tests, viability and phenotype tests, oncogenic tests, and endotoxin assay), clinical grade production (for example, a large number of cells), and clinical transition (for example, engraftment, angiogenesis, tissue remodelling, and modulation of the immune response) (Farini, Sitzia et al. 2014).

The following section will discuss MSCs from bone marrow, adipose tissue and dental pulp.

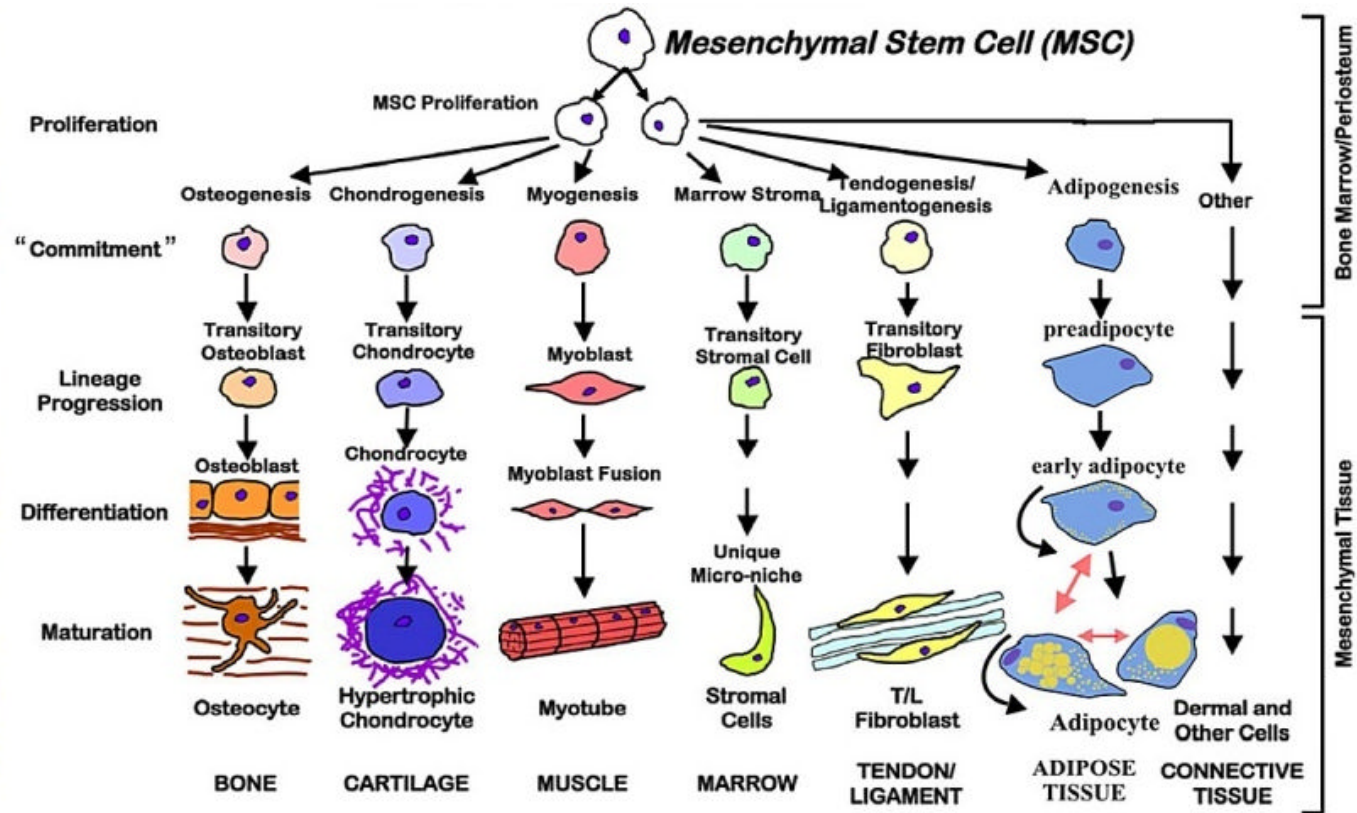


Figure 1.1 Differentiation capacities of multipotent MSCs.

Mesenchymal stem cells (MSCs) can be cultured *in vitro* to proliferate and differentiate into a number of phenotypes, which include cells capable of forming bone, cartilage, muscle, marrow, tendon/ligament, adipocytes, and connective tissue in certain culture conditions (Bonfield, Nolan Koloze et al. 2010).

1.2.1 Bone marrow mesenchymal stem cells

The most commonly studied mesenchymal stem cells are isolated from bone marrow (BM-MSCs) of various species, including human (Tao, Sun et al. 2011), rabbit (Deng, Sun et al. 2006), rat (Deng, Sun et al. 2006; Li, Deng et al. 2006) and mouse (Tao, Lau et al. 2007; Tao, Lau et al. 2008). An *in vitro* study using flow cytometry analysis showed that human BM-MSCs expressed stromal-derived factor 1 (STRO-1, a commonly used marker for MSCs), Oct4, Nanog, CD13 (aminopeptidase N), CD44 (an adhesion molecule for hyaluronate and lymphocyte homing-associated cells), CD90, CD146 (a melanoma cell adhesion molecule; a marker for endothelial cell lineage and perivascular cell), and CD166 (an activated leukocyte cell adhesion molecule; integrin $\alpha 3$; a MSCs marker), but not CD14, CD34, CD45 and CD117 (a c-kit receptor; a surface marker for hematopoietic stem cells) (Karaoz, Dogan et al. 2010). By using immunohistochemistry and reverse transcription-polymerase chain reaction (RT-PCR), it was demonstrated that human BM-MSCs under different *in vitro* differentiation conditions expressed osteogenic (alkaline phosphatase or ALP, osteonectin, osteocalcin, osteopontin, runt-related transcription factor 2, bone morphogenetic protein-2 or BMP-2, BMP-4, type I collagen), adipogenic (leptin, adipophilin, and peroxisomal proliferator activated receptor gamma 2 or PPAR γ 2), chondrogenic (type II collagen, type X collagen and cartilage oligomeric matrix protein), myogenic (desmin, myogenin, myosin IIa, and α -smooth muscle actin or α -SMA) and neurogenic (γ -enolase, microtubule-associated proteins 2 or MAP2, c-fos, nestin, neurofilament-heavy, neurofilament-light, β 3 tubulin, and glial fibrillary acid protein or GFAP) markers (Koyama, Okubo et al. 2009; Karaoz, Dogan et al. 2010). Other studies have reported that BM-MSCs have the ability to differentiate into a variety of lineages, such as osteoblasts, adipocytes, chondrocytes, skeletal muscle cells, neurons, and cardiomyocytes (Tao, Lau et al. 2008; Ferrari, Gulinelli et al. 2011).

Therefore, human BM-MSCs are attractive candidates for stem cell based tissue regeneration. For example, a gelatin/chondroitin-6-sulfate/hyaluronan tri-copolymer scaffold containing bone marrow fluid and dental bud cells was implanted into porcine mandibular alveolar sockets (Kuo, Lin et al. 2011). Histological analysis showed formation of the crown, root, pulp, enamel, dentin, odontoblast, cementum,

blood vessel, ameloblasts, periodontal ligament and dentin tubules, suggesting generation of dentin-pulp-like complex tooth structures and formation of periodontal tissues. However, many outstanding issues, including regulation of cell proliferation and differentiation, determination of tooth shape, and control of the size and eruption of the tooth, still need to be resolved.

Although BM-MSCs are still considered as the golden reference for the application of MSCs, there are several limitations. For example, the patients experienced pain during the cell isolation process (Scarfi 2014). Moreover, BM-MSCs appear low frequency of prevalence (0.001 - 0.01% of the total population) in BM tissues (Pittenger, Mackay et al. 1999) and must be expanded *in vitro* to obtain sufficient cells prior to use. Additionally, the differentiation potential of isolated BM-MSCs decreases with the age of the donor increasing (Tokalov, Gruner et al. 2007). Currently, there is increasing interest in MSCs from other tissues, such as adipose tissue and dental pulp.

1.2.2 Adipose tissue mesenchymal stem cells

Adipose tissue mesenchymal stem cells (AT-MSCs), also known as adipose-derived stem/stromal cells (ADSCs), as a source of MSCs have attracted much attention in recent years. Compared with BM-MSCs, a large number of AT-MSCs can be easily isolated from adipose tissues without any ethical concerns (Zuk, Zhu et al. 2001; Tobita and Mizuno 2013; Romagnoli and Brandi 2014). Generally, AT-MSCs can be isolated *in vitro* by density gradient centrifugation of collagenase-digested tissues after adipose tissues were lipoaspirated or minced (Boquest, Shahdadfar et al. 2006). These cells exhibited expression of the positive markers, including STRO-1, CD9, CD10, CD13, CD29, CD44, CD49, CD73, CD90, CD105 and CD166, but not the negative cell markers, such as CD14, CD16, CD34, CD45, CD56, CD61, CD104 and CD106 (an endothelial cell lineage marker) (Zuk, Zhu et al. 2002; Cao, Sun et al. 2005; Gimble, Guilak et al. 2008; Karaoz, Dogan et al. 2010; Baer and Geiger 2012; Baer, Kuci et al. 2013).

Studies have shown that AT-MSCs possess a high plasticity; they can differentiate into osteoblasts, adipocytes, chondrocytes, myocytes, neural cells, epithelial cells and hepatocytes (Safford, Hicok et al. 2002; Zuk, Zhu et al. 2002; Brzoska, Geiger et al. 2005; Banas, Teratani et al. 2007). Therefore, several tissue engineering and cell therapy approaches using AT-MSCs have been carried out to repair or regenerate cartilage (Mehlhorn, Zwingmann et al. 2009), bone (Chen, Yang et al. 2010), peripheral nerves (Santiago, Clavijo-Alvarez et al. 2009), hepatic integration (Aurich, Sgodda et al. 2009), liver failure (Banas, Teratani et al. 2009), insulin-producing islet cells (Kajiyama, Hamazaki et al. 2010), myocardial infarction (Schenke-Layland, Strem et al. 2009) and renal function (Li, Han et al. 2010). However, there are still many hurdles that need to be overcome for clinical applications, such as standardization in the isolation methods and culture protocols, and good manufacturing practices (Bourin, Gadelorge et al. 2008; Baer and Geiger 2012; Romagnoli and Brandi 2014).

1.2.3 Dental pulp mesenchymal stem cells

Dental pulp mesenchymal stem cells (DP-MSCs) have gained increasing attention. DP-MSCs were firstly isolated from permanent teeth by Gronthos in 2000 (known as dental pulp stem cells or DPSCs) (Gronthos, Mankani et al. 2000) and from exfoliated deciduous teeth by Miura in 2003 (known as stem cells from human exfoliated deciduous teeth (SHEDs) or immature DPSCs (Miura, Gronthos et al. 2003). Compared with BM-MSCs, DP-MSCs have advantages for clinical applications due to the fact that they are easily available from teeth after extraction with very low morbidity and no ethical issues (Galler, Schweikl et al. 2011). Moreover, DP-MSCs show high proliferation rates and potential of differentiation into osteoblasts, odontoblasts, ameloblasts, and nerve cells (Galler, Schweikl et al. 2011). In addition, DP-MSCs retain their multipotent ability to differentiate, even after temporary storage in liquid nitrogen (Perry, Zhou et al. 2008).

Immunohistochemical studies have shown that DP-MSCs, isolated from the dental pulp of human third molar teeth and cultured under *in vitro* basal or undifferentiated conditions, are positive for STRO-1, CD44, CD105, CD 106, CD146, VCAM-1 (vascular cell adhesion molecule 1, an endothelial cell lineage marker), α -SMA,

ALP, osteonectin (an osteogenic marker), osteopontin (an osteogenic marker), osteocalcin (an osteogenic marker), collagen type I (an osteogenic marker), collagen type II (a cartilage marker), collagen type III (a fibroblasts marker) and fibroblast growth factor 2 (FGF-2, a fibroblasts marker), but they are negative for CD14, CD31 (a marker for endothelial cell lineage), CD34, CD45, CD71 (a transferring receptor), MyoD (a myocyte marker), neurofilament (a neuronal marker), PPAR γ 2 (a fat marker), dentin sialophosphoprotein (DSPP, an odontoblast specific protein) (Gronthos, Mankani et al. 2000; Shi, Bartold et al. 2005; Karaoz, Dogan et al. 2010). Flow cytometry analysis has confirmed that human DP-MSCs express CD13, CD73, CD90 and CD166, but not CD15 and CD117 (Karaoz, Dogan et al. 2010).

Moreover, human DP-MSCs can be induced to express not only osteoblast markers such as osteocalcin and flk-1 (vascular endothelial growth factor receptor 2, VEGF-R2), but also endothelial markers including CD54, von-Willebrand (domain 1 and 2), CD31 and angiotensin-converting enzyme (d'Aquino, Graziano et al. 2007). Furthermore, immunohistochemical and RT-PCR analysis revealed that human DP-MSCs in different *in vitro* differentiation culture are able to express osteogenic markers (ALP, osteonectin, osteocalcin, osteopontin, runt-related transcription factor 2, type I collagen, BMP-2 and BMP-4), adipogenic markers (leptin, adipophilin, and PPAR γ 2), chondrogenic markers (type II collagen, type X collagen and cartilage oligomeric matrix protein), myogenic markers (desmin, myogenin, myosinIIa, and α -SMA) and neurogenic markers (γ -enolase, microtubule-associated proteins 2 or MAP 2, c-fos, nestin, neurofilament-heavy, neurofilament-light, β 3 tubulin, and GFAP) (Koyama, Okubo et al. 2009; Karaoz, Dogan et al. 2010). Therefore, when cultured *in vitro*, DP-MSCs show the ability to differentiate into odontoblasts, osteoblasts, adipocytes, chondrocytes, endotheliocytes, myocytes and neurons (Gronthos, Mankani et al. 2000; Gronthos, Brahim et al. 2002; d'Aquino, Graziano et al. 2007; Zhang, Chang et al. 2008; Koyama, Okubo et al. 2009; Yu, Damek-Poprawa et al. 2009).

DP-MSCs *in vivo* can produce many complex tissues. For example, an early study showed that human DP-MSCs could differentiate into adipocytes (PPAR γ 2 and lipoprotein lipase) and neural-like cells (nestin, and GFAP), and forming ectopic

dentin and dentin-pulp-like tissue *in vivo* (Gronthos, Brahim et al. 2002). More recent *in vivo* studies have reported that human DP-MSCs are able to form calcified bone tissue with Haversian canals and osteocytes (Laino, d'Aquino et al. 2005; Kumabe, Nakatsuka et al. 2006; Yu, Damek-Poprawa et al. 2009) and dentin-pulp-like tissue complexes (Gronthos, Mankani et al. 2000; El-Backly, Massoud et al. 2008). Therefore, DP-MSCs are promising for dental tissue engineering and tooth regeneration.

In a recent study, DP-MSCs have been demonstrated to be induced to undergo odontoblastic differentiation in response to optimal mechanical compression of three-dimensional (3D) scaffolds with dentinal tubule-like pores. This effect is through activation of mitogen-activated protein kinases (MAPK) signaling pathway and expression of BMP7 and Wnt10a (Miyashita, Ahmed et al. 2014). But the mechano-sensing mechanisms involved are not yet identified.

Therefore, a better understanding of the mechanisms of autocrine (such as bone morphogenetic protein 2 [BMP-2], adenosine 5'-triphosphate [ATP]) and paracrine (for example, interleukin-1 [IL-1]) extracellular signals involved in the regulation of MSCs behaviors, is expected to facilitate tissue engineering and clinical applications (Scarfi 2014). For example, BMP-2 secreted from MSCs has been shown to improve the production of bone extracellular matrix during the induction of bone formation (Lin, Wang et al. 2014). ATP released from MSCs also modulated hMSCs proliferation (Coppi, Pugliese et al. 2007), suggesting an important role for extracellular ATP in regulating stem cell functions through the P2 purinergic receptors (Pedata, Melani et al. 2007). In addition, it has been reported that MSCs were induced by IL-1 to secrete prostaglandin E 2 (PGE 2) and a group of cytokines (such as IL-6 and IL-8) (Li, Reinhardt et al. 2012).

1.3 Extracellular ATP Signalling

1.3.1 ATP release, degradation and purinergic signalling

Since the discovery of ATP in 1929, it is well known that ATP acts as the energy supplier for a variety of cellular and molecular processes inside the cell. ATP is released from dying or damaged cells at the tissue injury or inflammation sites. There is increasing evidence to show ATP release from healthy cells constitutively or in response to stimulations, such as sensory nerves (Holton and Holton 1954; Holton 1959), osteoclasts, osteoblasts (Burnstock 2009; Burnstock, Fredholm et al. 2010). There is a diversity of stimulations or conditions that cause ATP release from cells, such as mechanical stress, hypoxia and inflammation (Burnstock, Fredholm et al. 2010; Sun, Junger et al. 2013; Scarfi 2014). The mechanisms mediating ATP efflux from the cell is not completely understood. However, several possible mechanisms have been reported, such as ATP-conductive anion channels, hemi-gap-junction channels and exocytosis (Kawano, Otsu et al. 2006).

Extracellular ATP can be converted through the actions of ecto-nucleotidases, to adenosine 5'-diphosphate (ADP), adenosine 5'-monophosphate (AMP) and adenosine as shown in Figure 1.2 (Buckley, Golding et al. 2003). In 1972, 'purinergic signalling' concept was hypothesized by Burnstock (Burnstock 1972). In 1978, two different families of such 'purinoceptors' P1 for adenosine and P2 receptors for ADP/ATP, were proposed (Burnstock and Wong 1978).

Four different P1 receptors, which are more commonly referred to as the A1, A2A, A2B and A3 receptors, are identified; they are all guanosine nucleotide-binding proteins (G-proteins) coupled receptors. The P2 receptors are further divided into two subfamilies, the ionotropic P2X receptors as cation channels and the metabotropic P2Y receptors as G-protein-coupled receptors, as shown in Figure 1.2 (Burnstock and Kennedy 1985; Khakh and North 2006; Coddou, Yan et al. 2011; von Kugelgen and Harden 2011; Baroja-Mazo, Barbera-Cremades et al. 2013). Seven mammalian P2X receptor subunits and eight P2Y mammalian receptor subunits have been characterized (Khakh and North 2006; Pedata, Melani et al. 2007; Burnstock 2014).

Intracellular Ca^{2+} is a ubiquitous signalling molecule that is involved in the regulation of almost all known cellular functions and reactions (Berridge, Bootman et al. 2003; Petersen, Michalak et al. 2005). Calcium signalling was mediated directly through activation of Ca^{2+} permeable ion channels, for example, Ca^{2+} entry through P2X receptors and store operated calcium (SOC) channels (discussed further below), or indirectly via second messengers generated by signal transduction pathways, for example, intracellular Ca^{2+} release mediated by inositol 1,4,5-triphosphate (IP_3) following activation of the P2Y receptors. There is now strong evidence to show that the P2 purinergic receptors have many functional roles in a wide range of physiological processes (Lim and Mitchell 2012), including bone remodelling (Burnstock, Fredholm et al. 2010; Orriss, Burnstock et al. 2010), neuronal signalling (Burnstock 2011; Burnstock and Ulrich 2011), inflammation (Ohta and Sitkovsky 2009), and epithelial transport (Novak 2011).

The following section will describe the P2 purinergic receptors, P2X and P2Y, and P2Y-activated SOC channels.

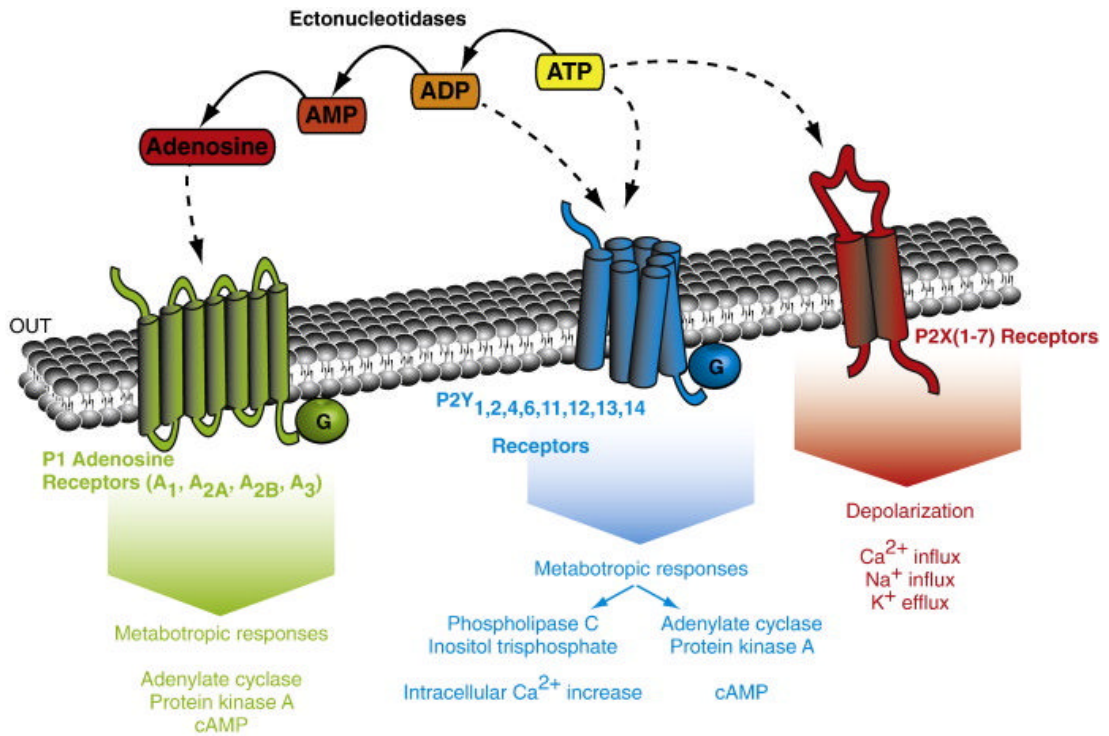


Figure 1.2 ATP degradation and the purinergic receptor family.

Extracellular ATP is the agonist for both P2X and P2Y receptors, and it can degrade to ADP, AMP and adenosine through actions of various ectonucleotidases. The activation of P2X receptors by ATP results in extracellular Na⁺ and Ca²⁺ influx and K⁺ efflux and thereby an increase in the intracellular Ca²⁺ concentrations and/or membrane depolarization. The activation of P2Y receptors by ATP and ADP leads to phospholipase C (PLC) activation, generation of IP₃ and release of cytosolic Ca²⁺ from intracellular stores to increase the intracellular Ca²⁺ concentrations, or inhibition of adenylate cyclase and reduction of the level of cyclic adenosine monophosphate (cAMP). Adenosine receptors are also coupled to G-proteins and regulate the production of cAMP through adenylate cyclase (Baroja-Mazo, Barbera-Cremades et al. 2013).

1.3.2 P2X receptors

There are seven P2X receptor protein or subunit subtypes (P2X1-P2X7) are identified (Khakh and North 2006). They range from 388 (P2X4) to 595 (P2X7) amino acid residues in length. Each subunit has two hydrophobic transmembrane (TM) domains connected by a large extracellular loop of about 280 amino acids residues, and both N- and C-termini are intracellular as shown in Figure 1.2. The P2X receptors are trimmers formed in a homomeric and heteromeric fashion (Jiang 2012). The experimental evidence so far shows that the P2X6 subunit does not form a homomeric receptor and the P2X7 subunit does not form a heteromeric receptor with other P2X subunits. Several heteromeric P2X receptors have been reported, including P2X1/2, P2X1/4, P2X1/5, P2X2/3, P2X2/5, P2X2/6, and P2X4/6 (Jiang 2012). P2X receptor are expressed in excitable cells like neurons and muscle cells and also in a diversity of non-excitable cells (Table 1.2), where they play an important role in a number of physiological and pathophysiological processes, including cell proliferation and differentiation (North 2002; Burnstock, Fredholm et al. 2010; Jiang 2012; Burnstock 2014).

All the P2X receptors are ligand-gated ion channels activated by extracellular ATP. P2X receptors mediate rapid non-selective passage of cations such as Na⁺, K⁺ and Ca²⁺ across the cell membrane, resulting in an increase in the intracellular Ca²⁺ concentrations and/or membrane depolarization (Burnstock, Fredholm et al. 2010). Membrane depolarization can induce further an increase in the intracellular Ca²⁺ concentration via activation of the voltage-gated Ca²⁺ (Ca_v) channels. This mechanism does not depend on the production and diffusion of second messengers within the cytosol or cell membrane. So, the P2X receptors play an important role in the rapid responses to extracellular ATP, during such as neuronal signalling and regulation of muscle contractility.

The P2X receptor ion channels have fast activation and deactivation kinetics, that is, they all open within a few milliseconds upon ATP binding and close within tens of milliseconds after ATP is removed. They exhibit strikingly different inactivation kinetics, manifested by the decline of the ionic currents during persistent application of ATP. The P2X1 and P2X3 receptors desensitize very fast, with ATP-induced

currents disappearing within tens or hundreds of milliseconds, whereas the P2X2, P2X4 and P2X5 receptors show modest desensitization in a few seconds and the P2X7 receptor exhibits no desensitization even over several minutes (Jarvis and Khakh 2009; North and Jarvis 2013). Further details are discussed in the following sections.

All P2X receptors are activated by ATP but show no or little sensitivity to ADP AMP, adenosine or other purines (for example, GTP) or pyrimidines (for example, UTP and CTP) (North and Jarvis 2013). However, there are several synthetic ATP analogues that act as the P2X receptor agonists, including 2-methylthioadenosine 5'-triphosphate (2-MeSATP), $\alpha\beta$ -methylene ATP ($\alpha\beta$ meATP) and 2',3'-O-(benzoyl-4-benzoyl)-ATP (BzATP). ATP and 2-MeSATP activate almost all P2X receptors (Jarvis and Khakh 2009; Khakh and North 2012). Suramin and PPADS are two generic antagonists that inhibit all P2X receptors except the P2X4 receptor (Jarvis and Khakh 2009; Khakh and North 2012).

In recent years, significant advances have been made in the development of more potent and selective antagonists with drug-like properties at certain P2X receptor subtypes, particularly the P2X3 and P2X7 receptors (Jiang 2012). The main distribution, agonists and antagonists of the P2X receptors are summarized in Table 1.2, and will be discussed further in the next section.

Table 1.2 Main distribution, agonists and antagonists of P2X receptors.

Receptor	Main distribution	Agonists	Antagonists
P2X1	Dorsal horn spinal neurons, cerebellum, smooth muscle, platelets	$\beta\gamma$ -meATP \geq α,β meATP \approx ATP \approx 2-MeSATP, BzATP, Ap4A	NF023, NF279, NF449, MRS2220, PPNDS, IP ₅ I, RO1, RO 0437626, TNP-ATP, BBG, Suramin, PPADS
P2X1/2	—	ATP, 2-MeSATP, α,β meATP, BzATP	—
P2X1/4	—	ATP, α,β meATP	TNP-ATP, Suramin, PPADS
P2X1/5	Submucosal arterioles	ATP, 2-MeSATP, α,β meATP	TNP-ATP, Suramin, PPADS
P2X2	Central nervous system (CNS) tissue, smooth muscle, retina, chromaffin cells, autonomic and sensory ganglia	ATP \geq ATP γ S \geq 2-MeSATP \gg α,β meATP	PPADS, TNP-ATP, BBG, PSB-1011, Suramin, PSB-1011, NF770, NF778
P2X2/3	Sensory neurons, sympathetic ganglion cells, brain neurons	ATP, α,β meATP, 2-MeSATP, BzATP	TNP-ATP, Suramin, PPADS, A317491, RO-3,
P2X2/5	Neurons	ATP, BzATP, ATP γ S	TNP-ATP
P2X2/6	Respiratory neurons	ATP, 2-MeSATP, α,β meATP	Suramin, PPADS

Receptor	Main distribution	Agonists	Antagonists
P2X3	Sensory neurons, some sympathetic neurones	BzATP, 2-MeSATP \geq ATP \geq α,β meATP \sim Ap ₄ A	Suramin, PPADS, IP ₅ I, TNP-ATP, A317491, RO-3, RO-4, RO-5, RO-51, RO-85, MK-3901, AF219
P2X4	CNS, epithelia of ducted glands and airways, smooth muscle of bladder, gastrointestinal tract, uterus, arteries, and fat cells	ATP, 2-MeSATP $>$ α,β meATP	TNP-ATP, BBG (weak antagonist), 5-BDBD, PSB-12062
P2X4/6	Hippocampal CA1 neurons	ATP, 2-MeSATP, α,β meATP	Suramin, PPADS
P2X5	Central neurons, bladder, thymus, spinal cord, cardiac muscle, skeletal muscle, skin, eye, and epithelia	ATP, 2-MeSATP	Suramin, PPADS
P2X6	Central nervous system tissue, pinal cord	(Does not function as homomultimer)	—
P2X7	CNS, peripheral nervous system, pancreas, skin, the immune system, and bone	BzATP $>$ ATP- γ -S $>$ ATP \geq 2-MeSATP $>$ α,β meATP	KN62, BBG, A-438079, A-839977, A-740003, A-759029, A-804598, AZ11645373, AZ10606120, CE-224535, AZD9056

[Most of the data presented in this table are considered fully in the following papers (Burnstock 2009; Jarvis and Khakh 2009; Khakh and North 2012; Nawazish-i-Husain Syed and Kennedy 2012; Burnstock 2013; Burnstock 2014)].

1.3.2.1 P2X1 subunit-containing receptors

The P2X1 receptor has been reported to be expressed at the mRNA or protein level in dorsal horn spinal neurons, cerebellum, smooth muscle, platelets (Burnstock and Knight 2004; Ashour, Atterbury-Thomas et al. 2006). It mediates muscle contraction, and activation of platelets leading to prothrombotic phenotype (Oury, Kuijpers et al. 2003; Surprenant and North 2009). The heteromeric P2X1/5 receptor has been observed in submucosal arterioles, and has a possible role in mediating excitatory junction potentials (Surprenant, Schneider et al. 2000).

Agonists

P2X1 receptor activation can be elicited by $\alpha\beta$ meATP at a half maximal effective concentration (EC_{50}) of 0.3 μ M, similar to that at the P2X3 receptor (0.8 μ M) (Jarvis and Khakh 2009; Khakh and North 2012). Therefore, $\alpha\beta$ meATP can be used to distinguish the P2X1 and P2X3 receptors from the other P2X receptors, but cannot be used to uniquely define P2X1 (Jarvis and Khakh 2009; Khakh and North 2012). Beta, gamma-methylene ATP ($\beta\gamma$ -meATP) is equipotent to $\alpha\beta$ meATP at P2X1, approximately 30-fold to 50-fold less potent at P2X3, and > 100-fold less potent at P2X2, P2X4, P2X5 and P2X7, indicating $\beta\gamma$ -meATP can be used as a selective agonist for P2X1 (North 2002; Gever, Cockayne et al. 2006). BzATP is also an effective agonist at the P2X1 receptor with an EC_{50} of 0.003 μ M when the receptor-mediated Ca^{2+} entry was measured, approximately 100-fold more potent than $\alpha\beta$ meATP (Bianchi, Lynch et al. 1999; Khakh and North 2012). Diadenosine polyphosphates such as Ap4A are also reported to be more selective agonists for P2X1 over P2X2, P2X3 and P2X4 (Wildman, Brown et al. 1999).

To the date, the P2X1 receptor subunit has been reported to participate in the formation of three heteromeric receptors: P2X1/2, P2X1/4 and P2X1/5 (Jarvis and Khakh 2009). The P2X1/2 receptor is reported to be activated by ATP ($EC_{50} \approx 0.5$ μ M), 2-MeSATP ($EC_{50} \approx 0.07$ μ M), $\alpha\beta$ meATP ($EC_{50} \approx 0.1$ μ M) and BzATP ($EC_{50} \approx 0.003$ μ M). The heteromeric P2X1/4 receptor can be activated by ATP ($EC_{50} \approx 10$ μ M) and $\alpha\beta$ meATP ($EC_{50} \approx 10$ μ M). Similar to the P2X1 receptor, the

heteromeric P2X1/5 receptor can be evoked by ATP ($EC_{50} \approx 1 \mu\text{M}$), 2-MeSATP ($EC_{50} \approx 1 \mu\text{M}$) and $\alpha\beta\text{meATP}$ ($EC_{50} \approx 3 \mu\text{M}$).

Antagonists

Several analogs of suramin (such as NF023, NF279 and NF449) are developed with improved potency and selectivity at the P2X1 receptor (Jiang 2012). NF023 was shown to have a half-maximal inhibitory concentration (IC_{50}) of 210-240 nM, less potent at the P2X2 ($IC_{50} > 50 \mu\text{M}$), P2X3 ($9 < IC_{50} < 29 \mu\text{M}$) and P2X4 ($IC_{50} \gg 100 \mu\text{M}$) receptors (Soto, Lambrecht et al. 1999). NF279 inhibits the P2X1 receptors with an IC_{50} of 19-50 nM, and much less potent at the P2X2 ($IC_{50} \approx 0.8 \mu\text{M}$), P2X3 ($IC_{50} \approx 1.6 \mu\text{M}$), P2X4 ($IC_{50} > 300 \mu\text{M}$) and P2X7 ($IC_{50} \approx 2.8 \mu\text{M}$) receptors (Klapperstuck, Buttner et al. 2000; Rettinger, Schmalzing et al. 2000). NF449 has the greater potency, with an IC_{50} of 0.3 nM (Kassack, Braun et al. 2004; Rettinger, Braun et al. 2005). NF449 can inhibit the heteromeric P2X1/2 receptors with an IC_{50} of 0.7 nM.

Numerous PPADS analogs with increased potency and selectivity for the P2X receptor have been identified, such as MRS2220, PPNDS, diinosine pentaphosphate (IP_5I) (Jacobson, Kim et al. 1998; King, Liu et al. 1999; Lambrecht, Rettinger et al. 2000; North 2002; Gevers, Cockayne et al. 2006). Particularly, IP_5I is highly potent and selective for P2X1 with an IC_{50} of 3 nM, and much less potent for P2X3 ($IC_{50} \approx 2.8 \mu\text{M}$) and P2X2 ($IC_{50} > 300 \mu\text{M}$), and inactive at the other P2X receptors (King, Liu et al. 1999; Khakh and North 2012). Finally, RO-1 or RO-0437626 has been described as a selective drug-like human P2X1 receptor antagonist with an IC_{50} of 3 μM in calcium entry assays, and > 30 -fold less potent at the human P2X2 and P2X3 receptors ($IC_{50} > 100 \mu\text{M}$) (Jaime-Figueroa, Greenhouse et al. 2005; Ford, Gevers et al. 2006).

The P2X1 receptors are also inhibited by 2',3'-O-(2,4,6-trinitrophenyl)-ATP (TNP-ATP) ($IC_{50} \approx 0.006 \mu\text{M}$) and Brilliant blue G (BBG) ($IC_{50} > 5 \mu\text{M}$) (Khakh, Burnstock et al. 2001; North 2002). TNP-ATP is a highly potent antagonist for the heteromeric P2X1/4 receptor with an IC_{50} of 0.5 μM , and the heteromeric P2X1/5 receptor with an IC_{50} of 0.4 μM (Jarvis and Khakh 2009).

1.3.2.2 P2X2 subunit-containing receptors

The P2X2 receptor is expressed in the central nervous system (CNS), smooth muscles, retina, chromaffin cells, autonomic and sensory ganglia (King, Housley et al. 1998; Burnstock and Knight 2004; Studeny, Torabi et al. 2005; Puthussery and Fletcher 2006). It has possible roles in mediating facilitation of synaptic transmission in hippocampal interneurons (Khakh, Gittermann et al. 2003), ventilatory responses to hypoxia in the carotid body (Rong, Gourine et al. 2003), and proliferation of glial cells differentiated from P19 murine embryonic carcinoma cells. The heteromeric P2X2/3 receptor is expressed in sensory neurons, sympathetic ganglion cells, and they are necessary for the initiation of sensory signalling in the pathways subserving taste, chemoreception, visceral distension, and neuropathic pain (Dunn, Zhong et al. 2001; Jiang, Kim et al. 2003; McGaraughty, Wismer et al. 2003; Surprenant and North 2009). The heteromeric P2X2/5 receptor is expressed in peripheral and central neurons, and display functional properties including pore dilatation, membrane blebbing, and phosphatidylserine exposure (Compan, Ulmann et al. 2012). The heteromeric P2X2/6 receptor is expressed in respiratory neurons in the brain (Schwindt, Trujillo et al. 2011).

Agonists

ATP, adenosine-5'-(γ -thio)-triphosphate (ATP γ S) and 2-MeSATP are reported to be the agonists for the P2X2 receptor, while BzATP is a less potent and partial agonist (Evans, Lewis et al. 1995; Bianchi, Lynch et al. 1999; Lynch, Touma et al. 1999). $\alpha\beta$ meATP, $\beta\gamma$ -meATP, ADP, and UTP are inactive up to 100-300 μ M (Evans, Lewis et al. 1995; Bianchi, Lynch et al. 1999; Lynch, Touma et al. 1999). The agonists for the heteromeric P2X1/2 receptor are described in section 1.3.2.1. The heteromeric P2X2/3 receptor is reported to be potently activated by ATP ($EC_{50} \approx 0.7$ μ M), BzATP ($EC_{50} \approx 0.8$ μ M), 2-MeSATP ($EC_{50} \approx 1$ μ M), and $\alpha\beta$ meATP ($EC_{50} \approx 5$ μ M). While a recent study has showed that the P2X2 and P2X5 subunits interact to form a heteromeric P2X2/5 receptor activated by ATP ($EC_{50} \approx 12$ μ M), BzATP ($EC_{50} \approx 82$ μ M) and ATP γ S ($EC_{50} \approx 22$ μ M) (Compan, Ulmann et al. 2012). The heteromeric P2X2/6 receptor is less sensitive to ATP ($EC_{50} \approx 30$ μ M), 2-MeSATP ($EC_{50} \approx 35$ μ M) and $\alpha\beta$ meATP ($EC_{50} > 100$ μ M) (Jarvis and Khakh 2009).

Antagonists

PPADS ($IC_{50} \approx 1 \mu\text{M}$), TNP-ATP ($IC_{50} \approx 1 \mu\text{M}$) and BBG ($IC_{50} \approx 1.4 \mu\text{M}$) have similar potency of antagonizing ATP-evoked currents mediated by human or rat P2X2 receptors, while suramin is less potent ($IC_{50} \approx 8\text{-}10 \mu\text{M}$) than these antagonists (Evans, Lewis et al. 1995; Bianchi, Lynch et al. 1999; Khakh, Burnstock et al. 2001). PSB-1011 has been identified to be a P2X2 antagonist with a high selectivity over the P2X1, P2X3, P2X4 and P2X7 receptors (Baqi, Hausmann et al. 2011). Moreover, NF770 and NF778 are potent P2X2 antagonists generated by structural modification of suramin (Wolf, Rosefort et al. 2011). The heteromeric P2X2/3 receptor is very potently blocked by TNP-ATP ($IC_{50} \approx 0.007 \mu\text{M}$) as well as PPADS and suramin (Jarvis and Khakh 2009). The P2X2/3 receptors is also potently inhibited by A-317491 with an IC_{50} of $0.1 \mu\text{M}$ (Jarvis, Burgard et al. 2002; Neelands, Burgard et al. 2003), and by RO-3 with an IC_{50} of $\sim 2 \mu\text{M}$ (Jarvis and Khakh 2009). The heteromeric P2X2/5 receptor is potently inhibited by $1 \mu\text{M}$ TNP-ATP (Compan, Ulmann et al. 2012).

1.3.2.3 P2X3 subunit-containing receptors

The P2X3 receptor is exclusively expressed in sensory neurons and some sympathetic neurones (Chen, Akopian et al. 1995; Lewis, Neidhart et al. 1995; Bradbury, Burnstock et al. 1998), where it is involved in the control of bladder function, taste, chemoreception and neuropathic pain (McGaraughty, Wismer et al. 2003; Burnstock 2006).

Agonists

The P2X3 receptor is highly sensitive to ATP ($EC_{50} \approx 0.5 \mu\text{M}$), 2-MeSATP ($EC_{50} \approx 0.3 \mu\text{M}$) and $\alpha\beta\text{meATP}$ ($EC_{50} \approx 0.8 \mu\text{M}$) (Khakh and North 2012). BzATP is the most potent agonist for the P2X3 receptors, with an EC_{50} of $0.08 \mu\text{M}$ (Khakh and North 2012). Overall, ATP, 2-MeSATP, $\alpha\beta\text{meATP}$, BzATP, $\beta\gamma\text{-meATP}$ and Ap4A have been reported to be less potent at the P2X3 receptor as compared to the P2X1 receptor (Khakh and North 2012). The heteromeric P2X2/3 receptor is described in section 1.3.2.2.

Antagonists

Suramin, PPADS, IP₅I and TNP-ATP are antagonists at the P2X₃ receptor (Khakh and North 2012). Particularly, TNP-ATP is a competitive potent P2X₃ antagonist with an IC₅₀ of 1 nM (Khakh and North 2012). A-317491 was the first competitive and selective P2X₃ receptor antagonist (IC₅₀ ≈ 20 nM) with drug-like properties (Jarvis, Burgard et al. 2002; Neelands, Burgard et al. 2003).

Other potent drug-like P2X₃ antagonists have been reported, including RO3 (Gever, Cockayne et al. 2006), RO4 (or AF353) (Gever, Soto et al. 2010), RO5 (or AF-792) (Kaan, Yip et al. 2010), RO-51 (Jahangir, Alam et al. 2009), RO-85 (Brotherton-Pleiss, Dillon et al. 2010), MK-3901 (Gum, Wakefield et al. 2012) and AF-219 (Gum, Wakefield et al. 2012; Ochoa-Cortes, Linan-Rico et al. 2014). Specially, AF-219 has an IC₅₀ of 30 nM and has been advanced into clinical studies (Ford 2012; Gum, Wakefield et al. 2012; Ford and Udem 2013; Ochoa-Cortes, Linan-Rico et al. 2014).

1.3.2.4 P2X₄ subunit-containing receptors

The P2X₄ receptor has a wide distribution in the CNS, epithelia of ducted glands and airways, smooth muscle of bladder, gastrointestinal tract, uterus, arteries, and fat cells (Bo, Kim et al. 2003). It is engaged in the regulation of capillary diameter, development of vascular inflammation and neuropathic pain (Coull, Beggs et al. 2005; Qureshi, Paramasivam et al. 2007). Mice lacking the P2X₄ receptor are hypertensive and have smaller-diameter arteries (Surprenant and North 2009). The P2X_{4/6} receptor is expressed in hippocampal CA1 neurons (Khakh, Proctor et al. 1999).

Agonists

The homomeric P2X₄ receptor is activated by ATP and 2-MeSATP with a similar EC₅₀ of ~ 10 μM, whereas αβmeATP and βγ-meATP are much less potent at the P2X₄ receptor (Garcia-Guzman, Soto et al. 1997). The heteromeric P2X_{1/4} receptor is described in section 1.3.2.1. The heteromeric P2X_{4/6} receptor can be activated by

ATP ($EC_{50} \approx 6 \mu\text{M}$), 2-MeSATP ($EC_{50} \approx 7 \mu\text{M}$) and $\alpha\beta\text{meATP}$ ($EC_{50} \approx 12 \mu\text{M}$) (Jarvis and Khakh 2009).

Antagonists

The P2X4 receptor is inhibited by TNP-ATP ($IC_{50} \approx 15 \mu\text{M}$) and BBG ($IC_{50} \approx 3\text{-}10 \mu\text{M}$), but insensitive to suramin and PPADS (Khakh, Burnstock et al. 2001; Gum, Wakefield et al. 2012; North and Jarvis 2013). 5-BDBD has been reported to be a potent P2X4 antagonist that blocks the P2X4 receptor-mediated currents ($IC_{50} \approx 0.50 \mu\text{M}$) (Casati, Frascoli et al. 2011). Furthermore, PSB-12062 is reported as a potent and selective antagonist for the P2X4 receptor ($IC_{50} \approx 0.9\text{-}1.8 \mu\text{M}$) and almost 35-fold less potent at the P2X1, P2X2, P2X3, and P2X7 receptors (Hernandez-Olmos, Abdelrahman et al. 2012). Suramin and PPADS are antagonists at the P2X4/6 receptor (Khakh and North 2012).

1.3.2.5 P2X5 subunit-containing receptors

The P2X5 receptor is localized in neurons in the CNS, bladder, thymus, spinal cord, cardiac muscle, skeletal muscle, skin, eye, and epithelia (Ryten, Dunn et al. 2002; Burnstock and Knight 2004; Nawazish-i-Husain Syed and Kennedy 2012). In an *in vivo* wound-healing study, the P2X5 receptor protein expression, as measured by immunohistochemistry, was reported to be significantly increased in keratinocytes of the regenerating epidermis (Greig, James et al. 2003). Particularly, the P2X5 receptor expression was reported to be increased in migratory keratinocytes at the wound edge, which indicates that the P2X5 receptor might be involved in cell migration.

Agonists and antagonists

The P2X5 receptor can be activated by ATP ($EC_{50} \approx 10 \mu\text{M}$) and 2-MeSATP ($EC_{50} \approx 10 \mu\text{M}$), and blocked by suramin ($IC_{50} \approx 40 \mu\text{M}$) and PPADS ($IC_{50} \approx 3 \mu\text{M}$) (Gever, Cockayne et al. 2006; Khakh and North 2012). The heteromeric P2X1/5 and P2X2/5 receptors are described in section 1.3.2.1 and section 1.3.2.2, respectively.

1.3.2.6 P2X6 subunit-containing receptors

The P2X6 protein is expressed in the CNS and spinal cord (Burnstock and Knight 2004), and is possibly involved in depolarization of medial habenula, medial vestibular and locus coeruleus neurons (Edwards, Gibb et al. 1992; Chessell, Michel et al. 1997; Sansum, Chessell et al. 1998). However, it is generally thought that the P2X6 subunit is incapable of forming functional homomeric receptors (Gever, Cockayne et al. 2006; Khakh and North 2012). However, the P2X6 subunit can interact with other P2X subunits to form heteromeric P2X receptors including the P2X2/6 and P2X4/6 receptors as described in section 1.3.2.2 and section 1.3.2.4, respectively.

1.3.2.7 P2X7 receptor

The P2X7 receptor is present in CNS, peripheral nervous system (PNS), pancreas, skin, the immune system, and bone (Collo, Neidhart et al. 1997; Ke, Qi et al. 2003; Burnstock and Knight 2004; Burnstock 2011), but not neuronal cells (Sim, Young et al. 2004). They are involved in the release of proinflammatory cytokines from macrophages and neuropathic chronic pain (Solle, Labasi et al. 2001; Chessell, Hatcher et al. 2005; Surprenant and North 2009). Some studies also have shown that the P2X7 receptor could promote cell proliferation, as shown in human neuroblastoma cells (Raffaghello, Chiozzi et al. 2006), microglial cells (Bianco, Ceruti et al. 2006; Monif, Reid et al. 2009; Sanz, Chiozzi et al. 2009), and mouse Neuro-2a (N2a) neuroblastoma cells (Wu, Lin et al. 2009). Additionally, activation of the P2X7 receptor in osteoblasts enhances bone formation (Panupinthu, Rogers et al. 2008; Li, Meyer et al. 2009), whereas activation of the P2X7 receptor in osteoclasts results in apoptosis and bone resorption (Korcok, Raimundo et al. 2004).

Agonists

Among the P2X receptors, the P2X7 receptor is least sensitive to activation by ATP ($EC_{50} \approx 100 \mu\text{M}$) and 2-MeSATP ($EC_{50} \approx 100 \mu\text{M}$) (Gever, Cockayne et al. 2006; Khakh and North 2012). BzATP exhibits greater potency ($EC_{50} \approx 20 \mu\text{M}$) than ATP, 2-MeSATP, ATP γ S ($EC_{50} \approx 20 \mu\text{M}$) and $\alpha\beta\text{meATP}$ ($EC_{50} > 300 \mu\text{M}$) (Gever, Cockayne et al. 2006; Jarvis and Khakh 2009; Khakh and North 2012), but it is

worth pointing out BzATP is also a full or partial agonist at the P2X1, P2X2, P2X3 and P2X4 receptors as described above.

Antagonists

Earlier studies have identified several potent P2X7 antagonists, such as BBG (Jiang, Mackenzie et al. 2000) and KN-62 (Gargett and Wiley 1997). These compounds exhibit striking species differences, for example, BBG with IC₅₀ of ~270 nM for the human P2X7 receptor and IC₅₀ of ~10 nM for the rat P2X7 receptor; KN-62 with an IC₅₀ of ~40-130 nM for the human P2X7 receptor and an IC₅₀ of ~86 nM for the rhesus macaque monkey P2X7 receptor (Bradley et al., 2011). Recently, a variety of as drug-like, potent and selective P2X7 receptor antagonists have been developed based on tetrazole/triazole (for example, A-438079 with an IC₅₀ of ~126-500 nM, A-839977 with an IC₅₀ of ~20-150 nM, A-740003 with an IC₅₀ of ~18-40 nM, A-759029 with an IC₅₀ of ~32-40 nM and A-804598 with an IC₅₀ of ~9-11 nM), cyclic imides (such as AZ11645373 with an IC₅₀ of ~5-20 nM), adamantane amides (such as AZ10606120 with an IC₅₀ < 10 nM for human P2X7 receptors and > 10-1000 nM for rat P2X7 receptors) and 6-azauracil derivatives (such as CE-224535) (Jiang 2012). To date, P2X7 antagonists AZD9056 and CE-224535 have been tested in clinical trials (Guile, Alcaraz et al. 2009; Elsby, Fox et al. 2011; Keystone, Wang et al. 2012; Stock, Bloom et al. 2012). AZD9056 is a potent (IC₅₀ of 10-13 nM) and high selective antagonist at the human P2X7 receptor (> 1000-fold) compared to the other P2X receptor subtypes, but it has little affinity for the mouse or rat P2X7 receptors (Keystone, Wang et al. 2012). CE-224535 is also a potent antagonist with an IC₅₀ of 2-13 nM, and is highly selective for the P2X7 receptor at least 500-fold relative to the P2X1 and P2Y1 receptors (Stock, Bloom et al. 2012). But both compounds AZD9056 and CE-224535 failed to bring about significant therapeutic benefits (Guile, Alcaraz et al. 2009; Elsby, Fox et al. 2011; Keystone, Wang et al. 2012; Stock, Bloom et al. 2012).

1.3.3 P2Y receptors

The P2Y receptors are widely expressed in neurons, muscle cells and many non-excitabile cells (cells lacking the ability to fire action potentials) (Burnstock,

Fredholm et al. 2010). Eight mammalian P2Y receptors have been identified: P2Y1, P2Y2, P2Y4, P2Y6, P2Y11, P2Y12, P2Y13 and P2Y14. The P2Y receptor proteins consist of 308 to 377 amino acid residues. They have seven transmembrane domains (7TM) with short extracellular N and intracellular C termini as shown in Figure 1.2 (Webb, Simon et al. 1994; Khakh and North 2006).

In contrast to the P2X receptors at which ATP is the only physiological activator as discussed above, the P2Y receptors are sensitive to activation by a variety of nucleotides: ATP (P2Y1, P2Y2, P2Y11), ADP (P2Y1, P2Y12, P2Y13), UTP (P2Y2, P2Y4), UDP (P2Y6, P2Y14) and UDP-glucose (P2Y14) (Burnstock 2006; Burnstock 2009). The responses mediated by the P2Y receptors are usually longer than those by the P2X receptors because they are coupled to G-proteins and involve generation of second messengers. The P2Y1, P2Y2, P2Y4, P2Y6, and P2Y11 receptors are coupled to G_{q/11} proteins to activate PLC, which leads to hydrolysis of phosphatidylinositol 4,5-bisphosphate (PIP₂) and subsequent generation of IP₃ and 1,2-diacylglycerol (DAG). Diffusible IP₃ binds to the IP₃ receptors (IP₃R) in the membrane of endoplasmic reticulum (ER) to cause Ca²⁺ release from the ER, as shown in Figure 1.2 and Figure 1.4 (Berridge 1993; Fahrner, Muik et al. 2009). The P2Y12, P2Y13, and P2Y14 are coupled to G_i to inhibit adenylyl cyclase (AC) to reduce the intracellular levels of cyclic adenosine monophosphate (cAMP) (Khakh and North 2006; Park, Hoover et al. 2009; Burnstock, Fredholm et al. 2010). The P2Y11 receptor is also coupled to G_s to stimulate AC to increase the cAMP levels (Torres, Zambon et al. 2002).

Like the P2X receptors, the P2Y receptors are also inhibited by suramin (P2Y1, P2Y2, P2Y6, P2Y11, P2Y12, P2Y13) and PPADS (P2Y1, P2Y4, P2Y6, P2Y13) (von Kugelgen 2006). The distribution, agonists and antagonists of the P2Y receptors are summarized in Table 1.3 and are discussed below.

Table 1.3 Main distribution, agonists and antagonists of P2Y receptors.

Receptor	Main distribution	Agonists	Antagonists
P2Y ₁	Brain, epithelial and endothelial cells, platelets, immune cells, osteoclasts	MRS2365 > 2-MeSADP >> ADP > ATP	MRS2500 > MRS2279 > MRS2179
P2Y ₂	Neurons, smooth muscle cells, epithelial and endothelial cells, osteoblasts, breast cancer cells	2-Thio-UTP > UTP, MRS2698 ≥ ATP, INS 365 > INS 37217, Ap ₄ A > MRS 2768	AR-C126313 > suramin > Reactive Blue 2, PSB-716
P2Y ₄	Intestine, epithelial cells, placenta, spleen and thymus	MRS4062, UTP ≥ ATP	ATP (human) > Reactive Blue 2 > suramin
P2Y ₆	Airway and intestinal epithelial cells, placenta, T cells, thymus	MRS2693 > UDPβS, PBS0474, UDP > UTP >> ATP	MRS2578 > Reactive Blue 2, PPADS
P2Y ₁₁	Macrophage, neurons, smooth muscle cells, spleen, intestine, granulocytes	ATPγS > AR-C67085 > BzATP ≥ ATP, NF546	NF157 > suramin > Reactive Blue 2

Receptor	Main distribution	Agonists	Antagonists
P2Y ₁₂	Platelets, glial cells, smooth muscle cells, endothelial cells, and chromaffin cells	ADP ~ 2-MeSADP > ATP	AR-C69931MX > AR-C67085, AZD6140, INS49266, INS50589
P2Y ₁₃	Spleen, placenta, brain, lymph nodes, bone marrow, osteoblasts, monocytes	2-MeSADP, ADP > ATP > 2-MeSATP	AR-C69931MX > AR-C67085 > MRS2211
P2Y ₁₄	Placenta, brain regions, adipose tissue, stomach, intestine, bone marrow, immune system	MRS2802, MRS2690 > UDP-glucose ≥ UDP-galactose, UDP-glucosamine	UDP

[Modified and updated from (von Kugelgen 2006; Burnstock 2009; von Kugelgen and Harden 2011; Burnstock 2013)]

1.3.3.1 P2Y1 receptor

The P2Y1 expression has been detected at the mRNA level in various tissues and cells, including brain, epithelial and endothelial cells, platelets, immune cells, osteoclasts (Burnstock 2013). Activation of the P2Y1 receptor by ADP stimulates osteoclast activity and bone resorption (Hoebertz, Arnett et al. 2003).

Agonists and antagonists

ATP is a partial agonist for the P2Y1 receptor and ADP is the most potent physiological agonist ($EC_{50} \approx 7.9 \mu\text{M}$) (Bodor, Waldo et al. 2004), and UTP, UDP, CTP, and GTP are all inactive. Moreover, 2-MeSADP is more potent at the P2Y1 receptor ($EC_{50} \approx 6.3 \text{ nM}$) than ADP. Particularly, MRS2365 (the N-methanocarba analogue of 2-MeSADP) represents a highly potent and selective agonist for the P2Y1 receptor with an EC_{50} of 0.4 nM, but exhibits no activity at the P2Y12 and only very low agonist activity at the P2Y13 receptor (at concentrations up to $1 \mu\text{M}$) (Chhatiwala, Ravi et al. 2004). MRS2179 ($IC_{50} \approx 0.3 \mu\text{M}$) (Nandanan, Camaioni et al. 1999), MRS2279 ($IC_{50} \approx 7.9 \text{ nM}$) (Kim, Ohno et al. 2003), and MRS2500 ($IC_{50} \approx 1 \text{ nM}$) (Kim, Ohno et al. 2003) represent the potent and selective antagonists at the P2Y1 receptor.

1.3.3.2 P2Y2 receptor

The P2Y2 receptor is expressed in many cells including neurons, smooth muscle cells, epithelial and endothelial cells, osteoblasts, breast cancer cells (Hoebertz, Arnett et al. 2003; Burnstock 2009; Burnstock 2013; Chadet, Jelassi et al. 2014). Activation of the P2Y2 receptors in osteoblasts by ATP and UTP inhibits bone growth and mineralization (Hoebertz, Arnett et al. 2003). It is also reported that activation of the P2Y2 receptor increases MCF-7 breast cancer cells migration (Chadet, Jelassi et al. 2014).

Agonists and antagonists

ATP ($EC_{50} \approx 79.4 \text{ nM}$), UTP ($EC_{50} \approx 7.9 \text{ nM}$), diadenosine tetraphosphate (Ap4A, $EC_{50} \approx 0.79 \mu\text{M}$) and γ -thiophosphate (UTP γ S, $EC_{50} \approx 0.25 \mu\text{M}$) are full agonists at

the P2Y2 receptor, whereas ADP and UDP are much less potent (von Kugelgen 2006; Burnstock 2009; von Kugelgen and Harden 2011). To date, there are several potent P2Y2 receptor agonists, such as MRS2698 ($EC_{50} \approx 8$ nM) (Ivanov, Ko et al. 2007) and selective agonists, such as MRS2768 ($EC_{50} \approx 1.89$ μ M) (Ko, Carter et al. 2008). 2-ThioUTP is a potent and selective agonist at the human P2Y2 (hP2Y2) receptor with an EC_{50} of 0.035 μ M, and it is much less potent at the hP2Y4 and hP2Y6 receptors with an EC_{50} of 0.35 and 1.5 μ M, respectively (El-Tayeb, Qi et al. 2006; Ko, Carter et al. 2008). Additionally, Up4U (INS365, Diquafosol, $EC_{50} \approx 0.1$ μ M) and dCp4U (INS37217, Denufosol, $EC_{50} \approx 0.22$ μ M) are drug-like agonists for the P2Y2 receptor. The P2Y2 receptor-mediated responses can be blocked by suramin ($IC_{50} \approx 50.0$ μ M), but not by PPADS (von Kugelgen 2006; Burnstock 2009; von Kugelgen and Harden 2011). AR-C126313 ($IC_{50} \approx 1$ μ M) (Jacobson, Costanzi et al. 2004), Reactive Blue 2 ($IC_{50} < \sim 100$ μ M) and PSB-716 ($IC_{50} \approx 10$ μ M) have been reported to be effective antagonists for the P2Y2 receptor (Burnstock 2009; Jacobson, Balasubramanian et al. 2012; Burnstock 2014).

1.3.3.3 P2Y4 receptor

The P2Y4 receptor is distributed in intestine, epithelial cells, placenta, spleen and thymus (Burnstock 2009; Burnstock 2013). The P2Y4 receptor has a role in mediating the regulation of chloride secretion by UTP in the jejuna epithelium (Robaye, Ghanem et al. 2003; Burnstock, Fredholm et al. 2010).

Agonists and antagonists

UTP is the most potent native agonist at the P2Y4 receptor ($EC_{50} \approx 2.5$ μ M for human), while ADP and UDP are inactive (von Kugelgen 2006; Burnstock 2009; von Kugelgen and Harden 2011). MRS4062 is a potent and selective agonist at the P2Y4 receptor with an EC_{50} of 23 nM, while it inhibits at the P2Y2 and P2Y6 receptors with an IC_{50} of 640 and 740 nM, respectively (Jacobson, Balasubramanian et al. 2012). There is no selective antagonist for the P2Y4 receptor. ATP acts as an antagonist at the human ($IC_{50} \approx 39.8$ μ M), but not the rat, P2Y4 receptors. Suramin is a weak P2Y4 receptor antagonist ($IC_{50} < 100$ μ M). Reactive Blue 2 is a potent

antagonist for the rat P2Y4 receptor, but only partially blocks the human P2Y4 receptor ($IC_{50} < 100 \mu\text{M}$) (Burnstock 2009; Burnstock 2013).

1.3.3.4 P2Y6 receptor

The P2Y6 receptor is expressed in airway and intestinal epithelial cells, placenta, T cells and thymus (Burnstock 2009; Burnstock 2013). It is involved in UDP-induced release of IL-6 and inflammatory protein-2 from macrophages, and production of inositol phosphate (Robaye, Ghanem et al. 2003; Burnstock, Fredholm et al. 2010).

Agonists and antagonists

ATP, ADP and their 2-methylthio derivatives are inactive at the P2Y6 receptor. UDP and UTP activate the P2Y6 receptor; UDP is approximately 100-fold more potent ($EC_{50} \approx 0.32 \mu\text{M}$) than UTP (Nicholas, Lazarowski et al. 1996; von Kugelgen 2006; von Kugelgen and Harden 2011). Uridine β -thiodiphosphate (UDP β S) ($EC_{50} \approx 0.05 \mu\text{M}$) and Up3U ($EC_{50} \approx 0.25 \mu\text{M}$) are more metabolically stable and selective agonists at the P2Y6 receptor than UDP (Hou, Harden et al. 2002; Ivanov, Ko et al. 2007). INS48823 is also a potent agonist with an EC_{50} of $\sim 125 \text{ nM}$ (Korcok, Raimundo et al. 2005). MRS2693 (5-iodo-UDP) is a selective agonist with an EC_{50} of $\sim 15 \text{ nM}$ (Besada, Shin et al. 2006). PSB0474 is a potent and selective agonist with an EC_{50} of 70 nM at the P2Y6 receptor and much less potent at the P2Y2 ($EC_{50} > 1 \mu\text{M}$) and P2Y4 receptors ($EC_{50} > 10 \mu\text{M}$) (El-Tayeb, Qi et al. 2006).

P2Y6 receptor-mediated responses can be inhibited by Reactive Blue 2 and PPADS (von Kugelgen 2006; Burnstock 2009; von Kugelgen and Harden 2011). To date, MRS2578 has been shown to be a non-competitive antagonist ($IC_{50} \approx 39.8 \text{ nM}$) for the P2Y6 receptor (Mamedova, Joshi et al. 2004).

1.3.3.5 P2Y11 receptor

The P2Y11 receptor is expressed in macrophage, neurons, smooth muscle cells, spleen, intestine and granulocytes (Burnstock 2013; Sakaki, Tsukimoto et al. 2013) and is involved in macrophage activation (Sakaki, Tsukimoto et al. 2013),

neuropathic pain (Barragan-Iglesias, Pineda-Farias et al. 2014), neutrophil apoptosis (Vaughan, Stokes et al. 2007), and relaxations of smooth muscle cells (King and Townsend-Nicholson 2008).

Agonists and antagonists

ATP is the native agonist at the P2Y₁₁ receptor ($EC_{50} \approx 15.8 \mu\text{M}$ for human P2Y₁₁). ATP γ S and BzATP are more potent agonists than ATP, with EC_{50} of $\sim 3.1 \mu\text{M}$ and $\sim 7.9 \mu\text{M}$, respectively (Communi, Robaye et al. 1999). AR-C67085 is a potent agonist at the P2Y₁₁ receptor with EC_{50} of $\sim 8.9 \mu\text{M}$ (Communi, Robaye et al. 1999), but acts as an antagonist at the P2Y₁₂ receptor) (Burnstock 2009; Burnstock 2013). NF546 has been shown to be a selective agonist for the P2Y₁₁ receptor ($EC_{50} \approx 53.7 \mu\text{M}$) over the other P2Y receptors, including P2Y₁, P2Y₂, P2Y₄, P2Y₆ and P2Y₁₂ receptors (Meis, Hamacher et al. 2010). P2Y₁₁receptor-mediated responses can be blocked by Reactive Blue 2 ($IC_{50} < \sim 100 \mu\text{M}$), but not by PPADS (Nicholas, Lazarowski et al. 1996; von Kugelgen 2006; von Kugelgen and Harden 2011). Suramin acts as a more potent antagonist at the human P2Y₁₁ receptor ($IC_{50} \approx 15.8 \mu\text{M}$) than the human P2Y₁ receptor (von Kugelgen 2006; Burnstock 2009; von Kugelgen and Harden 2011). NF157, derived from suramin, has been reported to be a potent and selective antagonist for the P2Y₁₁ receptor ($IC_{50} \approx 0.46 \mu\text{M}$) (Ullmann, Meis et al. 2005).

1.3.3.6 P2Y₁₂ receptor

The P2Y₁₂ receptor is present in platelets, glial cells, smooth muscle cells, endothelial cells, and chromaffin cells (Burnstock 2009; Burnstock 2013). They are involved in the inhibition of platelet aggregation by ADP, resistance to arterial thrombosis, and prolonged bleeding time (Burnstock 2009; Burnstock, Fredholm et al. 2010). Moreover, an *in vivo* study showed that the P2Y₁₂ receptor activated by ADP stimulates migration of microglial cells to the injury area at the early stages of the response to local CNS injury (Sharon, Levesque et al. 2006).

Agonists and antagonists

ADP is the native agonist at the P2Y₁₂ receptor ($EC_{50} \approx 63 \text{ nM}$ for human P2Y₁₂), at which ATP is inactive. 2-MeSADP is also a potent agonist with an EC_{50} of ~ 12.6

nM, similar to ADP. Currently, AR-C69931MX and AR-C67085 are two potent drug-like antagonists for the P2Y₁₂ receptor with an IC₅₀ of ~ 0.4 nM and ~30 μM, respectively (Springthorpe, Bailey et al. 2007). AZD6140 is a potent antagonist at P2Y₁₂ receptor with an IC₅₀ of ~ 12.6 nM (Springthorpe, Bailey et al. 2007; Ye, Chen et al. 2008). Other antagonists of the P2Y₁₂ receptor include INS49266 (an ADP derivative with an IC₅₀ of ~ 52 nM) and INS50589 (an AMP derivative with an IC₅₀ of ~ 11 nM) (Douglass, deCamp et al. 2008).

1.3.3.7 P2Y₁₃ receptor

The P2Y₁₃ receptor is distributed in spleen, placenta, brain, lymph nodes, bone marrow, osteoblasts, and monocytes (Burnstock 2009; Burnstock, Fredholm et al. 2010). It is involved in mediating osteogenic responses to mechanical stimulation by regulating ATP metabolism in osteoblasts (Wang, Rumney et al. 2013). Moreover, the P2Y₁₃ receptor contributes to the balance of osteoblast and adipocytes differentiation of BM-MSCs (Biver, Wang et al. 2013).

Agonists and antagonists

The P2Y₁₃ receptor can be activated by ADP, 2-MeSADP and ATP, with EC₅₀ of ~12.6 nM, 12.6 nM and 0.25 μM, respectively at the human P2Y₁₃ receptor for human (Jacobson and Boeynaems 2010; Burnstock 2014). ADP is more potent than ATP, and 3-5 folds more potent than 2-MeSADP at the rat P2Y₁₃ receptor. The P2Y₁₃ receptor can be inhibited by ARC69931MX (IC₅₀ ≈ 4.0 nM) and ARC67085 (IC₅₀ ≈ 0.2 μM). A derivative of PPADS, MRS2211, has been shown to be a selective antagonist for the P2Y₁₃ receptor with an IC₅₀ of ~1.1 μM (> 20-fold more selective over the P2Y₁ and P2Y₁₂ receptors) (Kim, Lee et al. 2005).

1.3.3.8 P2Y₁₄ receptor

The P2Y₁₄ receptor is widely expressed in placenta, brain regions, adipose tissue, stomach, intestine, bone marrow, and immune system (Lee, Cheng et al. 2003; Moore, Murdock et al. 2003; Burnstock 2009; Kobayashi, Yamanaka et al. 2012; Kobayashi, Yamanaka et al. 2013). It is involved in the recruitment of macrophages to liver, local inflammation, induction of insulin resistance, neuropathic pain and

chemoattractant functions (Lee, Cheng et al. 2003; Moore, Murdock et al. 2003; Burnstock 2009; Kobayashi, Yamanaka et al. 2012; Kobayashi, Yamanaka et al. 2013).

Agonists and antagonists

The P2Y₁₄ receptor can be activated by UDP-glucose, UDP-galactose, UDP-glucuronic acid, and UDP-*N*-acetylglucosamine (Burnstock 2009; Burnstock, Fredholm et al. 2010). MRS2690 is a 7-fold more potent agonist ($EC_{50} \approx 0.049 \mu\text{M}$) at the P2Y₁₄ receptor than UDP-glucose ($EC_{50} \approx 0.35 \mu\text{M}$), and is inactive at the P2Y₂ receptor (Ko, Fricks et al. 2007). Moreover, MRS2802 is shown to fully activate the human P2Y₁₄ receptor with an EC_{50} of $0.063 \mu\text{M}$, but it is inactive at the P2Y₆ receptor (Das, Ko et al. 2010). To the date, a study has shown that UDP acts an antagonist at the P2Y₁₄ receptor with an IC_{50} of $\sim 50 \text{ nM}$ (Fricks, Maddileti et al. 2008).

1.3.4 Store-operated calcium channels

As discussed above in section 1.3.3, activation of several P2Y receptors leads to cause Ca^{2+} release from the ER store (Figure 1.4) (Berridge 1993; Berridge, Bootman et al. 2003). Subsequently, the depletion of the Ca^{2+} store activates Ca^{2+} entry through the plasma membrane, a process commonly referred to as store-operated Ca^{2+} (SOC) entry (Lewis and Cahalan 1989; Zweifach and Lewis 1993). While, the Ca^{2+} currents passing through the plasma membrane via the SOC channels is well characterized electrophysiologically, termed Ca^{2+} release-activated Ca^{2+} (CRAC) currents (Hoth and Penner 1992; Hoth and Penner 1993). Experimentally, the depletion of the ER Ca^{2+} store can be evoked by reagents such as thapsigargin (TG, a sarco/endoplasmic Ca^{2+} -ATPase (SERCA) pump inhibitor), ionomycin (a Ca^{2+} ionophore), EGTA and TPEN (Ca^{2+} chelators) (Parekh and Putney 2005; Lewis 2011).

A Stim1



B Orai1

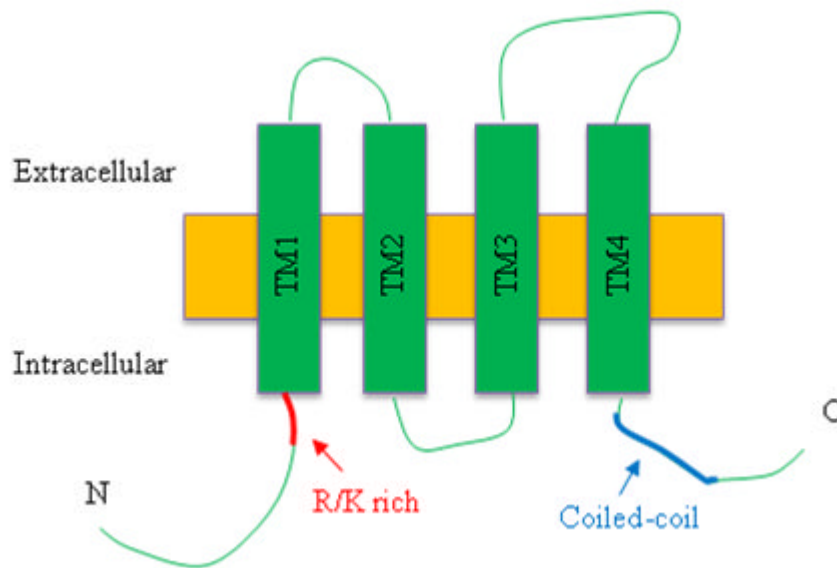


Figure 1.3 The structural features of Stim1 and Orai1.

(A) Stim1 is a single-transmembrane protein. The N terminus is directed to the lumen of the ER and contains an EF-hand domain, a Ca^{2+} sensor, followed by a sterile α -motif (SAM, a protein interaction domain) and the transmembrane (TM) domain. In the C terminus, within the coiled-coil domain, there is a Stim-Orai activating region (SOAR) involved in activation of the Orai1 channels, followed by a fast inactivation (FI) domain, a regulatory domain (potential phosphorylation sites that regulate Stim1 function) and a lysine-rich domain (K-rich, that may contribute to Stim1 localization in near-membrane puncta (see Figure 1.4) by interacting with the plasma membrane acidic lipids). (B) The single Orai1 channel subunit contains four transmembrane domains (TM1-4) with the α -helical TM1 lining the ion-conducting pore. An arginine/lysine-rich (R/K-rich) region in the N-terminus and the coiled-coil in the C-terminus are involved in coupling Orai1 to Stim1 (Putney 2010; Lewis 2011).

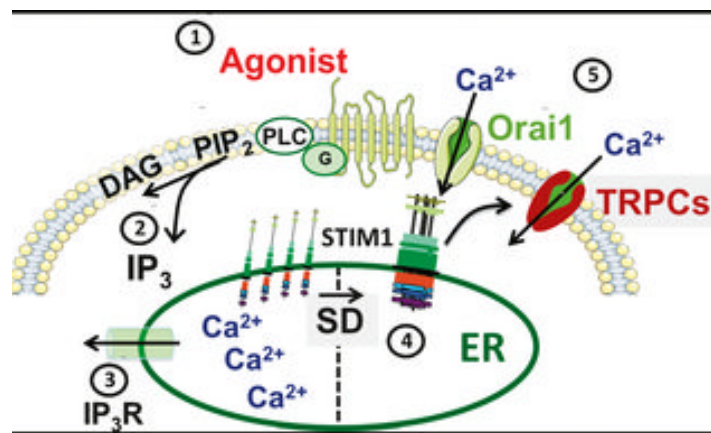


Figure 1.4 Store-operated Ca²⁺ entry (SOCE) pathways.

As depicted, SOCE is mediated by multiple sequential steps: (1) Binding of a variety of physiological agonists to their specific G-protein-coupled receptors results in activation of phospholipase C (PLC) leading to generation of the second messengers IP₃, and 1,2-diacylglycerol (DAG). (2) Diffusible IP₃ binds to the IP₃ receptors in the membrane of the ER to cause Ca²⁺ release and subsequent store depletion (SD). (3) The Ca²⁺ store depletion is sensed by the ER-resident Stim1 proteins. (4) Dissociation of Ca²⁺ from Stim1 results in Stim1 oligomerization into punctate structures and translocation to the junctional ER regions in close apposition with the plasma membrane. (5) Physical interactions between the C-terminus of Stim1 and C- and N-termini of plasma membrane Orai1 protein results in Ca²⁺ entry. Ca²⁺-permeable TRPC channels have been also proposed to act as SOC channels and are regulated by electrostatic interactions with Stim1 (Trebak, Zhang et al. 2013).

The SOCE pathway has been known for decades but our understanding at a molecular level remained elusive until the identification of ER Ca^{2+} -sensing protein Stim1 (stromal interaction molecule 1) in 2005 (Liou, Kim et al. 2005; Zhang, Yu et al. 2005) and plasma membrane protein Orai1 or Ca^{2+} release-activated Ca^{2+} modulator 1 (CRACM1) in 2006 (Feske, Prakriya et al. 2005; Feske, Gwack et al. 2006). So far, the ER Ca^{2+} -sensing protein family comprises Stim1 and Stim2 (Dziadek and Johnstone 2007), while the Orai protein family consists of Orai1, Orai2 and Orai3 (Yeromin, Zhang et al. 2006; Dziadek and Johnstone 2007). The Stim proteins are single transmembrane proteins (Fig. 1.3A) that are localized in the ER; their N-termini are directed to the lumen of the ER and contain an EF-hand Ca^{2+} binding domain. The Orai proteins consist of four transmembrane domains (TM1–TM4) with both C and N-termini residing in the cytoplasm (Fig.1.3B) (Fahrner, Muik et al. 2009). As illustrated in Figure 1.4, the depletion of the ER Ca^{2+} store causes Ca^{2+} to dissociate from Stim1, which results in Stim1 aggregation and movement to the closely apposed ER-plasma membrane junctions to physically interact with and thereby activate the Orai1 channels that mediate Ca^{2+} entry (Fahrner, Muik et al. 2009).

Besides the Orai proteins as the primary SOCs, a number of earlier studies suggested that the canonical transient receptor potential (TRPC) channels also act as SOC channels (Yuan, Kim et al. 2009; Lee, Yuan et al. 2010; Yuan, Lee et al. 2012). TRPC channels belong to the mammalian transient receptor potential (TRP) channel family with 28 members that contain other 5 subfamilies: TRPA (ankyrin-like), TRPM (melastatin), TRPML (mucolipin), TRPP (polycystin), and TRPV (vanilloid) (Ramsey, Delling et al. 2006). They are non-selective cation channels and are composed of six transmembrane domains (S1-S6) with a pore loop between the S5 and S6 (Ramsey, Delling et al. 2006). The TRP channels play an important role in mediating vision, taste, olfaction, hearing, touch and temperature (Venkatachalam and Montell 2007; Latorre, Zaelzer et al. 2009; Huynh, Cohen et al. 2014; Premkumar 2014). The TRPC channels are Ca^{2+} -permeable and activated through PLC-coupled receptor activation, which indicates their possible roles in mediating the SOCE pathway (Ramsey, Delling et al. 2006; Trebak, Zhang et al. 2013). There is evidence to suggest that the TRPC1 (Ambudkar, Ong et al. 2007; Yuan, Zeng et al. 2007; Cheng, Liu et al. 2008; Zeng, Yuan et al. 2008; Yuan, Kim et al. 2009; Dragoni,

Laforenza et al. 2014), TRPC4 (Zeng, Yuan et al. 2008; Sours-Brothers, Ding et al. 2009) and TRPC5 (Ma, Peng et al. 2008) channels interact with Stim1. While the TRPC3 and TRPC6 do not interact directly with Stim1 (Ambudkar, Ong et al. 2007; Yuan, Zeng et al. 2007; Cheng, Liu et al. 2008; Zeng, Yuan et al. 2008; Yuan, Kim et al. 2009; Dragoni, Laforenza et al. 2014), they are regulated by Stim1 due to Stim1-dependent heteromultimerization of TRPC1/TRPC3 and TRPC4/TRPC6 (Ambudkar, Ong et al. 2007; Yuan, Zeng et al. 2007; Cheng, Liu et al. 2008; Zeng, Yuan et al. 2008; Yuan, Kim et al. 2009; Dragoni, Laforenza et al. 2014). Recent studies have further shown that Stim1 facilitates formation of the Orai1/TRPC1 complex to mediate the SOC activity (Cheng, Liu et al. 2008; Liao, Erxleben et al. 2008; Lee, Yuan et al. 2010). Moreover, it has been reported that knockdown of TRPC1 by short hairpin RNA (shRNA) (Li, Chen et al. 2012) or TRPC5 by small interfering RNA (siRNA) (Shin, Hong et al. 2010) reduced the SOCE in neural progenitor cells (NPCs), indicating TRPC1 or TRPC5 as a molecular constituent of the SOC channels. Despite these studies, whether TRPC channels are involved in the SOCE is still debated (DeHaven, Jones et al. 2009; Lewis 2011).

It is now clear that the SOC channels not only mediate replenishment of the ER Ca^{2+} stores but also are coupled to downstream signalling pathways and transcription factors including c-fos and Nuclear Factor for Activated T cells (NFAT) (Trebak, Zhang et al. 2013; Xie, Xu et al. 2014). Described below are the main distribution and function, activators and inhibitors of the SOC channels.

1.3.4.1 Distribution and function

The SOC channels are now known to be present in almost all cells, including neurons, skeletal muscles and non-excitabile cells (Parekh and Putney 2005; Lewis 2011). Recent studies have revealed that Stim and Orai play important roles in the immune system, skeletal muscles, platelets, sweat glands, teeth and breast cancer cells (Lewis 2011; Trebak, Zhang et al. 2013). For example, previous studies reported that Stim1 and Orai1 were involved in cell migration and metastasis of breast cancer cells (Yang, Zhang et al. 2009; Hu, Qin et al. 2011). Orai3 channel-mediated SOCE has been also recently shown to be expressed in estrogen

receptor α -expressing (ER α (+)) breast cancer cells and to mediate cell tumorigenesis (Motiani, Zhang et al. 2013).

1.3.4.2 Activation

As mentioned above, the SOC channels are activated following the Ca²⁺ store depletion by activation of the IP₃ receptors, blockade of the SERCA pumps (e.g. TG, cyclopiazonic acid (CPA)) and use of a Ca²⁺ ionophore (e.g. ionomycin) (Putney 2010; Lewis 2011). Experimentally, 2-aminoethyldiphenyl borinate (2-APB) is widely considered as a small-molecular-weight activator for the SOC channels (DeHaven, Smyth et al. 2008; Putney 2010; Lewis 2011). 2-APB at low concentrations (3-20 μ M) potentiates, but at high concentrations (\geq 30 μ M) inhibits TG-mediated SOCE (DeHaven, Smyth et al. 2008; Putney 2010). Moreover, 2-APB is potent in activating the Orai1 channel at concentrations less than or equal to 20 μ M in cells co-expressing Orai1 and Stim1, and less potent in activating the Orai2 channel in cells co-expressing Orai2 and Stim1 (Lis, Peinelt et al. 2007; DeHaven, Smyth et al. 2008). Interestingly, 2-APB at higher concentrations (> 50 μ M) can evoke sustained currents in cells co-expressing Orai3 and Stim1 (Lis, Peinelt et al. 2007; DeHaven, Smyth et al. 2008). Furthermore, 2-APB can directly activate Orai3 without store depletion or co-expression of Stim1 (Lis, Peinelt et al. 2007; DeHaven, Smyth et al. 2008; Schindl, Bergsmann et al. 2008; Zhang, Kozak et al. 2008). Currently, one direct activator of the SOC channels is a peptide derived from the Orai-interacting domain of Stim1 (Putney 2010), which directly forms punctuate structures that move to the ER-plasma membrane junctions and activate the Orai channels without depletion of the Ca²⁺ store (Park, Hoover et al. 2009).

1.3.4.3 Inhibition

Experimentally, the SOC channels can be inhibited by La³⁺ and Gd³⁺ (Putney 2010; Dragoni, Laforenza et al. 2014). But, La³⁺ can also block voltage-gated sodium channels and Gd³⁺ is well known as an inhibitor of mechanosensitive ion channels (Tanaka, Tamba et al. 2002). Up to date, a number of agents (such as BTP-2, 2-APB, DPB162-AE, DPB163-AE, Synta66) are reported to block the SOC channels. BTP2 (YM-58483) has been shown to block the SOC channels with an IC₅₀ of \sim 10 nM, and displays \sim 31-fold greater selectivity over the voltage-dependent Ca²⁺ channels

(Zitt, Strauss et al. 2004; Ohga, Takezawa et al. 2008). Previous studies showed that 2-APB inhibited puncta formation of Stim1 at the plasma membrane, and subsequently blocked the SOC channels (DeHaven, Smyth et al. 2008; Peinelt, Lis et al. 2008). Additionally, 2-APB has been also reported to inhibit Orai1- and Orai2-mediated Ca^{2+} entry at high concentrations ($\geq 50 \mu\text{M}$) (Lis, Peinelt et al. 2007; DeHaven, Smyth et al. 2008). Two 2-APB analogues, DPB162-AE and DPB163-AE, have recently been reported; they are more potent and selective inhibitors for the Orai1 and Orai2 channels as compared to 2-APB (Goto, Suzuki et al. 2010). Synta66 (GSK1349571A) has been reported as a potent inhibitor of TG-induced SOCE (Li, Cubbon et al. 2011; Li, McKeown et al. 2011).

1.4 Extracellular ATP-evoked Ca^{2+} Signalling in Stem Cells

Several studies have shown that stem cell types release ATP constitutively, such as embryonic stem cells, hematopoietic stem cells, BM-MSCs, AT-MSCs, and DP-MSCs (Coppi, Pugliese et al. 2007; Burnstock and Ulrich 2011; Sun, Junger et al. 2013). Furthermore, it has been proposed that ATP is released via hemi-gap-junction channels in hBM-MSCs (Kawano, Otsu et al. 2006).

As described below, studies have provided increasing evidence to support the expression of the P2X, P2Y and SOC channels in stem cells. There is also emergent evidence to suggest the importance of ATP-induced purinergic signalling in stem cell functions (Coppi, Pugliese et al. 2007; Pedata, Melani et al. 2007; Burnstock and Ulrich 2011). A better understanding of ATP-induced purinergic signalling is interesting and potentially important in facilitating usage of stem cells for cell therapies and tissue regeneration.

1.4.1 Expression and function of the P2X receptors

Studies using RT-PCR, Western blotting and Ca^{2+} imaging show the expression of P2X1, P2X2, P2X3, P2X4, P2X6 and P2X7 receptors in undifferentiated pluripotent P19 murine embryonic carcinoma cells (Resende, Majumder et al. 2007; Resende, Britto et al. 2008; Yuahasi, Demasi et al. 2012). Additionally, the results from Ca^{2+}

imaging suggests that P2X4 receptor is the major receptor responsible for ATP-induced Ca^{2+} entry in undifferentiated P19 cells (Resende, Britto et al. 2008). RT-PCR analysis showed that all P2X receptors were expressed in human CD34^+ HSCs (Lemoli, Ferrari et al. 2004). The protein expression of P2X7 receptor in human CD34^+ HSCs was confirmed by Western blotting (Lemoli, Ferrari et al. 2004).

Expression of the P2X receptors in MSCs from several tissues (such as bone marrow, adipose tissue, skin biopsies) has been examined in recent studies. It has been shown that ATP-induced inward currents in BM-MSCs using patch-clamp recording (Coppi, Pugliese et al. 2007). It was also demonstrated that ATP increased intracellular Ca^{2+} levels in BM-MSCs (Ichikawa and Gemba 2009). More recent studies have reported that mRNAs for all the P2X receptors except P2X2 are expressed in BM-MSCs using RT-PCR (Ferrari, Gulinelli et al. 2011). In particular, it has been further demonstrated by Western blotting that the protein expression of P2X1, P2X4 and P2X7 receptors in BM-MSCs (Ferrari, Gulinelli et al. 2011; Sun, Junger et al. 2013). Up to date, the expression of the P2X receptors in dental pulp MSCs is still unknown, which will be one of the objectives of my study.

1.4.2 Roles of the P2X receptors

To date, a number of *in vitro* studies have shown that the P2X receptors play important roles in stem cell proliferation, migration, differentiation (Burnstock and Ulrich 2011; Glaser, Cappellari et al. 2012; Ulrich, Abbracchio et al. 2012; Scarfi 2014). The main proposed functional roles of ATP-sensitive P2 purinergic receptors in stem cells are summarized in Table 1.4, and will be discussed further in the next section.

1.4.2.1 Proliferation

A previous study demonstrated that ATP (10 μM) decreased by about 9% hBM-MSC proliferation using an Automated Coulter Counter (Coppi, Pugliese et al. 2007). In agreement, another study showed that treatment with ATP (1 mM) induced down-regulation of the genes required for cell proliferation in hBM-MSCs using

Affymetrix HG-U133 Plus 2 GeneChip array, and inhibited cell proliferation (Ferrari, Gulinelli et al. 2011).

It has been reported that stimulation of murine bone marrow-derived hematopoietic stem cells/progenitor cells with ATP at high concentrations (>1 mM) inhibited cell growth by driving cell death through the P2X7 receptors (Yoon, Lee et al. 2007). However, an early study showed using the 5-bromo-2-deoxyuridine (BrdU) incorporation assay that ATP (100 μ M) up-regulated cell proliferation of P19 embryonic carcinoma cells, which was inhibited by PPADS (10 μ M) (Resende, Britto et al. 2008). Similar results were reported by a more recent study, cell proliferation of mouse embryonic stem cells was inhibited by the specific P2X7 inhibitors KN62 (10 μ M) and A438079 (1 μ M) (Glaser, de Oliveira et al. 2014). Therefore, studies suggest that the P2X7 receptor might be involved in the regulation of the stem cell proliferation by ATP, with the effects being concentration-dependent.

1.4.2.2 Migration

There is evidence to suggest that the P2X receptors, such as P2X5, are involved in the modulation of cell migration (Greig, James et al. 2003). A recent study using Affymetrix HG-U133 Plus 2 GeneChip array has shown that genes required for cell migration were up-regulated in hBM-MSCs after treatment with ATP (1 mM) (Ferrari, Gulinelli et al. 2011). Moreover, ATP (1 mM) significantly enhanced cell migration of hBM-MSCs using a transwell assay. However, whether the P2X receptors are involved in ATP-induced BM-MSC migration is still unknown.

1.4.2.3 Differentiation

ATP has also been reported to modulate stem cell differentiation. ATP (0.1-100 μ M) increased the ALP activity, osteocalcin (OC) protein production, and formation of bone nodules assessed by Alizarin Red staining in hBM-MSCs, which was inhibited by reducing P2X7 receptor expression with P2X7-siRNA and/or inhibiting the P2X7 receptor using selective antagonist KN62 (0.1 μ M) (Sun, Junger et al. 2013), indicating that ATP activates the P2X7 receptor and downstream signalling

pathways to increase the osteogenic differentiation of MSCs. In addition, knockdown of the P2X7 receptor expression was reported to induce neuronal differentiation of Neuro-2a cells (Wu, Lin et al. 2009). Similarly, a more recent study has reported that suppression of the P2X7 receptor activity by KN62 (10 μ M) enhanced neuronal differentiation of embryonic stem cells (Glaser, de Oliveira et al. 2014). These studies suggest that the P2X7 receptor is involved in the regulation of stem cell differentiation by ATP.

1.4.3 Expression and function of the P2Y receptors

As discussed above, the P2Y receptors are expressed in many cells (Table 1.3). Studies were carried out to examine the expression of the P2Y receptors in MSCs from several tissues, such as adipose tissue, skin biopsies and bone marrow (Riddle, Taylor et al. 2007; Ichikawa and Gemba 2009; Ferrari, Gulinelli et al. 2011; Fruscione, Scarfi et al. 2011; Zippel, Limbach et al. 2012). Ferrari et al showed the mRNA expression of all the P2Y receptors in hBM-MSCs (Ferrari, Gulinelli et al. 2011). Studies further confirmed that the protein expression of the P2Y1, P2Y2 and P2Y11 receptors in the hBM-MSCs by immunostaining and Western blotting (Ichikawa and Gemba 2009).

The P2Y receptors are also expressed in other type of stem cells, such as P19 embryonic carcinoma cells, HSCs and hepatocellular carcinoma cells (as cancer stem cells) (Sainz and Heeschen 2013). The protein expression of the P2Y1, P2Y2, P2Y4, and P2Y6 receptors was detected in undifferentiated P19 embryonic carcinoma cells by immunostaining or Western blotting (Resende, Majumder et al. 2007). The mRNA expression of the P2Y1 and P2Y2 receptors was observed in HSCs by RT-PCR analysis, and the protein expression of the P2Y1 receptor was confirmed by Western blotting (Lemoli, Ferrari et al. 2004). Hepatocellular carcinoma cells were shown to express the P2Y2 and P2Y4 receptors by RT-PCR and Western blotting (Xie, Xu et al. 2014).

Table 1.4 Proposed function of ATP-sensitive P2 purinergic receptors in stem cells.

Receptors	Cells	Proposed functional roles	References
P2X7	ESCs	Cell proliferation	Glaser, de Oliveira et al. 2014
		Inhibition of neuronal differentiation	Glaser, de Oliveira et al. 2014
	HSCs	Active cell death at high ATP concentrations	Yoon, Lee et al. 2007
	BM-MSCs	ATP-increased osteogenic differentiation	Sun, Junger et al. 2013
	Neuro-2a cells	Inhibition of Neuronal differentiation	Wu, Lin et al. 2009
P2Y1	ESCs	ATP-increased cell proliferation	Resende, Britto et al. 2008
		ATP-induced neuronal differentiation	Resende, Britto et al. 2008
	HSCs	ATP-increased cell proliferation	Lemoli, Ferrari et al. 2004
	BM-MSCs	Inhibition of cell proliferation	Coppi, Pugliese et al. 2007
		ATP-increased adipogenic differentiation	Ciciarello, Zini et al. 2013
	AT-MSCs	Osteogenic differentiation	Zippel, Limbach et al. 2012
	Cancer stem cells	ATP-increased cell proliferation	Xie, Xu et al. 2014

Receptors	Cells	Proposed function	References
P2Y2	ESCs	ATP-induced cell proliferation	Resende, Britto et al. 2008
		ATP-induced neuronal differentiation	Resende, Britto et al. 2008
	HSCs	ATP-increased cell proliferation	Lemoli, Ferrari et al. 2004
		UTP-mediated cell migration	Lemoli, Ferrari et al. 2004
	BM-MSCs	NAD ⁺ -mediated cell migration	Fruscione, Scarfi et al. 2011
	AT-MSCs	Osteogenic differentiation	Zippel, Limbach et al. 2012
	Cancer stem cells	ATP-increased cell proliferation	Xie, Xu et al. 2014
ATP-mediated cell migration		Xie, Xu et al. 2014	
P2Y11	AT-MSCs	Adipogenic differentiation	Zippel, Limbach et al. 2012

1.4.4 Roles of the P2Y receptors

To date, several studies have shown that the ATP-sensitive P2Y receptors (P2Y1, P2Y2 and P2Y11) play important roles in stem cell proliferation, migration and differentiation (Table 1.4) (Burnstock and Ulrich 2011; Glaser, Cappellari et al. 2012; Scarfi 2014).

1.4.4.1 Proliferation

In an earlier study, BM-MSc proliferation was increased by ~26% by the P2 receptor generic antagonist PPADS (30 μ M) and ~12% by MRS2179 (10 μ M), a selective P2Y1 receptor antagonist (Coppi, Pugliese et al. 2007). In contrast, cell proliferation of undifferentiated P19 mouse embryonic carcinoma cells was reported to be increased by ATP (100 μ M), ADP (100 μ M) and UTP (100 μ M) using the BrdU-incorporation assay (Resende, Britto et al. 2008). Moreover, ATP or ADP-induced increase in cell proliferation was blocked by suramin (30 μ M) and PPADS (10 μ M), while UTP-induced cell proliferation was inhibited by suramin (30 μ M) but not PPADS (10 μ M). Since the P2Y11 receptor was not expressed in these cells (Resende, Majumder et al. 2007), the P2Y1 and P2Y2 receptors are thought to be involved in ATP-induced cell proliferation (Resende, Britto et al. 2008). Additionally, the P2Y1 and P2Y2 receptors were reported to be involved in cell proliferation of adult human (CD34⁺) HSCs stimulated by ATP (1-100 nM) (Lemoli, Ferrari et al. 2004). Knocking down the P2Y2 receptor inhibited (10 μ M) ATP-induced cell proliferation of hepatocellular carcinoma cells as assessed by MTT (methylthiazolotetrazolium) and BrdU-incorporation assays (Xie, Xu et al. 2014). These studies suggested that the P2Y1 and P2Y2 receptors are involved in the regulation of stem cell proliferation by ATP.

1.4.4.2 Migration

ATP has been reported to modulate hBM-MSc migration (Ferrari, Gulinelli et al. 2011). UTP at 10 μ M was also reported to increase cell migration of CD34⁺ HSCs using the transwell assays (Lemoli, Ferrari et al. 2004). Since the P2Y4 receptor was not expressed in CD34⁺ HSCs, the P2Y2 receptor is mainly involved in UTP-mediated cell migration (Lemoli, Ferrari et al. 2004). As shown using both

wound-healing and transwell migration assays, ATP at 20 μM induced cell migration of hepatocellular carcinoma cells, which was also inhibited by the P2Y2 receptor specific shRNA (Xie, Xu et al. 2014). The group of Fruscione (Fruscione, Scarfi et al. 2011) demonstrated that knockdown of the P2Y11 receptor with siRNA inhibited cell migration of hBM-MSCs induced by extracellular NAD^+ . In summary, these studies indicate that the ATP-sensitive P2Y2 and P2Y11 receptors are involved in the regulation of stem cell migration.

1.4.4.3 Differentiation

During neuronal differentiation of P19 EC cells, ATP (100 μM) increased gene mRNA and protein expression of nestin (a marker for neural progenitors) and neuron-specific enolase (a marker for neurons) by RT-PCR and Western blotting analysis respectively (Resende, Britto et al. 2008). Additionally, ATP-induced Ca^{2+} increase can be blocked by suramin (30 μM) and PPADS (10 μM). Due to the fact that P19 cells express the P2Y1 and P2Y2 not P2Y11 receptors, the P2Y1 and P2Y2 receptors are possibly involved in ATP-induced neuronal differentiation (Resende, Britto et al. 2008). Expression of the P2Y1 and P2Y2 receptors is down-regulated in osteogenic differentiation, while the P2Y11 is significantly up-regulated in adipogenic differentiation of AT-MSCs (Zippel, Limbach et al. 2012; Scarfi 2014). Recently, preincubation with 1 mM ATP for 24 hr improved lipid droplets formation and the expression level of $\text{PPAR}\gamma$ (an adipogenic master gene) in hBM-MSCs during adipogenic differentiation (Ciciarello, Zini et al. 2013). Such ATP-dependent $\text{PPAR}\gamma$ expression was decreased by MRS 2279 (a P2Y1 specific antagonist), not by MRS2768 (a P2Y2 agonist) (Ciciarello, Zini et al. 2013). These studies suggested that the P2Y1 and P2Y2 receptors might be involved in the regulation of stem cell neuronal differentiation and osteogenic differentiation, whereas the P2Y1 and P2Y11 receptors have a role in adipogenic differentiation.

1.4.5 Expression and function of the SOC channels

An early study reported that Ca^{2+} entry through activation of SOC channels by depletion the ER store with Ca^{2+} -ATPase blockers 10 μM CPA or 1 μM TG in hBM-MSCs (Kawano, Shoji et al. 2002). Recently, it has been shown that (20 μM)

ATP-induced Ca^{2+} entry was inhibited by 2-APB (30 μM) and specific shRNA for Stim1 in human hepatocellular carcinoma cells (Xie, Xu et al. 2014). Moreover, the SOC entry was inhibited by knockdown of STIM1, Orai1 or TRPC1 in adult neural progenitor cells (Li, Chen et al. 2012). In previous studies, five TRPC proteins (TRPC1, TRPC3, TRPC4, TRPC5, and TRPC6) were shown to be expressed in embryonic central nervous system by Western blotting (Strubing, Krapivinsky et al. 2003) and in neural progenitor cells by real-time RT-PCR analysis (Shin, Hong et al. 2010; Li, Chen et al. 2012).

1.4.6 Roles of the SOC channels

1.4.6.1 Proliferation

It has been demonstrated that the SOC channels inhibitor, 2-APB (30 μM) and knockdown of Stim1 expression using shRNA inhibited cell proliferation of hepatocellular carcinoma cells induced by ATP (10 μM) in the MTT (methylthiazoltetrazolium) and BrdU-incorporation assays (Xie, Xu et al. 2014). Another recent study has also shown that knockdown of Stim1, Orai1 by siRNA or TRPC1 by shRNA inhibited cell proliferation in adult neural progenitor cells using the BrdU-incorporation assay (Li, Chen et al. 2012). These studies suggest that the SOC channels are involved in the regulation of stem cell proliferation by ATP.

1.4.6.2 Migration

In a previous study, 2APB (30 μM) and knockdown of Stim1 were shown to inhibit cell migration of hepatocellular carcinoma cells induced by ATP (20 μM) using wound healing and transwell migration assays (Xie, Xu et al. 2014), suggesting that the SOC channels are involved in the regulation of stem cell migration by ATP.

1.4.6.3 Differentiation

To date, the role of the SOC channels has not been well defined in the differentiation of stem cells. A real-time RT-PCR analysis showed that the mRNA expression of TRPC1 and TRPC4 was down-regulated, while the mRNA expression of TRPC3, TRPC5, and TRPC6 was up-regulated during the neuronal differentiation of NPCs

(Shin, Hong et al. 2010). Particularly, the expression level of TRPC5 in differentiated neuronal cells was up-regulated by about 43-folds as compared to that in NPCs. Moreover, knockdown of TRPC5 by siRNA inhibited TG-stimulated SOC entry and induced NPCs to express nestin but not MAP2 (a mature neural cell marker) during neuronal differentiation, indicating that TRPC5 acts as a SOC channel and plays a key role in neuronal differentiation (Shin, Hong et al. 2010).

1.5 Aim and Objectives

As discussed above, there is strong evidence to support the great promise of using MSCs for tissue engineering and cell therapies. On the other hand, our understanding of the extracellular signalling molecules and intrinsic mechanisms that determine or regulate the MSCs functions is limited. ATP is an extracellular signalling molecule activating the P2X and P2Y receptors on the cell surface. P2X receptors are Ca^{2+} -permeable channels, and ATP-sensitive P2Y receptors are coupled to downstream signalling pathways that induce intracellular Ca^{2+} release from the ER, and depletion of the ER Ca^{2+} store in turn activates the SOC channels to mediate Ca^{2+} entry. It has well established these signalling molecules are important in mediating extracellular ATP-induced Ca^{2+} signalling mechanisms that determine functions of both excitable and non-excitable functional cells. However, our understanding of such signalling mechanisms in stem cells is just emerging but remains piecemeal. Therefore, the overall aim of the study presented in this thesis is to gain a better understanding of the ATP-induced effects on DP-MSC functions and the underlying molecular signalling mechanisms. The primary objectives of this study are as follows:

1. To isolate and characterize human dental pulp MSCs from different donors (chapter 3).
2. To determine the effects of extracellular ATP on cell proliferation, migration and differentiation (chapter 3).
3. To investigate the expression of ATP-sensitive P2X and P2Y receptors and their roles in mediating ATP-induced Ca^{2+} signalling (chapter 4).
4. To investigate the expression of the SOC channels and their roles in contributing ATP-induced Ca^{2+} signalling (chapter 5).
5. To determine the roles of P2X and P2Y receptors and SOC channels in the regulation by extracellular ATP of MSC proliferation, migration, differentiation (chapter 6).

Chapter 2

Materials and Methods

2.1 Materials

2.1.1 General materials

General chemicals or reagents are summarized in Table 2.1 and were purchased from Sigma unless otherwise indicated.

2.1.2 Solutions

Solutions are summarized in Table 2.2 and they were prepared with distilled water. Solutions for cell culture were sterilized by syringe filter (0.22 μm) or autoclaving.

2.2 Methods

2.2.1 Cell isolation and culture

Human MSCs were isolated from dental pulp of teeth (human molars) which were obtained from the Leeds Dental Institute Dental Clinic. The project has been approved by the Dental Research Ethics Committee (280211/LJ/60). The teeth from four donors (9, 21 and 32 years old, all female; 22 years old, male) were immersed in 70% (v:v) ethanol for 5 minutes. After removing the connective tissues by scalpel under sterile conditions, teeth were cracked into several parts (Figure 3.1). Pulp tissues were removed from the pulp chamber of the teeth and placed in a drop of phosphate-buffered saline (PBS) (Invitrogen/GIBCO) in a sterile Petri dish. The pulp tissues were minced into approximately 0.5 x 0.5 x 1 mm³ sized pieces using a sterile scalpel and transferred to a 15-ml tube with 2 ml of PBS containing 5 mg/ml collagenase P (Worthington Biochem, Freehold, NJ) for 45-60 minutes at 37°C and 5% CO₂ according to the size of the pulp pieces. Through the incubation the tube was removed and the contents were gently pipetted every 15 minutes. The reaction was stopped by adding 7 ml of DMEM with 10% heat-inactivated fetal bovine

serum (FBS) (Invitrogen) when pulp pieces were totally dispersed in the solutions. The cell suspension was then centrifuged at 200 x g for 10 minutes. The cell pellet was resuspended in 5 ml of Dulbecco's modified Eagle's medium (DMEM) (Invitrogen) supplemented with 20% (v: v) FBS, 2 mM L-glutamine, 100 units/ml penicillin and 100 µg/ml streptomycin (Biofluids, Rockville, MD). Single-cell suspension was obtained by passing the cells through a 70-µm cell strainer (BD Falcon™ California, USA). The cells were seeded into a T-25 (25 cm²) plastic tissue culture flask (BD Biosciences) and incubated in a humidified 5% CO₂ and 37°C air incubator (Heraeus HERAcell 240) with medium changes every 3-4 days until 90% confluency was reached. Cell growth was monitored everyday by examining under a light microscope (Olympus LH50A). The mesenchymal stromal cells were isolated based on their ability to adhere to the plastic surface of the culture flasks, while other non-adherent cells were removed by changing the growth medium. The adherent cells were grown to 90% confluency and were defined as passage zero (P0) cells. Later passages were named accordingly. All cell handling was carried out in a tissue culture hood (Wolf laboratories Aura-B6).

2.2.2 Cell subculture

When the cells reached around 90% confluency, they were subcultured as follows. Taking a T-75 (75cm²) flask as an example, after aspiration of the media, the cell monolayer was washed with 4 ml of PBS. Then 4 ml of 0.25% trypsin-EDTA solution (Invitrogen/GIBCO) was added to cover the cells and incubated at 37°C for 5-7 minutes to allow the cells to be dislodged from the bottom of the flask. Mixed with the same volume of growth medium, the detached cells were gently suspended. The detached cells were pelleted down by centrifuging at 1000 rotation per minute (rpm) for 5 minutes. The supernatant was aspirated and the cell pellet was resuspended in 3 ml of DMEM supplemented with 10% FBS. The number of cells per ml of the suspension was determined by a haemocytometer and seeded onto T25 or T75 fresh culture flasks (Greiner™) at a concentration of 1×10^4 cells/cm². Cell growth medium was replaced every 3-4 days until 90% confluency was reached. Cells within the fifth passage were used throughout the study.

Table 2.1 General chemical and reagents used.

Chemicals	Supplier
Ethanol	VWR International Poole, UK.
Phosphate-buffered saline (PBS)	Invitrogen, USA.
Collagenase P	Worthington Biochem, Freehold, NJ
Dulbecco's modified Eagle's medium (DMEM)	Invitrogen, USA.
Foetal bovine serum (FBS)	Invitrogen, USA.
L-glutamine	Sigma-Aldrich Ltd., UK.
Penicillin-streptomycin	Sigma-Aldrich Ltd., UK.
10× Trypsin-EDTA	Invitrogen, USA.
Dimethyl sulfoxide (DMSO)	Sigma-Aldrich Ltd., UK.
Sodium chloride	Fisher scientific, UK.
Potassium chloride	Fisher scientific, UK.
Calcium chloride solution	Sigma-Aldrich Ltd., USA
Magnesium chloride solution	Sigma-Aldrich Ltd., USA
N-(2-hydroxyethyl) piperazine-N'-(2-ethanulfonic acid) (HEPES)	Fisher scientific, UK.
Glucose	Fisher scientific, UK.
Ethylene diamine tetraacetic acid (EDTA)	Sigma-Aldrich Ltd., USA
Pluronic acid F-127	Invitrogen, USA.
Sodium hydroxide	Sigma-Aldrich Ltd., UK.
Agarose	Sigma-Aldrich Ltd., UK.
EtBr	Sigma-Aldrich Ltd., UK.
OPTI-MEM medium	Invitrogen, USA.
SYBR Green I Stain	Invitrogen, USA.
ATP	Sigma-Aldrich Ltd., UK.

$\alpha\beta$ meATP	Sigma-Aldrich Ltd., UK.
BzATP	Sigma-Aldrich Ltd., UK.
ADP	Sigma-Aldrich Ltd., UK.
UTP	Sigma-Aldrich Ltd., UK.
MRS4062	Tocris bioscience, UK
UDP	Sigma-Aldrich Ltd., UK.
PPADS	Tocris bioscience, UK
5-BDBD	Tocris bioscience, UK
AZ11645373	Sigma-Aldrich Ltd., UK.
Thapsigargin (TG)	Sigma-Aldrich Ltd., UK.
2-APB	Sigma-Aldrich Ltd., UK.
CGS15943	Tocris bioscience, UK

Table 2.2 Solutions and culture media used in the present study.

	For cell culture
Primary cell culture medium (only for Passage 0)	DMEM supplemented with 20% (v:v) FBS, 2 mM L-glutamine, 100 units/ml penicillin and 100 µg/ml streptomycin
Cell growth basal medium (BM)	DMEM was supplemented with 10% (v:v) FBS
	For FLEXstation
Extracellular Ca ²⁺ -containing solution (SBS) (in mM)	NaCl 147, KCl 2, CaCl ₂ 1.5 (or 7.5), MgCl ₂ 1, HEPES 10 and glucose 13, pH 7.3
Extracellular Ca ²⁺ -free solution (in mM)	NaCl 147, KCl 2, MgCl ₂ 1, HEPES 10, glucose 13 and EDTA 1. 147, pH 7.3
SBS-Fura-2/AM	2 µM Fura-2/AM and 0.1% pluronic acid in SBS
	For DNA preparation
10 mg/ml EtBr	Dissolved in TE buffer made of 10 mM Tris pH8.0, and 1 mM EDTA pH8.0
TAE buffer	40 mM Tris-Oac, 0.114% (v:v) glacial acetic acid, and 1 mM EDTA pH8.0
2% DNA agarose gel	2% (w:v) agarose dissolved in TAE buffer with EtBr (10 mg/ml)
6× DNA gel loading buffer	0.25% (w:v) bromopenol blue and 40% (w:v) sucrose, stored at 4°C
	Other
SYBR Green staining solution	0.1% SYBR Green I Stain in DMSO

Note: solutions which were generally used are summarized in this table, and some solutions which are not included are specified where they were applied.

2.2.3 Preparation of frozen cells

To prepare frozen cell stocks, cells were grown to reach a >90% confluency in T-75 flasks, and dislodged as described in section 2.2.2. The detached cells from each flask were then collected and resuspended in 1 ml of solution containing 90% FBS and 10% (v:v) DMSO, and were transferred into 2-ml cryostat vials. The vials were frozen at -80°C overnight and, on the next day were transferred into a liquid nitrogen cryostat.

2.2.4 Thawing and restoring frozen cells

Vials containing frozen cells were removed from a liquid nitrogen cryostat and quickly thawed by incubation at 37°C. The thawed cell suspension was transferred into a T-25 flask containing 5 ml of DMEM supplemented with 10% FBS. After incubation for 24 hours to allow the cells to attach the bottom of the flask, the growth medium was replaced with fresh basal growth medium. Cells were maintained at 37°C until they became confluent.

2.2.5 Colony-forming test

To assess the colony-forming capability, single cells were seeded into 6-well tissue culture plates (1×10^3 cells/well) and maintained in growth basal medium for 7 or 14 days with the medium changed every 3-4 days. At the end of 7 or 14 days, the cells were washed with PBS and fixed with 10% neutral buffered formalin (Sigma, UK) at room temperature for at least 30 minutes. The cells were then stained in Harris Hematoxylin staining solutions (VWR International) at room temperature for 2 minutes. The cells nuclei were stained blue-violet after extensively washing with distilled water to remove the staining solution. An aggregate of more than 50 cells in a small field was scored as one colony, and more than 100 cells in a large field as two colonies (Osathanon, Nowwarote et al. 2011). Colony-forming capability was determined by the number of colonies relative to the total number of seeded cells in each well (Ferrari, Gulinelli et al. 2011).

2.2.6 Flow cytometry

To confirm that hDP-MSCs maintain their phenotypic characteristics after growth in culture, cells were subjected to flow cytometry analysis. Cells were harvested as described in section 2.2.2 and suspended in 1 ml of flow cytometry staining buffer (PBS containing 0.5% (w:v) BSA and 2 mM EDTA) at a concentration of 1×10^7 cells/ml. The cell suspension was treated with 1mg/ml Fc receptor blocking solution (TruStain FcX™, Biolegend) at room temperature for 10 minutes. The cell suspension (1×10^6 cells) was transferred to 1.5-ml eppendorf tube and incubated at 4°C for 30 minutes with primary mouse anti-human antibodies: CD105-fluorescein isothiocyanate (FITC) (Biolegend), CD90-FITC (Biolegend), CD73-phycoerythrin (PE) (Biolegend), CD45-FITC (Biolegend), CD34-FITC (Biolegend), CD14-FITC (Biolegend), Isotype Control-FITC (Biolegend), Isotype Control-PE (Biolegend) and STRO-1 (Santa Cruz Biotechnology). After washing, cells were centrifuged at 2000 rpm for 5 minutes and resuspended in 400 µl of flow cytometry staining buffer. The cells labelled with the anti-STRO-1 antibody were then incubated with a secondary FITC-conjugated goat anti-mouse antibody (Invitrogen) at 4°C for 30 minutes in the dark and resuspended in 400 µl of flow cytometry staining buffer again after washing and centrifugation. Flow cytometry was performed using a FACSCalibur (BD Biosciences, San Diego, USA) and ten thousand events were recorded for each sample. The data were analyzed with Cell Quest software (BD Biosciences).

2.2.7 Osteogenic differentiation

Cells were harvested as described in section 2.2.2 and were seeded into 24-well plates with 4×10^4 cells/well. After incubation for 48 hours, cells were cultured for 2 weeks in osteogenic differentiation medium (ODM) containing 100 nM dexamethasone (Sigma-Aldrich) and 0.05 µM ascorbate-2-phosphate (Wako Chemicals, Richmond, VA, USA) in basal growth medium (BM). ATP from 0 µM to 300 µM was added into the culture medium and, in some experiments, after pretreatment with antagonists or inhibitors (CGS15943, AZ11645373, PPADS and 2-APB) for 30 minutes. The medium was replaced every 3 days. In some experiments, cells were transfected with siRNA for 48 hours and then cultured in BM or ODM, and transfected again with siRNA for 24 hours after 7 days during

osteogenesis and then cultured in BM or ODM. After 14 days, osteogenic differentiation was assessed using ALP staining (Sigma-Aldich, Fluka Chemie AG, Buchs, Switzerland), or determining the DNA content and ALP activity.

CGS15943, PPADS and 5-BDBD were prepared as 10 mM stock solutions in DMSO and were diluted in the culture medium to indicated final concentrations. All the other agonists or antagonists stock solutions were made in water or culture medium.

2.2.8 ALP staining assay

After 14 days in BM or ODM as described section 2.2.7, cells in each well were washed with PBS and fixed in 98% ethanol in a cold room for 10 minutes. Then, ethanol was removed and replaced by 4% (v:v) α -naphthol in distilled water containing 24 mg/ml of Fast violet. The cells were incubated at room temperature for 1 hour. After washing with distilled water, cells expressing ALP were stained in red and were visualized under a light microscope.

2.2.9 DNA content determination

After 14 days in BM or ODM as described section 2.2.7, cells were washed twice with PBS and 200 μ l of PBS containing 0.01% (v:v) Triton X-100 was added into each well. Cells were collected using a cell scraper and cells were lysed by freezing-thawing at -20 °C. The cell lysates were transferred to eppendroff tubes and centrifuged at 2000 rpm for 5 minutes to remove cellular debris. The resulting cell lysate (20 μ l) for each condition was transferred into 8 wells in a flat, clear bottom 96-well plate (Greiner Bio-One) which was used to determine the DNA content as well as the ALP activity. For each well, 80 μ l of TE buffer (Tris-EDTA buffer, containing 10 mM Tris-HCl and 1 mM EDTA, pH 8.0, Sigma) was added to make up a total volume of 100 μ l. DNA standard solutions in 100 μ l containing 0, 0.04, 0.2, 1, 1.5, 2 μ g/ml were transferred into 3 wells for each condition in the same 96-well plate. Then, an equivalent volume (100 μ l) of PicoGreen (Molecular Probes®, Invitrogen, Leiden), diluted at 1:200 in TE, was added into each well including the DNA standards and incubated for 5 minutes in the dark. The

fluorescence was measured using a fluorescence micro-plate reader (Varioskan™) with the excitation wavelength of 480 nm and the emission wavelength of 520 nm. The standard curves were constructed between the absorption values and DNA concentrations, and was linear ($R^2 \approx 0.99860$, $n/N = 2/6$). The DNA content ($\mu\text{g/ml}$) in the cell lysates was calculated from the standard curves.

2.2.10 ALP activity assay

The cell lysates (20 μl) prepared as described section 2.2.9 was also used to determine the ALP activity. The total volume was made up to 100 μl using p-Nitrophenol phosphate substrate (80 μl). An equivalent volume (100 μl) of ALP standard solutions ranging from 0, 10, 50, 100, 200 nmol/ml were transferred to 3 wells for each concentration in the same 96-well plate. The plate was incubated in the dark at 37°C for 60 minutes. The reaction was stopped by adding 100 μl of 1 M NaOH to each well including the standards. The optical density of the yellow product, para-nitrophenol, was determined by a VersaMax Microplate Reader (Varioskan™) at the wavelength of 405 nm. The standard curves were determined between the absorption values and ALP concentrations and were linear ($R^2 \approx 0.99587$, $n/N = 2/6$). The ALP concentration (nmol/ml) in each well was calculated from the standard curve. The ALP activity was expressed as the ALP amount (nmol) per μg DNA in each sample.

2.2.11 Adipogenic differentiation

Cells were harvested as described in section 2.2.2 and were seeded onto glass coverslips (BD Biosciences) in 24-well plates with 4×10^4 cells/well. After 48 hours, cells were cultured for 3 weeks in adipogenic differentiation medium (ADM) containing 0.5 mM isobutyl-methylxanthine (IBMX-Sigma-Aldrich), 10 μM dexamethasone (Sigma-Aldrich, Fluka Chemie AG, Buchs, Switzerland), 10 $\mu\text{g/ml}$ insulin (Invitrogen/GIBCO), and 200 μM indomethacin (Sigma-Aldrich) in BM. Cells were treated with ATP from 0 μM to 30 μM alone or after pretreatment with antagonists or inhibitors (CGS15943, AZ11645373, PPADS and 2-APB). The medium was replaced every 3 days. In some experiments, cells were transfected with siRNA for 48 hours and then cultured in ADM. Cells were transfected again

with siRNA for 24 hours after 9 days during induction of adipogenesis and then cultured in ADM. After 3 weeks, cells were stained with Oil Red O for detection of the fat droplets in adipocytes.

2.2.12 Oil red O staining

Oil red O staining was conducted as described by Perry (Perry, Zhou et al. 2008). After 3 weeks in BM or ADM as described section 2.2.11, cells were washed with PBS and fixed with 4% paraformaldehyde (PFA) at room temperature for at least 30 minutes. The cells were then washed with distilled water twice and incubate with 60% isopropanol in distilled water at room temperature for 5 minutes. After that, cells were stained for 15 minutes with 0.3% Oil red O, which was prepared by mixing 3 ml of 0.5% Oil red O (5mg/ml in isopropanol, Sigma) with 2 ml of distilled water and extensively washed with distilled water to remove the staining solution. The fat droplets were stained in red. For counting the cell number, cells were also stained by Harris Hematoxylin solution at room temperature for 2 minutes and nuclei were stained in blue-violet after extensively washing with distilled water to remove the staining solution. Stained cells were visualized under an Olympus inverted microscope and imaged five different fields in each well using a digital camera (Olympus 7 megapixel camera). Adipogenic differentiation was determined by the number of Oil red O-stained cells relative to the total number of cells in the same area. To distain cells, stained cells in each well were incubated with 100 μ l of isopropanol and rotated at room temperature for 15 minutes to distain red colour from the fat droplets. The distained isopropanol solutions (80 μ l) were transferred into a flat, clear bottom 96-well plate (Greiner Bio-One) and determined by a VersaMax Microplate Reader (Varioskan™) at the wavelength of 510 nm (Basseri, Lhotak et al. 2009; Xu, De Becker et al. 2010). The distained cells were washed with distilled water and the DNA content was determined as described section 2.2.9. Adipogenic differentiation was expressed as the OD₅₁₀ value per μ g/ml DNA in each sample.

2.2.13 Chondrogenic differentiation

Monolayer cells

Cells were harvested as described in section 2.2.2 and were seeded in 24-well plates with 4×10^4 cells/well for monolayer cell cultures. After 48 hours, cells were cultured for 3 weeks in chondrogenic differentiation medium (CDM) containing 0.1 μ M dexamethasone (Sigma, UK), 10 ng/mL TGF- β 3, 50 μ g/mL ascorbic acid 2-phosphate (Sigma, UK) and 1 \times insulin-transferrin-selenium supplement (ITS, Sigma) in BM. The medium was replaced every 3 days. After 3 weeks, monolayer cells were stained by Alcian blue staining.

Cell pellets

The cell suspension harvested as described in section 2.2.2 were also centrifuged in 14ml BD Falcon round bottom test tubes at 1100 rpm for 5 min to obtain cell pellets (1×10^6 cells/tube) for three-dimensional (3D) cell culture. Cell pellets were cultured in BM for 24 hours and then were encouraged to float freely for 48 hours by gentle shaking. Cell pellets were then cultured in CDM or BM for 3 weeks with the medium changed every 3 days. After 3 weeks, cell pellets were paraffin embedded, sectioned and stained with Alcian blue/Sirius red staining for the identification of glycosaminoglycans (GAG) and collagenous matrix.

2.2.14 Alcian blue staining for monolayer cells

Alcian blue dye stains sulfated proteoglycan in cartilage tissues to indicate cell chondrogenesis. Monolayer cells were washed with PBS and fixed with 10% neutral buffered formalin (Sigma, UK) at room temperature for at least 30 minutes. The cells were then washed with distilled water twice and incubate in 1% Alcian blue solution (in 3% acetic acid; Sigma) at room temperature for 30 minutes. After that, cells were washed with distilled water to remove the staining solution. Acid mucosubstances were stained in blue. In order to determine the total number of cells in each well, cells were stained with 1:100 (v:v) SYBR Green diluted in staining solution/water for 15 minutes in the dark. The nuclei were stained in green. Stained cells were visualized and imaged five different areas in each well under an Olympus inverted fluorescence microscope (Olympus IX51) using a digital camera (Olympus

7 megapixel camera). Chondrogenic differentiation was determined by comparing the density of blue colour, normalized by the total number of cells in each image.

2.2.15 Alcian blue/Sirius red staining for cell pellets

After 3 weeks, cell pellets were washed with PBS twice and fixed with 10% neutral buffered formalin (Sigma, UK) and a drop of 0.1% Nuclear Fast Red solution (0.1 g nuclear fast red in 100 ml of 5% aluminum sulphate in distilled water; Sigma) for at least 24 hours at room temperature before processing. Cell pellets were then placed in the embedding cassettes (Simport, Canada) with a metal lid and were processed in a tissue processor (Tissue-Tek VIP) for a 16-hour program. The processor is an automated machine which dehydrates the samples through a series of treatments with ethanol (50%, 70%, 90%, 100%, 100%, and 100%) for 1 hour each treatment, xylene (100%, 100%, and 100%) for 1.5 hour each time, and molten paraffin wax four times at 65°C. For embedding, the cell pellets were transferred onto a metal tissue-holding tray and fully covered with additional hot wax (65°C). The embedding cassette was then placed on top of the tray following addition of hot wax to the brim of the tray. After that, the tray was placed on the cold plate for overnight to make the wax completely solidified. Samples were then sectioned at 5 µm thickness using N35 blades (Surgipath, UK) on an Ultra microtome (Jung Biocut, UK) and the slices were placed and floated in water at 40°C. These slices were attached on to poly-L-lysine-coated slides (VWR, UK), after a drop of 20% ethanol was placed on the slice. The slides were incubated at 37°C for at least 16 hours for histological examination.

Paraffin embedded slices were de-waxed in xylene for 5 minutes, and were immersed in absolute alcohol twice for 5 minutes each time. After washing under tap water, the slices were stained with a mixed solution containing Weigart's haematoxylin A (Fisher scientific, UK) and B (Fisher scientific, UK) in a ratio of 1:1 for 10 minutes and rinsed with tap water for 10 minutes. Slides were stained with 1% Alcian blue in 3% acetic acid (Sigma) for 10 minutes, and washed with tap water for 1 minute, and were stained with 1% aqueous phosphomolybdic acid in distilled water (Fluka, UK) for 20 minutes and then washed in tap water for 1 minute. Sections were then stained with 0.1% Sirius red in saturated picric acid

(Fluka, UK) for 60 minutes. The sections were dehydrated through absolute alcohol twice for 5 minutes each time and immersed in xylene twice for 1 minute each time before mounting in dibutyl phthalate xylene (DPX). Stained slices were then visualized under an Olympus inverted light microscope (Olympus LH50A). Alcian blue binds to proteoglycans while the Sirius red stain binds to collagen types I, II and III (Lee, Choi et al. 2006).

2.2.16 Cell proliferation assays

The proliferation capacity of cells was measured using a XTT cell viability assay kit (Biotium). Cells were seeded at 5,000 cells/well into 4-6 wells of flat, clear bottom 96-well plates (Greiner Bio-One) for each condition. After 48 hours, the culture medium was replaced with fresh medium and cells were incubated with ATP at concentrations from 0, 0.3, 3, 30 to 300 μM in 5% CO_2 at 37°C for 72 hours in BM. The medium was replaced every 24 hours.

For the XTT cell viability assay, the activated-XTT solution was prepared by adding the activation reagent to the XTT solution (v:v = 1:50). Cells were washed twice with PBS and then incubated with 25 μl of the activated-XTT solution in 100 μl BM for 4 hours in the dark, including 3 control wells containing no cells as blank absorbance readings. The numbers of living cells were determined by measuring the absorbance at the wavelength of 475 nm and 650 nm by a spectrophotometer microplate reader (Varioskan™). The specific absorbance of the sample is expressed as follows:

$$\text{Specific Absorbance} = A_{475\text{nm}}(\text{Test}) - A_{650\text{nm}}(\text{Test}) - A_{475\text{nm}}(\text{Blank})$$

The cell proliferation was also examined by cell counting. In order to estimate the numbers of cells in 4-6 wells for each condition in the 96-well plates (Greiner Bio-One), cells with 98 μl / well BM were treated with 2 μl / well of SYBR Green staining solution (see Table 2.2) for 15 minutes in the dark. Stained cells were imaged at the same two areas of each well and counted by IncuCyte (Essen BioScience).

2.2.17 Cell migration assays

Cells were seeded at 40,000 cells/well in 96-well plates (Thermo Scientific) and incubated in a tissue incubator with 5% CO₂ at 37°C. After 48 hours, the 96-pin Wound Maker (Essen BioScience) was used to produce the wounds in all wells of a 96-well plate by gently removing cells from the confluent monolayer using an array of 96 pins. Cells were then washed with PBS twice to remove the detached cells and cultured in BM, before plates were placed in the IncuCyte. ATP at concentrations from 0, 3, 30 to 300 µM was added into 4-6 wells for each condition, or after cells were pretreated with antagonists or inhibitors (CGS15943, AZ11645373, PPADS and 2-APB) for 30 minutes. In order to count the number of cells migrating into the wound area in each well, cells in 98 µl/well BM were treated with 2 µl/well SYBR Green staining solution (see Table 2.2) for 15 minutes in the dark at 24, 48 or 72 hours. Cells in each well were imaged by IncuCyte. Cell migration was determined by counting the number of cells migrating into the wound area relative to the cell density in the adjacent and healthy area in each well. The values obtained were expressed as percentage of relative cell migration.

Cell migration was more closely examined by measuring the width of the wound area that is reduced as cells migrate into the wound area. The 96-well cell migration software (Essen BioScience) was set to scan the wells to measure the wound width every hour. The wound width by obtained automatically using the cell migration software is the average distance from 924 random lines of resolution between the edges of the scratch wound within an image, and the migration distance at a given time is the difference between the initial wound width (at time 0) and wound width at that time (24 hours, as illustrated in Figure 3.6A). The migration distance was collected every hour and the migration time courses were obtained. The areas covered by the time course curves are calculated and the migration is expressed as percentage of the area for control cells (no treatment with ATP).

2.2.18 Measurements of the intracellular Ca²⁺ levels

The changes in the intracellular Ca²⁺ levels ([Ca²⁺]_i) were measured using both single cell Ca²⁺ imaging and FLEXstation. Cell suspension was harvested as

described in section 2.2.2. Cells were then seeded on type I collagen-coated coverslips placed in 24-well plates (Greiner Bio-one) at a density of 2×10^3 cells/cm² for single cell Ca²⁺ imaging and in 96-well assay plates (black and µclear, Greiner Bio-one GmbH,) at 40,000 cells/well for FLEXstation.

After 48 hours, cells were washed with PBS and incubated with 4 µM Fura-2/AM (Molecular Probes) and 0.4% pluronic acid in standard bath solution (SBS, see Table 2.2) at 37°C for 1 hour in the dark. Then, the cells were extensively washed twice in SBS in the dark. After incubation at 37°C for 30 minutes in SBS, cells were washed and replaced with fresh SBS or extracellular Ca²⁺-free solution (see Table 2.2). Both extracellular Ca²⁺-containing and Ca²⁺-free solutions were adjusted to pH 7.4 with 4 M NaOH. All agonists or antagonists stock solutions were diluted in the extracellular solutions to the indicated final concentrations. Cells were pretreated with antagonists or inhibitors (PPADS, 5-BDBD, AZ11645373, 2-APB and Synta66) before treatment with ATP. Synta66 (GSK1349571A) was obtained as a gift from Prof David J. Beech (University of Leeds).

For single cell Ca²⁺ imaging, a coverslip with cells were placed in a chamber which was fixed onto the microscope (Axiovert S100 TV, Zeiss). Cells were perfused with the SBS or extracellular Ca²⁺-free solution. Individual cells in one field were selected to be measured as well as the background region. After the recording started, images were acquired by exciting the cells at 340 nm and 380 nm every 10 seconds.

For the FLEXstation experiments, a 96-well U-bottomed compound plate (Greiner Bio-one) was prepared in advance with the correct layout, concentrations, and volumes of solutions (up to 250 µl each well). Then the cell assay plate, the compound plate and pipette tips were loaded into the FLEXstation (FLEXstation II 384, Molecular Devices), setting up and running the experiments using FLEXstation software Softmax Pro (Molecular Devices). The FLEXstation uses tips to transfer compounds from the compound plate to designated wells in the cell assay plate. 40 or 50 µl of compounds at 5× working concentrations were added to wells (for cells

containing 160 μl or 200 μl of $1\times$ working concentrations) in the assay plate (final volume each well is 200 μl or 250 μl). ATP or other P2 receptor agonists were applied after 60 seconds to establish the baseline. In the experiments examining P2 receptor antagonists, cells were treated for 300 seconds before agonist application. Intracellular Ca^{2+} levels were monitored by measuring the ratio of fluorescence intensity at emission of 510 nm alternatively excited by 340 nm and 380 nm (F_{340}/F_{380}).

Data analysis was carried out using OriginPro 8.0. The receptor agonist concentration–response curve was least squared fit to the Hill equation:

$$\Delta F_{340}/F_{380} = \Delta F_{340}/F_{380 \text{ max}} / (1 + (\text{EC}_{50}/ [\text{agonist}])^{n_H})$$

Where $\Delta F_{340}/F_{380}$ is the change in the ratio of fluorescent intensities (F_{340}/F_{380}) induced by the receptor agonist, $\Delta F_{340}/F_{380 \text{ max}}$ is the maximal change, EC_{50} is the receptor agonist concentration evoking half of the maximal change, and n_H is the Hill coefficient.

2.2.19 Real-time reverse transcription polymerase chain reaction (RT-PCR)

RNA was extracted from one T75 flask of cells for each condition. RNA extraction was carried out using the TRI reagents (Sigma) as follows. 75% ethanol solution was prepared using RNase-free water and cooled on ice. After removing the growth medium, cells were washed once in PBS, and treated with 1 ml of TRI reagent. The cell lysates were transferred to a 1.5-ml eppendorf and left on ice for 5 min. After adding 100 μl of bromochloropropane (BCP, Sigma) and vortexing thoroughly, cell lysates were left at room temperature for 15 minutes before centrifuging at 13,000 rpm at 4°C for 15 minutes. The top RNA-containing aqueous layer was carefully transferred into a fresh eppendorf, without disturbing the DNA in the middle white layer or protein in the bottom pink layer. After mixing thoroughly with an equal volume of ice cold isopropanol thoroughly for 15 minutes on ice, the RNA sample was centrifuged at 13,000 rpm at 4°C for 20 minutes. After the supernatant was removed, 750 μl of 75% ethanol solution was added. Followed by vortexing thoroughly and centrifuged at 13,000 rpm at 4°C for 5 minutes, ethanol was

removed. After air dried for about 5 minutes or all the ethanol was removed, the white and shiny RNA pellet was resuspended in 10 µl of RNase-free water. The RNA samples were subjected to DNase digestion or stored at -80°C.

DNase digestion of the RNA samples to remove the DNA contamination was performed as follows. The digestion was assembled by adding 3 µl of RQ1 RNase-free DNase enzyme and 1.3 µl of RQ1 RNase-free DNase 10× Reaction Buffer (Ambion) into 10 µl of the RNA sample and the mix was incubated at 37°C for 1 hour. After brief centrifugation using a bench centrifuge, 3 µl of Stop Reagent was added and left on ice for 2 minutes. Then the samples were subjected to the Ribogreen assay or were stored at -80°C after centrifugation for 1 minute.

The Ribogreen assay was carried out as follows to determine the RNA concentration. 10 µl of Ribogreen solutions (Invitrogen) (dilute at 1:200 in TE buffer) were mixed with 10 µl of the RNA sample (dilute at 1:100 in TE buffer) or TE buffer alone as blank control in capillaries. After centrifugation using the Light Cycler centrifuge, capillaries were loaded in the Light Cycler for F1 readings through running Real Time Fluorimeter by Light Cycler 3 computer program. The RNA concentration in the samples was estimated according to the following equation:

$$\text{RNA concentration } (\mu\text{g}/\mu\text{l}) = 0.2 \times [(\text{Ribogreen F1 reading} - \text{blank control}) + 0.2607] / 15.96$$

The RNA was reverse-transcribed into cDNA in a total reaction volume of 20 µl containing 0.6 µg of RNA sample and 4 µl of High Capacity RNA-to-cDNA Master Mix (Applied Biosystems). The same procedure was used for preparing No RT control with Master Mix without reverse transcriptase (Applied Biosystems). Reverse transcription was performed using a Mastercycler Gradient PCR machine (Eppendorf) with the following parameters (one cycle): 25°C for 5 minutes, 42°C for 30 minutes, 85°C for 5 minutes and holding at 4°C.

The cDNA samples were amplified using PCR and primers specific to the target genes as shown in Table 2.3. The PCR reaction samples in 5 μ l were made in the dark, containing 0.5 μ l of the cDNA sample, 2.9 μ l of H₂O, 0.6 μ l of 4 mM MgCl₂, 0.5 μ l of SYBR Green (Applied Biosystems), 0.25 μ l of 0.5 μ M forward primers and 0.25 μ l of 0.5 μ M reverse primers. The PCR protocols were composed of 95°C for 10 minutes, 45 cycles of 95°C for 10 seconds, 60°C for 6 seconds (55°C for Orai1, Orai2, Orai3, Stim1 and Stim2) and 72°C for 16 seconds, and a final melting step from 65°C to 95°C before the samples were maintained at 4°C (Li, Cubbon et al. 2011). The minimal cycle threshold values (Ct) were calculated from each of the quadruplicate reactions and the mean was obtained. The mRNA expression level for the gene under investigation was normalized to that of β -actin based on the following equation (Livak and Schmittgen 2001):

$$\text{Normalized expression} = 2^{[-(Ct_{\text{sample}} - Ct_{\beta\text{-actin}})]}$$

The difference in the relative gene expression fold after gene knockdown with siRNA (Time x), was calculated using the $2^{-\Delta\Delta Ct}$ method (Livak and Schmittgen 2001) relative to the gene expression level (Time 0, untreated control). The mean fold change in the expression of the target gene at each time point was calculated using following equation: $\Delta\Delta Ct = [(Ct_{\text{sample}} - Ct_{\beta\text{-actin}})_{\text{Time x}} - (Ct_{\text{sample}} - Ct_{\beta\text{-actin}})_{\text{Time 0}}]$.

The PCR products were analyzed by electrophoresis on 2% agarose gels. To prepare an agarose gel, the required amount of agarose was dissolved in TAE electrophoresis buffer by heating using a microwave oven until the solution appeared clear. After the agarose gel solution was cooled down to 50-60 °C, ethidium bromide (EtBr) (10 mg/ml) (Sigma) with the final concentration of 0.5 μ g/ml was added into agarose gel solution and mixed by gently swirling. The gel tray was prepared and the prepared agarose gel solution was poured carefully into it. The well-forming gel comb was inserted into the tray after removing air bubbles. The gel tray was left at room temperature for 1 hour for polymerisation of the agarose. Then, the comb was carefully removed from the gel and the tray was transferred into the gel tank covered with TAE buffer. Samples were prepared for gel loading by mixing 10 μ l of PCR products with 2 μ l of 6 \times gel loading buffer (Biolabs). The PCR samples were then transferred into the well of the gel merged in

running buffer in the tank. 0.5 μl of 100 bp DNA ladder (500 $\mu\text{g}/\text{ml}$, Biolabs) was mixed with 1 μl of 6 \times loading buffer and 4.5 μl of RNase-free water, and loaded along side with the PCR samples. The electrophoresis was run at 70 V for 60 minutes at room temperature. The DNA in the gel was visualized under the UV trans-illuminator. Gel images were captured with a Biorad Molecular Imager Gel Doc XR+ System (Biorad) and analyzed with Quantity One 1-D Analysis Software (Biorad). The size of PCR products was estimated based on the DNA ladders.

2.2.20 Transfection with siRNA

Cells were harvested as described in section 2.2.2 and seeded in 96-well plates for measurements of intracellular Ca^{2+} levels and migration tests, in 24-well plates for differentiation tests, or in 6-well plates for measurements of gene expression using RT-PCR. After 24 hours, cells were transfected with siRNA directed against targets or a negative siControl 1# (Ambion) (Table 2.4). For each transfection, 4 μl of siRNA (20 μM stock prepared in nuclease-free water) (Ambion) and 4 μl of LipofectamineTM 2000 (Invitrogen) was separately diluted in 200 μl of OPTI-MEM medium, and was incubated for 5 minutes at room temperature. Diluted siRNA and LipofectamineTM 2000 were mixed gently with a total volume of 400 μl and incubated for 20 minutes at room temperature. Cells in each well of 96-well plates were covered by 100 μl of the mixed transfection solution, 400 μl for cells in each well of 24-well plates, or 1 ml for cells in each well of 6-well plates. Cells were cultured for 48-72 hours before they were used in experiments. During the osteogenesis and adipogenesis study, cells were transfected twice with siRNA (see section 2.2.7 and 2.2.11).

2.2.21 Data analysis

All data are presented as mean \pm standard error of mean (S.E.M.), where appropriate, with n indicating the number of independent experiments and N indicating the number of wells of cells or cells from all preparations. Statistical analysis was performed using Student's unpaired t -test and one-way ANOVA (with Tukey post hoc test) by Origin software (Origin Lab Corporation, Northampton, MA, USA), with $p < 0.05$ being indicative of significance.

Table 2.3 Primers used for PCR.

Primer	Sequence (5'-3')	Expected Size
P2X1 forward primer	TTTCATCGTGACCCCGAAGCAG	633
P2X1 reverse primer	TCAAAGCGAATCCCAAACACC	
P2X2 forward primer	ACCTGCCCCGAGAGCATAAG	426
P2X2 reverse primer	AATGACCCCGATGACACCACCC	
P2X3 forward primer	CACCTCGGTCTTTGTCATCATCAC	695
P2X3 reverse primer	TGTTGAACTTGCCAGCATTC	
P2X4 forward primer	ACAGCAACGGAGTCTCAACAGG	561
P2X4 reverse primer	CCTTCCCAAACACAATGATGTCG	
P2X5 forward primer	AACCTGATTGTGACCCCAACC	683
P2X5 reverse primer	TCGCAGAAGAAAGCACCCCTTGC	
P2X6 forward primer	GGTGACCACTTCCTTGTGACG	476
P2X6 reverse primer	CCCAGTGA ACTCTGATGCCTACAG	
P2X7 forward primer	TGCGATGGACTTCACAGATTTG	465
P2X7 reverse primer	TGCCCTTCACTCTTCGGAAAC	
β -Actin forward primer	TTGAGACCTTCAACACCC	300
β -Actin reverse primer	TCTCTTGCTCGAAGTCC	
P2Y1 forward primer	CCGGCTGTCTACATCTTGGT	152
P2Y1 reverse primer	GGCAGAGTCAGCACGTACAA	

Primer	Sequence (5'-3')	Expected Size
P2Y2 forward primer	CCACCTGCCTTCTCACTAGC	163
P2Y2 reverse primer	TGGGAAATCTCAAGGACTGG	
P2Y4 forward primer	TGCCTGGTCACTCTTGTTG	205
P2Y4 reverse primer	GTACTCGGCAGTCAGCTTCC	
P2Y6 forward primer	CGACCACATGAGCTCCTACA	198
P2Y6 reverse primer	GAGCTTCTGGGTCCTGTGAG	
P2Y11 forward primer	AGGGCAAAGTGATGTTCCAC	175
P2Y11 reverse primer	CCCTCCAGGCTCTTCTTTCT	
Orai1 forward primer	GCACAATCTCAACTCGG	300
Orai1 reverse primer	GCGAAGACGATAAAGATCAG	
Orai2 forward primer	GCTGAGCTTAACGTGCCTATC	406
Orai2 reverse primer	GGAGTTCAGGTTGTGGATGTT	
Orai3 forward primer	CAAGGCATTGGTCTAGC	298
Orai3 reverse primer	AATTCAGTGTCAGAAGAGC	
Stim1 forward primer	CTCTCTTGACTCGCCA	276
Stim1 reverse primer	GCTTAGCAAGGTTGATCT	
Stim2 forward primer	TGGACCTCTAACACGC	351
Stim2 reverse primer	GCATACTGACGTCTACTCAA	

Table 2.4 siRNAs used.

siRNA	Sense (5'-3')	Ambion Catalogue No.
siP2X7	GCUUUGCUCUGGUGAGUGAtt	S9959
siP2Y1	GCCCUGAUCUUCUACUACUtt	S9962
siP2Y11	CACCCUAGGUGUUGCUGGAtt	S194676
siOrai1	GGGAAGAGGAUUUUUAUAAtt	34616
siOrai2	GACCAAAGUUUCCUCUUGtt	131489
siOrai3	CAUCCACAACCUCAACUCUtt	S41088
siStim1	GCAGAGUUUUGCCGAAUUGtt	138791
siStim2	GGAACGACACUUCCCAGGAtt	133273

Chapter 3

Effect of ATP on Cell Proliferation, Migration and Differentiation of Human Dental Pulp Mesenchymal Stem Cells

3.1 Introduction

Human DP-MSCs provide a promising stem cell source that can have possible clinical applications as cell therapy for regenerative medicine and dental tissue engineering due to the fact that they are easily available from teeth after extraction with very low morbidity and little ethical issues (Batouli, Miura et al. 2003; Yen and Sharpe 2006; Otaki, Ueshima et al. 2007). A clear understanding of extracellular signalling molecule and intrinsic mechanism that regulating proliferation, migration and differentiation of hDP-MSCs is expected to support better use in clinical applications. It has been demonstrated that hMSCs are strongly influenced by extracellular signalling molecules such as growth factors and extracellular matrix protein (Shi and Li 2008; Biver, Wang et al. 2013; Biver, Thouverey et al. 2014). As a signalling molecule, extracellular ATP has been shown to play a significant role in a diversity of cell functions, including proliferation, migration and differentiation in BM-MSCs (Coppi, Pugliese et al. 2007; Ferrari, Gulinelli et al. 2011; Sun, Junger et al. 2013), embryonic stem cells (Resende, Britto et al. 2008), hematopoietic stem cells (Lemoli, Ferrari et al. 2004), and neuronal progenitor stem cells (Wu, Lin et al. 2009). However, to date, the effects of extracellular ATP on such function of hDP-MSCs were unknown.

Therefore, the aim of the study described in this chapter was to investigate the effects of extracellular ATP on proliferation, migration and differentiation of hMSCs from dental pulp. The study started with characterization of hMSCs isolated from dental pulp in order to determine whether such cell preparations meet the minimal criteria for hMSCs (Dominici, Le Blanc et al. 2006), including plastic adherence, colony formation, specific surface marker expression and multipotent differentiation potential. Then, the effects of extracellular ATP on their proliferation,

migration, osteogenic differentiation and adipogenic differentiation under established *in vitro* differentiation conditions were determined.

3.2 Results

3.2.1 Isolation and characterization of cells

3.2.1.1 Isolation of cells from human dental pulp

Human MSCs were isolated from dental pulp tissues from 4 donors: 9F (9 years old, female), 21F (21 years old, female), 32F (32 years old, female) and 22M (22 years old, male). The donors frequently used in this study were female due to they were isolated earlier than the male donor. Figure 3.1A illustrates the dental pulp tissues in the pulp chamber from the donor 21F. Figure 3.1B shows one single cell adhering to the plastic bottom of a tissue culture flask following 4 days of culture. The cells (Passage [P] 0) proliferated and formed small colonies, called colony-forming units after incubation for 14 days (Figure 3.1C). Most of the cells exhibited the fibroblast-like and spindle-shaped morphology. These primary cells were subcultured when reaching 90% confluency. During their later passages (Passage 4), a majority of cells maintained such morphology (Figure 3.1D).

3.2.1.2 Formation of colony-forming units

The colony-forming unit-fibroblast (CFU-F) assay has been used as an important assay for the quality of MSCs to determine the incidence of clonogenic cell preparations (stem-like cells) after they are plated at a low density (Huang, Gronthos et al. 2009; Vemuri, Chase et al. 2011). P4 cultured cells were seeded at a low cell density (1×10^3 cells/well) in 6-well plates and the colony-forming efficiency was evaluated after 7 days. These cells became adherent onto the plastic surface and grew to form colonies that were composed of ≥ 50 cells identified upon staining in blue using Harris hematoxylin solution. The cells in the colonies, displayed typical fibroblast-like morphology and alignments in a similar direction (Figure 3.1E-G). Figure 2.1E and F show typical one single colony (Figure 3.1E) and two adjacent colonies (Figure 3.1F). There was 31.2 ± 1.2 colonies per 1000 cells from the donor 9F after 7 days in culture (Figure 3.1G). The ability to form CFU-F was also

examined for cells after storage at -80°C . There were 32.4 ± 1.8 colonies after 14 days in culture (Figure 3.1H). Similarly, there were 29.2 ± 1.4 colonies per 1000 cells after storage at -80°C from the donor 22M after 14 days in culture (Figure 3.1I). These results suggest that these cells from dental pulp were able to self-renew and form new cell population.

3.2.1.3 Expression of MSC positive and negative markers

To further characterize these cell preparations from the dental pulp, flow cytometry analysis was performed using well-known MSC positive and negative cell surface markers (Dominici, Le Blanc et al. 2006). A typical set of flow cytometry histograms from the donor 9F are shown in Figure 3.2, and the results from all 4 donors (9F, 21F, 22M and 32F) are summarized in Table 3.1. These cells exhibited strong expression of positive MSCs markers, such as CD105, CD90 and CD73, but no or very weak expression of negative MSC markers, such as hematopoietic lineage markers CD45, CD34, CD14. Furthermore, a substantial proportion of cells ($27.5 \pm 9.5\%$) also expressed STRO-1 (Table 3.1).

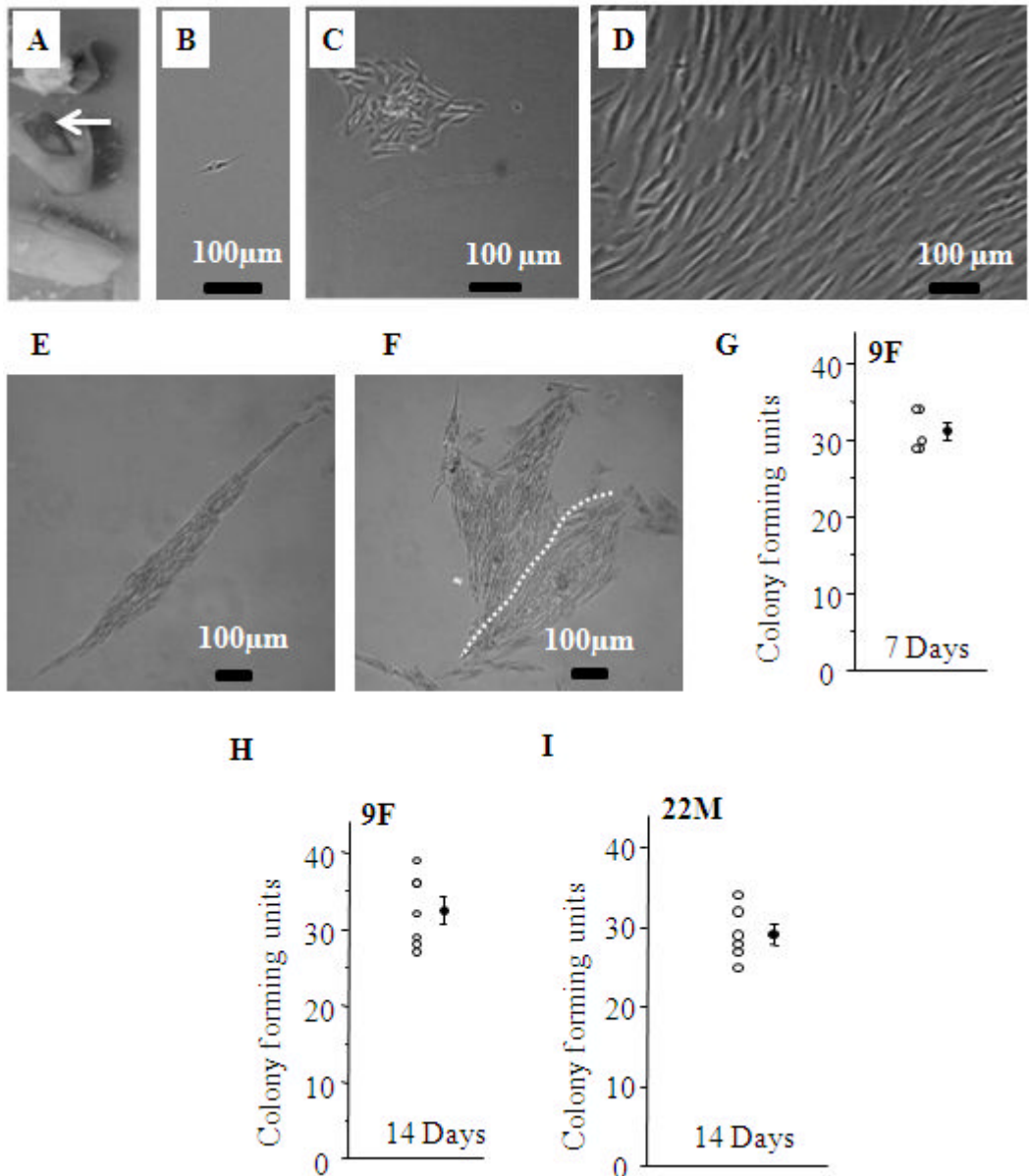


Figure 3.1 Isolation, morphology and colony-forming units of hDP-MSCs.

(A) Representative human dental pulp (white arrow, 21F). (B) Single primary hDP-MSC (P0) cultured for 4 days after treatment with collagenase P. (C) Representative primary hDP-MSCs (P0) cultured for 14 days. (D) Typical cultured hDP-MSCs (P4) cultured for 7 days. (E-I) Representative images are showing one (E) or two colonies (F) formed by hDP-MSCs (P4, 9F) after 7 days in culture. The number (open circle) and the average number (solid circle) of colony-forming unit per 1000 P4 cells prepared from the donor 9F after 7 days (G, N = 5) and 14 days (H, N = 6), and from the donor 22M after 14 days (I, N = 6) are shown.

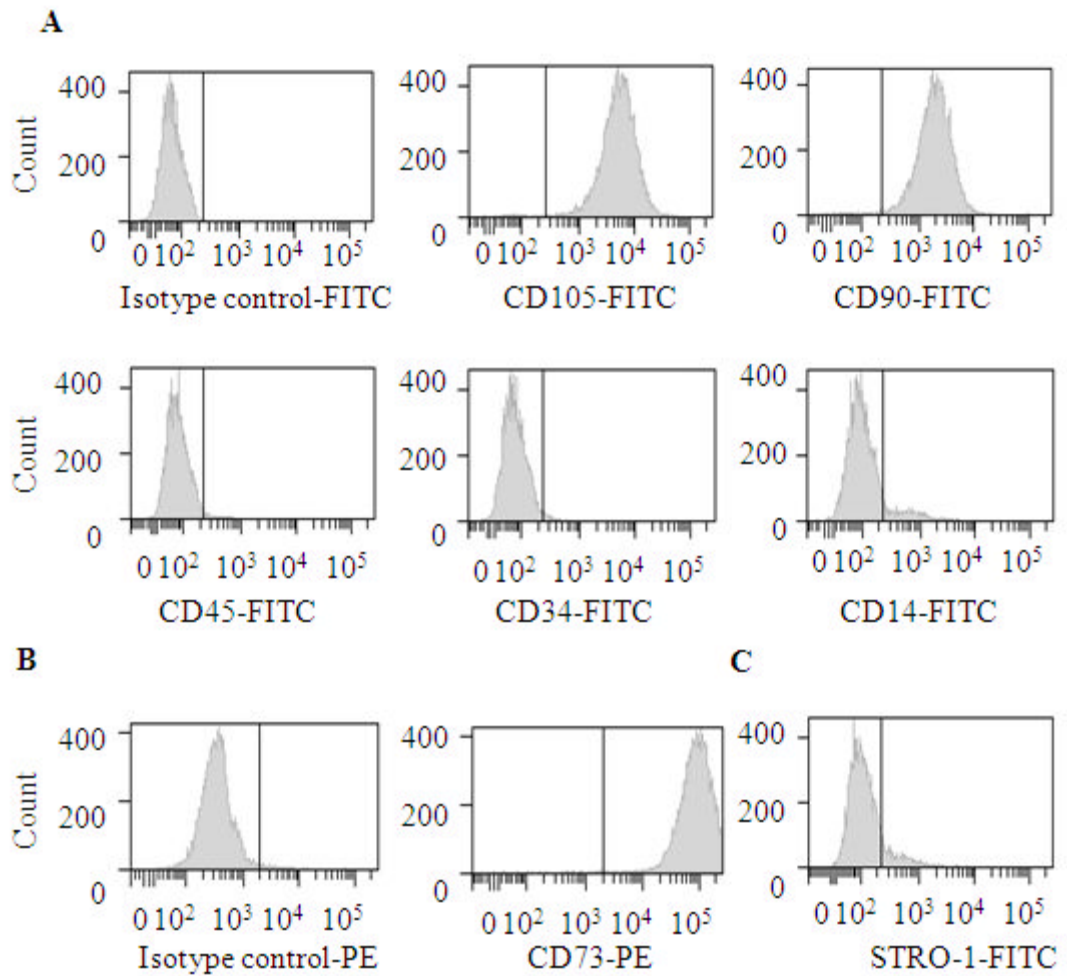


Figure 3.2 Flow cytometry analysis of expression of cell-surface markers in hDP-MSCs.

(A) Isotype control-FITC, CD105-FITC (98.5%), CD90-FITC (99.9%), CD45-FITC (1.3%), CD34-FITC (1.5%), and CD14-FITC (9.4%). (B) Isotype control-PE, CD73-PE (99.9%); (C) STRO-1-FITC (11.3%). P4 cells from the donor 9F were used.

Table 3.1 Summary of expression of cell surface markers in hDP-MSCs from four donors.

Donors Markers	9 Female (%)	21 Female (%)	22 Male (%)	32 Female (%)	Mean (%)	N
CD105	93.4 (2) ^a	40.9 (2)	60.1	51.9(4) ^a	59.6±7.0	9
CD90	99.9 (2) ^a	99.1	99.4	99.8	99.6±0.2	5
CD73	99.9 (2) ^a	98.6	99.8	93.4	98.3±1.3	5
CD45	1.2 (2) ^a	1.4	4.2	6.4	2.9±1.1	5
CD34	1.2 (2) ^a	0.9	12.5	0.4	3.2±2.3	5
CD14	8.1 (2) ^a	10.1 (2) ^a	3.6	8.9 (2) ^a	8.2±1.3	7
STRO-1	11.3	28.3	53.8	16.6	27.5±9.5	4

^aNote: mean values from two or four independent experiments.

3.2.1.4 Osteogenic, adipogenic and chondrogenic differentiation

To evaluate the multipotent differentiation capacity of these cells, they were induced using well-established *in vitro* osteogenic, adipogenic and chondrogenic differentiation media (Koyama, Okubo et al. 2009; Karaoz, Dogan et al. 2010). Representative results are shown in Figure 3.3. The osteogenic differentiation was examined by ALP staining. The cells cultured under osteogenic conditions displayed more extensive ALP staining as compared to the control cells or cells cultured under basal medium (Figure 3.3A-D), demonstrating osteogenic differentiation. The ALP expression was quantified by the ALP activity assay (see details in the section 2.2.10 in chapter 2).

To examine adipogenic differentiation, the cells were stained by Oil red O staining (Figure 3.3F-H). Red lipid droplets were discerned in cells cultured in adipogenic differentiation medium (ADM), but not in cells cultured in basal medium (BM). In addition, the cells cultured in ADM proliferated more slowly, and exhibited dramatic changes in their morphologies from a fibroblast-like shape to oval-like adipocyte one. These observations indicate differentiation into adipocytes.

To test chondrogenic differentiation, cells cultured in a monolayer were analyzed using Alcian blue staining (Figure 3.3I-L), and cells cultured in pellets by Alcian blue/Sirius red staining (Figure 3.3M-O). The monolayer cells were also stained by SYBR Green nucleus staining (Figure 3.3I and K). The cells cultured in chondrogenic differentiation medium had similar or less cell density as compared with the cells in basal medium (Figure 3.3I and K), but alcian blue staining of the cells cultured in chondrogenic differentiation medium (Figure 3.3L) was stronger as compared to that of the cells in basal medium (Figure 3.3J). Pellets cultured in the chondrogenic differentiation medium (Figure 3.3O) also showed stronger blue staining of proteoglycans by Alcian blue and less red staining of collagenous matrix formation by Sirius red compared to those in basal medium (Figure 3.3N), suggesting that the cells differentiated into chondrocytes.

3.2.2 Effects of extracellular ATP on cell proliferation

To examine the influence of extracellular ATP on cell proliferation, cells were cultured without or with ATP in different concentrations (0.3 μ M, 3 μ M, 30 μ M and 300 μ M) in BM for 72 hours and the number of cells was determined using the XTT assay. Cells from the donor 9F cultured in the absence and presence of ATP after 48 or 72 hours significantly increased in number compared with cells cultured for 24 and 48 hours (Figure 3.4A). However, there was no significant difference in percentage of cell proliferation among the different culture conditions (Figure 3.4B). The exception was that the cell proliferation was slightly reduced with ATP at 300 μ M at 48 hours (Figure 3.4B). Similar results were found for cells from the donor 21F (Figure 3.4C) and the donor 32F (Figure 3.4D). Overall, the results from all 3 donors show that ATP at the concentrations examined did not have any significant effect on cell proliferation (Figure 3.4E).

Such findings were observed using cell counting after SYBR Green staining of cells from the donor 9F. Figure 3.5A-C shows representative phase-contrast SYBR Green staining and merged images captured using IncuCyte. Typical SYBR Green staining images of cells cultured without or with ATP from 3 μ M to 300 μ M at 24, 48, 72 hours as shown in Figure 3.5D. The number of cells as indicated in the Figure 3.5D was counted and the results are presented in Figure 3.5E. The results show that the number of cells without or with ATP at 48 or 72 hours increased as compared to that at 24 hours (Figure 3.5E). However, there was no significant difference in cells cultured under the basal medium and basal medium containing different concentrations of ATP at 24, 48 and 72 hours (Figure 3.5F).

3.2.3 Effects of extracellular ATP on cell migration

To assess whether extracellular ATP affected cell migration, scratch wound healing assays were performed. Cells were stained by SYBR Green and captured by IncuCyte 24 hours after wounds were introduced, and the number of cells migrating into the wound area was counted in each image and corrected by the average cell density in the adjacent and healthy areas on both sides, resulting in the relative cell density (%) in the wound area (Figure 3.6A). Representative SYBR Green staining

images of cells cultured without or with ATP from 3 μM to 300 μM in the wound areas are shown in Figure 3.6B. The average relative cell density (%) is presented in Figure 3.6C, and the results after normalized to cells in the basal medium are shown in Figure 3.6D. While there was no difference in the migration between cells cultured in basal conditions and cells exposed to ATP at 3 μM (Figure 3.6D). ATP at 30 μM and 300 μM significantly increased the cell migration. Similar results were observed for cells from the donor 21F (Figure 3.6E) and the donor 32F (Figure 3.6F). The mean data from all 3 donors are shown in Figure 3.6G.

The wound areas are reduced or narrowed as cells migrate into and fill the wound areas (Figure 3.7A). The time course of migrated distance was measured using IncuCyte in the absence of ATP or in the presence of ATP at 3 μM and 30 μM for cells from the donor 9F are shown Figure 3.7 B. The migration areas at 24, 36 and 48 hours were calculated (see section-2.2.17 in chapter 2) and shown in Figure 3.7C, and further expressed as percentage of the migration area in the basal medium (Figure 3.7D). ATP at 3 μM did not change the cell migration area, whereas ATP at 30 μM significantly increased the cell migration at 24, 36 and 48 hours. Similar results were obtained for cells from the donor 21F (Figure 3.7E) and the donor 32F (Figure 3.7F). The mean data from all 3 donors are summarized in Figure 3.7G. Overall, these results are consistent with those from cell counting and support that ATP at 30 μM significantly promotes cell migration.

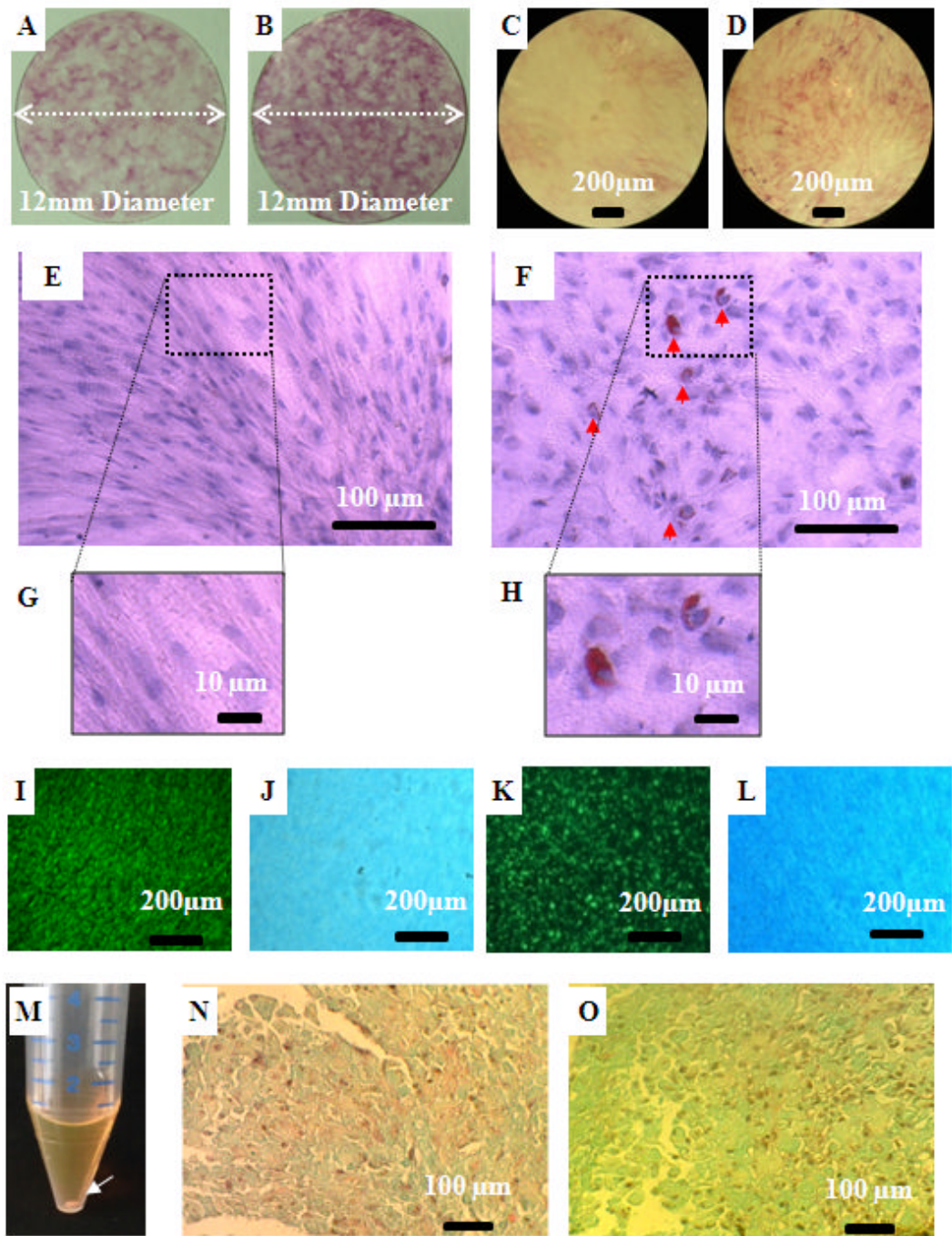
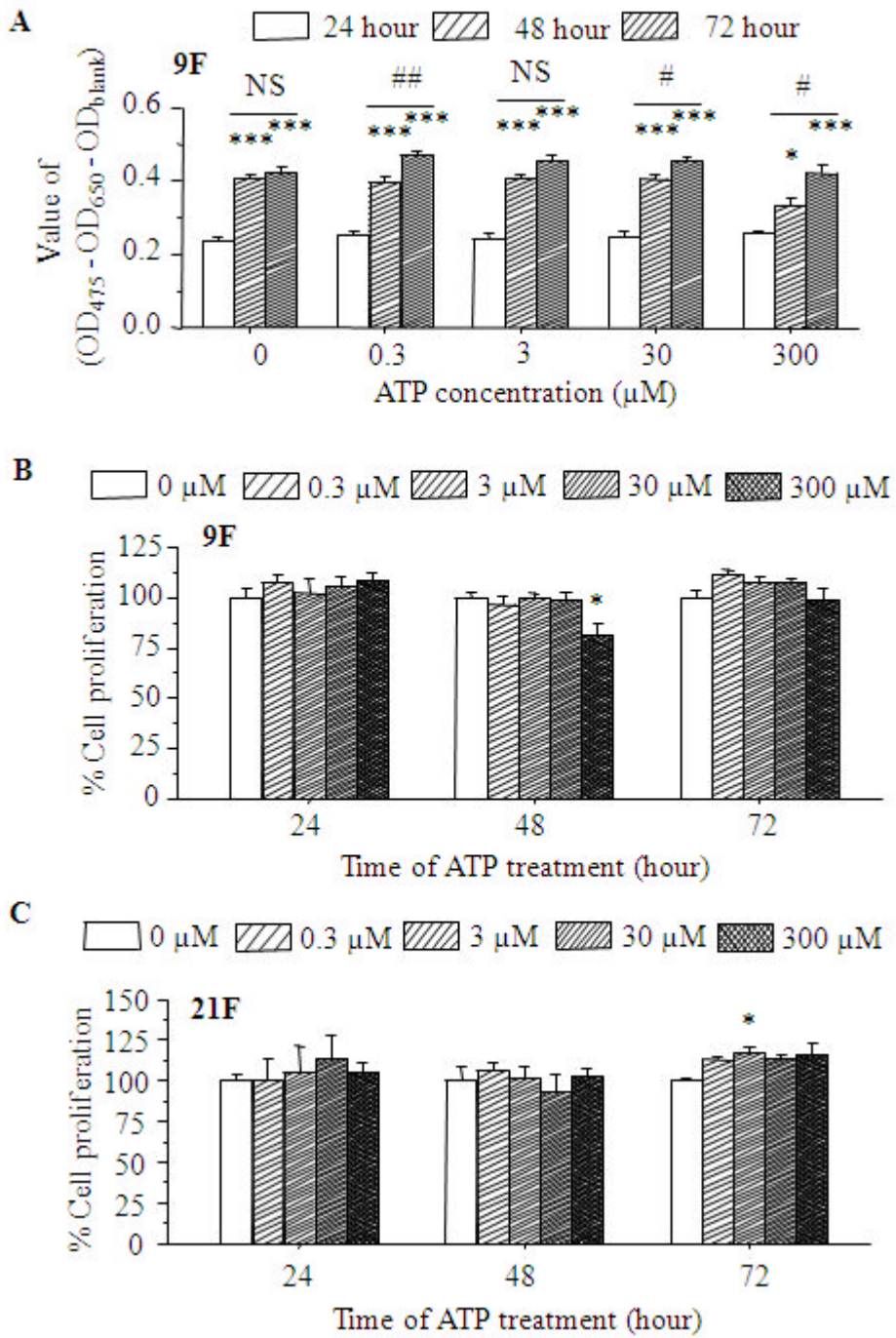


Figure 3.3 Differentiation potential of hDP-MSCs.

(A-D) ALP staining of hDP-MSCs (P4, 9F) cultured in the basal medium (A, C) and osteogenic differentiation medium (B, D). (E-H) Oil red O and Hematoxylin staining of hDP-MSCs cultured in the basal medium (E, G) and adipogenic differentiation medium (F, H). (K-J) SYBR Green and Alcian blue staining of hDP-MSCs cultured in the basal medium (I, J) and chondrogenic differentiation medium (K, L). (M-O) Alcian blue and Sirius red staining of hDP-MSCs pellets (M, chondrogenic differentiation medium) cultured in the basal medium (N) and chondrogenic differentiation medium (O).



(Figure 3.4)

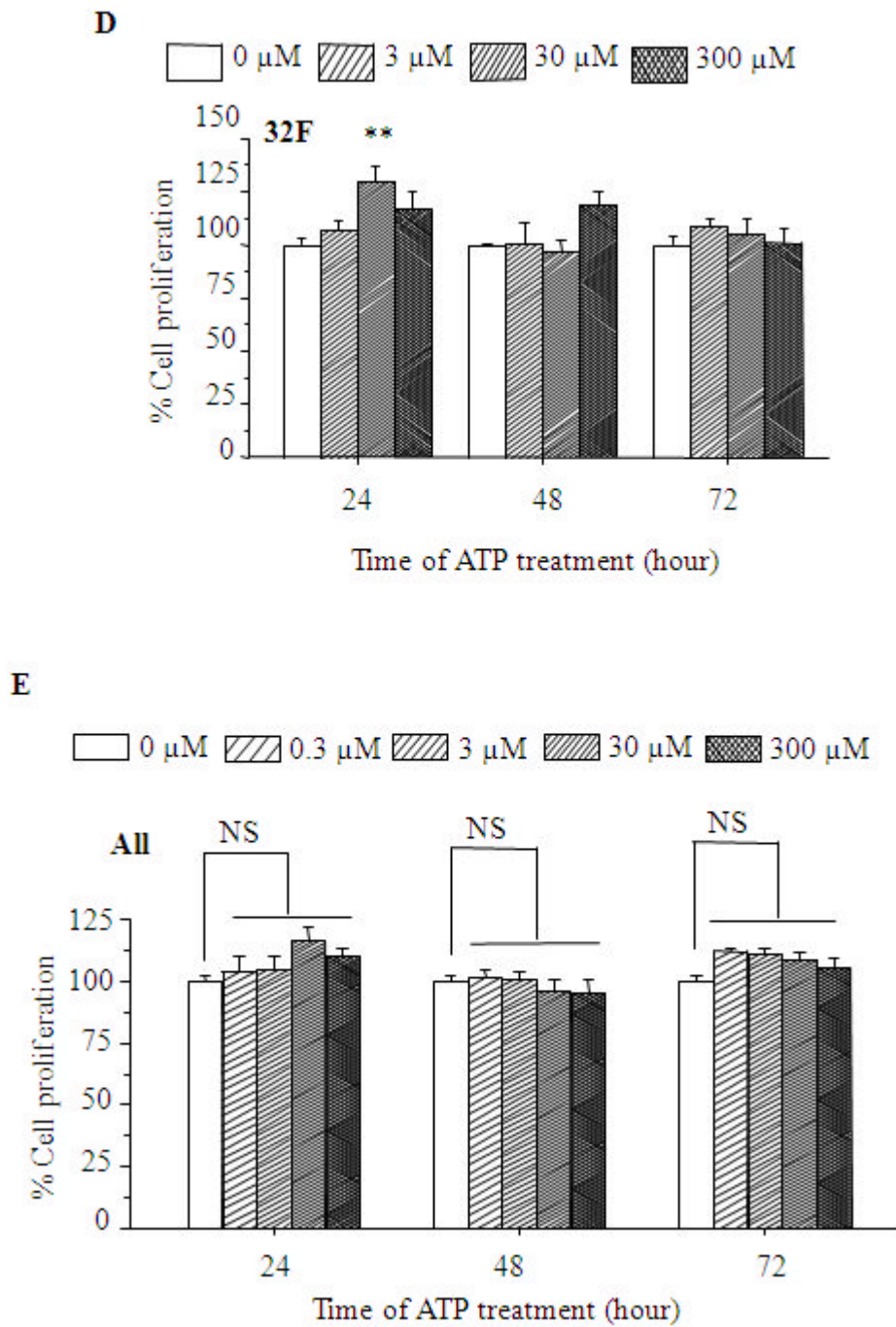
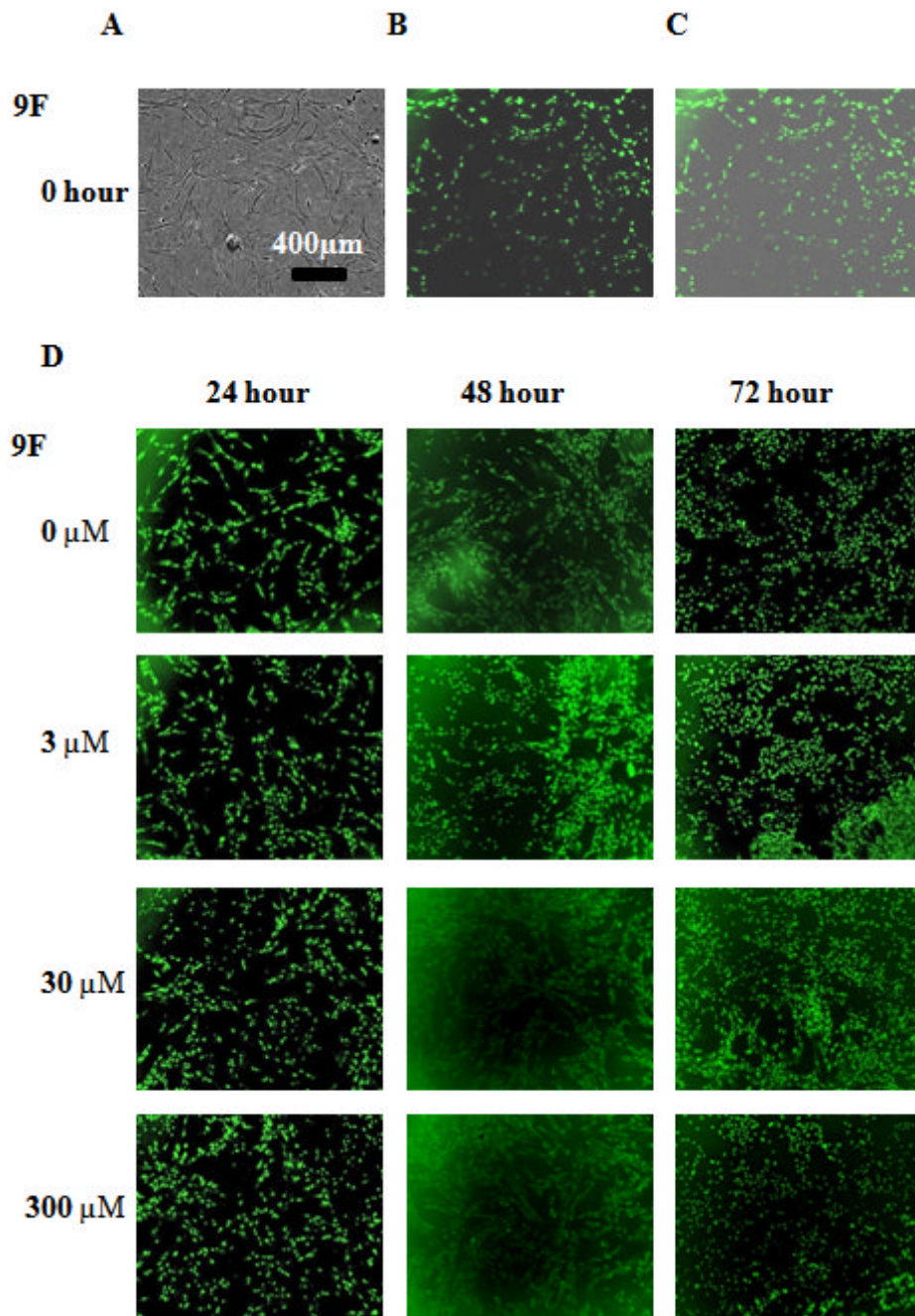


Figure 3.4 No effect of ATP on hDP-MSC proliferation by XTT assay.

(A-B) hDP-MSCs (P4, 9F) were cultured in basal medium without or with ATP from 0.3 μM to 300 μM for 24, 48 and 72 hours. The number of live cells are determined by the XTT assays and are presented as the OD value (A) and percentage of those in the basal medium alone (B), $N = 6$ wells. (C-E) The average percentage of cell proliferation in hDP-MSCs is shown: (C) 21F, P4, $N = 6$ wells; (D) 32F, P4, $N = 4$ wells; (E) 9F, 21F and 32F, $n/N = 3/16$. *, $p < 0.05$, **, $p < 0.01$, ***, $p < 0.001$; compared to the control (no ATP). #, $p < 0.05$, ##, $p < 0.01$.



(Figure 3.5)

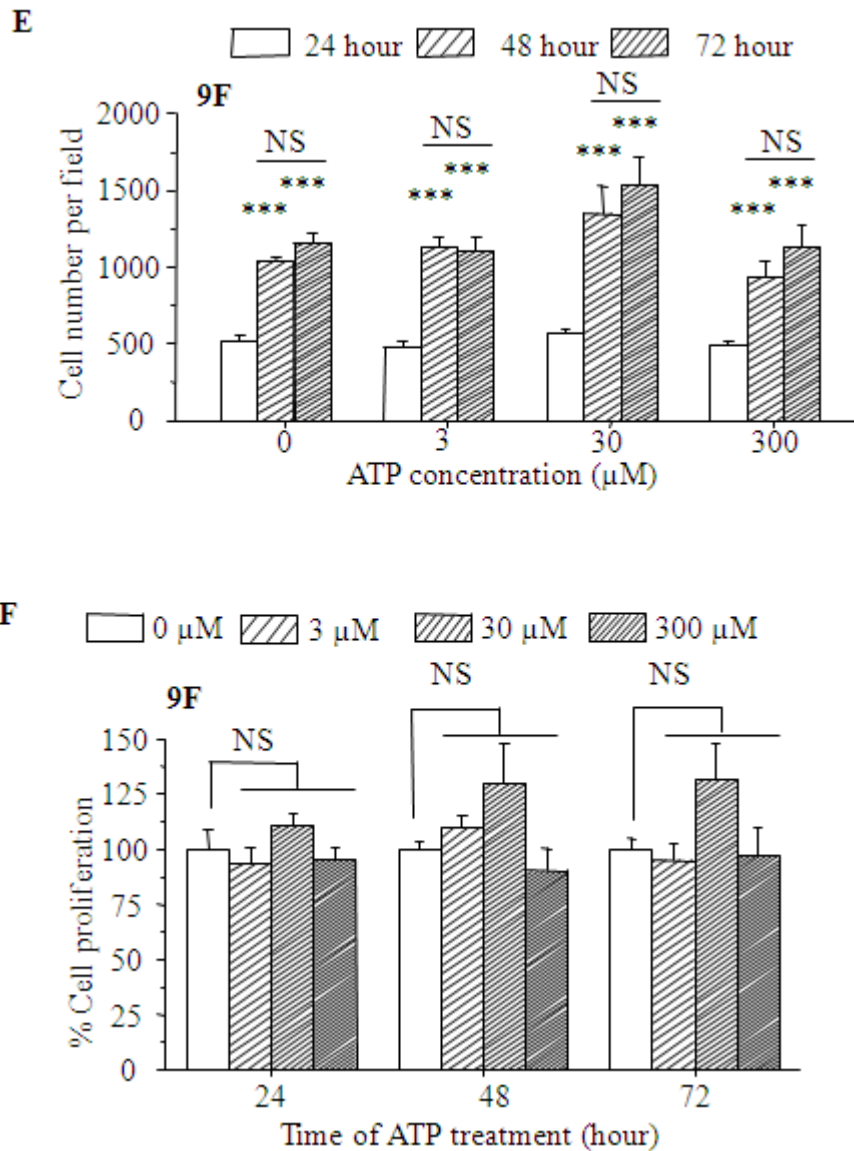


Figure 3.5 No effect of ATP on hDP-MSC proliferation by cell counting.

(A-C) Phase-contrast (A) and fluorescent SYBR Green staining (B) images of hDP-MSCs (9F, P4) under the indicated conditions. The merged images are shown in (C). (D-E) SYBR Green staining imaging (D) and the cell number per field (E) of hDP-MSCs cultured in basal medium without or with ATP from 3 μ M to 300 μ M for 24 hours, 48 hours and 72 hours. (F) The percentage of cell proliferation in hDP-MSCs cultured in basal medium alone are shown, N = 4 wells. *, $p < 0.05$, **, $p < 0.01$, ***, $p < 0.001$; compared to the control (no ATP).

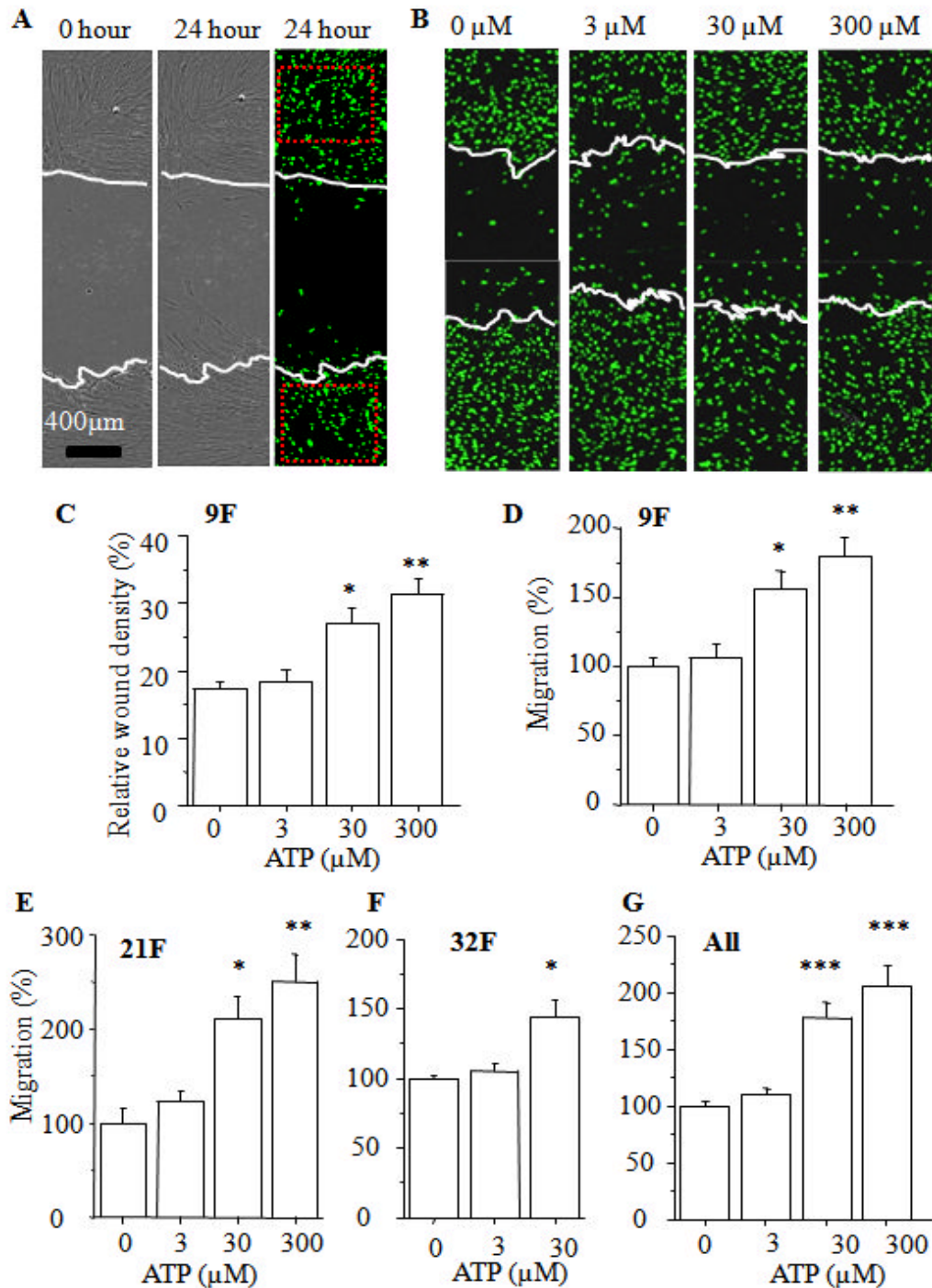


Figure 3.6 Effects of ATP on hDP-MSC migration by counting cells.

(A) Typical images showing the wound area immediately after being introduced by scratching and 24 hours later. From left to right, images are phase-contrast at the start time (0 hour), and phase-contrast and SYBR Green staining at 24 hours. (B) Typical images showing the wound after 24 hours in the basal medium without or with ATP from 0.3 μM to 300 μM (P4, 9F). (C-D) The relative density of cells in the wound area were calculated (C) and expressed as percentage of that in the basal medium without ATP (D), N = 7 wells. (E-G) The average percentage of hDP-MSC migration is shown: (E) 21F, P4, N = 5 wells; (F) 32F, P4, N = 5 wells; (G) all three donors, n/N = 3/17. *, $p < 0.05$, **, $p < 0.01$, ***, $p < 0.001$; compared to the control (no ATP).

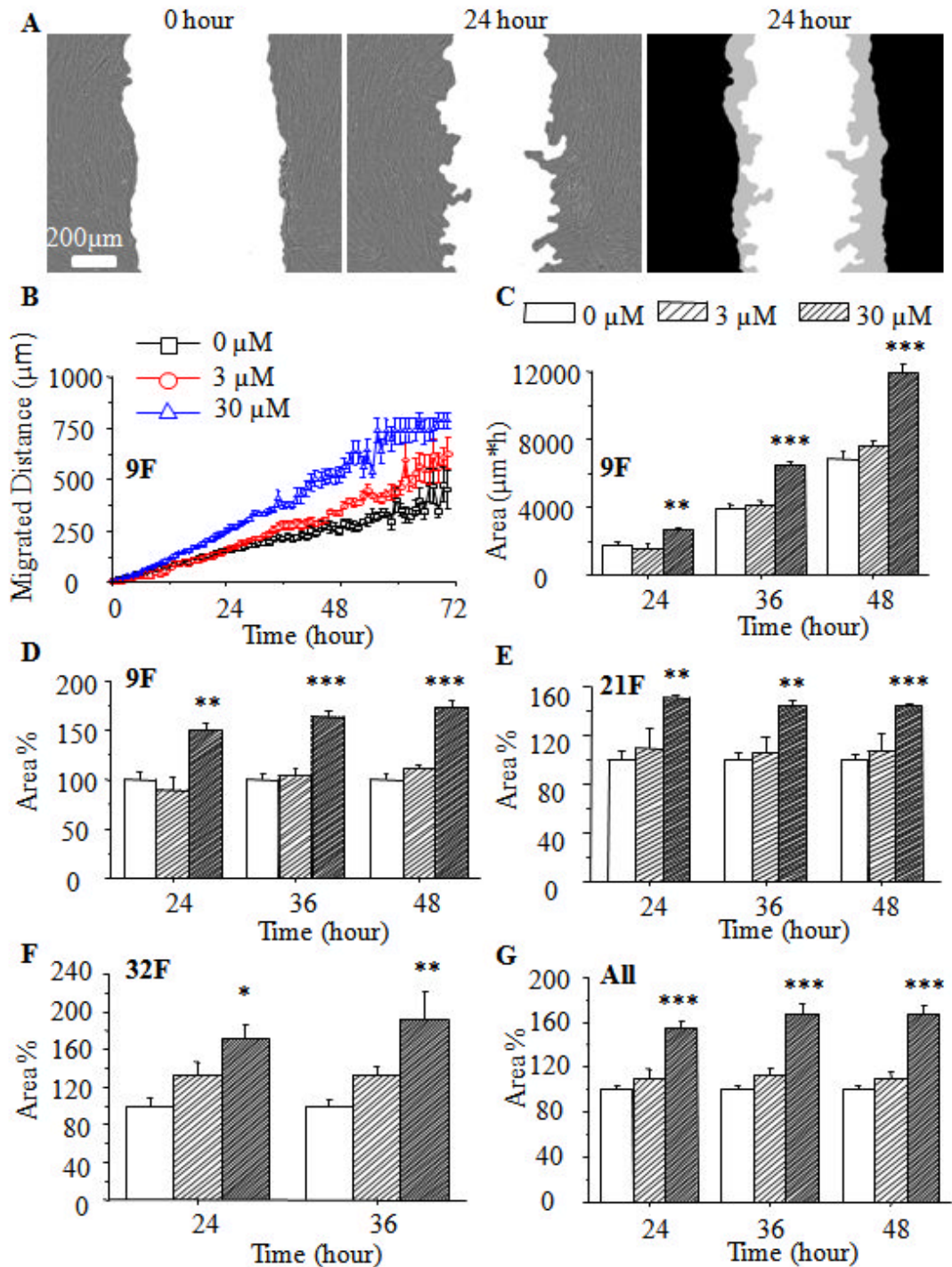


Figure 3.7 Effects of ATP on hDP-MSC migration determined by real-time imaging.

(A) Typical images showing the wound at 0 hour and 24 hours later. From left to right, images are the initial wound at the start time (0 hour), the wound at 24 hours, and the superimposition view (the white grey indicates the migrated width). (B) The changes in the migration distance in the basal medium without or with ATP from 3 μM to 30 μM for 72 hours (P4, 9F), N = 5 wells. (C-D) The relative migration area was calculated (C) and expressed as percentage of that in basal medium without ATP (D), N = 5 wells. (E-G) The average percentage of cell migration is shown: (E) 21F, P4, N = 5 wells; (F) 32F, P4, N = 5 wells; (G) all three donors, n/N = 3/15. *, $p < 0.05$, **, $p < 0.01$, ***, $p < 0.001$; compared to the control (no ATP).

3.2.4 Effects of extracellular ATP on osteogenic differentiation

As mentioned above, the ALP staining was considerably increased in cells cultured for 14 days in ODM. Treatment with ATP (3 μ M and 30 μ M) caused a noticeable reduction in the ALP staining in cells cultured in both BM and ODM (Figure 3.8A). To quantitatively evaluate the effect of extracellular ATP on the osteogenic differentiation, the ALP activity assays were conducted. The DNA content (μ g/ml), an indicator of the cell number, in BM showed significantly higher than that in ODM (Figure 3.8B). However, treatment with ATP did not have any significant effect on the DNA content of cells cultured in both BM and ODM. To minimise the potential effect of the difference in the cell proliferation, the ALP activity per microgram of DNA was used to indicate the ability of cells to undergo osteogenic differentiation. The ALP activity in cells from the donor 9F, before and after normalized to that in the control cells or cells that were not treated with ATP are shown in Figure 3.8C-D. The ALP activity in cells in ODM exhibited significantly higher than that in BM (Figure 3.8C), consistent with the increase in the ALP staining (Figure 3.8A and Figure 3.3A-D). The ALP activity (%) in cells in both BM and ODM was significantly decreased by ATP at 30 μ M, not at 3 μ M. Similar inhibition of the ALP activity by ATP were obtained in cells from the donor 21F (Figure 3.8E) and the donor 32F (Figure 3.8F). The mean data from all 3 donors are shown in Figure 3.8G. These results support that ATP inhibits osteogenic differentiation of hDP-MSCs.

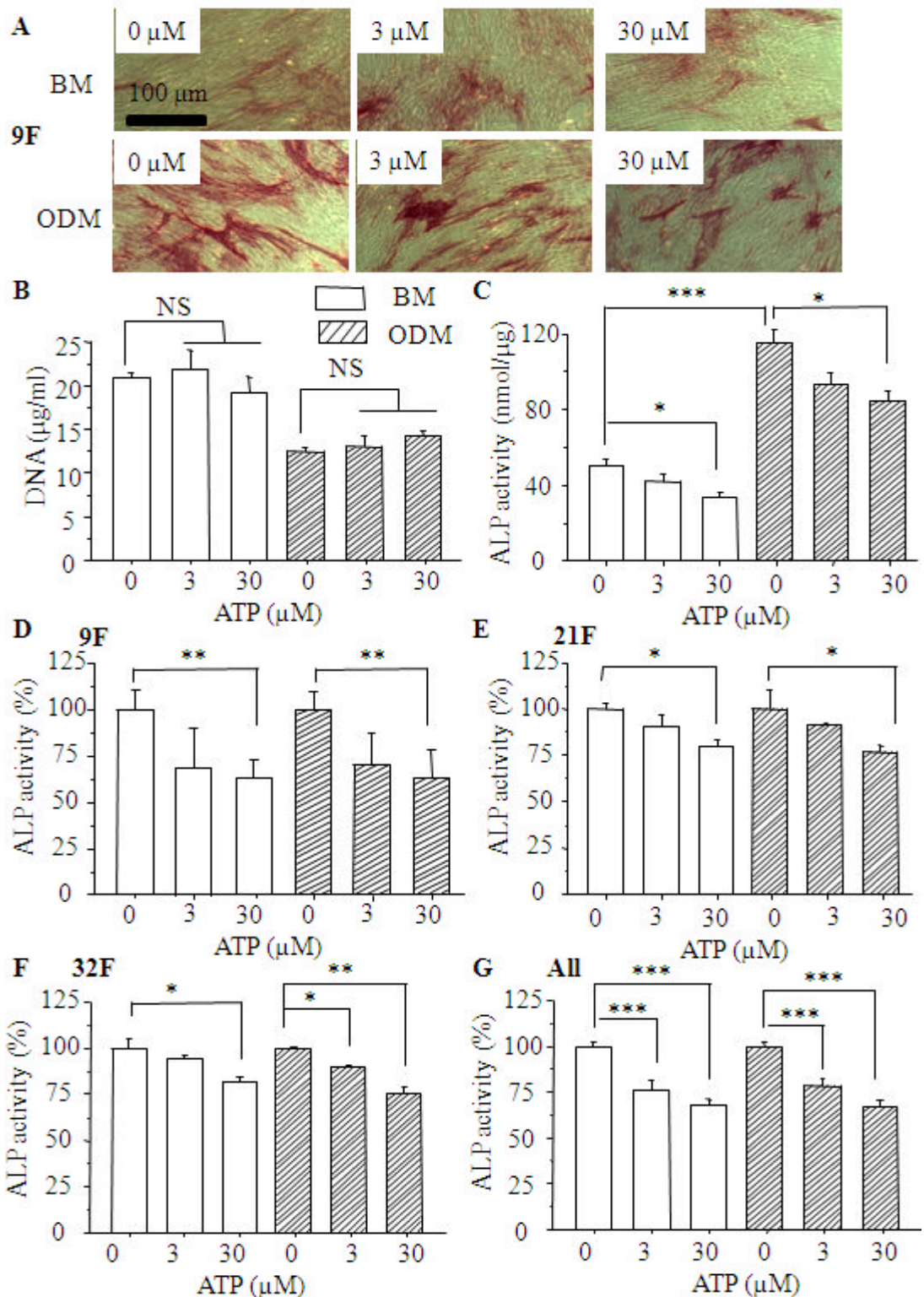


Figure 3.8 Effects of ATP on osteogenic differentiation of hDP-MSCs.

(A) Typical ALP staining of hDP-MSCs (P4, 9F) cultured for 14 days in the basal medium and osteogenic differentiation medium without or with ATP at 3 μM and 30 μM. (B-D) The DNA content (B) and ALP activity per μg of DNA (C) were calculated and expressed as percentage of that in the basal medium without ATP (D), n/N = 3/12. (E-G) The average percentage of the ALP activity in hDP-MSCs is shown: (E) P4, 21F, N = 4; (F) P4, 32F, N = 4; (G) 9F, 21F and 32F, n/N = 5/20. *, $p < 0.05$, **, $p < 0.01$, ***, $p < 0.001$; compared to the control (no ATP).

3.2.5 Effects of extracellular ATP on adipogenic differentiation

To evaluate the influence of extracellular ATP on adipogenic differentiation, cells were incubated in BM and ADM without or with ATP at 3 μ M and 30 μ M for 21 days and were stained with Oil red O to identify the lipid droplets-containing adipocytes. Lipid droplets were not detected in the cells cultured in BM, but were clearly visible in a subset of cells cultured in ADM (Figure 3.9A). The number of adipogenic cells from the donor 9F is shown in Figure 3.9B, and the data expressed as percentage of the control cells in ADM alone without ATP are shown in Figure 3.9C. ATP alone did not induce adipogenic differentiation of hDP-MSCs cultured in BM. However, ATP at 30 μ M, but not at 3 μ M, significantly increased the adipogenic differentiation of hDP-MSC in ADM. Similar results were observed in cells from the donor 21F (Figure 3.9D) and the donor 32F (Figure 3.9E). The mean data from all 3 donors are shown in Figure 3.9F. Taken together, these results show that ATP cannot induce but can facilitate the adipogenic differentiation.

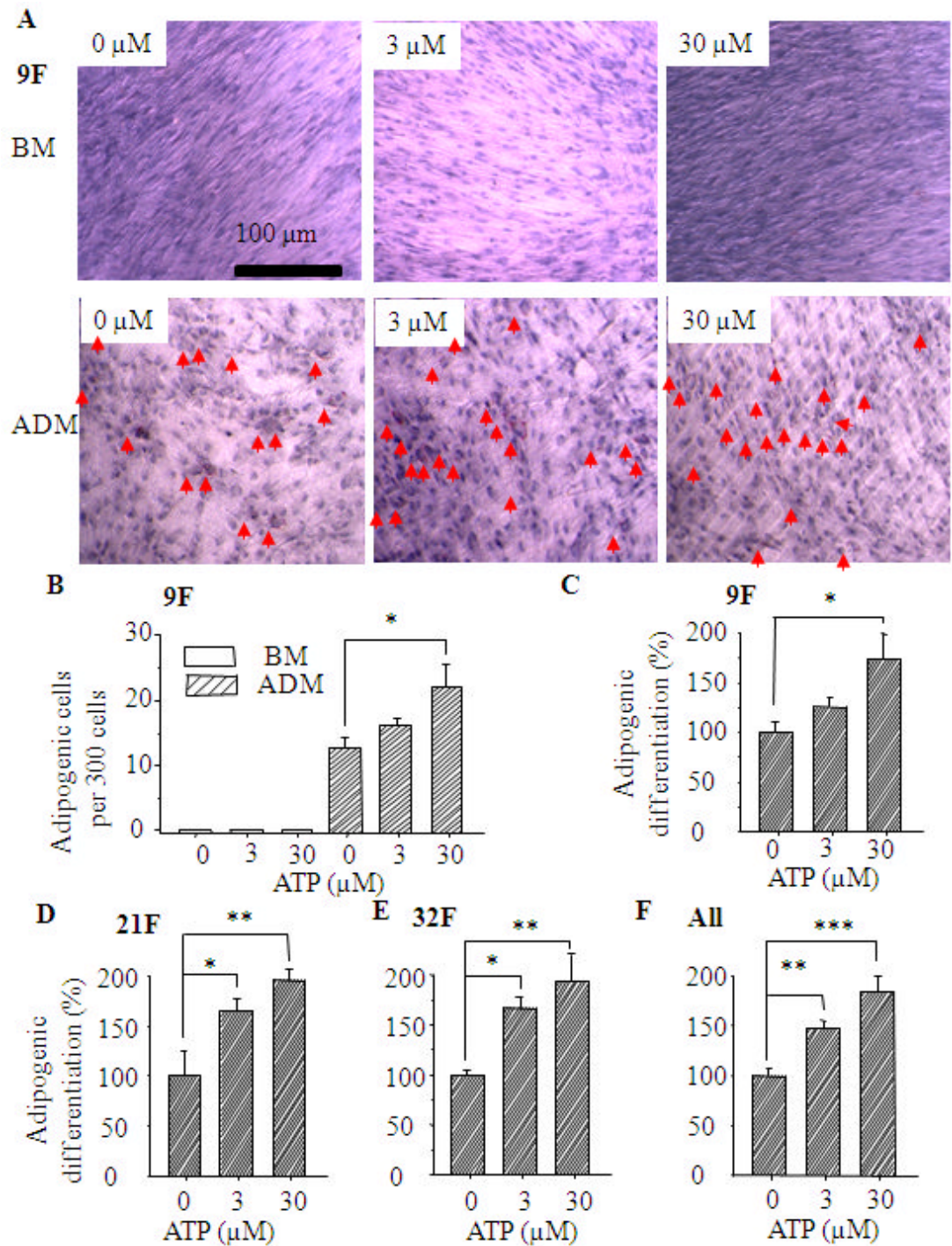


Figure 3.9 Effects of ATP on adipogenic differentiation of hDP-MSCs.

(A) Typical Oil red O staining after cells (P4, 9F) cultured for 21 days in BM and adipogenic differentiation medium (ADM) with or without ATP at 3 μM or 30 μM. Red arrows indicate fat-containing cells or adipocytes. (B) The positively-stained cells were counted and expressed as the number of adipogenic cells in every 300 cells. (C-F) The average percentage of adipogenic differentiation of hDP-MSCs as compared to cells without ATP in ADM is shown: (C) P4, 9F, N = 4 wells; (D) P4, 21F, N = 4 wells; (E) P4, 32F, N = 4 wells; (F) 9F, 21F and 32F, n/N = 3/12 wells. *, $p < 0.05$, **, $p < 0.01$, ***, $p < 0.001$; compared to the control (no ATP).

3.3 Discussion

In this chapter, MSC cells from human dental pulp were isolated as described by previous studies to isolate MSCs from adipose tissue (Rubio, Garcia-Castro et al. 2005) and placenta (Chang, Kao et al. 2007). Early passages (<5) of these cells were used to avoid loss of their stem cell characteristics during *in vitro* culture (Bonab, Alimoghaddam et al. 2006; Coppi, Pugliese et al. 2007; Ferro, Spelat et al. 2012). The results show that these cells can form CFU-F, express the positive MSC markers and no or a very low level of the negative MSC markers, and exhibit osteogenic, adipogenic and chondrogenic differentiation. In summary, the cells isolated from human dental pulp meet the criteria for MSCs (Dominici, Le Blanc et al. 2006).

First of all, these cells were plastic-adherent and grew well on plastic surfaces (Figure 3.1B and C). The colony-forming efficiency assay demonstrated that a small subsets of cells was clonogenic (Figure 3.1E-I), as previously reported for the BM-MSCs (Gronthos, Mankani et al. 2000). The results from the present study also showed that there was no significant difference in the colony-forming efficiency (~ 30 colonies/10³ cells) between the donors 9F and 22M (Figure 3.1H and I), indicating hDP-MSCs from different donors had similar clonogenic capability. Secondly, Flow cytometry assays showed that these cells expressed a high level of CD105, CD90 and CD73, and a very low level of CD45, CD34 and CD14 (Table 3.1). However, the prevalence of the CD105 expression observed in the present study, $59.6 \pm 7.0\%$, was slightly low. The cells with a similar expression level of CD105 (51.7%) were able to maintain mesenchymal multipotent differentiation potential and thus can be considered as MSCs (Mark, Kleinsorge et al. 2013). The expression level of CD14 ($8.2 \pm 1.3\%$) was slightly high, but a similar expression level of CD14 (5-9%) was also observed in hBM-MSCs (Pilz, Braun et al. 2011). Furthermore, the present study shows the MSC positive marker STRO-1 was expressed in a substantial number of cells ($27.5 \pm 9.5\%$), which was similar to that reported in BM-MSCs (Mafi, Hindocha et al. 2011). Therefore, the results from flow cytometry assay indicate that these cells show a similar expression profile of the surface markers of MSCs (Mark, Kleinsorge et al. 2013). Finally, these cells also displayed the ability of osteogenic, adipogenic, chondrogenic differentiation using

well-established *in vitro* differentiation inducing media and examination methods (Pittenger, Mackay et al. 1999; Augello and De Bari 2010), indicating that these cells have multipotent differentiation potential (Figure 3.3). Therefore, the cells isolated from dental pulp in this study have similar cell properties as MSCs reported in previous studies and thus termed hDP-MSCs in the rest of this thesis.

The study described in this chapter further examined the effects of extracellular ATP on several functional properties of hDP-MSCs, including cell proliferation, migration, adipogenic and osteogenic differentiation. The results from both XTT assay and cell counting indicate that ATP (0.3-300 μ M) did not have any significant effect on hDP-MSC proliferation of (Figure 3.4 and 3.5). This is similar with a previous study that demonstrated that ATP (1-100 μ M) had no significant effect on hBM-MSC proliferation although ATP at a higher concentration (1 mM) decreased cell proliferation (Ferrari, Gulinelli et al. 2011). However, another previous study showed that ATP at low concentration of 10 μ M decreased hBM-MSC proliferation (Coppi, Pugliese et al. 2007). In contrast, another early study reported that ATP at 25-250 μ M increased hBM-MSCs proliferation (Riddle, Taylor et al. 2007). Such discrepancies among different studies may arise from different cell preparations, different durations of ATP treatment and also proliferation assays used.

The present study using wound healing assays demonstrates that hDP-MSC migration was enhanced by exposure to extracellular ATP at 30- 300 μ M for 24-72 hours (Figure 3.6 and 3.7). ATP at 1 mM was reported to induce hBM-MSC migration using transwell assays (Ferrari, Gulinelli et al. 2011). Similar to what observed in the present study, ATP at 20 μ M stimulated migration of hepatocellular carcinoma cells using both wound healing and transwell migration assays (Xie, Xu et al. 2014).

The results obtained in the present study also show that extracellular ATP (30 μ M) significantly decreased the ALP activity in hDP-MSCs cultured in both BM and ODM (Figure 3.8), suggesting that ATP significantly inhibits or down-regulates the osteogenic differentiation. However, a previous study reported that pretreatment

with of ATP (0.1 – 100 μ M) for 5 minutes enhanced the ALP activity in hBM-MSCs (Sun, Junger et al. 2013). In addition, pretreatment of hBM-MSCs with 1 mM ATP for 24 hours promoted mineralization as shown by increased Alizarin Red staining and expression of RUNX2 (runt-related transcription factor 2, an osteoblast-related gene) (Ciciarello, Zini et al. 2013). In this study, hDP-MSCs were cultured in ODM along with ATP during the differentiation process. It is possible that the different results observed by the previous and present studies are due to the different treatment durations used. In contrast with the inhibitory effects on the osteogenic differentiation potential, treatment with extracellular ATP (30 μ M) increased the number of cells containing lipid droplets in hDP-MSCs cultured in ADM, indicating that extracellular ATP enhances adipogenic differentiation potential (Figure 3.9). This is consistent with the recent findings that lipid droplets formation and the expression level of PPAR γ are improved during adipogenic differentiation of hBM-MSCs after preincubation with 1 mM ATP for 24 hours (Ciciarello, Zini et al. 2013).

In summary, the studies presented in this chapter show that extracellular ATP promotes hDP-MSC migration, but has no effect on cell proliferation. In addition, ATP inhibits the osteogenic differentiation potential and by contrast enhances the adipogenic differentiation potential of hDP-MSCs. The following chapters will investigate the expression of signalling mechanisms activated by extracellular and their role in ATP-induced regulation of migration, osteogenesis and adipogenesis of hDP-MSCs.

Chapter 4

Expression of P2 Purinergic Receptors in Human Dental Pulp Mesenchymal Stem Cells

4.1 Introduction

The results presented in chapter 3 have shown that extracellular ATP significantly promotes cell migration and regulates adipogenic and osteogenic differentiation potential of hDP-MSCs. It is well established that ATP imposes various effects via activating P2X and P2Y receptors as discussed in Introduction chapter (see section 1.4.2 and 1.4.4). It has been reported that hBM-MSCs express both P2X and P2Y receptors (Ferrari, Gulinelli et al. 2011). The mRNA expression for all P2X and P2Y receptors except P2X2 was observed in hBM-MSCs by real-time RT-PCR, and the protein expression of the P2X1, P2X4, P2X7, P2Y1, P2Y2 and P2Y11 receptors were demonstrated by Western blotting (Ferrari, Gulinelli et al. 2011). Other studies provide evidence to suggest the functional expression of P2Y1 (Coppi, Pugliese et al. 2007) and P2X7 receptors in hBM-MSCs (Sun, Junger et al. 2013). Furthermore, recent studies suggest ATP via the P2X7 receptor regulates the osteogenic differentiation of hBM-MSCs (Sun, Junger et al. 2013), and via the P2Y receptors to regulate adipogenic differentiation (Ciciarello, Zini et al. 2013). However, the current understanding of the ATP-sensitive P2X and P2Y receptors in hBM-MSCs remains incomplete and inconsistent, which prevent a clear understanding of the intrinsic mechanisms that are responsible for the various effects of extracellular ATP on hMSCs.

Nothing is known regarding the expression of the P2 purinergic receptors in hDP-MSCs. Therefore, the aim of the study described in this chapter was to investigate the functional expression of the P2X and P2Y purinergic receptors for extracellular ATP in hDP-MSCs. Activation of ATP-sensitive P2X and P2Y receptors lead to increases in the $[Ca^{2+}]_i$, which were measured using single cell Ca^{2+} imaging and FLEXstation, in a combination of P2 purinergic receptors agonists,

antagonists and specific siRNAs. Moreover, the mRNA expression of P2X and P2Y receptors was examined by real-time RT-PCR.

4.2 Results

4.2.1 Ca^{2+} oscillations and ATP-induced Ca^{2+} responses in individual cells

Single cell Ca^{2+} imaging was firstly used to measure the changes in the $[\text{Ca}^{2+}]_i$ in individual cells. In the extracellular Ca^{2+} -containing solutions, 12 out of 40 cells examined displayed spontaneous Ca^{2+} oscillations in the absence of exogenous application of ATP. Examples are shown in Figure 4.1A and B. The average number of the Ca^{2+} spike events ($\Delta F_{340}/F_{380} \geq 0.05$) during a period of 10-minute recording was about 3 (Figure 4.1C) and the average amplitude was 0.06 (Figure 4.1D).

Cells not exhibiting Ca^{2+} oscillations were used to study ATP-induced Ca^{2+} responses. Cells responded with a rapid increase in the $[\text{Ca}^{2+}]_i$ to application of extracellular ATP at 100 μM (Figure 4.1E). Such ATP-induced Ca^{2+} responses were observed in 16 of 17 cells examined. ATP also induced strong Ca^{2+} responses in a majority of individual cells (14 of 15 cells) in the extracellular Ca^{2+} -free solutions (Figure 4.1F). The peak amplitude of ATP-induced Ca^{2+} responses was not significantly different in the extracellular Ca^{2+} -containing and Ca^{2+} -free solutions. However, the ATP-induced Ca^{2+} responses in the extracellular Ca^{2+} -containing solutions were sustained significantly longer than those in the extracellular Ca^{2+} -free solutions (Figure 4.1G). These results indicate expression of ATP-sensitive P2 receptors in hDP-MSCs.

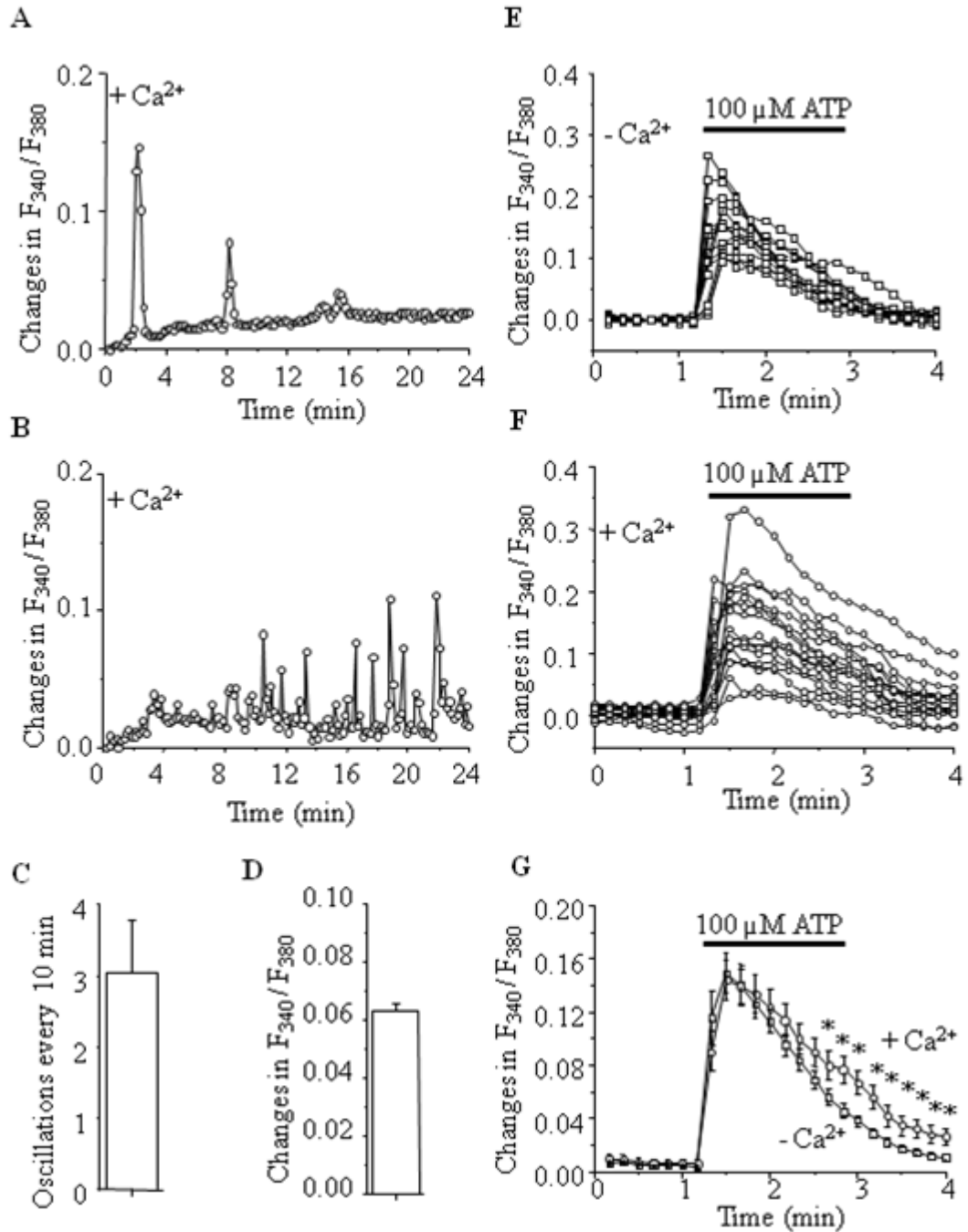


Figure 4.1 Spontaneous and ATP-induced Ca^{2+} responses in single hDP-MSCs.

(A-B) Typical spontaneous Ca^{2+} oscillations in individual cells (P4, 9F) are shown. (C-D) Summary of the average number of the Ca^{2+} spikes (C) and changes in F_{340}/F_{380} during a period of 10-minute recording (D), $N = 12$ out of 40 cells. (E-F) Changes in the F_{340}/F_{380} in individual cells treated with ATP at $100 \mu\text{M}$ in the absence (E, $N = 14$ out of 15 cells) and presence (F, $N = 16$ out of 17 cells) of extracellular Ca^{2+} . (G) The average change in the F_{340}/F_{380} in cells treated with ATP at $100 \mu\text{M}$ in the extracellular Ca^{2+} -containing solutions and extracellular Ca^{2+} -free solutions. *, $p < 0.05$, compared the amplitude of Ca^{2+} responses in the extracellular Ca^{2+} -containing and Ca^{2+} -free solutions at the same time points.

4.2.2 RT-PCR analysis of mRNA expression of P2 receptors

The mRNA expression of the P2 receptors in hDP-MSCs was examined using real-time RT-PCR. The primers and PCR protocols were validated using plasmids. In addition, the mRNA for β -actin was consistently detected. As shown in Figure 4.2 A and B, the mRNA expression for P2X4, P2X6, P2X7, P2Y1, P2Y4, P2Y6 and P2Y11 was detected in hDP-MSCs from all three donors examined (Figure 4.2A, B). The P2Y2 mRNA was detected in hDP-MSCs from one donor (9F) but very weak or not in hDP-MSCs from other two donors (21F and 32F) (Figure 4.2B). In contrast, the mRNA expression for P2X1, P2X2, P2X3 and P2X5 was not detected in hDP-MSCs from all three donors. The mRNA expression levels for each of these P2 receptors relative to β -actin from two independent preparations, each in triplicates ($n/N = 2/6$) is summarized in Figure 4.2C. There are noticeable variations in the mRNA expression level among the three donors. The P2Y11 is most abundant in hDP-MSCs from all three donors.

To further investigate the functional expression of the P2 receptors for extracellular ATP, the increases in the $[Ca^{2+}]_i$ induced by ATP and other known P2 receptor subtypes selective agonists and the effects of known P2 receptor antagonists on agonist-induced Ca^{2+} responses were examined using FLEXstation.

4.2.3 Effects of PPADS on ATP-induced Ca^{2+} responses

As seen in Figure 4.3A, ATP induced significant Ca^{2+} responses in the extracellular Ca^{2+} -containing solutions that reached the maximum after 20-40 seconds and gradually declined (Figure 4.3A). The maximum Ca^{2+} responses induced with 300 μ M ATP are shown in Figure 4.3B and C. The effect of PPADS, a generic P2 receptor antagonist (see section 1.3.1), on the ATP-induced Ca^{2+} responses was measured. Pre-treatment with PPADS at 10 μ M for 30 minutes significantly inhibited ATP-evoked increases in the $[Ca^{2+}]_i$ in hDP-MSCs from all three donors (Figure 4.3D-G), indicating that ATP-sensitive P2 receptors are functionally expressed.

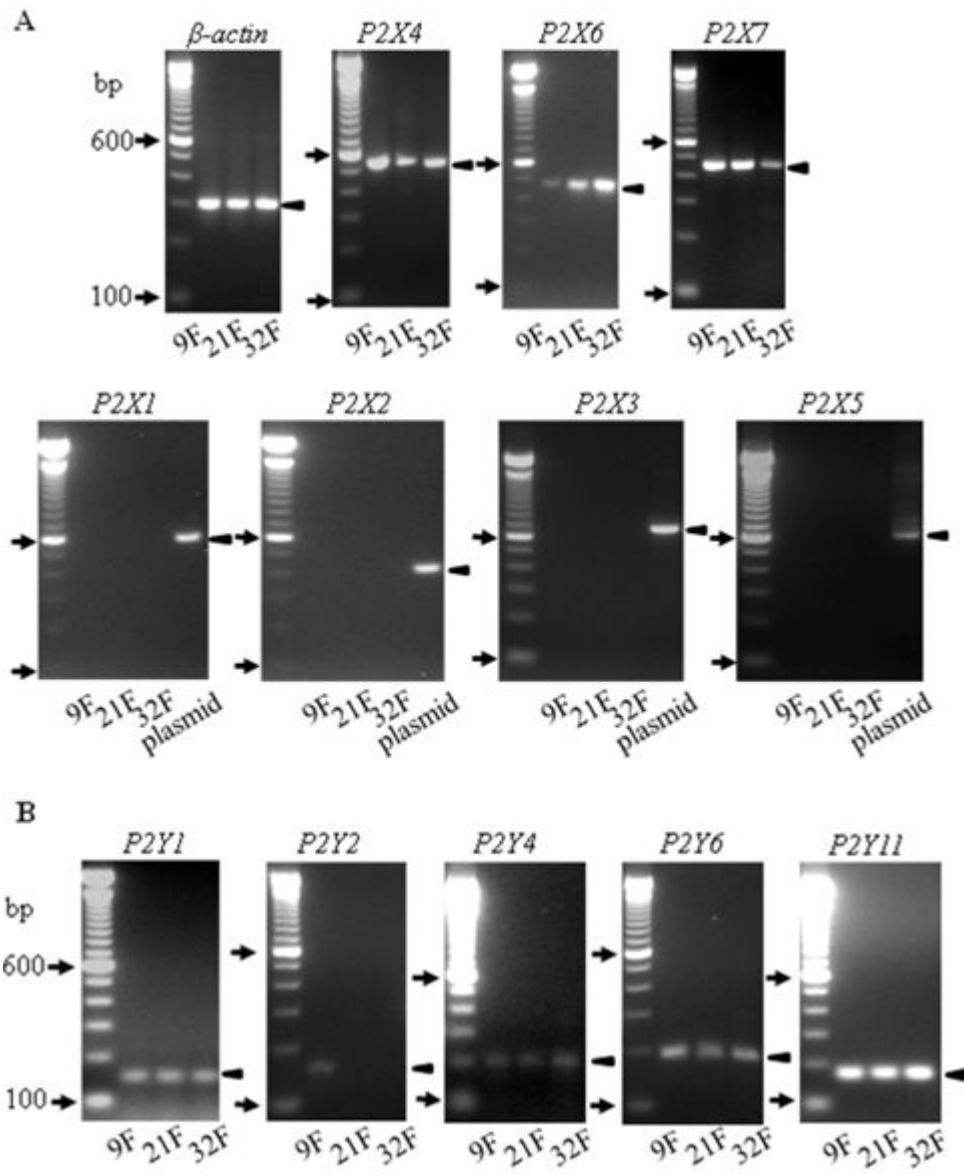


(Figure 4.2)

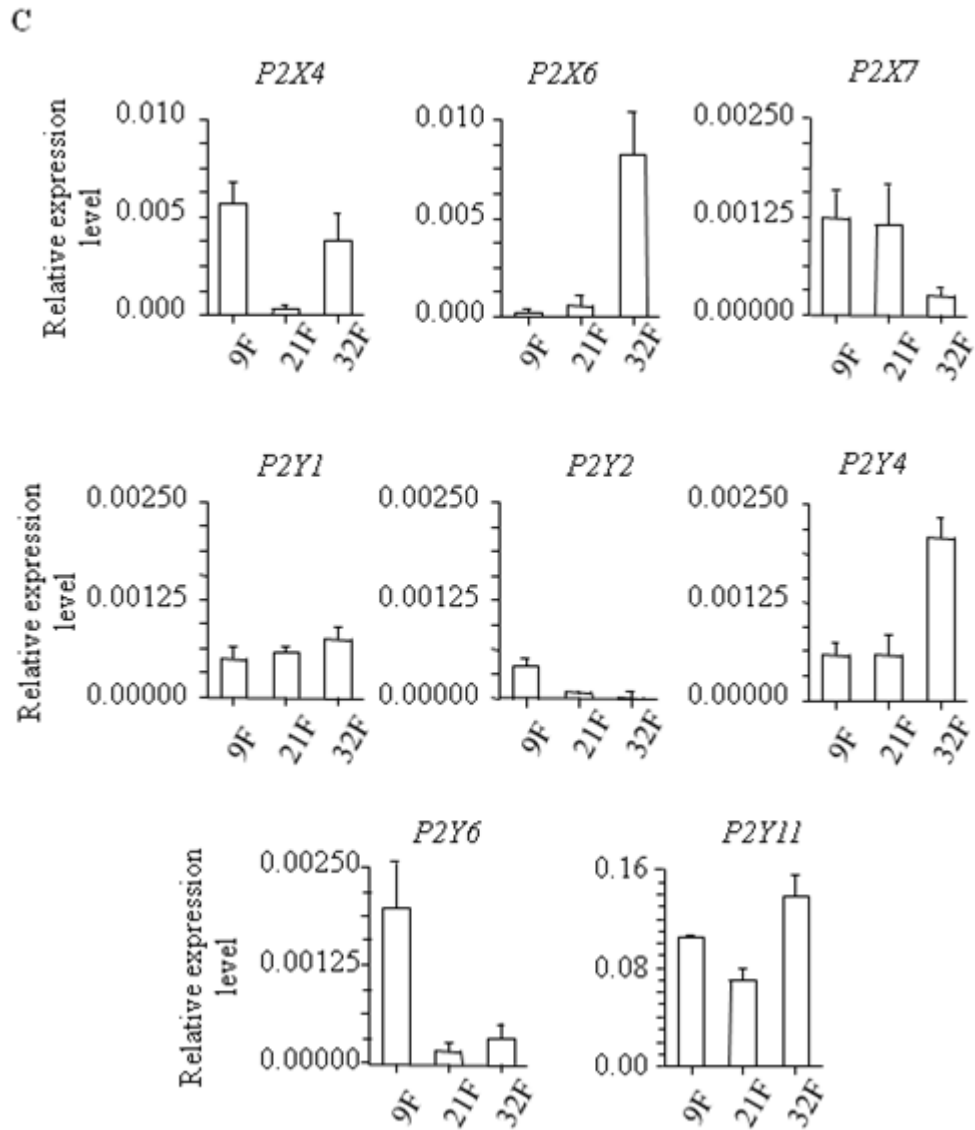
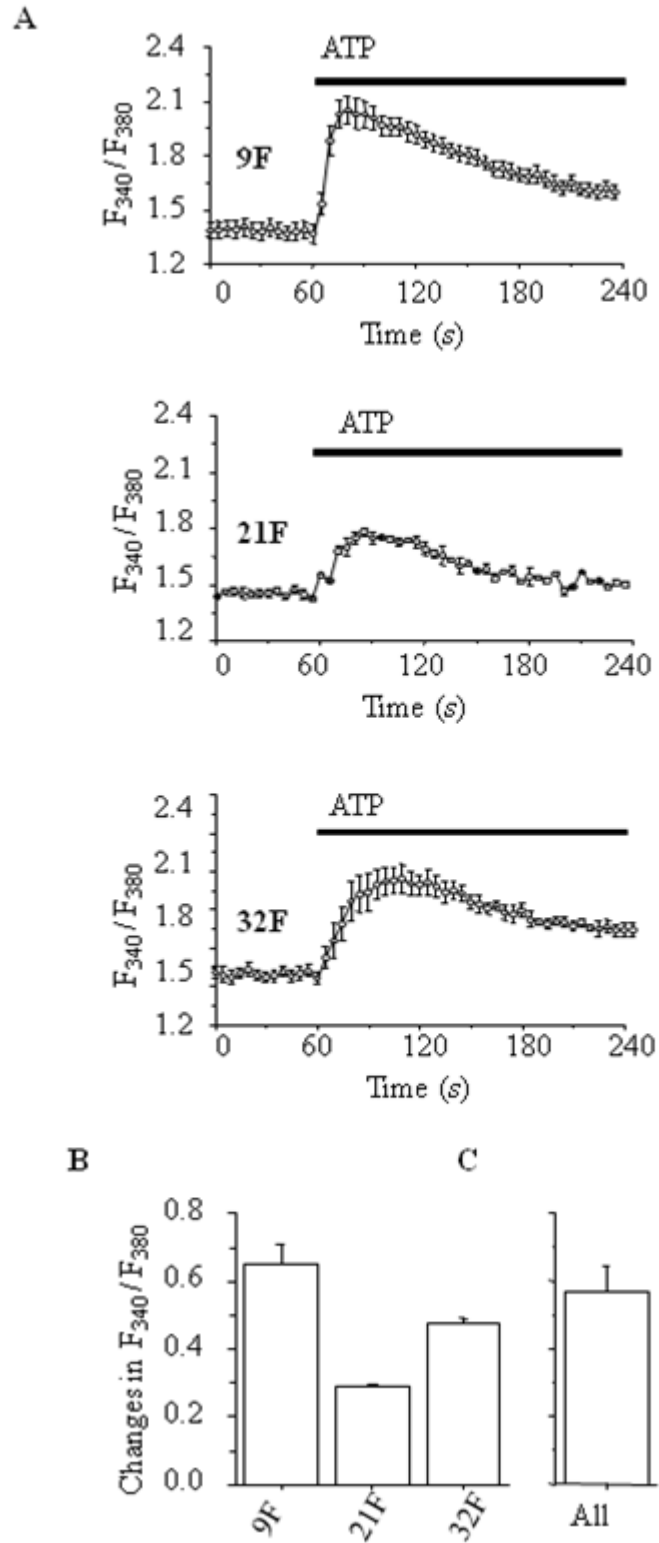


Figure 4.2 The mRNA expression of P2 receptors in hDP-MSCs.

(A) Representative images of agarose gel analysis of PCR products. The expression of P2X4, P2X6 and P2X7 was consistently observed, while the expression of P2X1, P2X2, P2X3 and P2X5 was not detected. The primers for the latter group of P2X receptors were validated using plasmids. (B) The expression of P2Y1, P2Y4, P2Y6 and P2Y11 receptors was detected, whereas the P2Y2 expression was detected only in the donor 9F. (C) The mRNA expression levels of the indicated P2 receptors relative to that of β -actin are shown ($n/N = 2/6$).



(Figure 4.3)

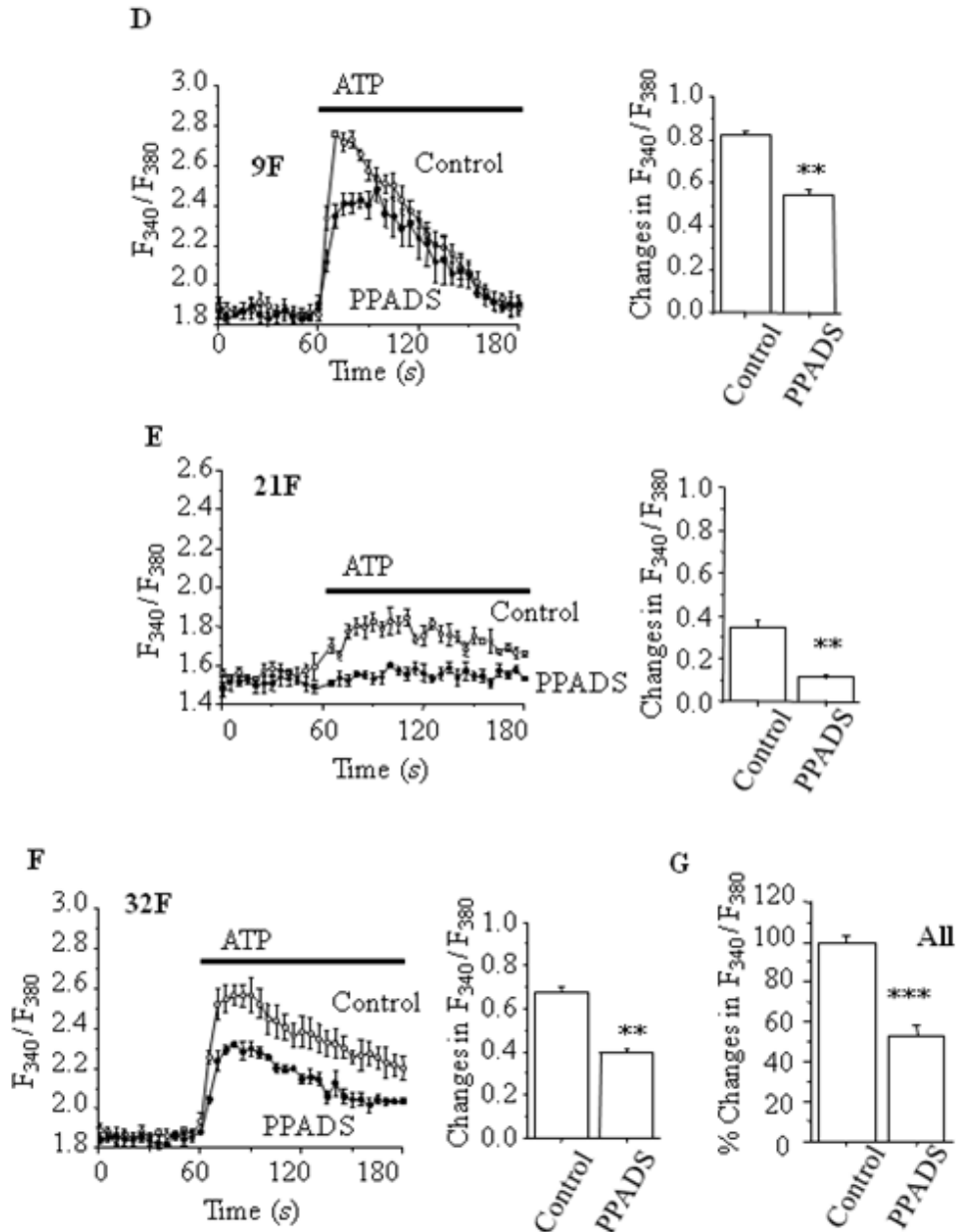


Figure 4.3 ATP-induced Ca^{2+} responses and inhibition by PPADS.

(A-C) Typical Ca^{2+} responses (A: 9F, 21F, 32F, P4, N = 4 wells for each case), and summary of the average maximum change in the F_{340}/F_{380} in cells for each donor (B) and average maximum changes from all three donors (C). ATP at 300 μ M was used. (D-F) The effect of PPADS at 10 μ M on ATP-induced Ca^{2+} responses: (D) 9F; (E) 21F; (F) 32F. P4, N = 4 wells for each case. (G) Summary of the average percentage of inhibition by PPADS in cells (9F, 21F and 32F) (n/N = 5/20). *, $p < 0.05$, **, $p < 0.01$, ***, $p < 0.001$; compared to the control (ATP alone).

4.2.4 Ca^{2+} responses to P2X receptor agonists

In the following experiments, the Ca^{2+} responses induced by P2X receptor subtype selective agonists, BzATP and $\alpha\beta\text{meATP}$ were investigated in order to further define the P2X receptors expressed in hDP-MSCs. Figure 4.4A-C show the Ca^{2+} responses to ATP at 300 μM , $\alpha\beta\text{meATP}$ at 100 μM , and BzATP at 300 μM in the presence of extracellular Ca^{2+} . While $\alpha\beta\text{meATP}$ did not evoke discernible increases in the $[\text{Ca}^{2+}]_i$ (Figure 4.4B), BzATP induced strong Ca^{2+} responses (Figure 4.4C). The maximum Ca^{2+} responses induced by BzATP were significantly higher than that by ATP in hDP-MSCs from all three donors (Figure 4.4D-F).

4.2.5 ATP and BzATP concentration-response relationships

In order to determine the sensitivity to ATP and BzATP, agonist concentration- Ca^{2+} response relationship curves were constructed. Figure 4.5A shows the Ca^{2+} responses to ATP at 0.3 μM , 3 μM , 30 μM and 300 μM in hDP-MSCs from the 9F donor. Figure 4.5B summarizes the ATP concentration-response relationship curve; fitting the data to the Hill equation yielded an EC_{50} of 22 μM and Hill coefficient (n_H) of 0.5 (Figure 4.5B). Figure 4.5C shows the Ca^{2+} responses induced by BzATP at 10 μM , 30 μM , 100 μM and 300 μM in hDP-MSCs from the 9F donor. The EC_{50} for BzATP was 87 μM and n_H value was 1.4 (Figure 4.5D).

4.2.6 Effects of P2X antagonists on ATP-induced Ca^{2+} responses

To further assess whether the cells express functional P2X4 and P2X7 receptors, the effects of 5-BDBD and AZ11645373 on ATP-induced Ca^{2+} responses were examined. 5-BDBD is a P2X4 selective antagonist with an IC_{50} of ~ 0.50 μM (see section 1.3.2.4). Pre-treatment with 5-BDBD at 10 μM for 30 minutes before exposure to ATP produced no significant inhibition on ATP-evoked Ca^{2+} responses in hDP-MSCs from all three donors (Figure 4.6A-E), indicating no functional expression of the P2X4 receptor.

AZ11645373 is a P2X7 selective antagonist with an IC_{50} of ~ 5 -20 nM for the hP2X7 receptor (see section 1.3.2.7). Pre-treatment with AZ11645373 at 1 μM for 30 minutes caused significant inhibition on ATP-evoked Ca^{2+} responses in hDP-MSCs

from all three donors (Figure 4.7A-D). On average, AZ11645373 blocked ATP-induced Ca^{2+} responses by $35 \pm 5\%$ (Figure 4.7E), indicating that functional expression of the P2X7 receptor.

4.2.7 Ca^{2+} responses induced by P2Y receptor agonists

To assess functional expression of the P2Y receptors, the increases in the $[\text{Ca}^{2+}]_i$ in response to several P2Y receptor subtype selective agonists were measured. These experiments were conducted in the extracellular Ca^{2+} -free solutions in order to avoid the contribution of Ca^{2+} entry through the P2X receptors as described above and also the contribution of Ca^{2+} entry through the SOC channels that are activated as a result of the P2Y receptor activation (see section 1.3.4 in the Introduction chapter), which is to be examined in the next chapter. ATP is a full and partial agonist at P2Y1, P2Y2 and P2Y11, ADP at P2Y1, UTP at P2Y2 and P2Y4, MRS4062 at P2Y4, UDP at P2Y6, and BzATP at P2Y1 and P2Y11 (see section 1.3.3 in the Introduction chapter). Figure 4.8A-F show representative Ca^{2+} responses to ATP, ADP, UTP, MRS4062, UDP and BzATP all at 100 μM . Figure 4.8G-I summarize the mean amplitude of Ca^{2+} responses in hDP-MSCs from all three donors. Figure 4.8J shows the mean Ca^{2+} responses expressed as percentage of the Ca^{2+} responses induced by ATP in each of three donors. There was no significant difference in the Ca^{2+} responses induced by ATP, ADP, UTP and BzATP. In contrast, the Ca^{2+} responses induced by MRS4062 were significantly lower than those by ATP. UDP-evoked responses were very small or undetectable in all three donors (Fig.4.8E and G-J). These results suggest that the P2Y1, P2Y2, P2Y4 and P2Y11 receptors are functionally expressed, but the P2Y6 receptor is not or very weakly expressed in hDP-MSCs.

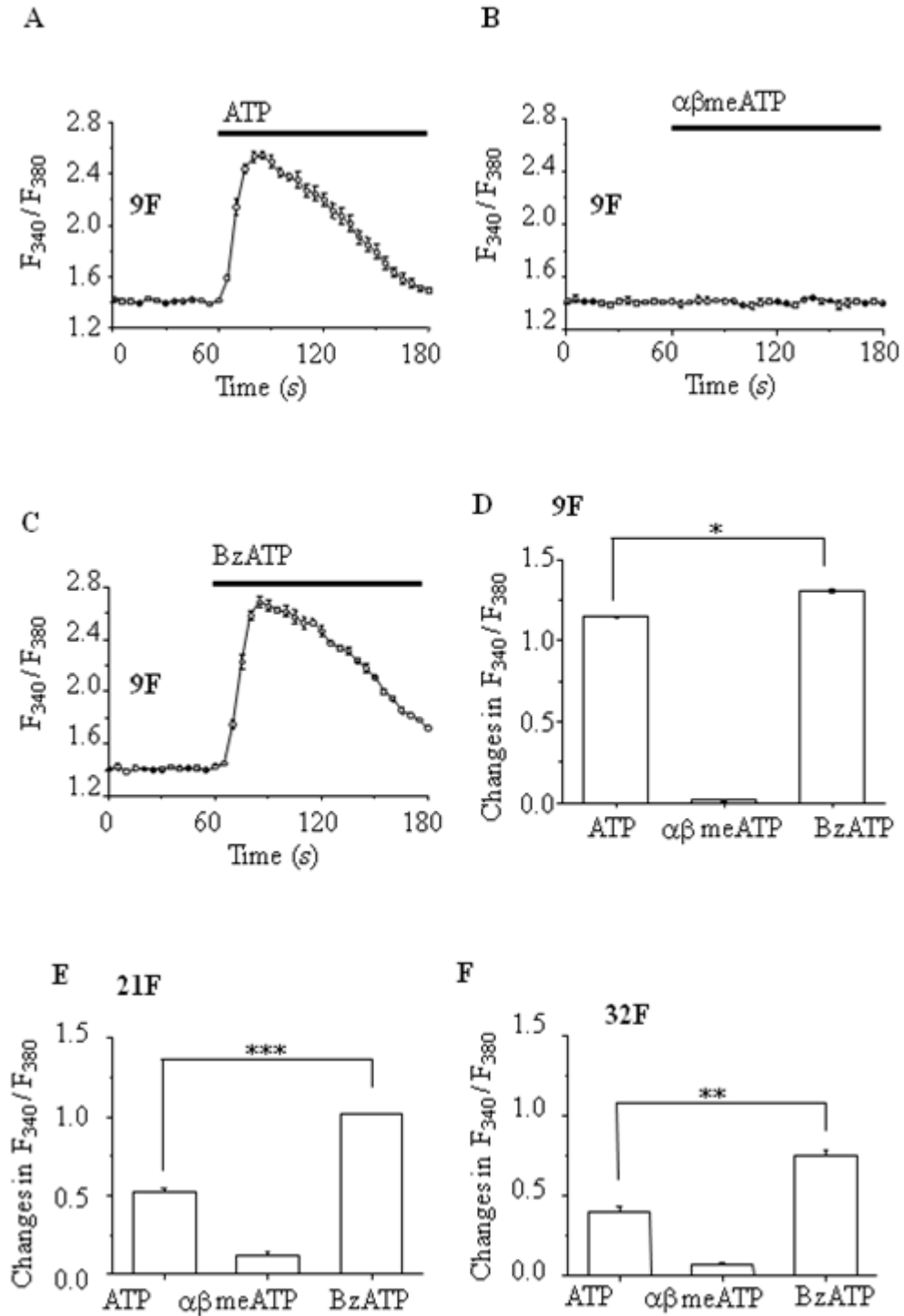


Figure 4.4 Ca^{2+} responses to P2X receptor agonists in hDP-MSCs.

(A-C) Representative Ca^{2+} responses to ATP at 300 μM (A), $\alpha\beta\text{meATP}$ at 100 μM (B) and BzATP at 300 μM (C) in the presence of extracellular Ca^{2+} . (D-F) The average change in F_{340}/F_{380} induced by ATP, $\alpha\beta\text{meATP}$ and BzATP as shown in A-C: (D) 9F; (E) 21F; (F) 32F. P4, N = 4 wells for each case. *, $p < 0.05$, **, $p < 0.01$, ***, $p < 0.001$; compared to ATP.

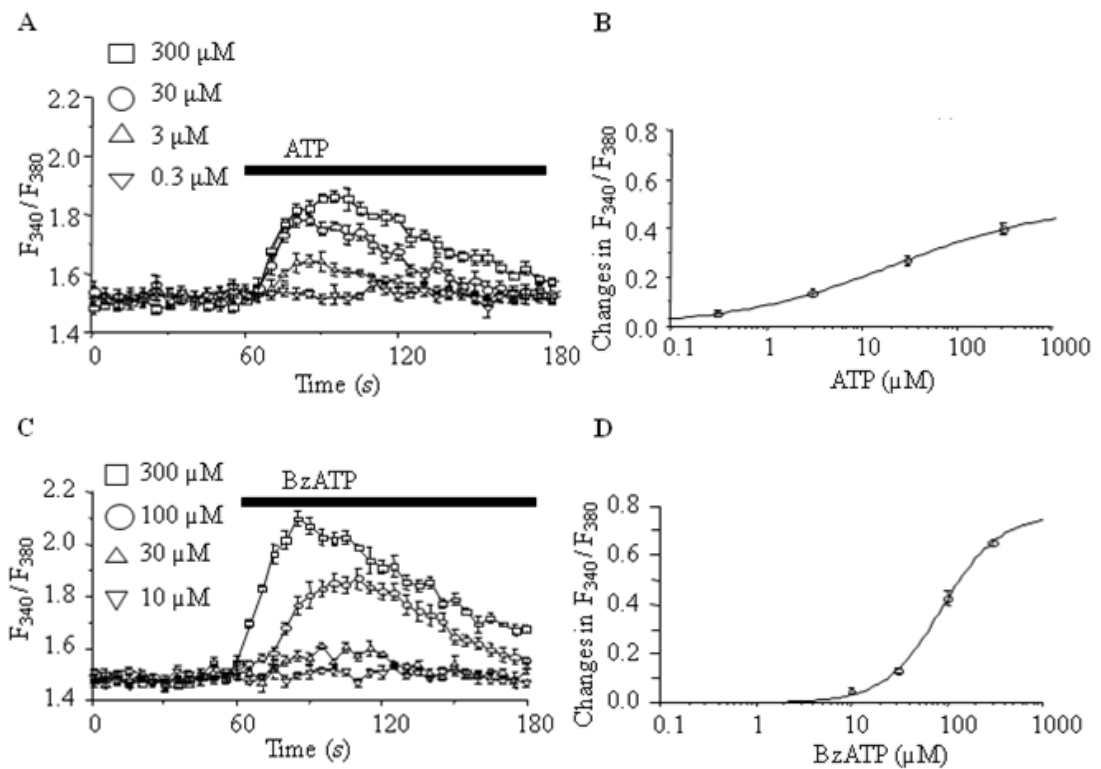


Figure 4.5 Agonist concentration- Ca^{2+} response relationship curves for ATP and BzATP.

(A) The Ca^{2+} responses to ATP at 0.3 μM , 3 μM , 30 μM and 300 μM in hDP-MSCs (P4, 9F) in the presence of extracellular Ca^{2+} ; $N = 4$ wells for each case. (B) The ATP concentration-response relationship curve derived from fitting the data to the Hill equation ($EC_{50} = 22 \mu\text{M}$ and $n_H = 0.5$). (C) The Ca^{2+} responses induced by BzATP at 10 μM , 30 μM , 100 μM and 300 μM in hDP-MSCs (P4, 9F) in the presence of extracellular Ca^{2+} . $N = 4$ wells for each case. (D) The BzATP concentration-response relationship curve from fitting to the Hill equation ($EC_{50} = 87 \mu\text{M}$ and $n_H = 1.4$).

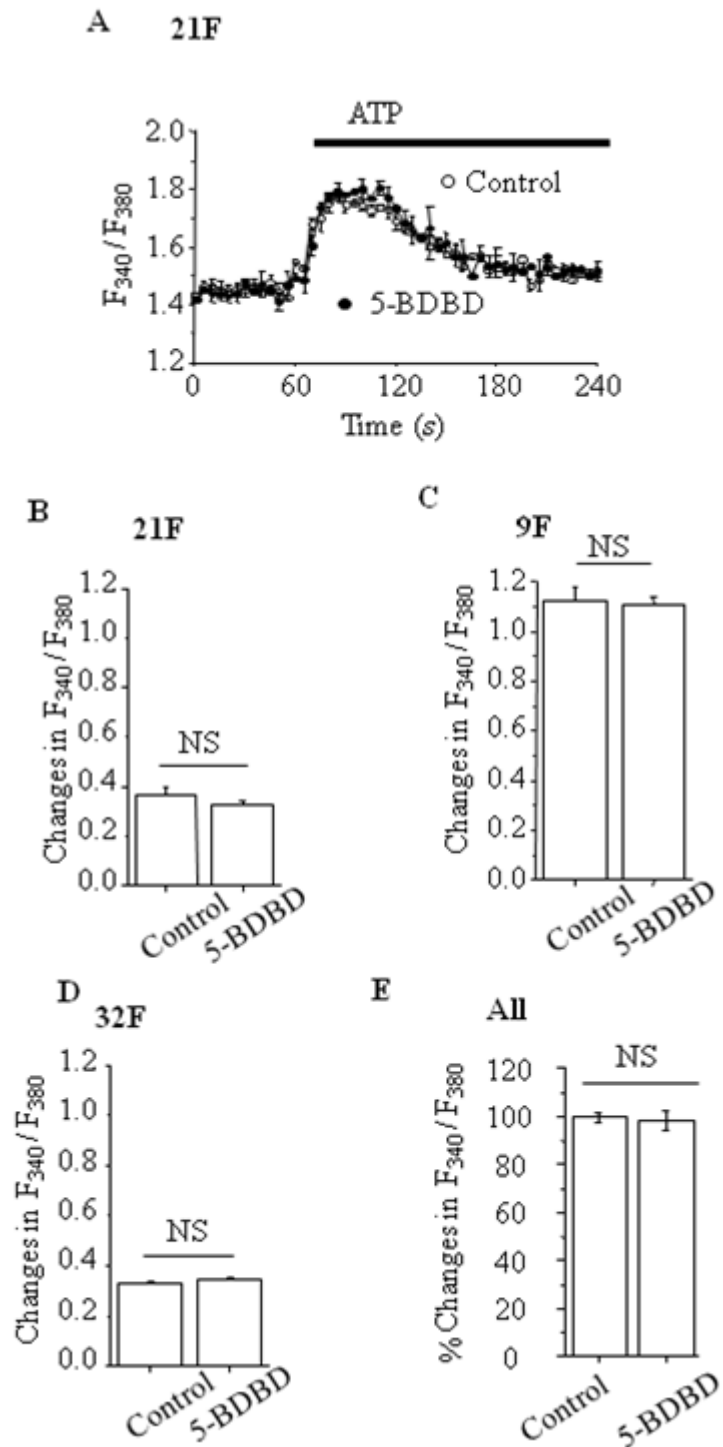


Figure 4.6 No effect of P2X4 receptor antagonist 5-BDBD on ATP-induced Ca^{2+} responses.

(A) Representative Ca^{2+} responses to ATP in hDP-MSCs (P4, 21F) pretreated without or with 5-BDBD at 10 μ M. ATP at 300 μ M was used. (B-D) Summary of the average maximum change in F_{340}/F_{380} in hDP-MSCs: (B) 21F; (C) 9F; (D) 32F. P4, N = 4 wells for each case. (E) The percentage of inhibition by 5-BDBD in hDP-MSCs from all three donors, n/N = 3/12 wells. NS, no significant difference compared to ATP alone.

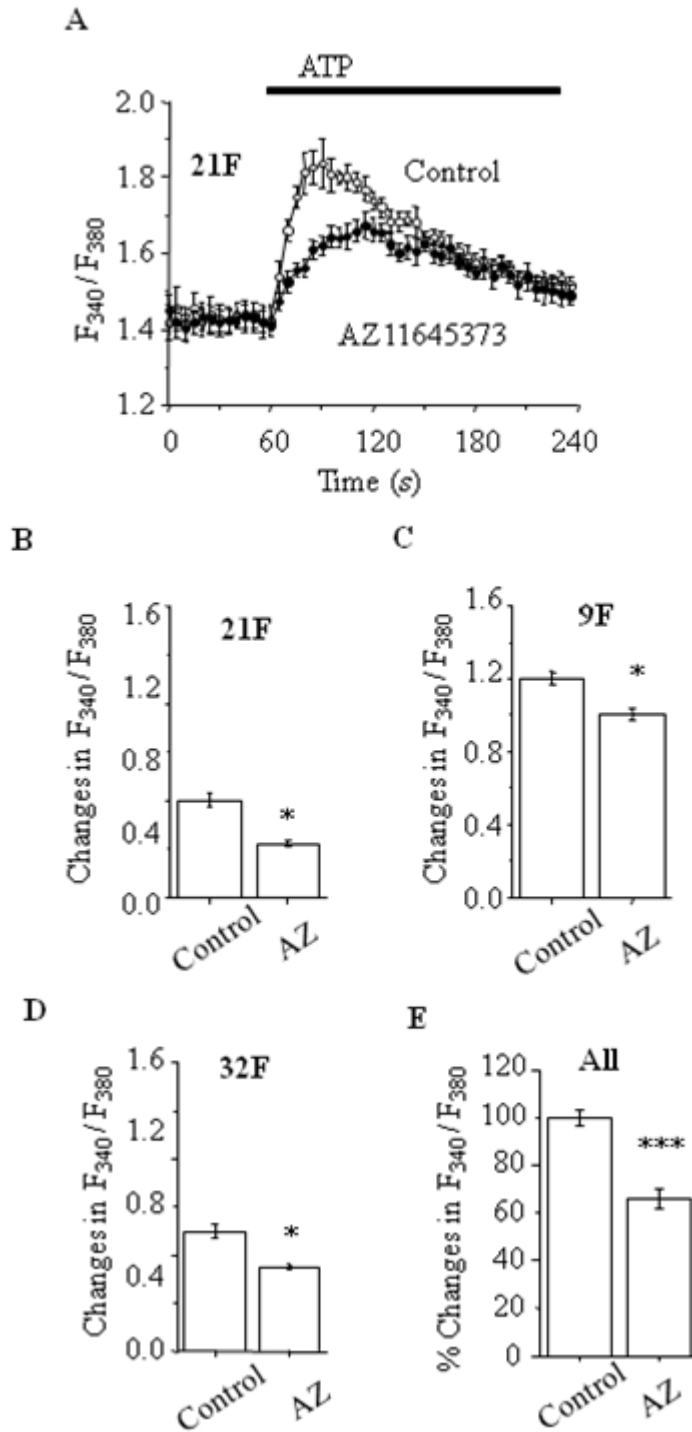
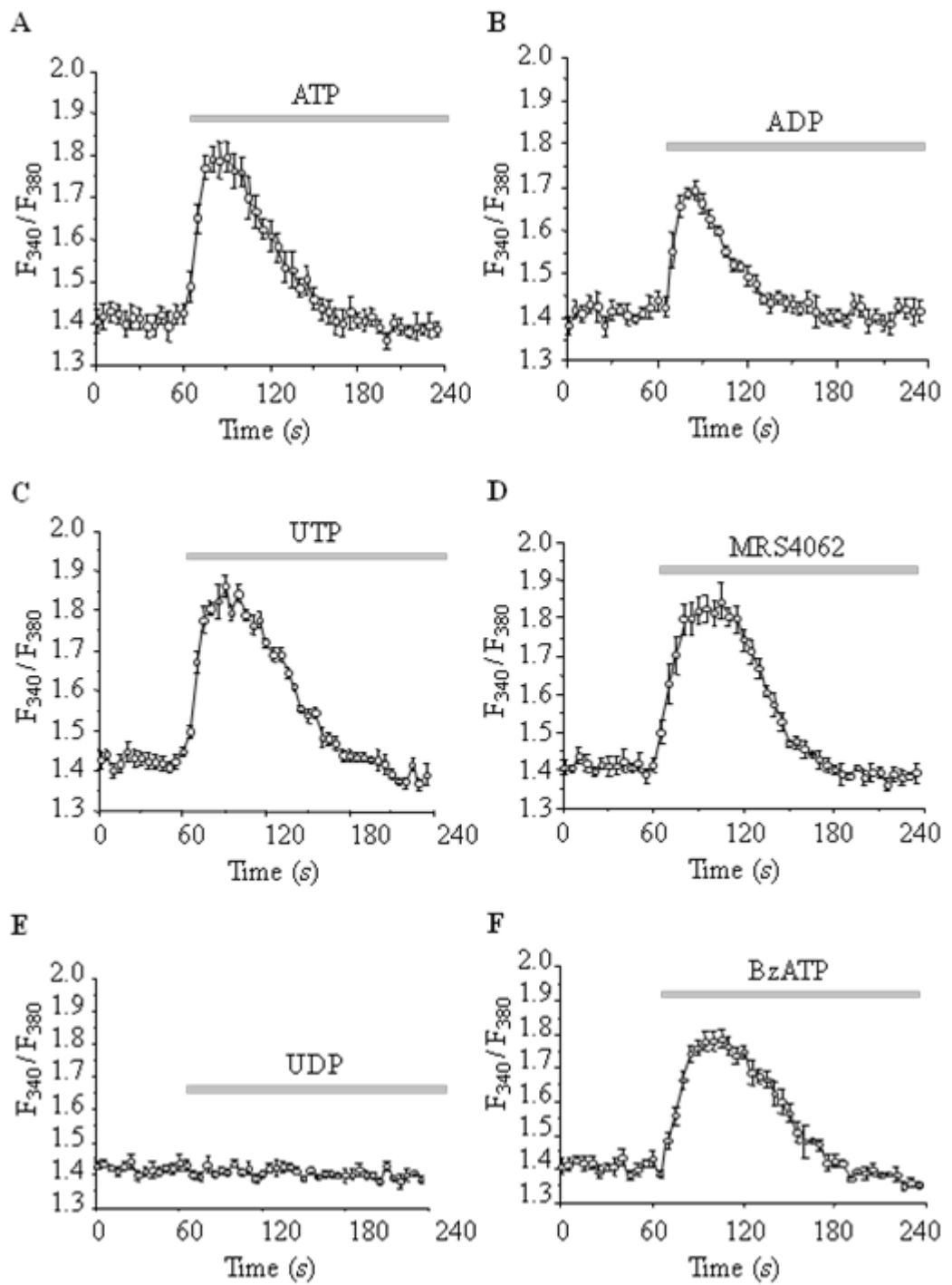


Figure 4.7 Inhibition of ATP-induced Ca^{2+} responses by P2X7 receptor antagonist AZ11645373.

(A) Representative Ca^{2+} responses to ATP in hDP-MSCs (P4, 21F) pretreated without or with AZ11645373 at 1 μ M. ATP at 300 μ M was used. (B-D) Summary of the average maximum change in the F_{340}/F_{380} in hDP-MSCs: (B) 21F; (C) 9F; (D) 32F. P4, N = 4 wells for each case. (E) The percentage of inhibition by AZ11645373 in hDP-MSCs from all three donors, n/N = 3/12 wells. *, $p < 0.05$, **, $p < 0.01$, ***, $p < 0.001$; compared to ATP alone.



(Figure 4.8)

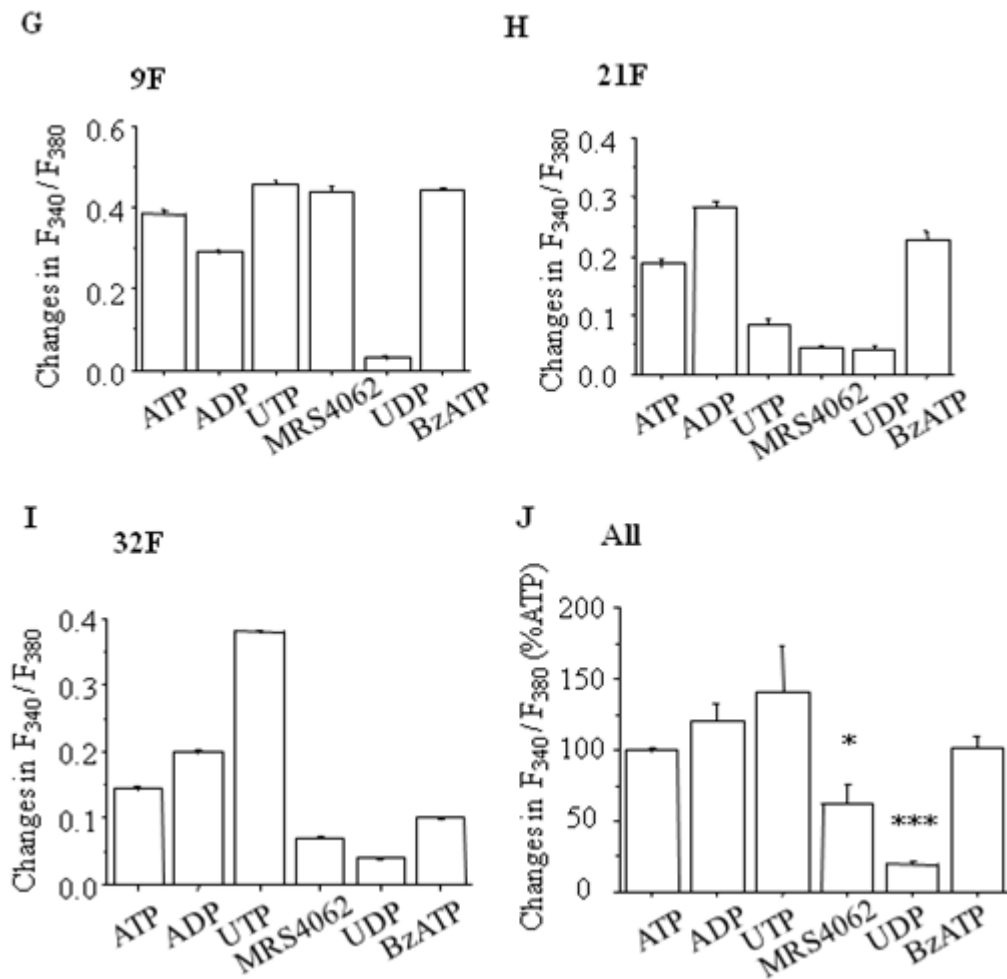


Figure 4.8 Ca^{2+} responses to P2Y receptor agonists in hDP-MSCs.

(A-F) Representative Ca^{2+} responses to 100 μ M ATP (A), ADP (B), UTP (C), MRS4062 (D), UDP (E) and BzATP (F) in hDP-MSCs (P4, 9F) in the absence of extracellular Ca^{2+} . (G-J) Summary of the average change in F_{340}/F_{380} as shown in A-F: (G) 9F, P4, N = 4 wells; (H) 21F, P4, N = 4 wells; (I) 32F, P4, N = 4 wells; (J) all donors, n/N = 3/12 wells. *, $p < 0.05$, **, $p < 0.01$, ***, $p < 0.001$; compared to ATP.

4.2.8 The role of P2X7 receptor in ATP-induced Ca²⁺ responses

The P2X7 mRNA expression and the sensitivity of ATP-induced Ca²⁺ responses to AZ11645373 support expression of the P2X7 receptor. In order to provide further evidence support contribution of the P2X7 receptor in ATP-induced Ca²⁺ signalling, Ca²⁺ responses to ATP or BzATP in cells transfected with P2X7 specific siRNA (siP2X7) were examined.

In order rule out the potential non-specific effect of scrambled or control siRNA (siControl), used as a negative control, the Ca²⁺ responses induced by 300 μM ATP in untransfected hDP-MSCs and hDP-MSCs transfected with siControl were examined. There was no significant difference in ATP-induced Ca²⁺ responses between untransfected and siControl-transfected cells (Figure 4.9A). Such observations were made in hDP-MSCs from all three donors (Figure 4.9B-E), suggesting that transfection with siControl has no discernible specific effect.

The mRNA expression level of the P2X7 receptor in hDP-MSCs transfected with siControl and siP2X7 was determined by real-time RT-PCR. Compared with cells treated with siControl, the mRNA expression level of the P2X7 receptor was reduced by 55 ± 5% using siP2X7 in hDP-MSCs from the donors 21F and 32F (n/N = 2/6) (Figure 4.10A-B). The reduced P2X7 expression by siRNA resulted in a significant decrease in ATP-induced Ca²⁺ responses in hDP-MSCs from all three donors (Figure 4.10C-F). The average decrease reached 27 ± 4% (n/N = 3/12) (Figure 4.10G). Treatment with siP2X7 also significantly decreased the Ca²⁺ responses induced by 300 μM BzATP (Figure 4.10H-K). The BzATP-induced Ca²⁺ responses were decreased on average by 34 ± 3% (Figure 4.10L). These results provide further evidence to support that the P2X7 receptor is expressed in hDP-MSCs and contributes to ATP-induced Ca²⁺ responses.

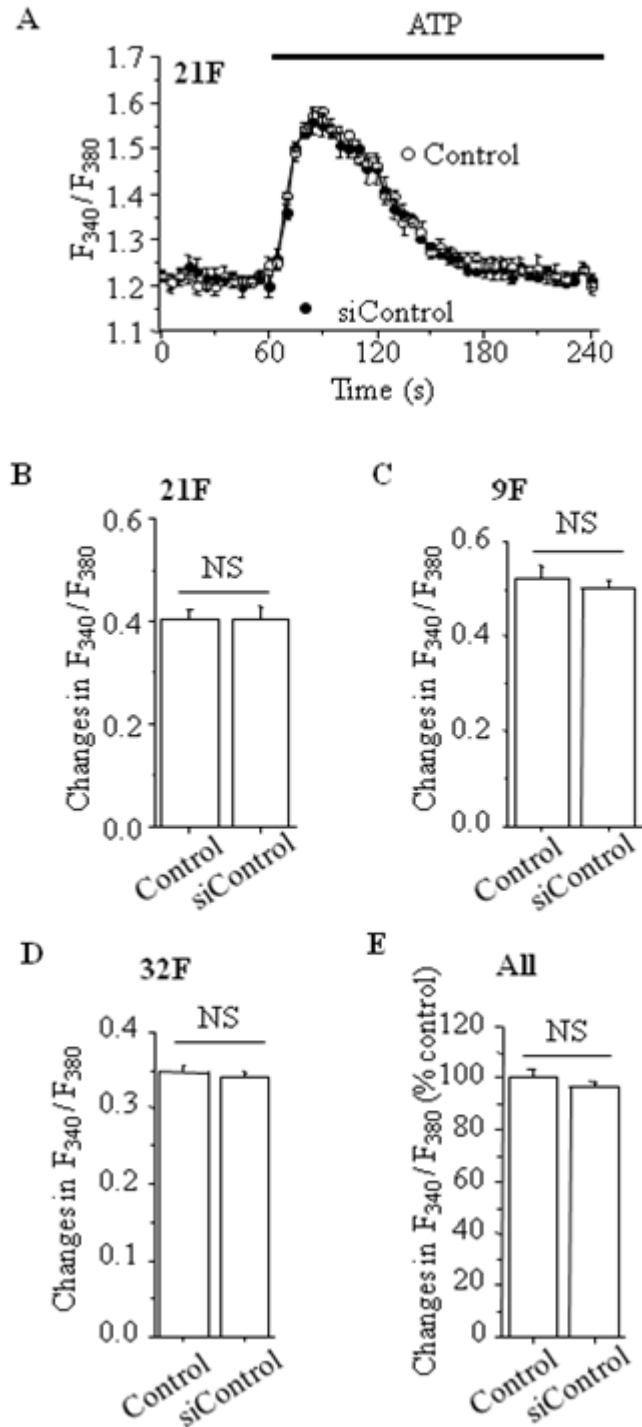
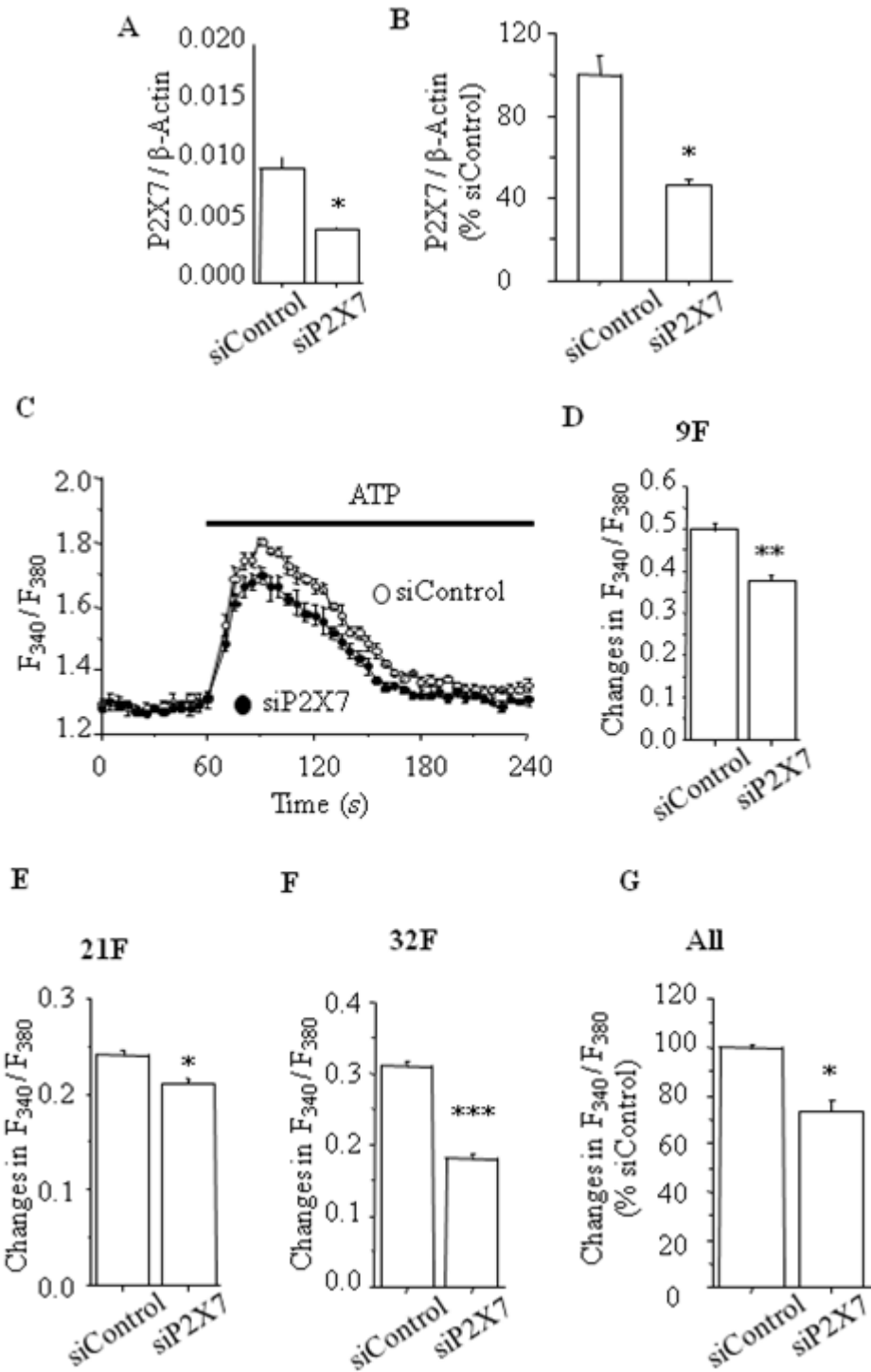


Figure 4.9 Effect of siControl on ATP-induced Ca²⁺ responses in hDP-MSCs.

(A) Typical ATP-induced Ca²⁺ responses in untransfected (control) or transfected hDP-MSCs (P4, 21F) with siControl. (B-D) Summary of the average maximum change in F_{340}/F_{380} : (B) 21F; (C) 9F; (D) 32F. P4, N = 4 wells for each case. ATP at 300 μ M was used. (E) Summary of the average maximum change of the F_{340}/F_{380} in all donors, n/N = 3/12 wells. NS, no significant difference compared to the control.



(Figure 4.10)

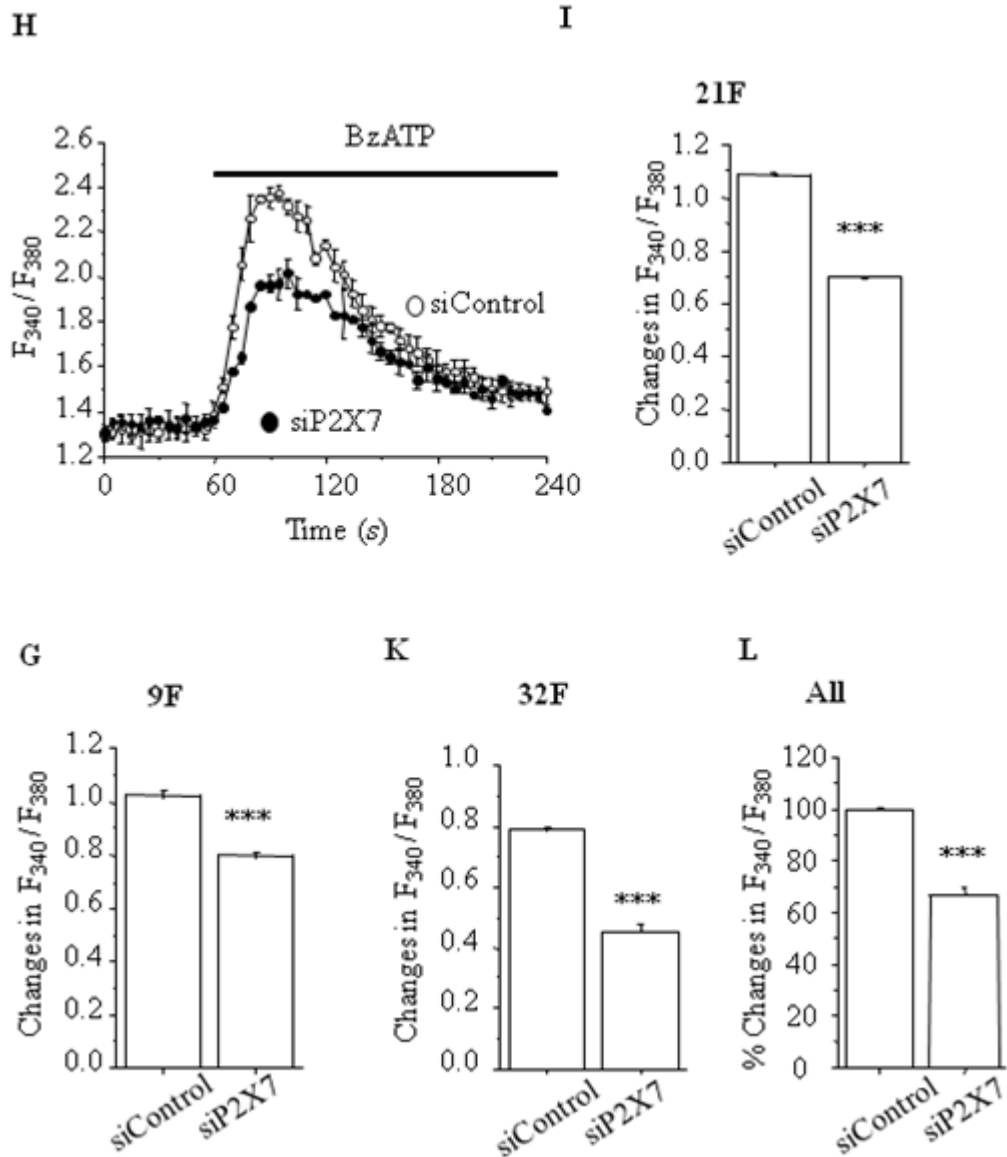


Figure 4.10 Effects of knocking down the P2X7 expression on Ca²⁺ responses by ATP and BzATP in hDP-MSCs.

(A) The mRNA expression level of P2X7 relative to that of β -actin in hDP-MSCs transfected with siP2X7 and siControl. $n/N = 2/6$ (21F, P4, $N = 3$ wells; and 32F, P4, $N = 3$ wells). (B) The mRNA expression level of P2X7 receptor in hDP-MSCs transfected with siP2X7 ($n/N = 2/6$) as percentage of that in hDP-MSCs transfected with siControl. (C) Typical ATP-induced Ca²⁺ responses in hDP-MSCs (9F, $N = 4$ wells) transfected with siP2X7 and siControl. ATP at 300 μ M was used. (D-G) Summary of the average maximum change in F_{340}/F_{380} : (D) 9F, P4, $N = 4$ wells; (E) 21F, P4, $N = 4$ wells; (F) 32F, P4, $N = 4$ wells; (G) all donors, $n/N = 3/12$. (H) Typical BzATP-induced Ca²⁺ responses in hDP-MSCs (9F, $N = 4$ wells) transfected with siP2X7 and siControl. BzATP at 300 μ M was used. (I-G) Summary of the average maximum change in F_{340}/F_{380} : (I) 21F, P4, $N = 4$ wells; (J) 9F, P4, $N = 4$ wells; (K) 32F, P4, $N = 4$ wells; (L) all donors, $n/N = 3/12$. *, $p < 0.05$, **, $p < 0.01$, ***, $p < 0.001$; compared to siControl.

4.2.9 The role of P2Y1 receptor in ATP-induced Ca²⁺ responses

The P2Y1 mRNA expression and ADP-induced Ca²⁺ responses support functional expression of P2Y1 receptors. To provide further independent evidence to support the P2Y1 receptor is involved in extracellular ATP-induced Ca²⁺ signalling, the Ca²⁺ responses to ATP or ADP in cells transfected with P2Y1 specific siRNA (siP2Y1) were determined. The mRNA expression level of the P2Y1 receptor in hDP-MSCs transfected with siControl and siP2Y1 was examined by real-time RT-PCR. Compared with cells treated with siControl, the mRNA expression level of the P2Y1 receptor was decreased by $81 \pm 5\%$ using siP2Y1 (Figure 4.11A-B). The reduced P2Y1 expression using siP2Y1 resulted in a significant decrease in ADP-induced Ca²⁺ responses in hDP-MSCs from all three donors (Figure 4.11C-F). The average decrease reached $51 \pm 9\%$ (Figure 4.11G). Knockdown of the P2Y1 receptor expression with siP2Y1 also significantly decreased the Ca²⁺ responses induced by ATP (Figure 4.12H-K). The average ATP-induced Ca²⁺ responses were attenuated by $43 \pm 8\%$ (Figure 4.11L). These results provide further strong evidence to support that the P2Y1 receptor is expressed in hDP-MSCs and contributes to ATP-evoked Ca²⁺ responses.

4.2.10 The role of P2Y11 receptor in ATP-induced Ca²⁺ responses

The P2Y11 mRNA expression and BzATP-induced Ca²⁺ responses in the extracellular Ca²⁺-free solutions support functional expression of the P2Y11 receptor. In order to investigate further contribution of the P2Y11 receptor in ATP-induced Ca²⁺ signalling, Ca²⁺ responses to ATP in cells transfected with P2Y11 specific siRNA (siP2Y11) were performed. The mRNA expression levels of the P2Y11 receptor were determined by RT-PCR in cells transfected with siControl and siP2Y11. Compared with cells treated with siControl, the mRNA expression level of the P2Y11 receptor was reduced by $51 \pm 5\%$ using siP2Y11 (Figure 4.12A-B). Reduced P2Y11 expression by siP2Y11 resulted in a significant decrease in ATP-induced Ca²⁺ responses in cells from all three donors (Figure 4.12C-F). The average decrease reached $35 \pm 6\%$ (Figure 4.12G). These results provide further evidence to support that P2Y11 receptor is expressed in these cells and contributes to ATP-evoked Ca²⁺ responses.

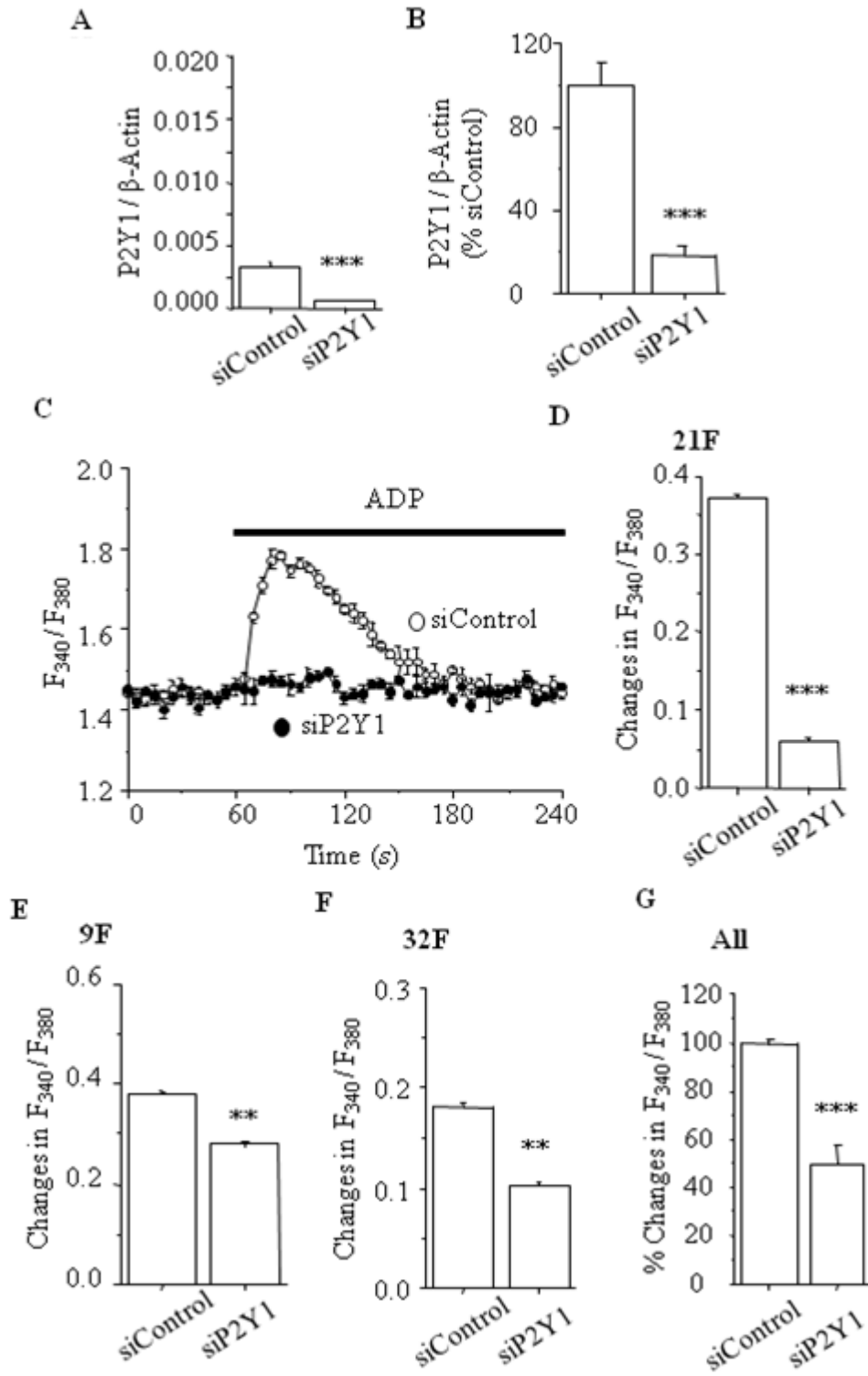


(Figure 4.11)

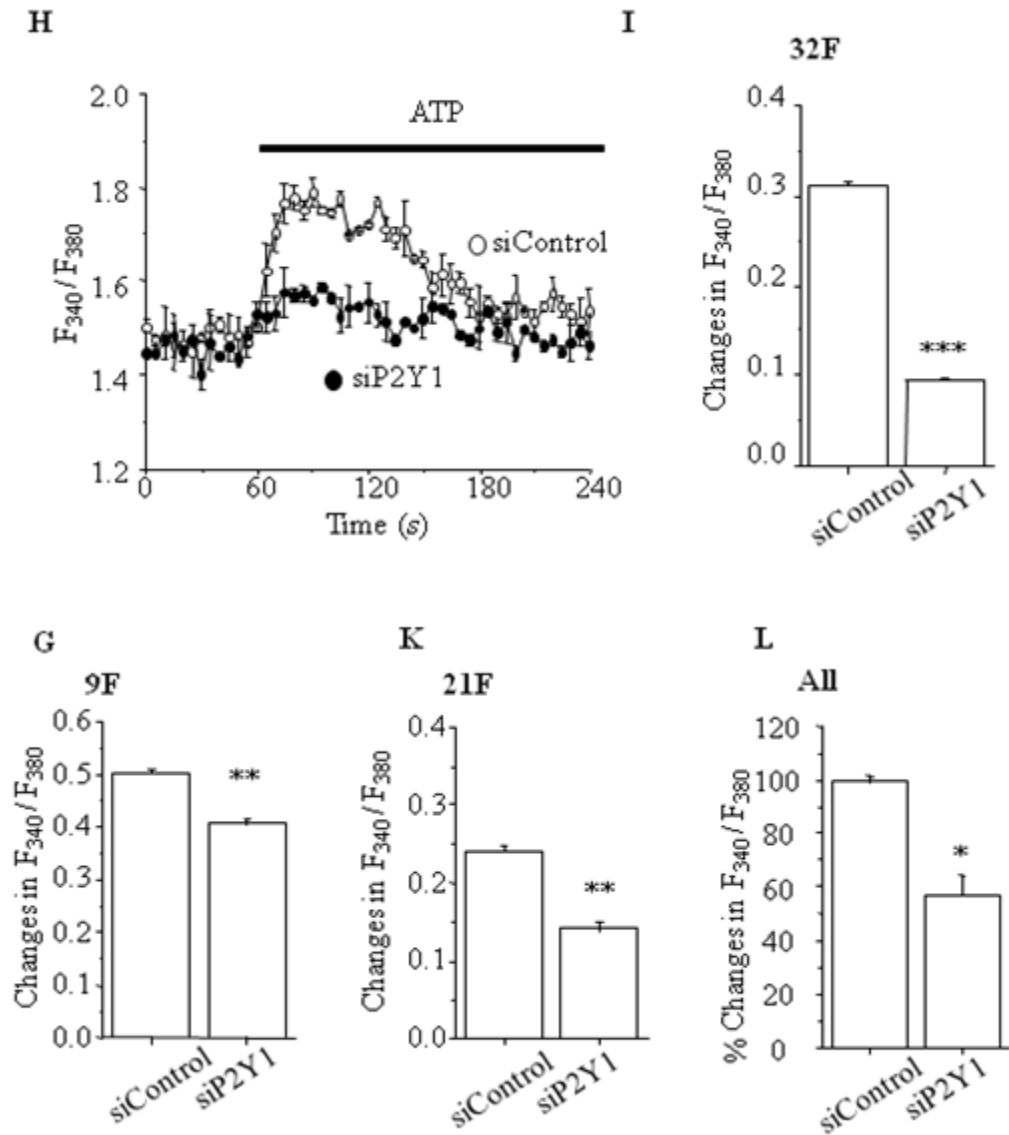


Figure 4.11 Effects of knocking down the P2Y1 expression on the Ca^{2+} responses by ADP and ATP in hDP-MSCs.

(A) The mRNA expression level of P2Y1 relative to that of β -actin in hDP-MSC from 21F and 32F transfected with siP2Y1 and siControl. 21F, P4, N = 3 wells and 32F, P4, N = 3 wells; n/N = 2/6. (B) The mRNA expression level of P2Y1 receptor in hDP-MSCs transfected with siP2Y1 (n/N = 2/6) as percentage of that in hDP-MSCs transfected with siControl. (C) Typical ADP-induced Ca^{2+} responses in hDP-MSCs (21F, P4, N = 4 wells) transfected with siP2Y1 and siControl. ADP at 100 μM was used. (D-G) Summary of the average maximum change in F_{340}/F_{380} : (D) 21F, P4, N = 4 wells; (E) 9F, P4, N = 4 wells; (F) 32F, P4, N = 4 wells; (G) all donors, n/N = 3/12. (H) Typical ATP-induced Ca^{2+} responses in hDP-MSCs (32F, N = 4 wells) transfected with siP2Y1 and siControl. ATP at 300 μM was used. (I-G) Summary of the average maximum change in F_{340}/F_{380} : (I) 32F, P4, N = 4 wells; (J) 9F, P4, N = 4 wells; (K) 21F, P4, N = 4 wells; (L) all donors, n/N = 3/12 wells. *, $p < 0.05$, **, $p < 0.01$, ***, $p < 0.001$; compared to siControl.

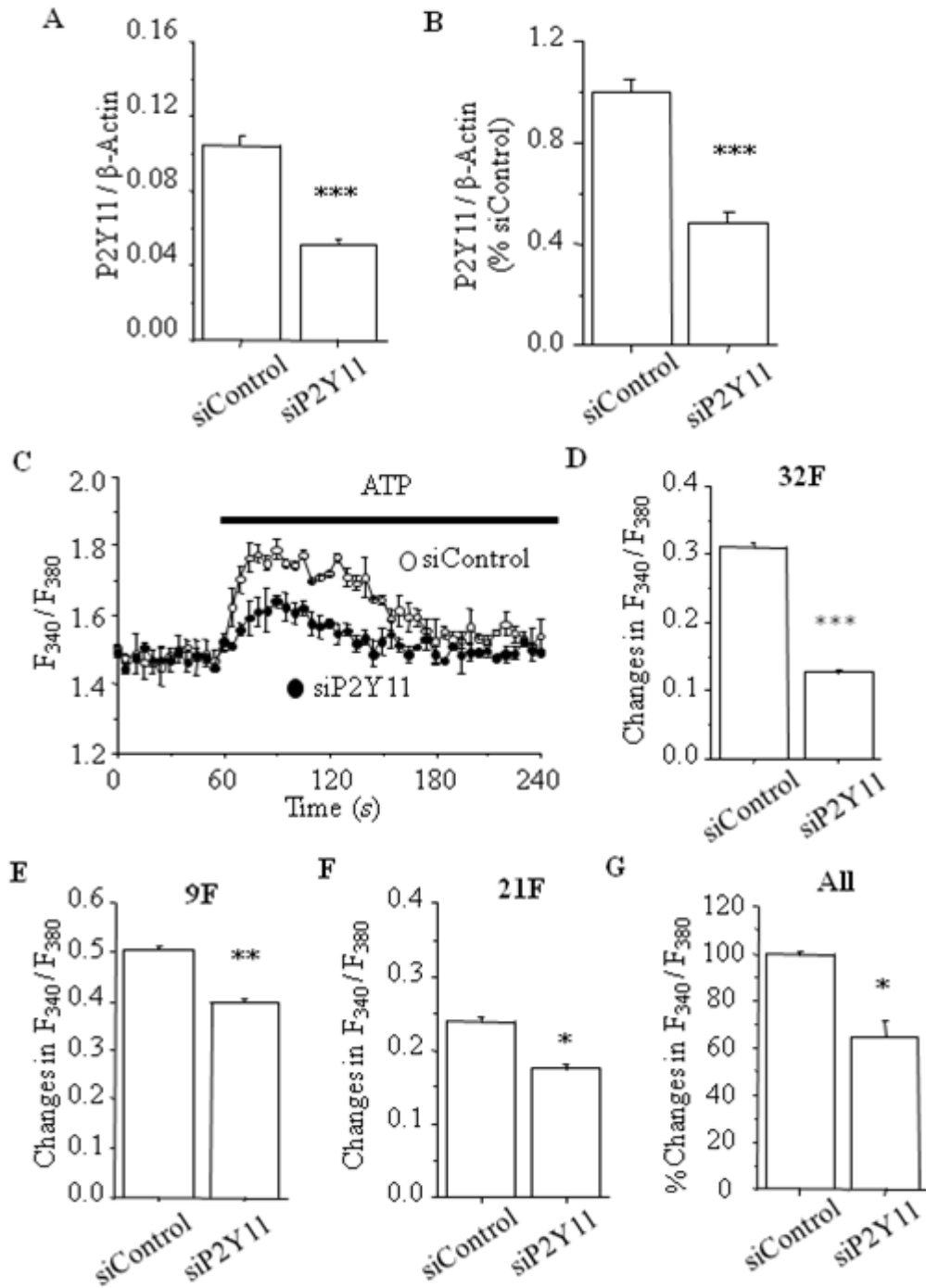


Figure 4.12 Effects of knocking down the P2Y11 expression on the Ca^{2+} responses by ATP in hDP-MSCs.

(A) The mRNA expression level of P2Y11 relative to that of β -actin in hDP-MSCs transfected with siP2Y11 and siControl. 21F, P4, N = 3 wells and 32F, P4, N = 3 wells; n/N = 2/6. (B) The mRNA expression level of P2Y11 receptor in hDP-MSCs transfected with siP2Y11 (n/N = 2/6) as percentage of that in hDP-MSCs transfected with siControl. (C) Typical ATP-induced Ca^{2+} responses in hDP-MSCs (32F, P4, N = 4 wells) transfected with siP2Y11 and siControl. ATP at 300 μ M was used. (D-G) Summary of the average maximum change in F_{340}/F_{380} : (D) 32F, P4, N = 4 wells; (E) 9F, P4, N = 4 wells; (F) 21F, P4, N = 4 wells; (G) all donors, n/N = 3/12. *, $p < 0.05$, **, $p < 0.01$, ***, $p < 0.001$; compared to siControl.

4.3 Discussion

The results described in this chapter have provided compelling evidence to demonstrate functional expression of several ATP-sensitive P2 receptors in hDP-MSCs, including the P2X7, P2Y1 and P2Y11 receptors.

Single cell imaging analyzing the Ca^{2+} responses in individual cells showed that ~30% cells displayed spontaneous Ca^{2+} oscillations (Figure 4.1C). Such spontaneous Ca^{2+} oscillations were reported in hBM-MSCs by previous studies (Kawano, Shoji et al. 2002; Kawano, Otsu et al. 2003; Kawano, Otsu et al. 2006). An early study reported a much higher proportion of cells exhibited spontaneous Ca^{2+} oscillations in the presence of extracellular Ca^{2+} (72%) and in the absence of extracellular Ca^{2+} (67%) (Kawano, Shoji et al. 2002). The frequencies of the Ca^{2+} oscillations were virtually the same in the extracellular Ca^{2+} -containing and Ca^{2+} -free solutions. However, increasing the extracellular Ca^{2+} concentration significantly enhanced the amplitude of Ca^{2+} oscillations without effect on the frequency of Ca^{2+} oscillations, indicating that the Ca^{2+} entry across the plasma membrane does not directly determine the frequency of Ca^{2+} oscillations but is required to refill the intracellular Ca^{2+} stores and increase the intensity of subsequent Ca^{2+} oscillations. The spontaneous Ca^{2+} oscillations were prevented by application of TG (1 μM), demonstrating that the Ca^{2+} oscillations result mainly from Ca^{2+} release from the ER (Kawano, Shoji et al. 2002). A later study further demonstrated that hBM-MSCs secreted ATP, and that ATP release was important in sustaining the spontaneous Ca^{2+} oscillations. The spontaneous Ca^{2+} oscillations were completely blocked by PPADS (100 μM), U73122 (a PLC blocker; 10 μM) or transfection with an IP_3 -binding protein (pTRE- IP_3 sponge) to buffer the cytosolic IP_3 and prevent IP_3 -induced Ca^{2+} release, and also abolished by 2-APB (an IP_3 receptor and SOC blocker, 75 μM) (Kawano, Otsu et al. 2006). The authors of these studies have proposed that the Ca^{2+} oscillations result from ATP release and subsequent activation of the P2Y receptors leads to activation of

PLC to generation of IP₃, which binds to the IP₃ receptors to cause Ca²⁺ release from ER and subsequent Ca²⁺ entry through the plasma membrane to refill the ER store. Such mechanisms may also explain the spontaneous Ca²⁺ oscillations in hDP-MSCs observed in the present study.

A majority of hDP-MSC responded to extracellular ATP in the extracellular Ca²⁺-free solutions with strong and rapid increases in the [Ca²⁺]_i (Figure 4.1E), indicating that intracellular Ca²⁺ is released, most likely from the ER store subsequent to activation of the ATP-sensitive P2Y receptors (Burnstock, Fredholm et al. 2010). The ATP-induced increases in the [Ca²⁺]_i in the extracellular Ca²⁺-containing solutions were significantly prolonged as compared those in the extracellular Ca²⁺-free solutions (Figure 4.1G), suggesting that extracellular Ca²⁺ entry also contributes to increases in the [Ca²⁺]_i. As discussed in the Introduction chapter (see section 1.3.3), extracellular ATP can activate two structurally and functional subfamilies of P2 purinergic receptors, P2X and P2Y. All the P2X receptors are activated by ATP and mediate extracellular Ca²⁺ entry, while five of the eight P2Y receptors, P2Y1, P2Y2, P2Y4, P2Y6 and P2Y11, are coupled to the PLC-IP₃ signalling that can mobilize the intracellular Ca²⁺ release from the ER, and three of them are sensitive to ATP, P2Y1, P2Y2 and P2Y11. The results from real-time RT-PCR in the present study show the mRNA expression of the P2X4, P2X6, P2X7, P2Y1, P2Y4, P2Y6 and P2Y11 receptors in hDP-MSCs (Figure 4.2A-B). The P2Y2 mRNA expression was detected in only the 9F donor and at a low level. There was no detectable mRNA expression of the P2X1, P2X2, P2X3 and P2X5 receptors (Figure 4.2A-B). A previous study using RT-PCR detected the mRNA expression of all PX and P2Y receptors except P2X2 in hBM-MSCs (Ferrari, Gulinelli et al. 2011). Taken together, the present and previous studies are consistent in showing the mRNA expression of the P2X4, P2X6 and P2X7 and P2Y1, P2Y4, P2Y6 and P2Y11 and lack of the P2X2 mRNA expression in hDP-MSCs and hBM-MSCs. The two studies also indicate difference in MSCs from two different origins in terms of the mRNA expression for the P2X1, P2X3, P2X5 and

P2Y2 receptors.

A functional characterization of the P2 receptors expression in hDP-MSCs cells was further carried out to examine the functional expression of these receptors by monitoring the changes in the $[Ca^{2+}]_i$ in response to ATP and other receptor subtype selective agonists and the effects of generic and receptor selective antagonists. First of all, ATP evoked a strong increase in the $[Ca^{2+}]_i$ in the presence of extracellular Ca^{2+} (Figure 4.3A-C). ATP-induced responses were significantly inhibited by PPADS (Figure 4.3 D-G), supporting the expression of ATP-sensitive P2 receptors.

The mRNA expression of P2X1, P2X2, P2X3 and P2X5 was undetected (Figure 4.2B). There was no discernible response to $\alpha\beta$ meATP up to 100 μ M (Figure 4.4B, D-F). This is consistent with lack of mRNA expression of P2X1 and P2X3. Taken together, these results support no functional expression of the P2X1 and P2X3 receptors. ATP-evoked Ca^{2+} responses were not inhibited by 5-BDBD at 10 μ M (Figure 4.6A-E) that is a potent and selective antagonist at the P2X4 receptor and shows no activity at other P2 receptors (Casati, Frascoli et al. 2011), suggesting no expression of the functional P2X4 receptor despite that the P2X4 mRNA expression was consistently detected in these cells from all three donors (Figure 4.2A).

BzATP is more potent than ATP for the P2X7 receptor but equipotent with or less potent than ATP for other P2X receptors (North and Surprenant 2000) (see section 1.3.2.7). BzATP evoked greater responses than ATP at the same concentration (300 μ M) in the extracellular Ca^{2+} -containing solutions (Figure 4.4D-F). In addition, ATP-evoked responses were substantially reduced by AZ11645373 (Figure 4.7A-E), a hP2X7 receptor selective antagonist (Stokes, Jiang et al. 2006; Jiang 2012). Furthermore, down-regulation of the P2X7 expression using siRNA resulted in a significant reduction in the Ca^{2+} responses induced by ATP (Figure 4.10C-G) and

BzATP (Figure 4.10H-L). Taken together, these results provided consistent evidence to support expression of the functional P2X7 receptor in hDP-MSCs. Consistently, several studies have shown the expression of P2X7 receptor in hBM-MSCs, using RT-PCR, Western blotting and immunofluorescent staining (Sun, Junger et al. 2013), and using KN-62 to show significant inhibition of ATP-induced Ca^{2+} responses (Ferrari, Gulinelli et al. 2011). Therefore, the P2X7 receptor is expressed in MSCs from dental pulp and bone marrow, and contributes in mediating ATP-induced Ca^{2+} signalling.

The present study also provided strong evidence for functional expression of several P2Y receptors in hDP-MSCs. Activation of the P2Y1-like receptors can lead to intracellular Ca^{2+} release; ADP acts as an agonist at the P2Y1 receptor, while UTP activates the P2Y2 and P2Y4 receptors, MRS4062 is a selective agonist for the P2Y4 receptor, UDP for the P2Y6 receptor, and BzATP for the P2Y11 receptor (see section 1.3.3 in the Introductory chapter). In hDP-MSCs, ATP, ADP, UTP, MRS4062 and BzATP evoked considerable Ca^{2+} responses in the extracellular Ca^{2+} -free solution, whereas UDP induced very low or undetectable responses (Figure 4.8A-J). These results taken together with the results from RT-PCR (Figure 4.2C), suggest that hDP-MSC mainly functionally express the P2Y1, P2Y4 and P2Y11 receptors, but not the P2Y2 and P2Y6 receptors. Therefore, ATP-induced intracellular Ca^{2+} release are mainly mediated by the P2Y1 or/and P2Y11 receptor in hDP-MSCs. Transfection with siP2Y1 significantly decreased Ca^{2+} responses evoked by ATP as well as by ADP (Figure 4.11C-L), while transfection with siP2Y11 reduced ATP-evoked Ca^{2+} responses (Figure 4.12C-G), confirming functional expression of the P2Y1 and P2Y11 receptors. These results provide compelling evidence to indicate that a significant contribution of the P2Y1 and P2Y11 in ATP-induced Ca^{2+} signalling in hDP-MSCs. The expression of ATP-sensitive P2Y receptors in BM-MSCs from human and rabbit was examined in several studies. The protein expression of the P2Y1, P2Y2 and P2Y11 receptors were demonstrated in hBM-MSCs by

immunostaining and Western blotting (Ichikawa and Gemba 2009). Activation of the P2Y1 receptor has been implicated in ATP-induced outward K^+ currents (Coppi, Pugliese et al. 2007) and spontaneous Ca^{2+} oscillations (Kawano, Otsu et al. 2006). However, another study suggests expression of the P2Y11 but not the P2Y1 receptor using immunofluorescent staining (Riddle, Taylor et al. 2007).

In conclusion, the results from the experiments presented in this chapter show that the P2X7, P2Y1 and P2Y11 receptors are functionally expressed and contribute to extracellular ATP-induced Ca^{2+} signalling in hDP-MSCs.

Chapter 5

Expression of Stim/Orai SOC Channels in Human Dental Pulp

Mesenchymal Stem Cells

5.1 Introduction

The results described in chapter 4 provide evidence to show that ATP-sensitive P2Y1 and P2Y11 receptors are functionally expressed in hDP-MSCs and contribute in ATP-evoked Ca^{2+} signalling by inducing Ca^{2+} release from the ER store. As discussed in the Introduction chapter (see section 1.3.4), Ca^{2+} release from the ER can activate the SOC channels on the cell surface that mediate extracellular Ca^{2+} entry into the cell in order to refill the Ca^{2+} store in the ER (McHale, Hollywood et al. 2006). Previous studies have reported that such Ca^{2+} entry is mediated through the SOC channels upon depletion of the ER Ca^{2+} store in stem cells (Yanagida, Shoji et al. 2004), including BM-MSCs (Kawano, Shoji et al. 2002), but the molecular components forming the SOC channels remain elusive. Recent studies have shown that Ca^{2+} entry through the SOC channels plays a significant role in the proliferation, migration and differentiation of stem cells (Shin, Hong et al. 2010; Li, Chen et al. 2012; Xie, Xu et al. 2014).

Therefore, the aim of the study described in this chapter was to investigate expression of the SOC channels and their contribution in ATP-induced Ca^{2+} signalling mechanism in hDP-MSCs. The changes in the $[\text{Ca}^{2+}]_i$ in hDP-MSCs were measured using single cell Ca^{2+} imaging and FLEXstation. The mRNA expression level of the SOC channel components was examined by real-time RT-PCR. Finally, the role of the SOC channels in ATP-induced Ca^{2+} signalling was evaluated using SOC channel

inhibitors to suppress the channel function and specific siRNA to reduce the expression of the SOC channels.

5.2 Results

5.2.1 Single cell Ca^{2+} responses to TG and ATP

To investigate the functional expression of the SOC channels in individual hDP-MSCs, single cell Ca^{2+} imaging was carried out using in combination with the widely used Ca^{2+} add-back protocols; pretreatment of cells with TG depleted the Ca^{2+} store in the ER in the extracellular Ca^{2+} -free solutions and thereby activated the SOC channels, and the Ca^{2+} entry through the activated SOC channels were measured by adding Ca^{2+} back to the extracellular solution.

In hDP-MSCs pre-treated with 1 μM TG for 30 minutes in the absence of extracellular Ca^{2+} , addition of extracellular Ca^{2+} resulted in a strong increase in the $[\text{Ca}^{2+}]_i$ in all individual cells (N = 18 in 18 cells), whereas a small increase in the $[\text{Ca}^{2+}]_i$ was observed in control cells or DMSO-treated cells (N = 15 in 15 cells) (Figure 5.1A-D), indicating emptying the Ca^{2+} store in the ER induces robust SOCE in all individual cells.

Experiments were also conducted to examine ATP-induced SOCE. Treatment with 100 μM ATP evoked intracellular Ca^{2+} release, as shown by a transient increase in the $[\text{Ca}^{2+}]_i$ in the absence of extracellular Ca^{2+} solutions. There were robust increases in the $[\text{Ca}^{2+}]_i$ upon addition of Ca^{2+} into the extracellular solutions, after ATP was washed (Figure 5.1E). These results from single cell Ca^{2+} imaging suggest that the SOC channels are functionally expressed in hDP-MSCs that can be activated by ATP via activation of the P2Y receptors

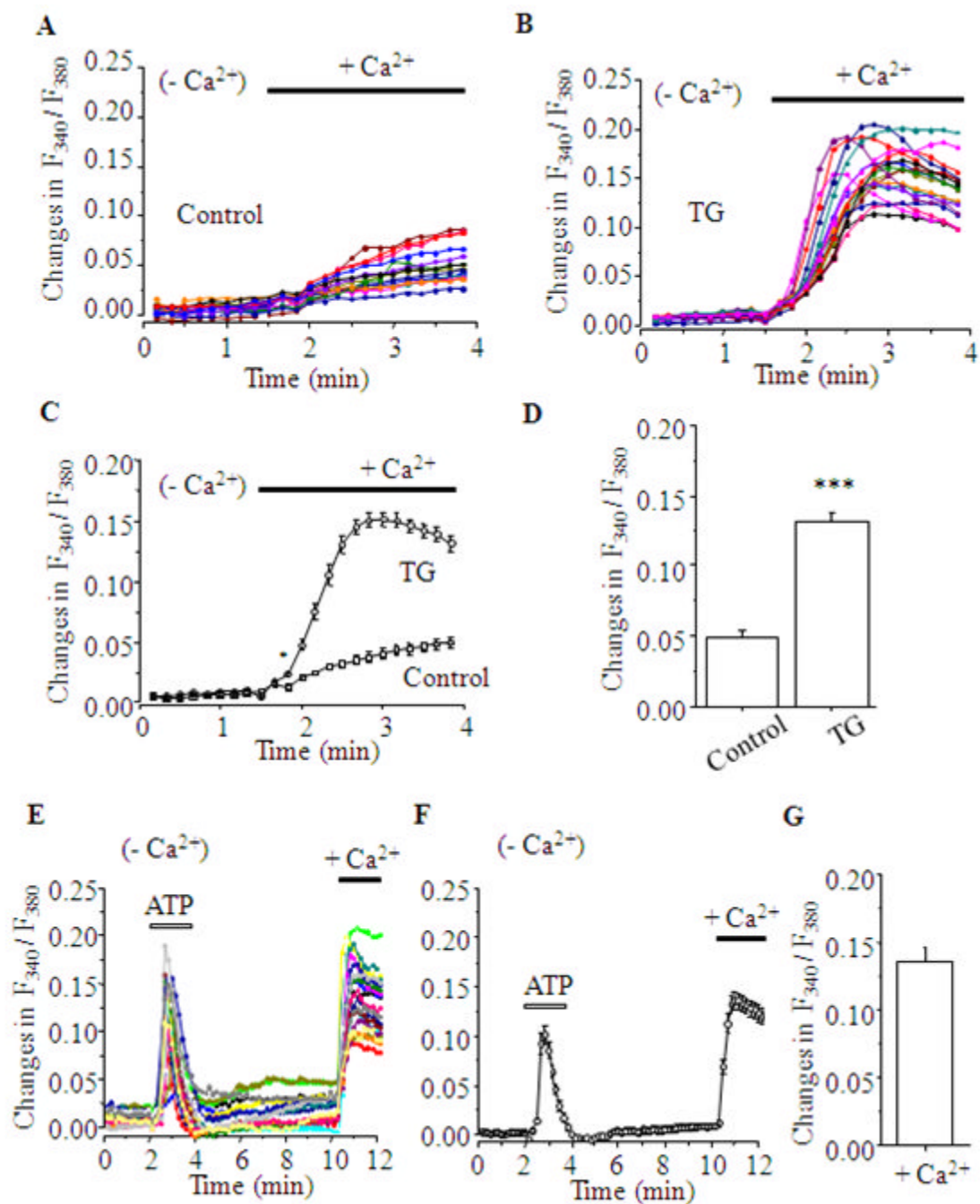


Figure 5.1 Single cell Ca^{2+} responses to TG and ATP in hDP-MSCs.

(A-B) Typical Ca^{2+} responses in single hDP-MSC (P4, 9F) without (A, N = 15 in 15 cells) and with pretreatment with TG at 1 μM (B, N = 18 in 18 cells). (C) Summary of the average change in F_{340}/F_{380} in individual cells. (D) Summary of the average maximum change in F_{340}/F_{380} after Ca^{2+} add-back in the control cells and cells pretreated with TG. (E-F) Typical Ca^{2+} responses (E, N = 19 in 19 cells) and the average change in F_{340}/F_{380} (F) in cells treated with ATP at 100 μM in the absence of extracellular Ca^{2+} and after Ca^{2+} add-back. (G) Summary of the average maximum change in F_{340}/F_{380} in cells treated with ATP after Ca^{2+} add-back. *, $p < 0.05$; **, $p < 0.01$; ***, $p < 0.001$; compared to the control.

5.2.2 mRNA expression levels of SOC channel component proteins

As discussed in the Introduction chapter (see section 1.3.4), Orai and Stim proteins have been identified as the key components of the SOC channels. Therefore, the expression of Orai and Stim in hDP-MSCs was examined using real-time RT-PCR. As shown in Figure 5.2A, the mRNA transcripts for Orai1, Orai2, Orai3, Stim1 and Stim2 were detected in hDP-MSCs from all three donors. The mRNA expression level relative to β -actin is summarized in Figure 5.2 B. In hDP-MSCs from all three donors, Orai3 showed the highest expression level among three Orai genes, and the expression level for Stim1 and Stim2 was similar.

5.3.3 Effects of extracellular Ca^{2+} on constitutively active Ca^{2+} -permeable conductance

Removal of the extracellular Ca^{2+} and subsequent addition of Ca^{2+} back into the extracellular solutions revealed a constitutively active Ca^{2+} conductance in hDP-MSCs (Figure 5.1A). To better understand this Ca^{2+} conductance, changes in the $[\text{Ca}^{2+}]_i$ upon addition of various concentrations of extracellular Ca^{2+} were measured using FLEXstation (Figure 5.3A). The $[\text{Ca}^{2+}]_i$ was rapidly increased as the extracellular Ca^{2+} concentration was increased from 0 mM to 0.03, 0.1, 0.3, 1, 3, 5 mM (Figure 5.3B). These results support the Ca^{2+} entry take place through such constitutively active Ca^{2+} -permeable conductance in cells.

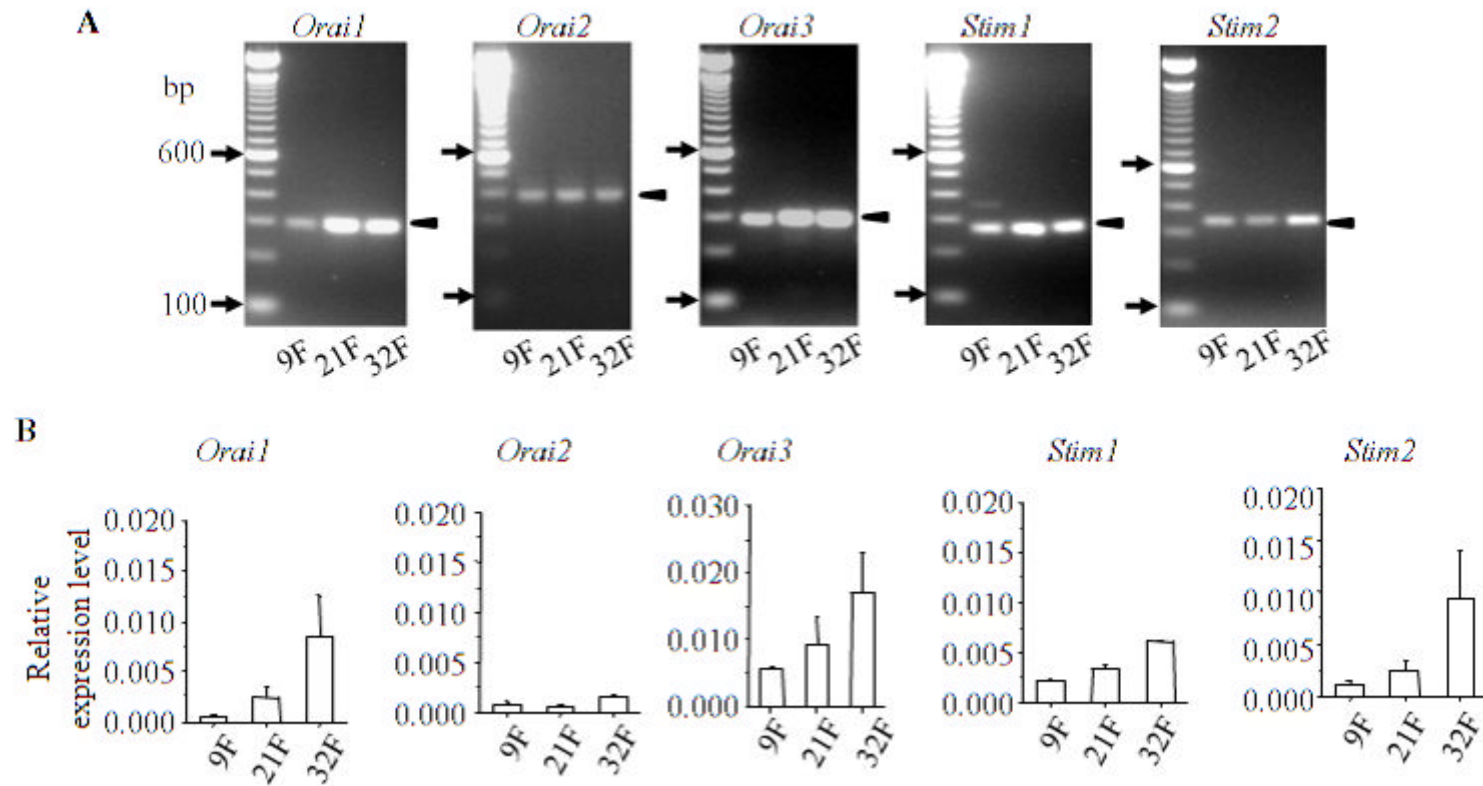


Figure 5.2 The mRNA expression of the SOC channels in hDP-MSCs.

(A) Representative images of agarose gel analysis of PCR products. The expression of *Orai1*, *Orai2*, *Orai3*, and *Stim1*, *Stim2* was consistently observed. (B) Summary of the mRNA expression level relative to β -actin for *Orai1*, *Orai2*, *Orai3*, and *Stim1*, *Stim2* in hDP-MSCs for each of the three donors (P4; 9F, 21F and 32F) from two independent experiments, each in triplicate ($n/N = 2/6$).

5.3.4 Effects of 2-APB on the constitutively active Ca^{2+} -permeable conductance

Further experiments were conducted to characterize the constitutively active Ca^{2+} -permeable conductance by determining the effect of 2-APB. Figure 5.3C illustrates the Ca^{2+} responses in the absence of extracellular Ca^{2+} and subsequent addition of extracellular Ca^{2+} in hDP-MSCs pretreated with 2-APB at different concentrations for 10 minutes. As summarized in Figure 5.3D, 2-APB from 1 μM to 30 μM did not significantly alter the $[\text{Ca}^{2+}]_i$, but it at 50 μM and 100 μM induced detectable intracellular Ca^{2+} release. Pretreatment with 2-APB at 1 μM and 5 μM did not significantly inhibit the increases in the $[\text{Ca}^{2+}]_i$ upon addition of extracellular Ca^{2+} , but it at high concentrations from 10 μM to 100 μM significantly blocked such increases, with 100 μM resulting in a complete inhibition (Figure 5.3D). These results show that 2-APB at concentrations of 10-100 μM cause a concentration-dependent inhibition of the constitutively active Ca^{2+} -permeable conductance. In addition, these results show 2-APB at high concentrations (50-100 μM) can induce intracellular Ca^{2+} release.

5.3.5 Effects of Synta66 on the constitutively active Ca^{2+} -permeable conductance

Synta66 is a selective SOC channel inhibitor (Putney 2010; Li, Cubbon et al. 2011; van Kruchten, Braun et al. 2012). The effect of Synta66 on the constitutively active Ca^{2+} -permeable conductance was also examined. As shown in Figure 5.3E and F, Synta66 from 1 μM to 10 μM did not significantly change the $[\text{Ca}^{2+}]_i$ in the extracellular Ca^{2+} -free solutions, suggesting no Ca^{2+} release. It also did not significantly inhibit the increases on the $[\text{Ca}^{2+}]_i$ after addition of extracellular Ca^{2+} , suggesting Synta66 at the concentrations (1-10 μM) examined have no effect on the constitutively active Ca^{2+} -permeable conductance.

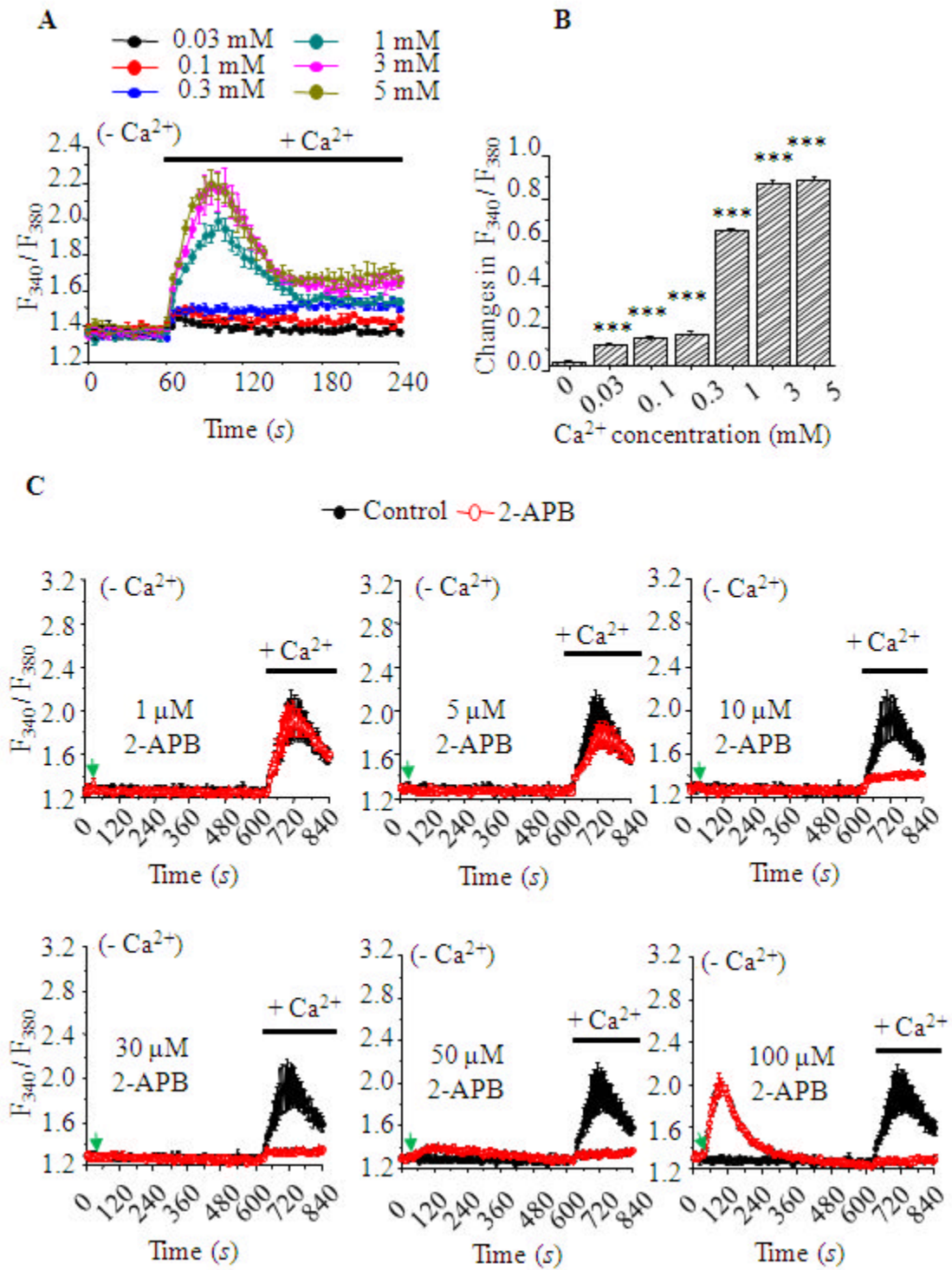


(Figure 5.3)

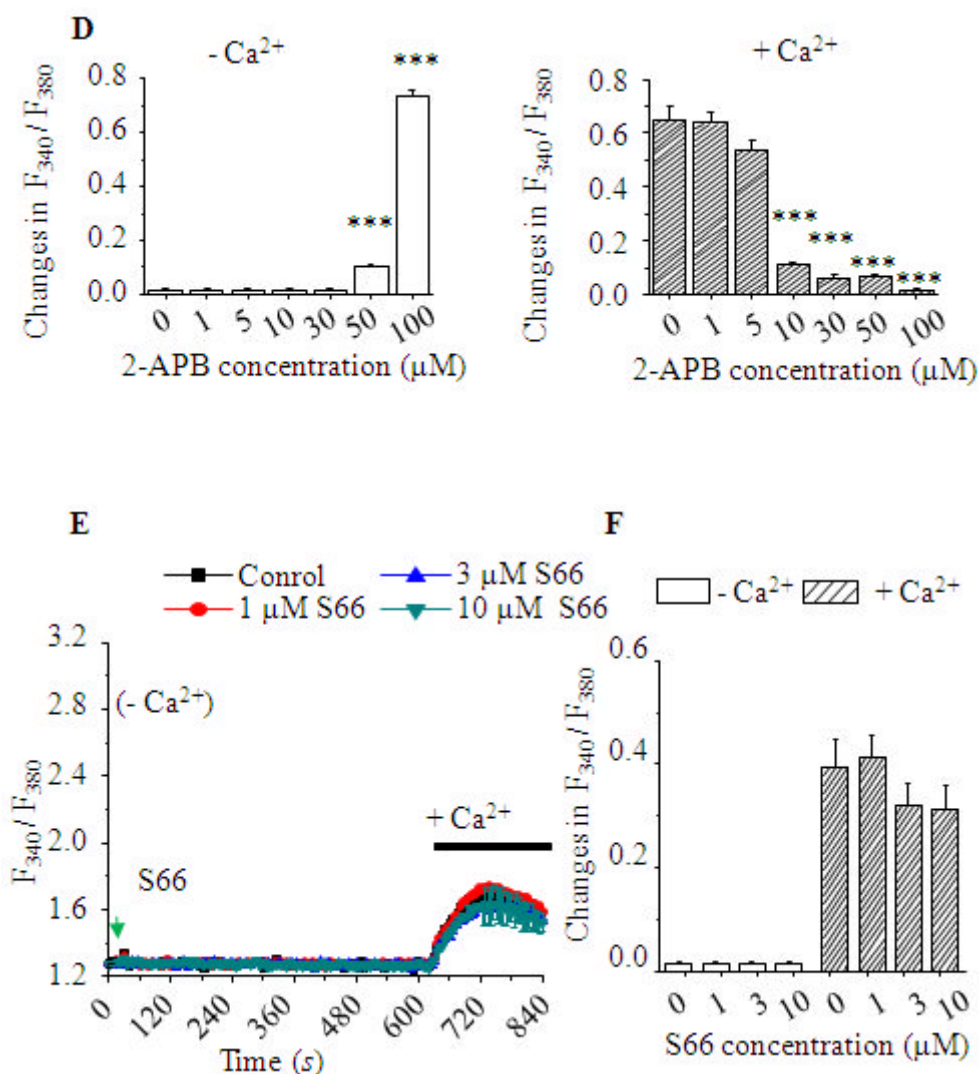


Figure 5.3 Characterization of the constitutively active Ca²⁺ conductance.

(A) Typical Ca²⁺ responses in hDP-MSCs (P4, 9F) after addition of Ca²⁺ from 0.03 mM to 5 mM into the extracellular Ca²⁺-free solution. (B) Summary of the average change in F₃₄₀/F₃₈₀ in cells shown in (A). N = 4 wells (C) The Ca²⁺ responses in the absence of extracellular Ca²⁺ and subsequent addition of extracellular Ca²⁺ in control cells (9F) and cells treated with 2-APB at 1, 5, 10, 30, 50 and 100 μM. (D) Summary of the average maximum change in F₃₄₀/F₃₈₀ in control cells (9F, P4, n/N = 3/12 wells) and cells treated with 2-APB in the extracellular Ca²⁺-free solution and after addition of Ca²⁺. (E) The Ca²⁺ responses in control cells (9F) without and with treatment with Synta66 (S66) at 1, 3 and 10 μM. (F) Summary of the average maximum change in F₃₄₀/F₃₈₀ in control cells (9F, P4, n/N = 3/12 wells) and cells treated with Synta66 in the extracellular Ca²⁺-free solution and after addition of Ca²⁺. *, *p* < 0.05; **, *p* < 0.01; ***, *p* < 0.001; compared to the control.

5.3.6 Ca^{2+} responses in TG-treated cells

To further investigate the functional expression of the SOC channels in hDP-MSCs, $[\text{Ca}^{2+}]_i$ in cells treated without and with TG were measured. As expected, treatment with TG at 1 μM induced significant Ca^{2+} release in the absence of extracellular Ca^{2+} solutions (Figure 5.4A and B). Subsequent addition of extracellular Ca^{2+} resulted in increases in the $[\text{Ca}^{2+}]_i$ (Figure 5.4A and B), which are much greater in TG-treated cells than in control cells without treatment with TG. These results indicate that TG induces extracellular Ca^{2+} entry through the SOC channels in hDP-MSCs.

5.3.7 Effects of 2-APB on TG-induced Ca^{2+} responses

The effects of 2-APB on TG-induced Ca^{2+} responses were investigated. As described in Figure 5.3D, 2-APB at 1 μM and 5 μM had no effect on the Ca^{2+} responses mediated by the constitutively active Ca^{2+} -permeable conductance in control cells without treatment with TG. 2-APB at these concentrations also did not affect TG-induced Ca^{2+} release in the extracellular Ca^{2+} -free solutions (Figure 5.4C-D). However, 2-APB at 5 μM significantly reduced the increases in the $[\text{Ca}^{2+}]_i$ following addition of extracellular Ca^{2+} in TG-treated cells (Figure 5.4C-D). TG-induced Ca^{2+} responses were obtained by subtracting the contribution of the constitutively active Ca^{2+} -permeable conductance in the matched control cells. 2-APB at 5 μM had no significant effect on the peak amplitude of TG-induced Ca^{2+} responses but significantly inhibited the sustained Ca^{2+} responses at the end of the experiments that is, measured at 210 seconds after addition of extracellular Ca^{2+} (Figure 5.4E). These results provide further evidence to support functional expression of the SOC channels in hDP-MSCs.

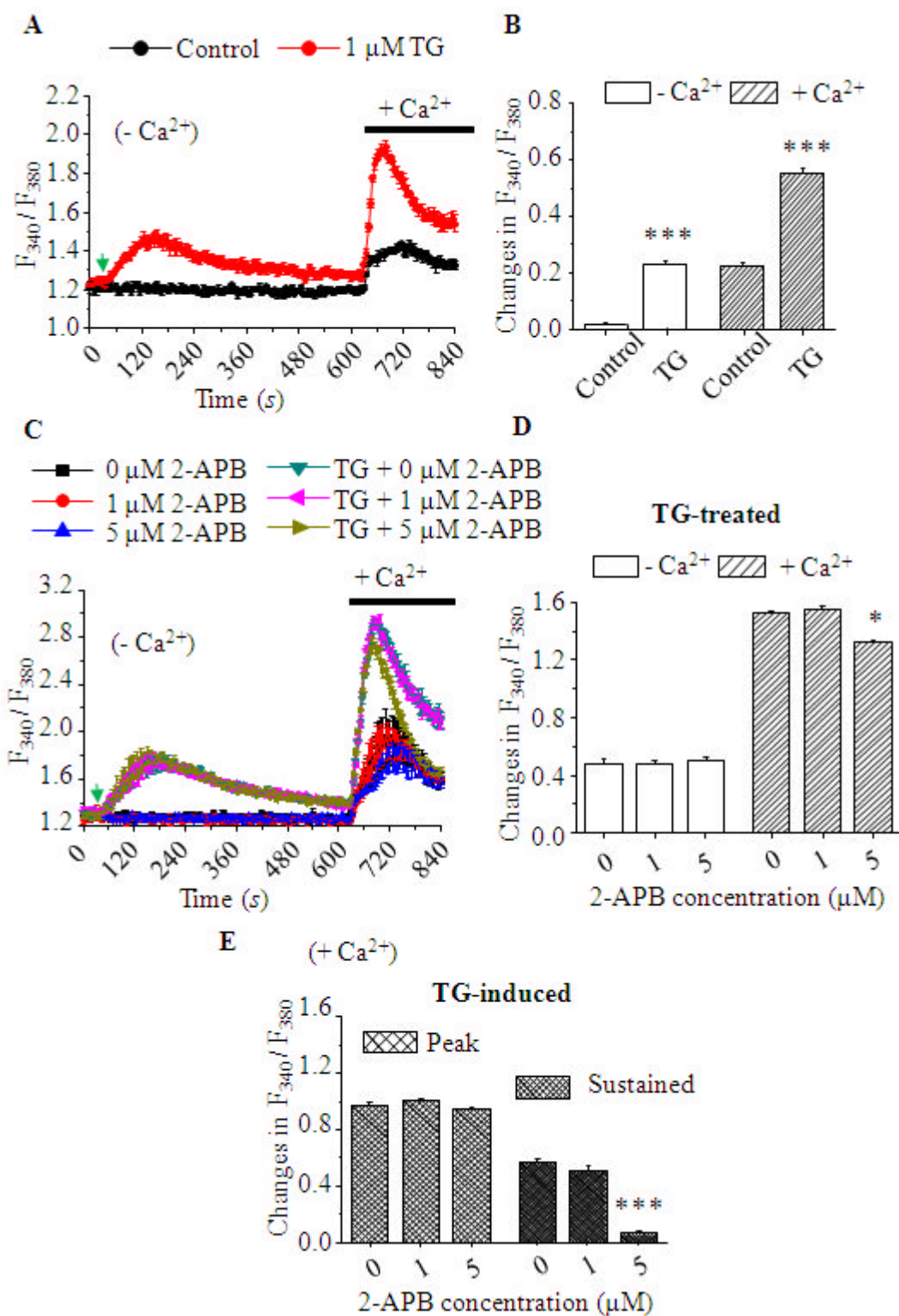


(Figure 5.4)

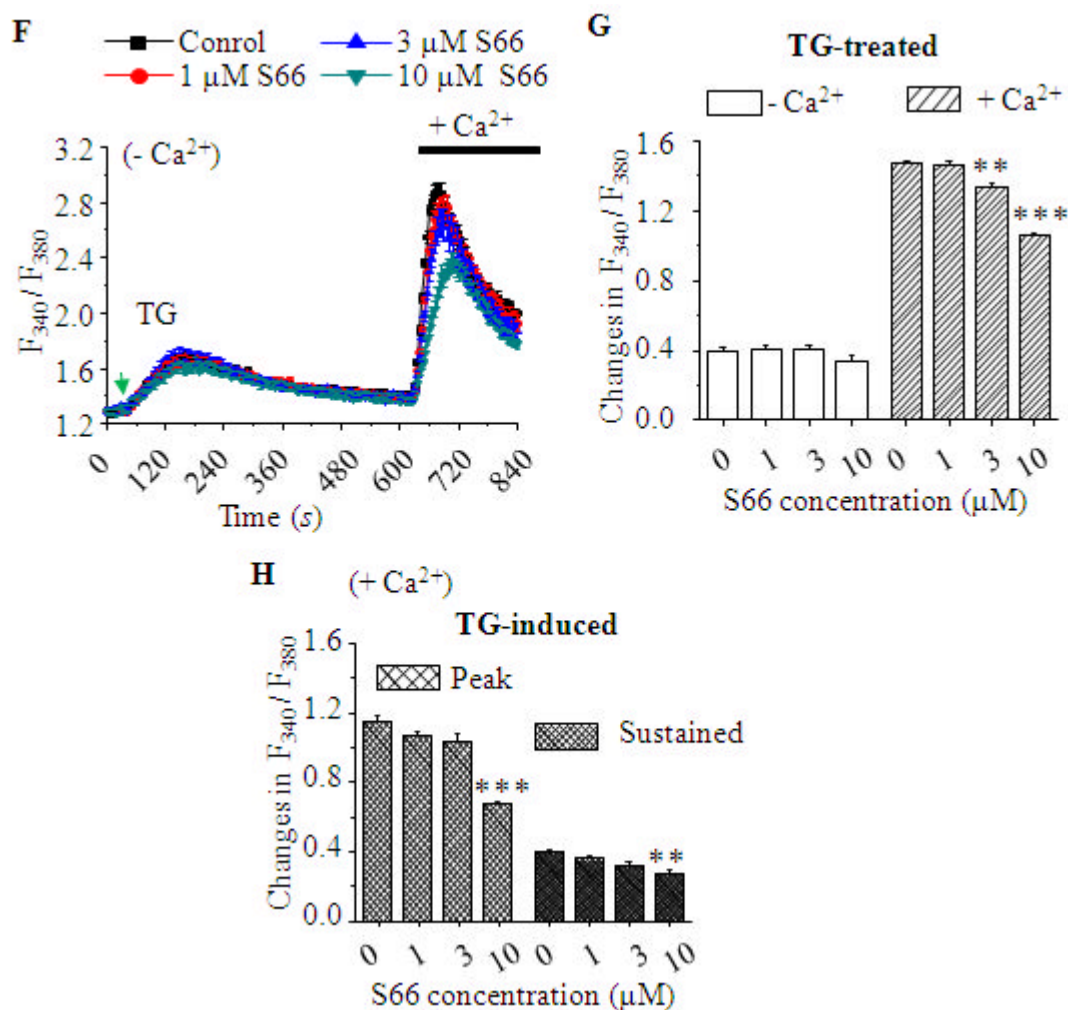


Figure 5.4 The SOC channel-mediated Ca²⁺ responses in hDP-MSCs.

(A) Typical Ca²⁺ responses in the absence of extracellular Ca²⁺ and subsequent addition of extracellular Ca²⁺ in hDP-MSCs (P4, 9F) without and with pretreatment with TG at 1 μM. (B) Summary of the average change in F₃₄₀/F₃₈₀ in cells shown in (A). *, *p* < 0.05; **, *p* < 0.01; ***, *p* < 0.001; compared to the control. (C) The effects of 2-APB at 1 and 5 μM on Ca²⁺ responses to in control cells (without TG) and TG-treated hDP-MSCs. (D) Summary of the average change in F₃₄₀/F₃₈₀ in hDP-MSCs in the extracellular Ca²⁺-free solution and after addition of Ca²⁺. (E) The peak amplitude (Peak) of TG-induced Ca²⁺ responses and sustained Ca²⁺ responses (Sustained) at 210 seconds after addition of extracellular Ca²⁺ in control cells or cells pretreated with 2-APB. 9F, P4, n/N = 3/12 wells. *, *p* < 0.05; **, *p* < 0.01; ***, *p* < 0.001; compared to the control (no 2-APB). (F) The effect of Synta66 at 1, 3, 10 μM on the Ca²⁺ responses in TG-treated hDP-MSCs. (G) Summary of the average change in F₃₄₀/F₃₈₀ in hDP-MSCs in the extracellular Ca²⁺-free solution and after addition of Ca²⁺. (H) The peak amplitude (Peak) of TG-induced Ca²⁺ responses and sustained Ca²⁺ responses (Sustained) at 210 seconds after addition of extracellular Ca²⁺ in control cells and cells pretreated with Synta66. 9F, P4, n/N = 3/12 wells. *, *p* < 0.05; **, *p* < 0.01; ***, *p* < 0.001; compared to the control (no Synta66).

5.3.8 Effects of Synta66 on TG-induced Ca²⁺ responses

The effects of Synta66 on TG-induced responses were examined. As shown in Figure 5.4F-G, while Synta66 at 1-10 μM did not change TG-induced intracellular Ca²⁺ release in the extracellular Ca²⁺-free solutions, it at 3 μM and 10 μM significantly reduced the increases in the [Ca²⁺]_i after addition of extracellular Ca²⁺, that is, the extracellular Ca²⁺ entry in TG-treated cells. Synta66 at 10 μM significantly inhibited both the peak and sustained amplitude of TG-induced Ca²⁺ entry (Figure 5.4H), supporting that the SOC channels are functionally expressed in hDP-MSCs.

5.3.9 Effects of 2-APB on ATP-induced Ca²⁺ responses

To investigate whether the SOC channels were involved in extracellular ATP induced-Ca²⁺ signalling, the effects of 2-APB on ATP-induced Ca²⁺ responses in the extracellular Ca²⁺-containing solutions were measured using FLEXstation.

The typical Ca²⁺ responses activated by 300 μM ATP in hDP-MSCs pretreated with 2-APB are shown in Figure 5.5A. Pre-treatment with 2-APB at 5 μM for 30 minutes significantly inhibited ATP-evoked Ca²⁺ responses in hDP-MSCs from three donors (Figure 5.5B-D), with an average inhibition of $37.5 \pm 3.1\%$ (Figure 5.5E). These results support that the SOC channels are involved in ATP-induced Ca²⁺ signalling

5.3.10 Effects of Synta66 on ATP-induced Ca²⁺ responses

The effects of Synta66 on ATP-activated Ca²⁺ responses were also examined. As shown in Figure 5.6A, pre-treatment with Synta66 at 10 μM for 30 minutes significantly reduced the amplitude of the sustained Ca²⁺ responses induced by 300 μM ATP without effect on the peak amplitude in hDP-MSCs from all three donors (Figure 5.6B-D). The average inhibition was $58.3 \pm 6.2\%$ at 240 seconds after treatment with ATP (Figure 5.6E).

These results, taken together with the inhibition by 2-APB described above show that the extracellular Ca^{2+} entry mediated by the SOC channels contribute to ATP-induced Ca^{2+} signalling.

5.3.11 Effects of reducing Stim and Orai expression using siRNA on ATP-induced Ca^{2+} responses

As shown above using RT-PCR, Stim1, Stim2, Orai1, Orai2 and Orai3 are expressed in hDP-MSCs. In order to identify which of these SOC channel proteins are important in forming the SOC channels mediating extracellular ATP-induced Ca^{2+} signalling, TG-induced Ca^{2+} responses in hDP-MSCs transfected with siRNA that specifically reduce the expression of each of these proteins (Li, Cubbon et al. 2011) were examined using the Ca^{2+} add-back protocols. In order to rule out the potential non-specific effect of transfection, the Ca^{2+} responses to TG in untransfected cells and siControl-transfected cells were compared. Cells transfected with siControl resulted in no significant difference in TG-induced Ca^{2+} release and extracellular Ca^{2+} entry (Figure 5.7A-C). Moreover, transfection with siControl had no significant effect on extracellular Ca^{2+} entry through constitutively active Ca^{2+} -permeable conductance (Figure 5.7D-F). Such observations suggest that transfection with siControl has no non-specific effect.

Figure 5.8 shows the mRNA expression level in hDP-MSCs transfected with siControl or siRNA for Stim1, Stim2, Orai1, Orai2 and Orai3. Treatment with specific siRNA resulted in a significant reduction in the mRNA expression level for Stim1 ($68 \pm 7\%$), Stim2 ($38 \pm 7\%$), Orai1 ($55 \pm 4\%$), Orai2 ($66 \pm 4\%$) and Orai3 ($41 \pm 5\%$).

Figure 5.9A-B show the typical Ca^{2+} responses following addition of extracellular Ca^{2+} in control hDP-MSCs (Figure 5.9A) and cells pretreated with TG (Figure 5.9B). Figure 5.9C-E summarizes the Ca^{2+} entry in control cells and TG-treated cells, and

the TG-induced Ca^{2+} entry in hDP-MSCs from each of the three donors. Figure 5.9F shows the Ca^{2+} responses in cells transfected with indicated siRNA presented as the percentage of those from cells transfected with siControl. The results show that siRNA for Orai1, Orai2, Orai3, Stim1 and Stim2 had no significant effect in the Ca^{2+} entry through constitutively active Ca^{2+} -permeable conductance. Knockdown in the expression of Orai1, Orai2, Orai3 and Stim1 and Stim2 by siRNA resulted in significant inhibition, but to various degrees, on the Ca^{2+} entry in TG-treated cells from three donors (Figure 5.9F). In contrast, the reduced expression of Stim2 had no significant effect on TG-induced Ca^{2+} entry (Figure 5.9 F). These results suggest Orai1, Orai2, Orai3 and Stim1 contribute significantly to formation of the SOC channels.

The effects of treatments with siRNA on ATP-induced Ca^{2+} responses were also examined. Representative Ca^{2+} responses induced by ATP at 300 μM are shown in Figure 5.10A. The results in cells from all three donors are summarized in Figure 5.10B-D. Treatment with Orai1, Orai2, Orai3 and Stim1 but not with Stim2 significantly attenuated ATP-induced Ca^{2+} responses in hDP-MSCs from two of the three donors (9F and 32F) (Figure 5.10B-C). ATP-induced Ca^{2+} responses in hDP-MSCs from the third donor (21F) was significantly reduced by treatment with siStim1 (Figure 5.10D). On average, the ATP-induced Ca^{2+} responses were attenuated by siRNA for Orai1 ($36.2 \pm 6.4\%$), Orai2 ($28.0 \pm 6.0\%$), Orai3 ($42.2 \pm 5.7\%$) and Stim1 ($48.7 \pm 9.2\%$) while siRNA for Stim2 had no significant effect (Figure 5.10E). These results are consistent with the effects of TG-induced Ca^{2+} entry and, taken together, support involvement of all three Orai and Stim1 proteins in ATP-induced Ca^{2+} responses in hDP-MSCs from two of three donors.

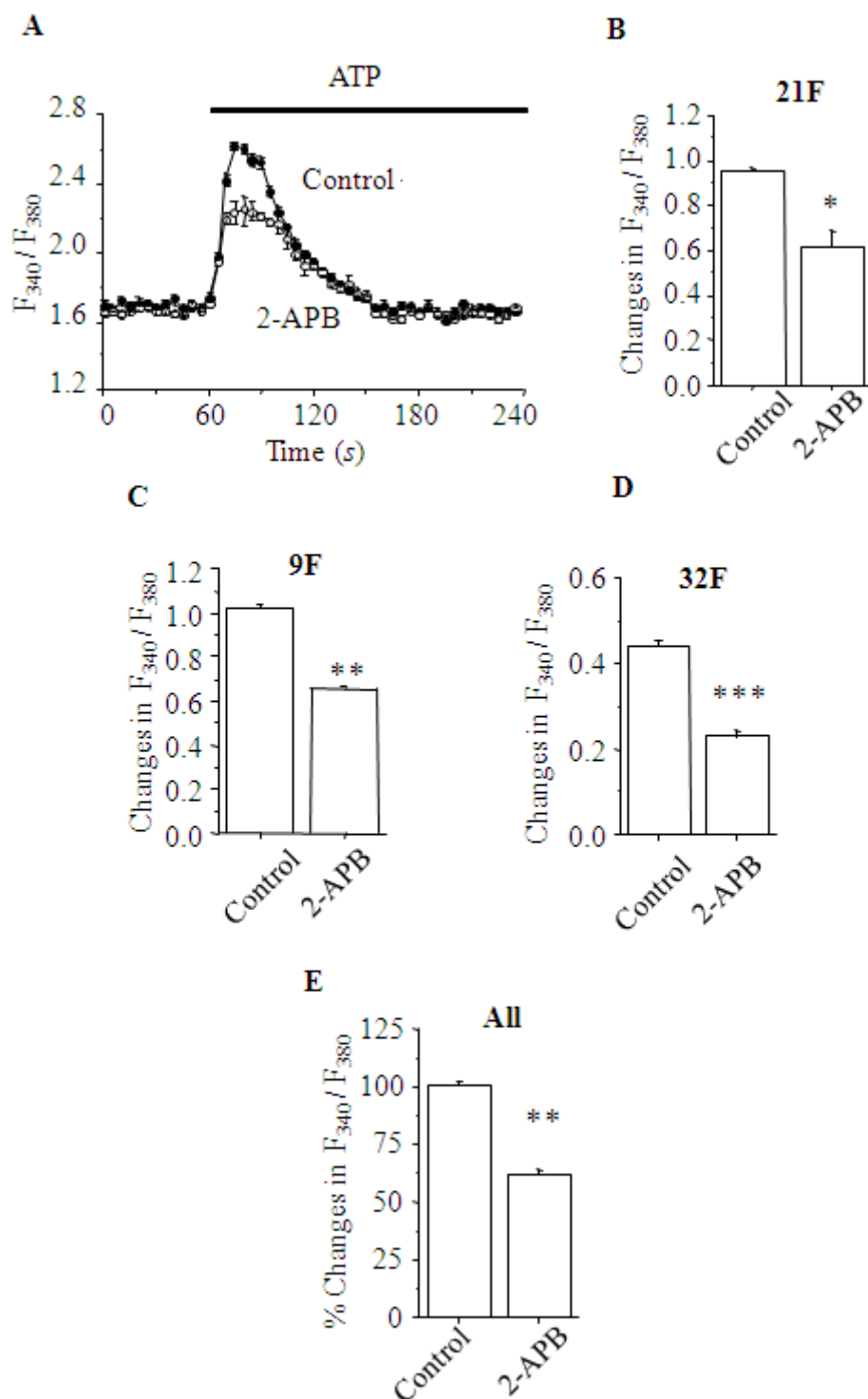


Figure 5.5 Effects of 2-APB on ATP-induced Ca^{2+} responses in hDP-MSCs.

(A) ATP-induced Ca^{2+} responses in cells (P4, 21F) treated without and with 2-APB at 5 μ M. (B-D) Summary of the average maximum changes in F_{340}/F_{380} in cells: (B) 21F; (C) 9F; (D) 32F. P4, N = 4 wells for each case. ATP at 300 μ M was used. (E) The percentages of inhibition by 2-APB in cells (P4; 9F, 21F and 32F) compared to the control. *, $p < 0.05$; **, $p < 0.01$; ***, $p < 0.001$; compared to the control.

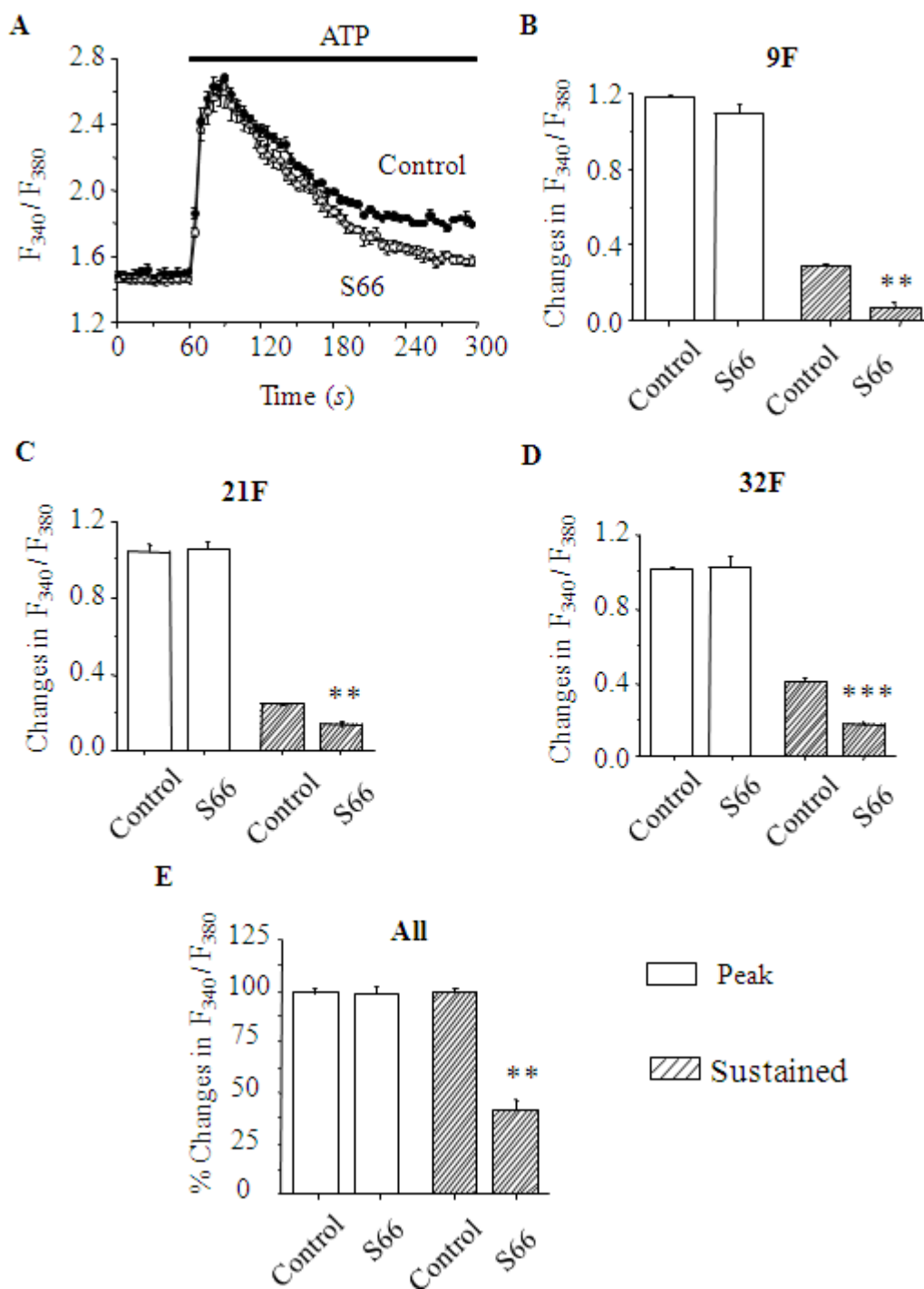


Figure 5.6 Effects of Synta66 on ATP-induced Ca^{2+} responses in hDP-MSCs. (A) ATP-induced Ca^{2+} responses in hDP-MSCs (P4, 9F) with or without pretreated with Synta66 (S66) at 10 μ M. (B-D) Summary of the average peak amplitude (Peak) of Ca^{2+} responses and sustained Ca^{2+} responses (Sustained) at the end of recording (240 seconds after addition of 300 μ M ATP): (B) 9F; (C) 21F; (D) 32F. P4, N = 4 wells for each case. (E) The percentage of inhibition by Synta66 of ATP-induced Ca^{2+} responses in hDP-MSCs (9F, 21F and 32F). *, $p < 0.05$; **, $p < 0.01$; ***, $p < 0.001$; compared to the control.

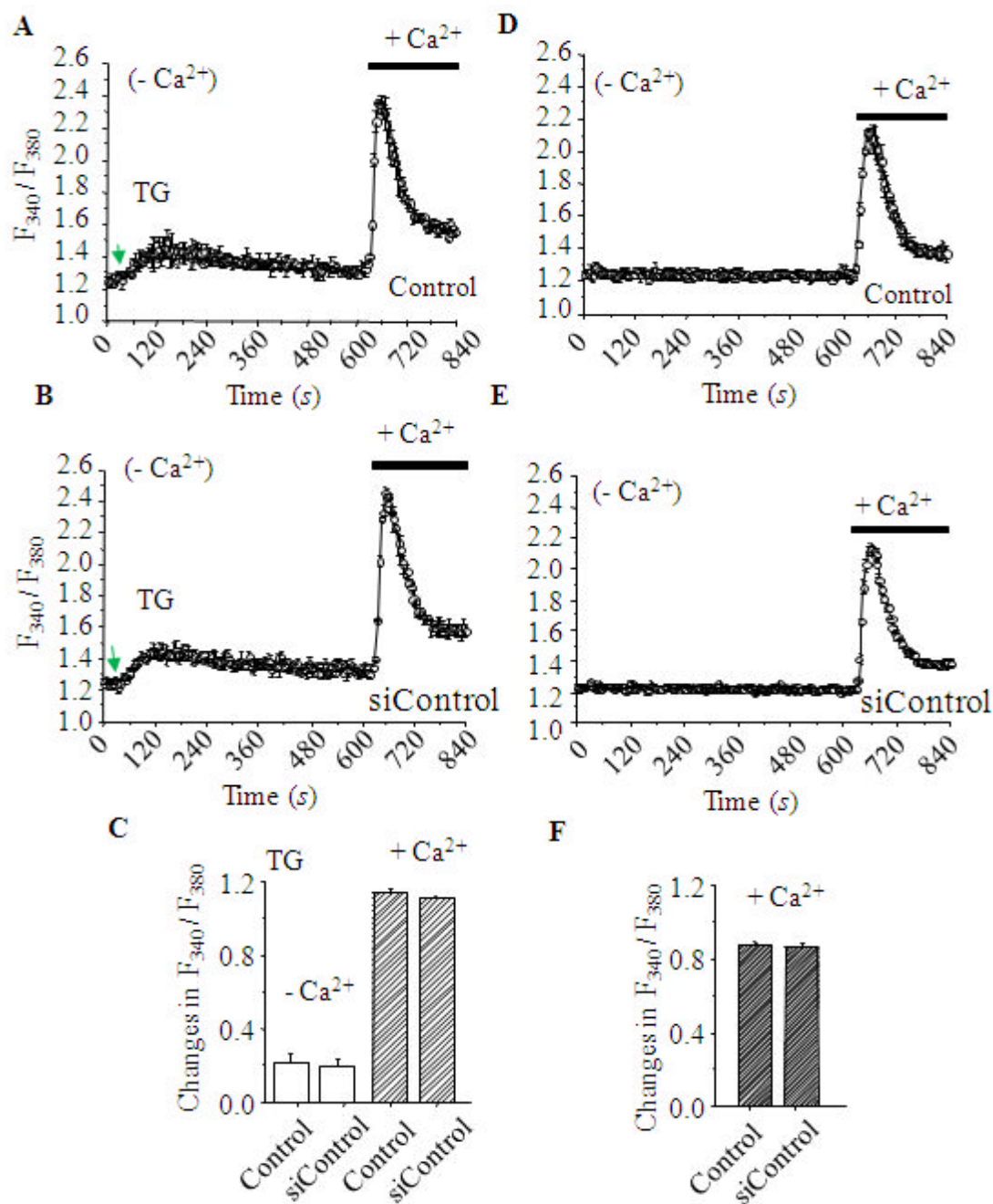


Figure 5.7 Effects of transfection with siControl on Ca^{2+} responses in hDP-MSCs without or with TG treatment.

(A-B) Typical Ca^{2+} responses to TG in untransfected (A, control) and siControl-transfected hDP-MSCs (P4, 9F) (B) in the absence of extracellular Ca^{2+} and subsequent addition of extracellular Ca^{2+} . (C) Summary of the average maximum change in F_{340}/F_{380} in cells treated with TG in the absence of extracellular Ca^{2+} and after addition of extracellular Ca^{2+} . (D-E) Ca^{2+} responses in untransfected (A, control) and siControl-transfected hDP-MSCs (P4, 9F) not treated with TG. (F) Summary of the average maximum change in F_{340}/F_{380} after addition of extracellular Ca^{2+} in cells without TG treatment. *, $p < 0.05$; **, $p < 0.01$; ***, $p < 0.001$; compared to the control.

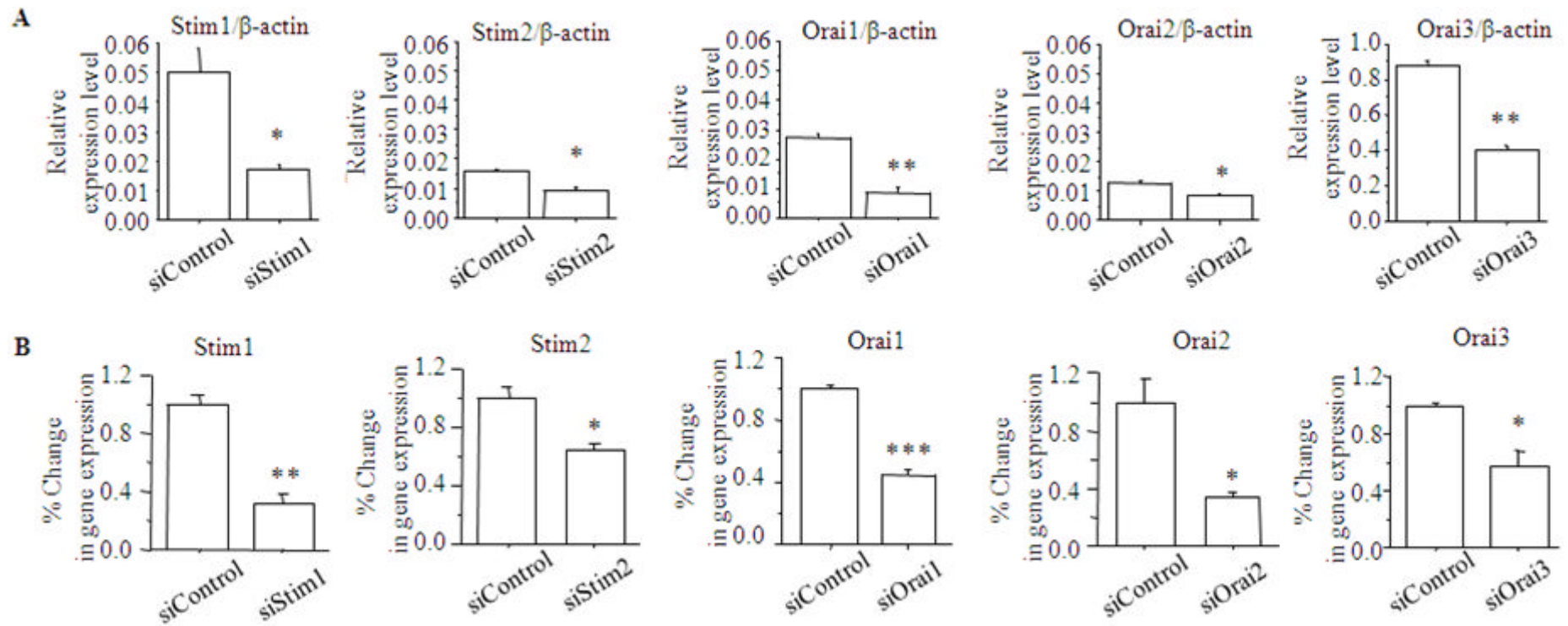
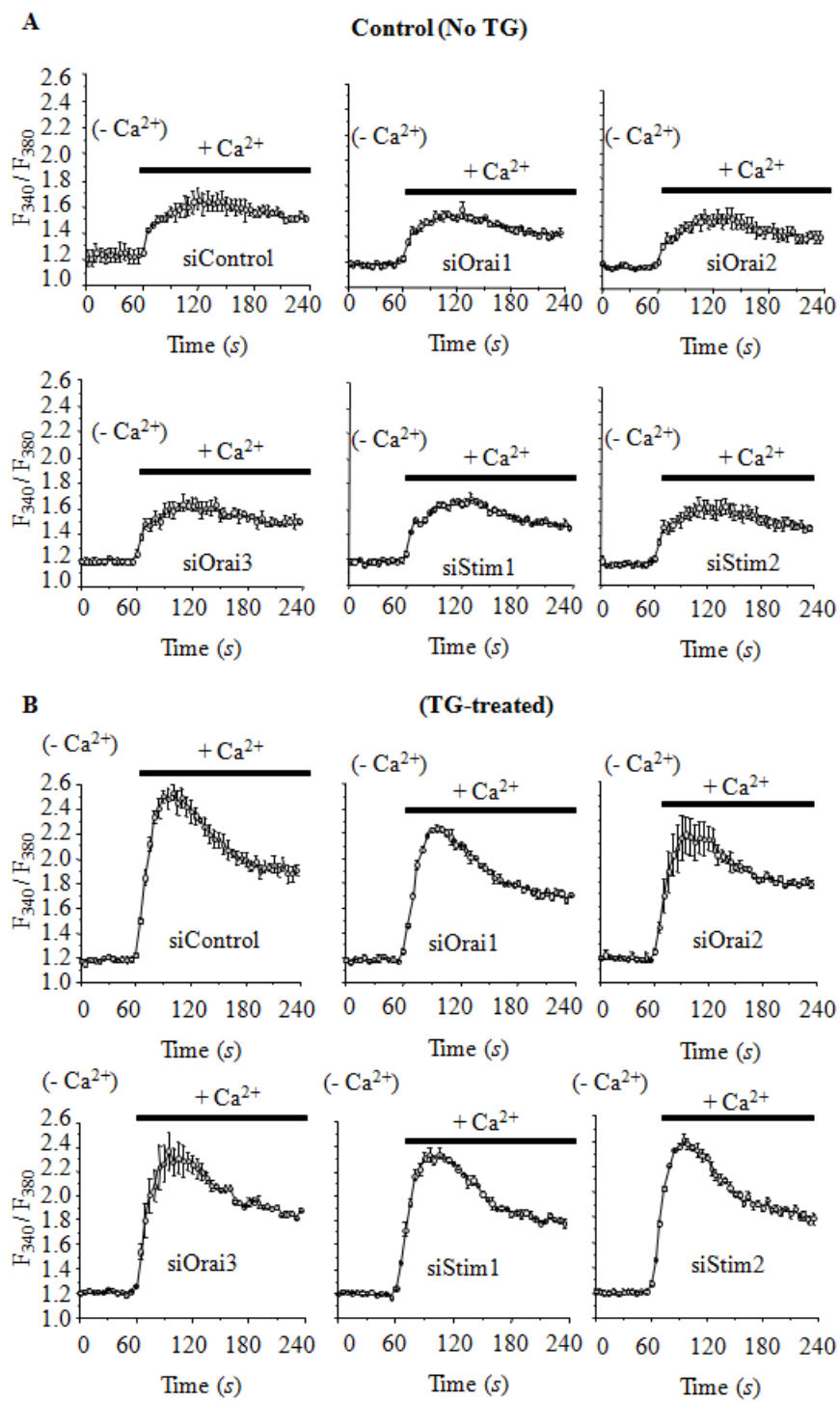
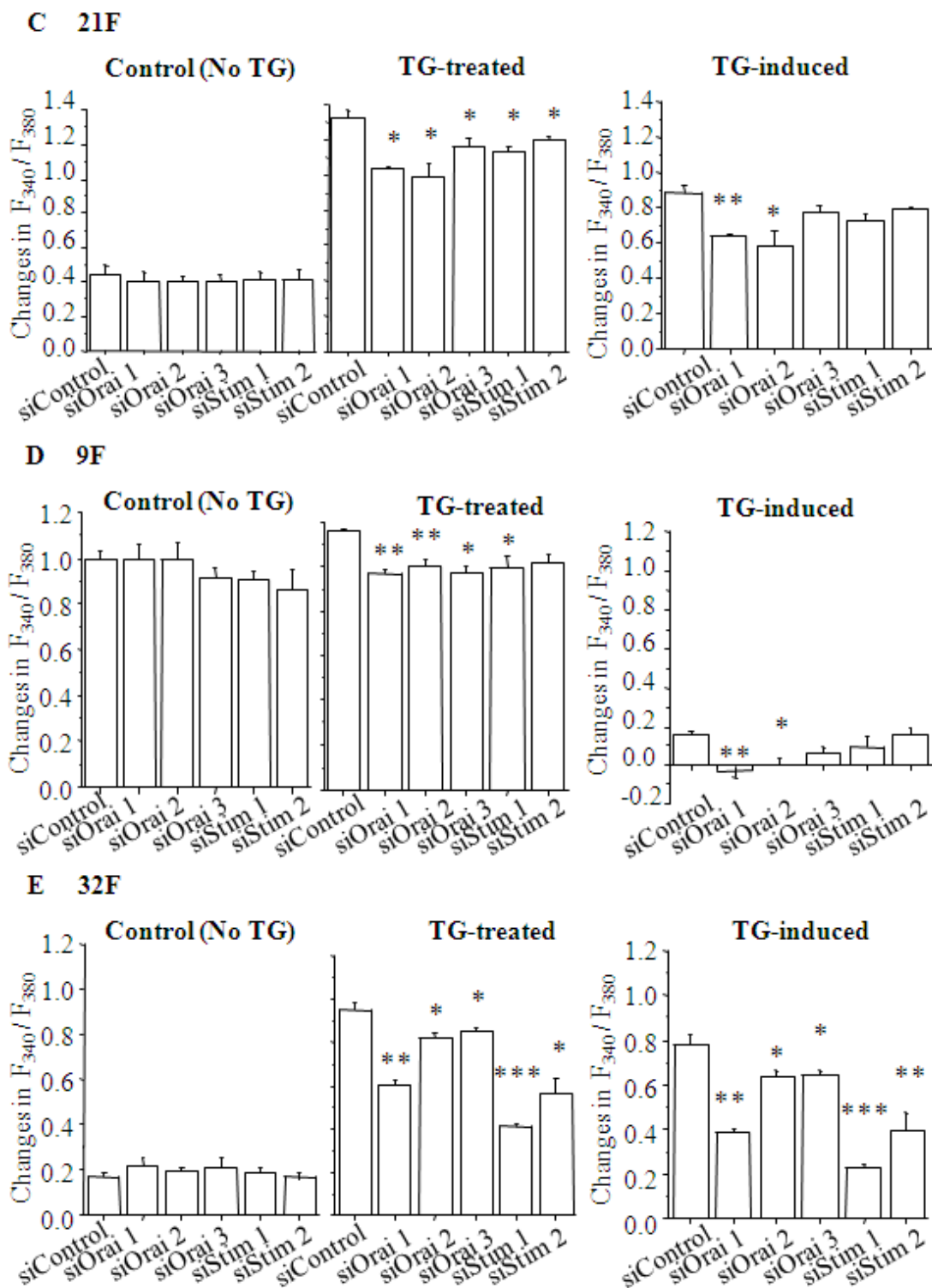


Figure 5.8 Effects of transfection with siRNA on the mRNA expression of Stim and Orai in hDP-MSCs.

(A) The mRNA expression level of Stim1, Stim2, Orai1, Orai2 and Orai3 relative to that of β -actin in hDP-MSCs from 21F and 32F transfected with specific siRNA and siControl. 21F, P4, N = 3 wells and 32F, P4, N = 3 wells; n/N = 2/6. (B) The mRNA expression level of Stim1, Stim2, Orai1, Orai2 and Orai3 in hDP-MSCs transfected with specific siRNA (n/N = 2/6) as percentage of that in cells transfected with siControl. *, $p < 0.05$; **, $p < 0.01$; ***, $p < 0.001$; compared to siControl.



(Figure 5.9)



(Figure 5.9)

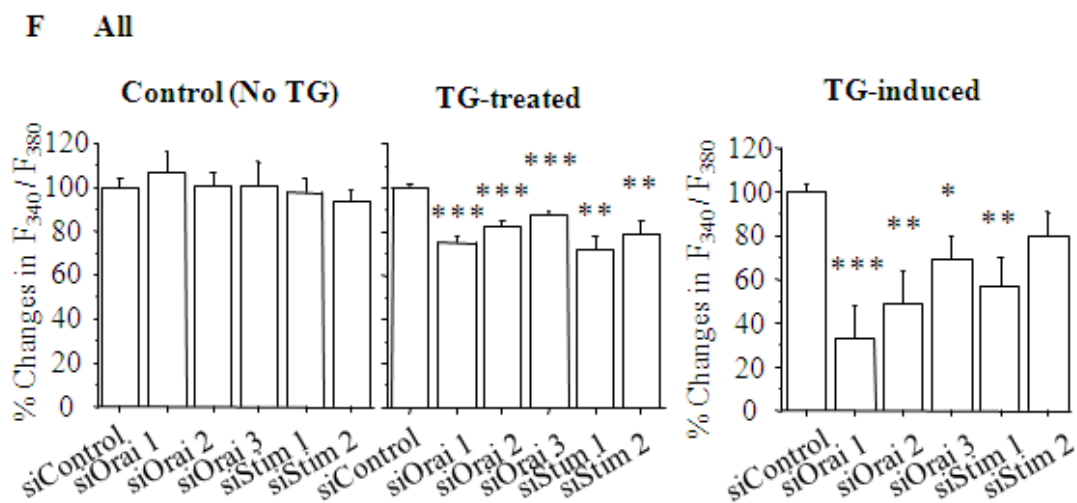
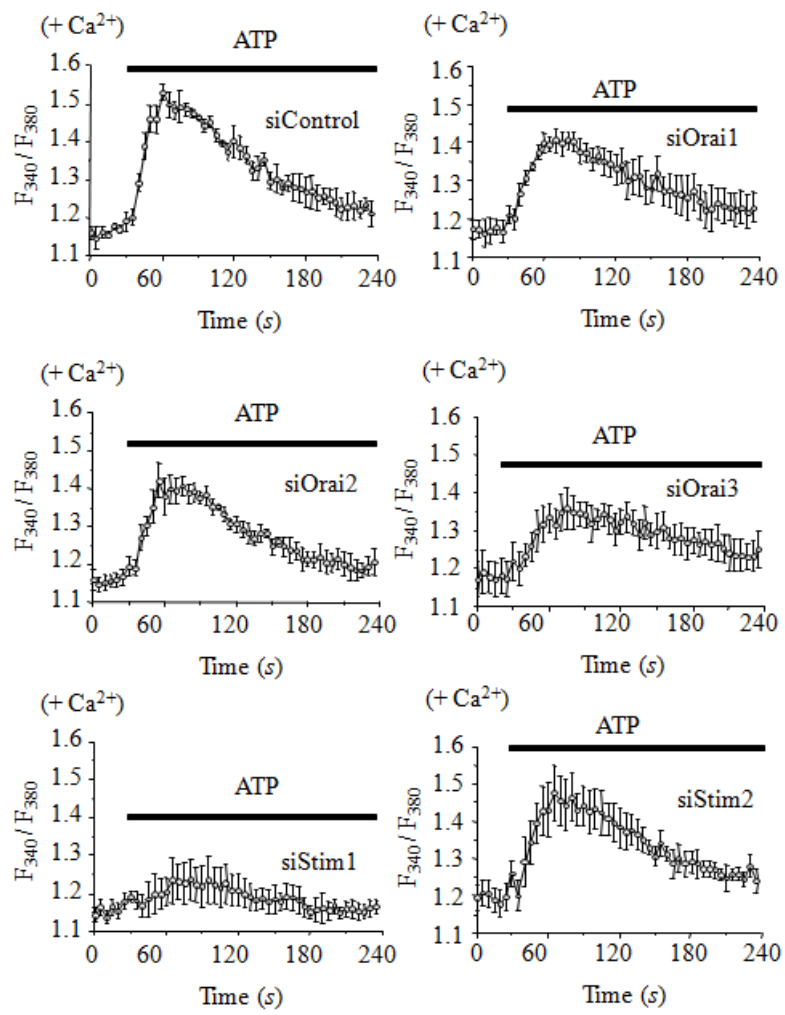


Figure 5.9 Effects of transfection with siRNA for Orai and Stim on TG-induced Ca^{2+} responses in hDP-MSCs.

(A-B) Typical Ca^{2+} responses in hDP-MSCs (P4, 21F) transfected with siControl and siRNA for Orai1, Orai2, Orai3, Stim1 and Stim2 without (A) and with (B) treatment with TG at 10 μM after addition of Ca^{2+} into the extracellular Ca^{2+} -free solutions. (C-E) Summary of the average maximum change in F_{340}/F_{380} in control cells and TG-treated cells, and TG-induced increases in the $[\text{Ca}^{2+}]_i$ after addition of Ca^{2+} into the extracellular Ca^{2+} -free solutions in hDP-MSCs: (C) 21F; (D) 9F; (E) 32F. P4, N = 4 wells for each case. (F) The change in F_{340}/F_{380} in hDP-MSCs transfected with siRNA for Orai and Stim (9F, 21F and 32F) as percentage of those in cells transfected with siControl. *, $p < 0.05$; **, $p < 0.01$; ***, $p < 0.001$; compared to siControl.

A



(Figure 5.10)

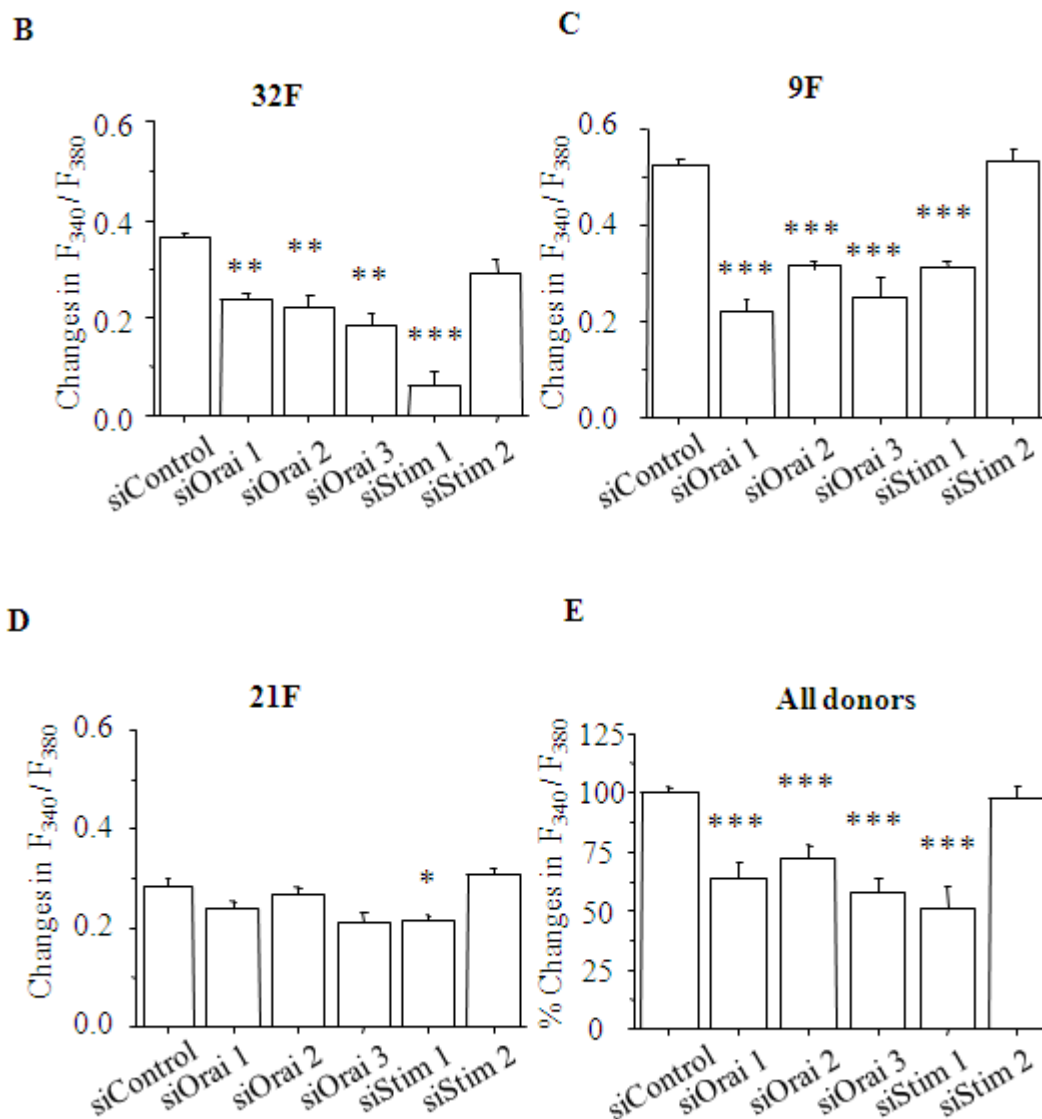


Figure 5.10 Effects of transfection with siRNA for Orai and Stim on ATP-induced Ca^{2+} responses in hDP-MSCs.

(A) Typical Ca^{2+} responses to ATP in hDP-MSCs (P4, 32F) transfected with siControl and siRNA for Orai1, Orai2, Orai3, Stim1 and Stim2 in the presence of extracellular Ca^{2+} . ATP at 300 μ M was used. (B-D) Summary of the average maximum change of F_{340}/F_{380} in cells: (B) 32F; (C) 9F; (D) 21F. P4, N = 4 wells for each case. (E) The change in F_{340}/F_{380} in hDP-MSCs (9F, 21F and 32F) as percentage of that in cells transfected with siControl. *, $p < 0.05$; **, $p < 0.01$; ***, $p < 0.001$; compared to siControl.

5.3.12 Effects of co-transfection with siRNA for Stim1 and Orai on ATP-induced Ca²⁺ responses

In order to further investigate that the molecular composition of the SOC channels were responsible for extracellular ATP-induced Ca²⁺ signalling, TG-induced Ca²⁺ entry and ATP-induced Ca²⁺ responses were examined in hDP-MSCs co-transfected with siStim1/siOrai (siStim1/siOrai1, siStim1/siOrai2 and siStim1/siOrai3).

Figure 5.11A-B show typical Ca²⁺ responses in control cells or TG-treated cells after co-transfection with siStim1/siOrai. Figure 5.11C-E summarize the increases in the [Ca²⁺]_i after addition of extracellular Ca²⁺ in cells from three donors. Figure 5.11F shows the increases in the [Ca²⁺]_i in control cells and TG-treated cells, and TG-induced increases in the [Ca²⁺]_i, expressed as percentage of those in cells transfected with siControl. The results show that without TG treatment there was no significant difference in extracellular Ca²⁺ entry between cells transfected with siControl and cells co-transfected with siStim1/siOrai (Figure 5.11F). However, co-transfection with siStim1/siOrai resulted in significant decrease in the extracellular Ca²⁺ entry in TG-treated cells, and TG-induced extracellular Ca²⁺ entry (Figure 5.11F).

The effects of co-transfection with such siRNAs on ATP-induced Ca²⁺ responses were also examined. As shown in Figure 5.12, co-transfection with siStim1/siOrai1, siStim1/siOrai2, and siStim1/siOrai3 resulted in similar attenuation of the Ca²⁺ responses induced by 300 μM ATP in hDP-MSCs from all three donors. These results indicated that all three Orai proteins may contribute to SOC channels and ATP-induced Ca²⁺ signalling in hDP-MSCs.

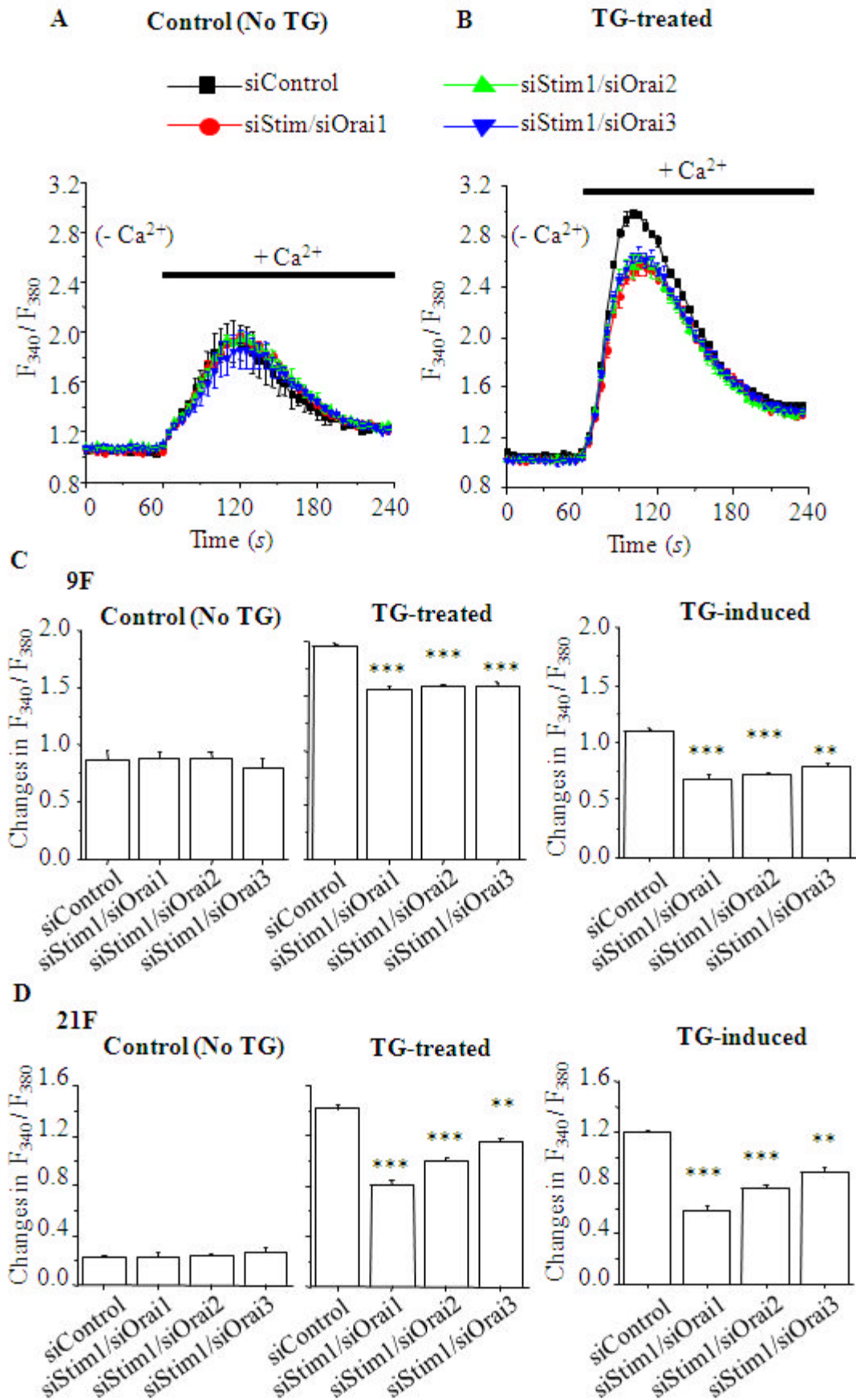


(Figure 5.11)

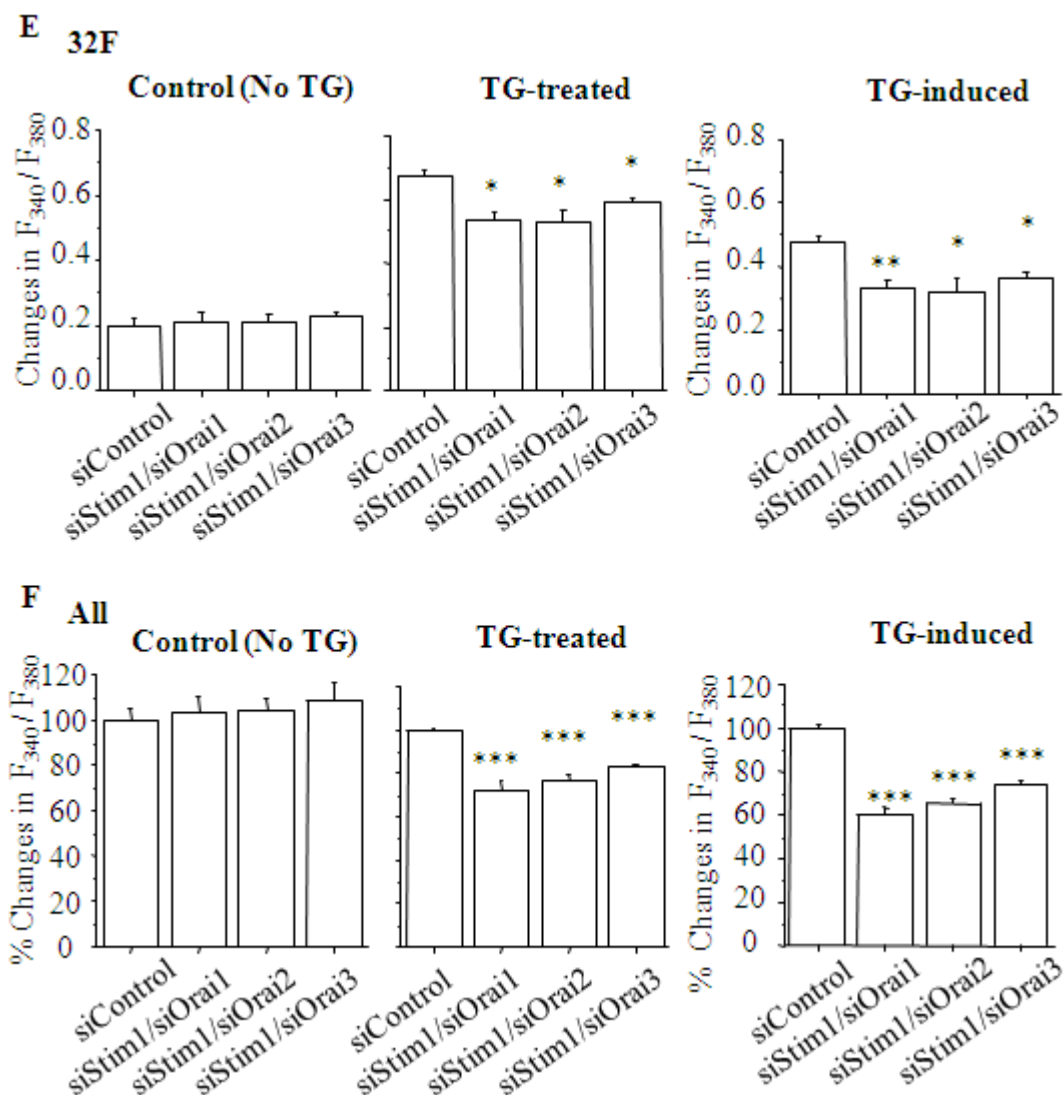


Figure 5.11 Effects of co-transfected with siRNAs for Stim1 and Orai on TG-induced Ca^{2+} responses in hDP-MSCs.

(A-B) Typical Ca^{2+} responses without (A) or with (B) treatment with TG at 10 μM in hDP-MSCs (P4, 9F) transfected with siControl, siStim1/siOrai1, siStim1/siOrai2, and siStim1/siOrai3 after addition of Ca^{2+} into the extracellular Ca^{2+} -free solutions. (C-E) Summary of the average maximum change in F_{340}/F_{380} in control cells (untreated with TG) and TG-treated cells, and TG-induced maximal change in F_{340}/F_{380} after addition of Ca^{2+} into the extracellular Ca^{2+} -free solutions in cells: (C) 9F; (D) 21F; (E) 32F. P4, N = 4 wells for each case. (F) The change in F_{340}/F_{380} in hDP-MSCs co-transfected with siRNA for Stim1 and Orai (9F, 21F and 32F) as percentage of that in cells transfected with siControl. *, $p < 0.05$; **, $p < 0.01$; ***, $p < 0.001$; compared to siControl.

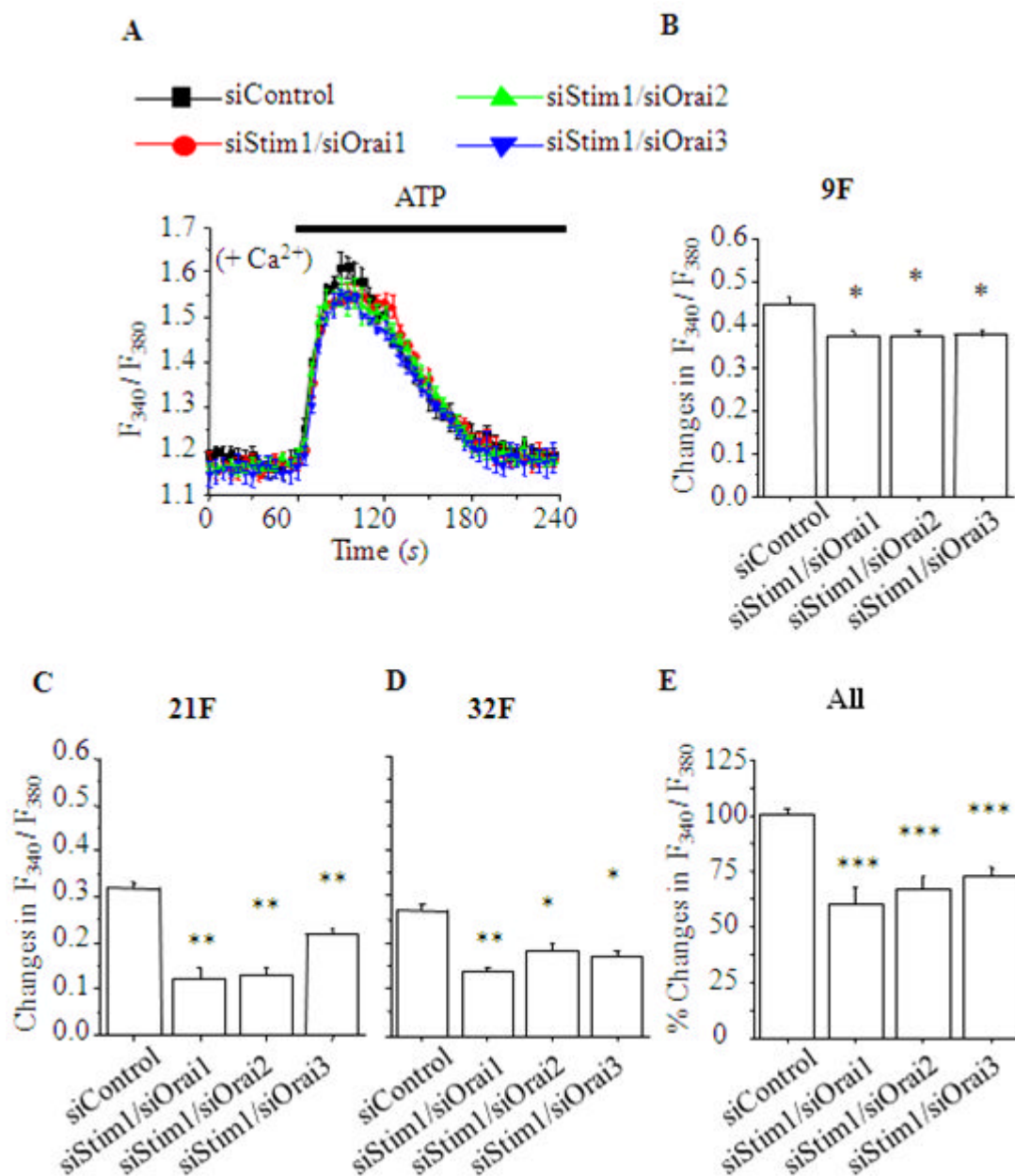


Figure 5.12 Effects of co-transfected with siRNAs for Stim1 and Orai on ATP-induced Ca^{2+} responses in hDP-MSCs.

(A) Typical ATP-induced Ca^{2+} responses in the presence of extracellular Ca^{2+} in hDP-MSCs (P4, 9F) co-transfected with siControl, siStim1/siOrai1, siStim1/siOrai2, and Stim1/Orai3. ATP at 300 μM was used. (B-D) Summary of the average maximum change of F_{340}/F_{380} in cells: (B) 9F; (C) 21F; (D) 32F. P4, N = 4 wells for each case. (E) The change in hDP-MSCs (9F, 21F and 32F) as percentage of that in siControl-transfected cells. *, $p < 0.05$; **, $p < 0.01$; ***, $p < 0.001$; compared to siControl.

5.3 Discussion

The results from the study described in this chapter provide evidence to show that Orai and Stim1 participate in formation of the SOC channels and contribute to ATP-induced Ca^{2+} signaling in hDP-MSCs. In addition, the study has also revealed a constitutively active Ca^{2+} conductance in the plasma membrane, which does not contribute to ATP-induced Ca^{2+} signaling.

The results from single cell Ca^{2+} imaging and FLEXstation consistently showed a modest increase in the $[\text{Ca}^{2+}]_i$ in hDP-MSCs upon addition of extracellular Ca^{2+} back into the extracellular Ca^{2+} -free solution, indicating presence of a constitutively active Ca^{2+} conductance (Figure 5.1A). Such increases in the $[\text{Ca}^{2+}]_i$ has not been reported in previous studies of hBM-MSCs (Kawano, Shoji et al. 2002). The functional characterization of such a constitutively active Ca^{2+} conductance in hDP-MSCs showed that the $[\text{Ca}^{2+}]_i$ through the constitutively active Ca^{2+} conductance was increased as in the extracellular Ca^{2+} concentration raised from 30 μM to 5 mM and the increase was very fast (Figure 5.3B), suggesting that such Ca^{2+} entry may be mediated by Ca^{2+} -permeable channels. Pretreatment with 2-APB at 10-100 μM significantly inhibited the Ca^{2+} entry via the constitutively active Ca^{2+} conductance (Figure 5.3D). In contrast, pretreatment with Synta66 up to 10 μM , a potent SOC inhibitor (see 1.3.4.3), had no effect (Figure 5.3F). Furthermore, the reduction in the expression of Orai and Stim alone or in combination did not also affect the Ca^{2+} entry via the constitutively active Ca^{2+} conductance (Figure 5.9F and Figure 5.10E), indicating that Orai and Stim proteins are unlikely involved in the formation of constitutively active Ca^{2+} conductance. Thus the molecular identify of the constitutively active Ca^{2+} conductance is elusive and further studies are needed.

As discussed in the Introduction chapter (see section 1.3.4), depleting the ER Ca^{2+}

store with TG can induce extracellular Ca^{2+} entry via the SOC channels. In hDP-MSCs, the increase in the $[\text{Ca}^{2+}]_i$ upon Ca^{2+} add-back was remarkably larger after treatment with TG (Figure 5.1C-D and Figure 5.4A-B). Moreover, pretreatment of 2-APB at 5 μM , which did not induce intracellular Ca^{2+} release and did not alter the Ca^{2+} entry via the constitutively active Ca^{2+} conductance (Figure 5.3D), significantly inhibited TG-induced Ca^{2+} entry (Figure 5.4E), indicating that 2-APB inhibits the SOC channels without altering intracellular Ca^{2+} release mechanisms. Synta66 at 10 μM also significantly blocked TG-induced Ca^{2+} entry without altering the basal $[\text{Ca}^{2+}]_i$ and extracellular Ca^{2+} entry through the constitutively active Ca^{2+} conductance (Figure 5.3F and Figure 5.4H). Taken together, these results suggest that the SOC channels are functionally expressed in hDP-MSCs. The functional expression of the SOC channels was also reported for hBM-MSCs (Kawano, Shoji et al. 2002). Therefore, the present and previous studies are consistent in supporting the expression of SOC channels in MSCs.

As described in the previous chapter, ATP in the absence of extracellular Ca^{2+} induced intracellular Ca^{2+} release by activating P2Y receptors, particularly P2Y1 and P2Y11 via the PLC-IP₃ signalling pathway in hDP-MSCs. Subsequent addition of extracellular Ca^{2+} resulted in significant extracellular Ca^{2+} entry (Figure 5.1E-F). In the experiments shown in Figure 5.1E-F, ATP was removed before addition of extracellular Ca^{2+} and therefore ATP-induced Ca^{2+} entry is mainly mediated by the SOC channels. Consistent with this notion is that 2-APB at 5 μM and Synta66 at 10 μM , blocked ATP-induced Ca^{2+} responses as well as TG-induced activation of the SOC channels (Figure 5.5E and Figure 5.6E). Therefore, these results suggest that functional SOC channels contribute to extracellular ATP-induced Ca^{2+} signalling in hDP-MSCs as previously reported in hBM-MSCs (Kawano, Shoji et al. 2002).

The molecular components of the SOC channels in MSCs remained unclear. The RT-PCR results presented in this study for the first time showed that hDP-MSCs expressed the mRNA transcripts for all the three SOC channel-forming proteins, Orai1, Orai2, Orai3, and the two ER Ca²⁺ sensing proteins Stim1 and Stim2 (Figure 5.2 A). Transfection with specific siRNA significantly decreased their expression levels (Figure 5.8), as reported in previous studies of the expression of these molecules in endothelial cells (Li, Cubbon et al. 2011). Down-regulation of the expression of each of these three Orai proteins and also Stim1, but not Stim2, significantly inhibited TG-induced Ca²⁺ entry (Figure 5.9F), indicating that Orai and Stim1 contribute to formation of SOC channels in hDP-MSCs. Similarly, the ATP-induced Ca²⁺ responses were significantly inhibited in hDP-MSCs transfected with siRNA for each of the three Orai and Stim1, but not Stim2 (Figure 5.10E). Furthermore, co-transfection with siStim1/siOrai1, siStim1/siOrai2, and siStim1/siOrai3 inhibited TG-induced extracellular Ca²⁺ entry (Figure 5.11F) and ATP-induced Ca²⁺ responses (Figure 5.11E), further supporting that Orai and Stim1 are important in forming the SOC channels contributing ATP-induced Ca²⁺ signalling in hDP-MSCs.

In summary, the results described in this chapter have shown that Orai and Stim1 contribute to formation of the SOC channels that are significantly involved in extracellular ATP-induced Ca²⁺ signalling in hDP-MSCs.

Chapter 6

Roles of P2 Purinergic Receptors and SOC Channels in MSC

Migration and Differentiation

6.1 Introduction

Previous studies suggest that several P2 receptors and downstream signalling are involved in the modulation of stem cells functions. For example, the P2Y11 receptor was shown to be involved in the modulation by NAD^+ of hBM-MSC migration (Fruscione, Scarfi et al. 2011). The P2Y2 receptor and Stim1-mediated SOC channels were also involved in ATP-induced cell migration of cancer stem cells (Xie, Xu et al. 2014). Recent studies have shown that stimulation by ATP of the P2X7 receptor induced osteogenic differentiation of hBM-MSCs (Sun, Junger et al. 2013), whereas activation of the P2Y1 and P2Y4 receptors by ATP might be involved in adipogenic differentiation of hBM-MSCs (Ciciarello, Zini et al. 2013). The results in chapter 3 show ATP can significantly regulate cell migration and differentiation of hDP-MSCs.

The results in chapter 4 and chapter 5 have shown that P2X7, P2Y1 and P2Y11 receptors, and Stim1/Orai SOC channels are critically involved in extracellular ATP-stimulated Ca^{2+} signalling in hDP-MSCs. It was interesting to determine whether such signalling mechanisms are important in ATP-induced cell migration and regulation of adipogenic and osteogenic differentiation. Therefore, the study presented in this chapter aimed to investigate the role of P2X7, P2Y1 and P2Y11 receptors, and Stim1/Orai-mediated SOC channels in the regulation by extracellular ATP of cell migration and differentiation of hDP-MSCs.

6.2 Results

6.2.1 The role in hDP-MSC migration

6.2.1.1 Effects of inhibitors for P2 receptors and SOC channels

In order to investigate the potential role of P2X7, P2Y1 and P2Y11 receptors, and Stim1/Orai SOC channels in mediating ATP-induced stimulation of hDP-MSC migration, the effects of the inhibitors for these receptors and channels were examined using the wound healing assays in combination with the IncuCyte real-time imaging system. Figure 6.1A shows the reduction in the wound width as results of cell migration for control cells, cells treated with 30 μ M ATP alone or cells treated with 1 μ M AZ11645373, 10 μ M PPADS and 5 μ M 2-APB together with ATP. Figure 6.1B summarizes the migration area at 24, 36 or 48 hours and Figure 6.1C shows the migration of cells treated with ATP alone or together with indicated inhibitors, expressed as % of migration for the control cells. As described above in section 3.2.3, ATP increased hDP-MSC migration. Treatment with PPADS resulted in significant inhibition of cell migration at 24, 36 and 48 hours. Treatment with AZ11645373 significantly inhibited cell migration at 48 hours. Like PPADS, 2-APB was also effective in blocking cell migration at 24, 36 and 48 hours. Unlike ATP-induced Ca^{2+} responses described in previous chapters that occurred within a few minutes after addition of extracellular ATP, ATP-induced effects on cell migration was determined over a much longer period of time. Under such conditions, ATP is degraded to ADP and adenosine (see section in 1.3.1), and thus it remained possible that ATP-induced increase in cell migration was in part or as a whole mediated indirectly by adenosine receptors. In order to study such a possibility, cells were treated with ATP together with CGS15943, a generic and potent antagonist of adenosine receptors with the K_i values of 3.5, 4.2, 16 and 51 nM for the human A1, A2A, A2B and A3 adenosine receptors, respectively (Ghai, Francis et al. 1987). There was no significant effect of CGS15943 at 100 nM on ATP-induced increase in cell migration (Figure 6.1B-F).

Taken together, the results from pharmacological interventions suggest that the P2X7, P2Y receptor and SOC channels, but not the adenosine receptors, contribute in mediating ATP-induced increase in hDP-MSC migration.

6.2.1.2 Effects of transfection with siRNAs on ATP-induced increase in cell migration

The results described in previous chapters show that P2X7, P2Y1, P2Y11, Stim1 and Orai1 are significantly engaged in extracellular ATP-induced Ca^{2+} signalling. In order to further investigate their roles in ATP-stimulated cell migration, hDP-MSCs transfected with siRNAs were examined. Figure 6.2A shows the representative results of cell migration or reduction in the wound width for cells transfected with siControl and siRNA for P2X7, P2Y1, P2Y11, Stim1 and Orai1. The results from hDP-MSCs from the donor 9F at 24, 36 and 48 hours are summarized in Figure 6.2B, and expressed as the percentage of those in cells transfected with siControl in Figure 6.2C. The results from the cells from the 32F and 21F donors are summarized in Figure 6.2D-E. As described in chapter 3, these results show that ATP significantly enhanced cell migration for hDP-MSCs from all three donors. Transfection with siRNA for P2X7, P2Y1, P2Y11, Stim1 and Orai1 significantly reduced the stimulatory effect of ATP on cell migration in cells from two of three donors (9F: Figure 6.2C; 32F: Figure 6.2D) but not the other (21F: Figure 6.2E). However, co-transfection with siStim1/siOrai1 consistently resulted in a significant inhibition of ATP-induced increase in cell migration at 24 and 36 hours for cells from all three donors (Figure 6.2E-F). The inhibition resulting from co-transfection with siStim1/siOrai1 was slightly greater than that from transfection with siOrai1 alone. These results are consistent with the results obtained using inhibitors, suggesting a significant role for the P2X7, P2Y1 and P2Y11 and particularly Stim1/Orai1 SOC channels in mediating ATP-induced stimulation of hDP-MSC migration.

A

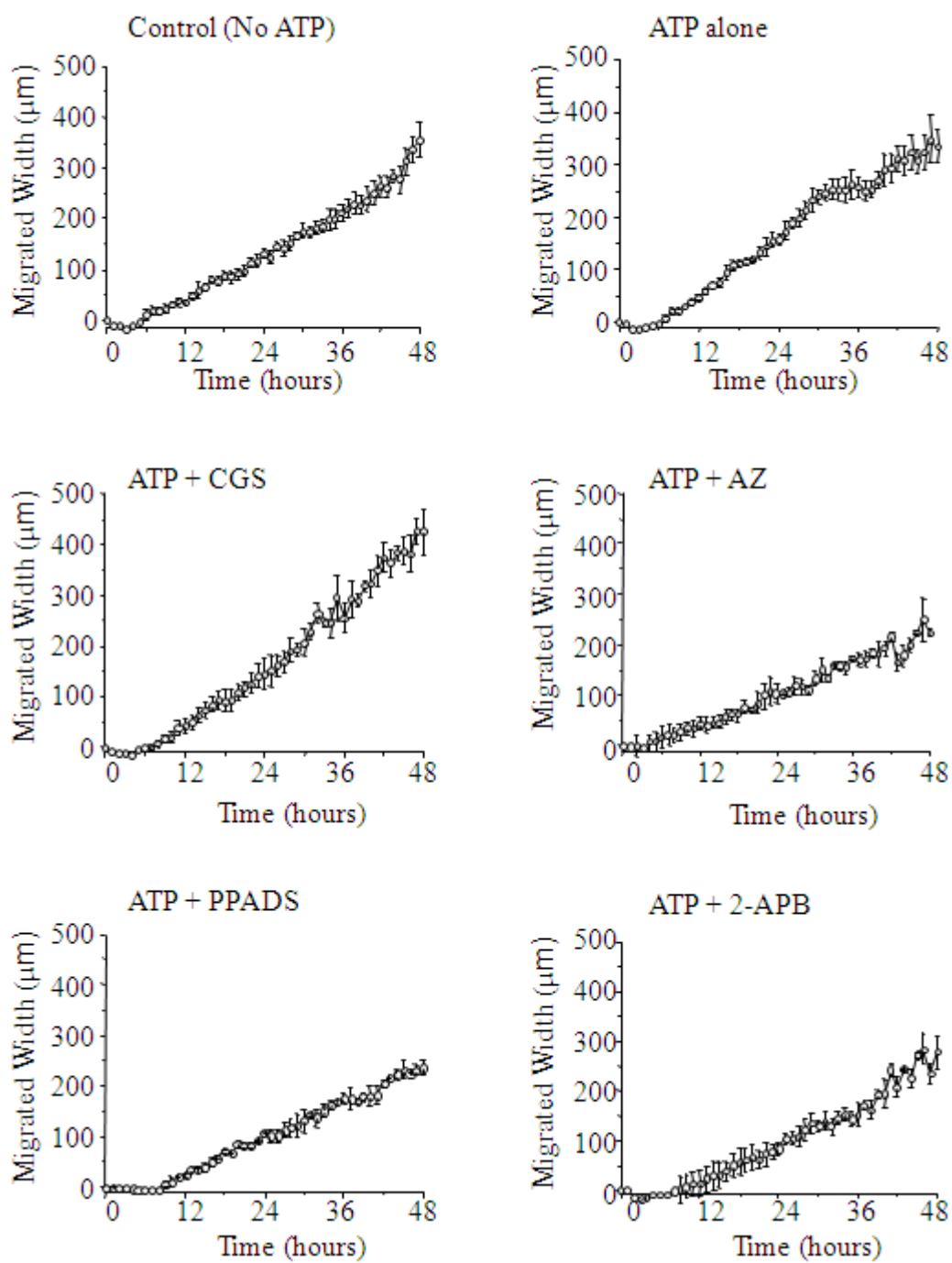


(Figure 6.1)

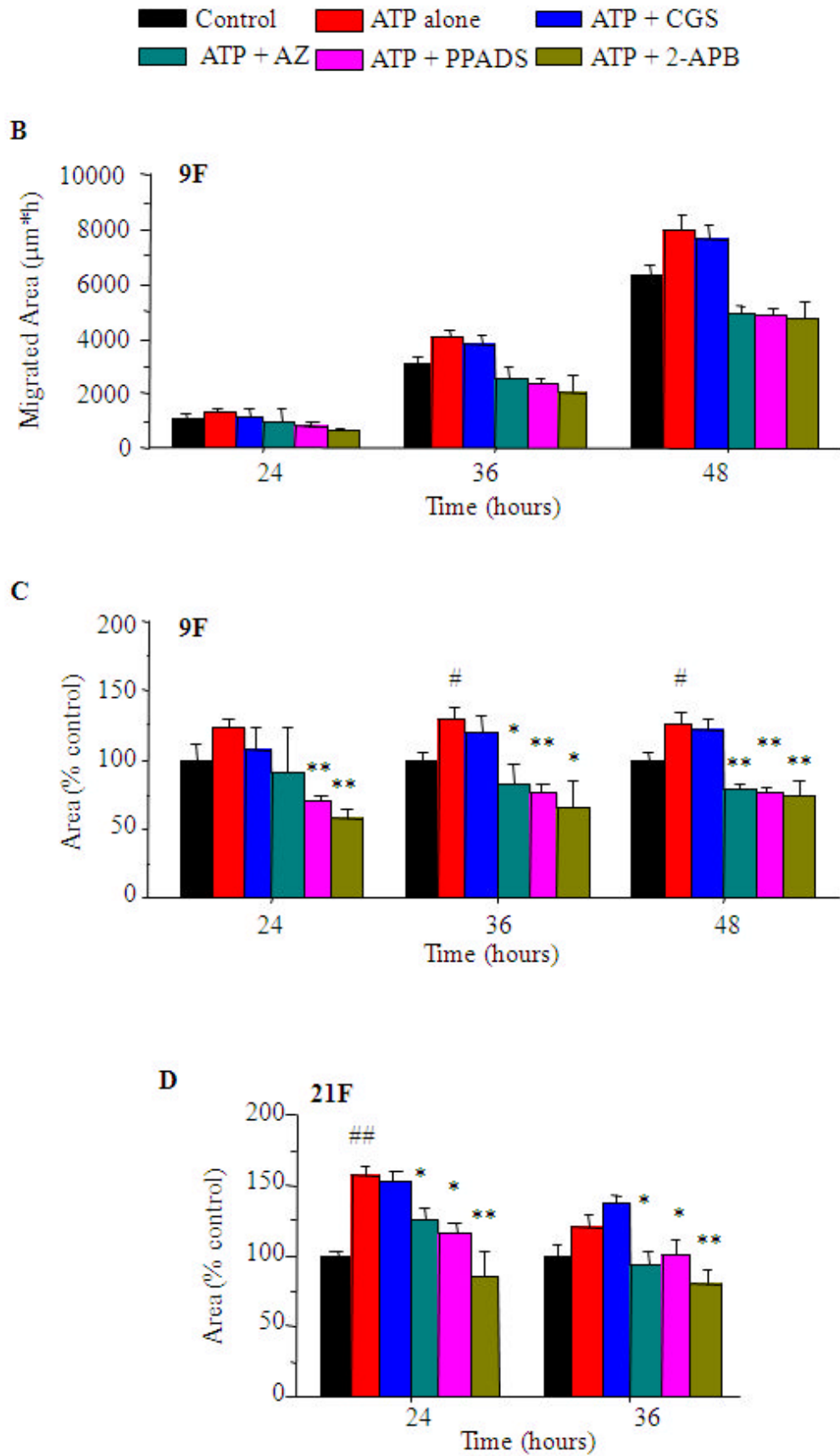


(Figure 6.1)

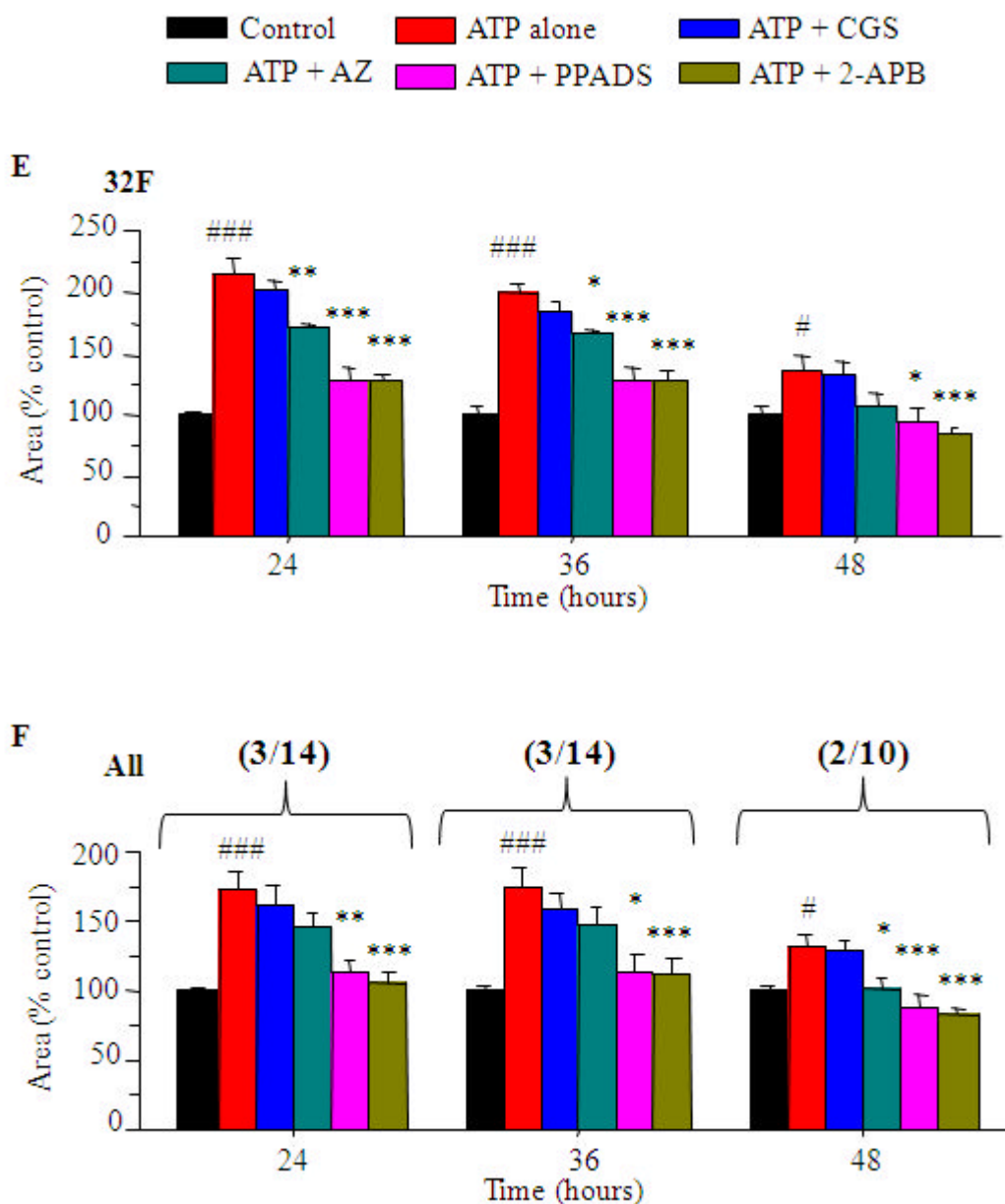
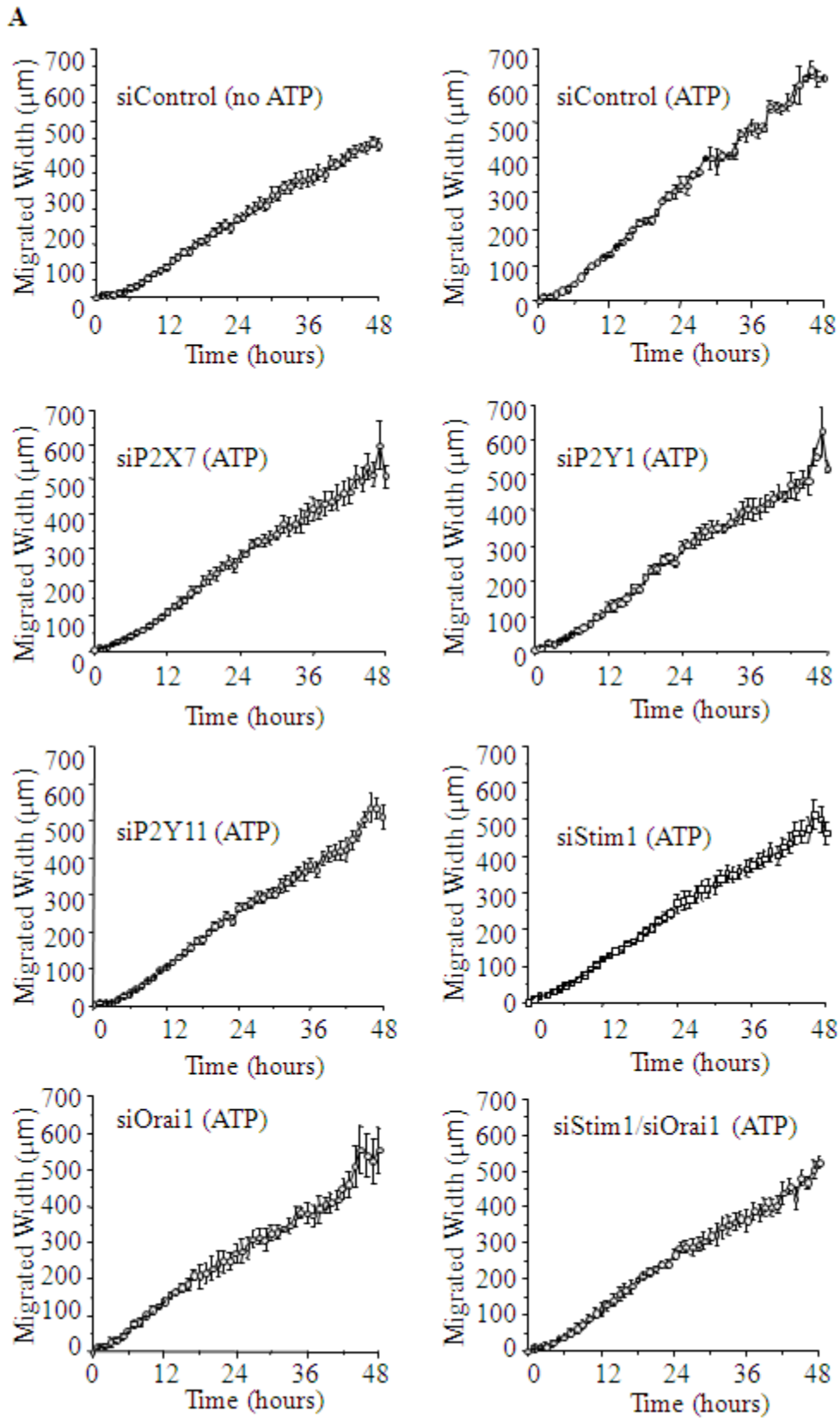
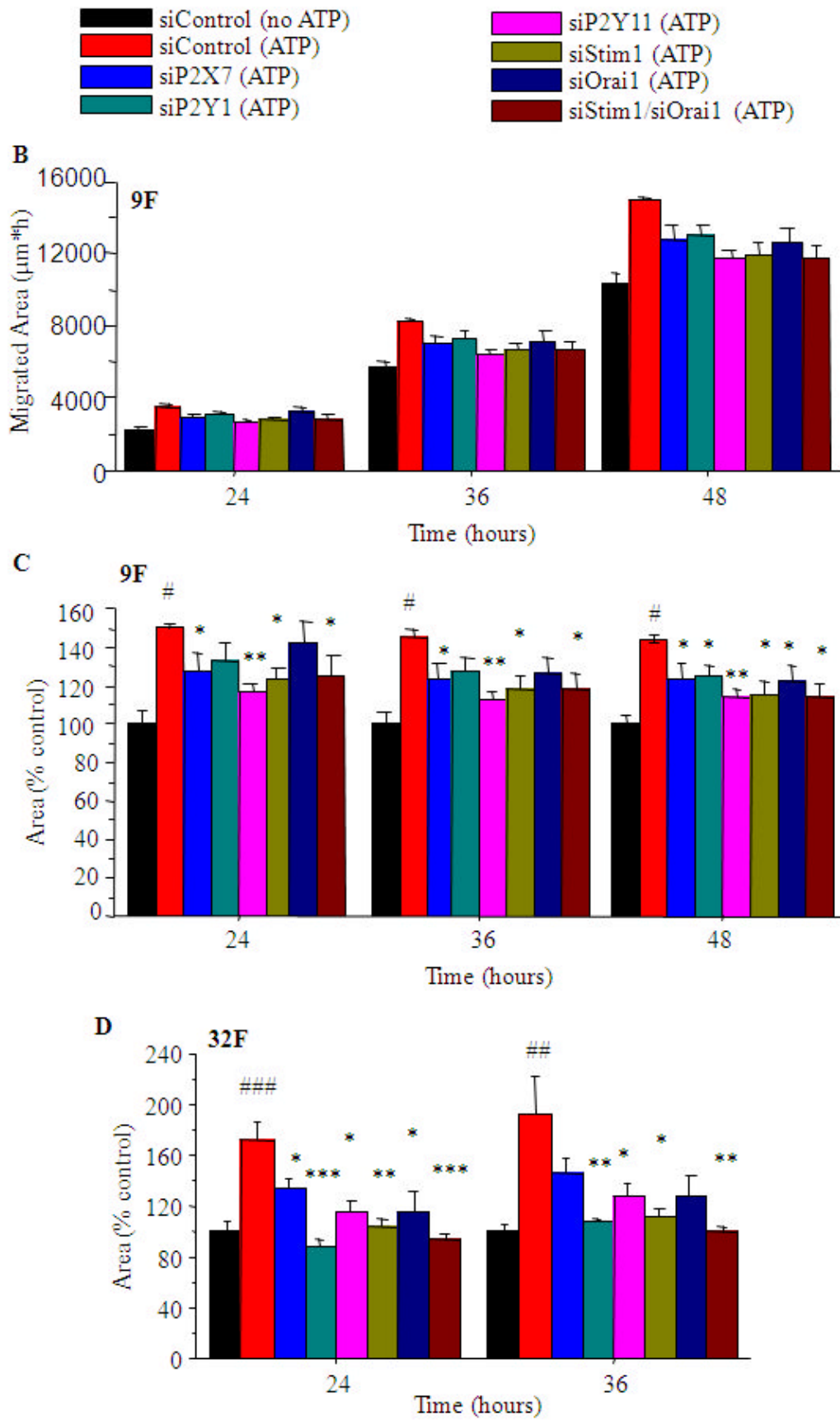


Figure 6.1 Effects of inhibitors on ATP-induced increase in hDP-MSC migration.

(A) Reduction in the wound width or cell migration for control or untreated cells (P4, 9F) and cells treated with ATP at 30 μ M alone or together with CGS15943 (CGS) at 0.1 μ M, AZ11645373 (AZ) at 1 μ M, PPADS at 10 μ M, and 2-APB at 5 μ M. (B) Summary of the migration areas at 24, 36 or 48 hours for cells (9F). (C-F) Summary of the cell migration expressed as percentage of cell migration for matched control cells at 24, 36 or 48 hours: (C) 9F, P4, N = 4 wells; (D) 21F, P4, N = 4 wells; (E) 32F, P4, N = 4 wells; (F) 9F, 21F and 32F, n/N = 3/12. #, $p < 0.05$; ##, $p < 0.01$; ###, $p < 0.001$; compared to the control without ATP. *, $p < 0.05$; **, $p < 0.01$; ***, $p < 0.001$; compared to ATP alone.



(Figure 6.2)



(Figure 6.2)

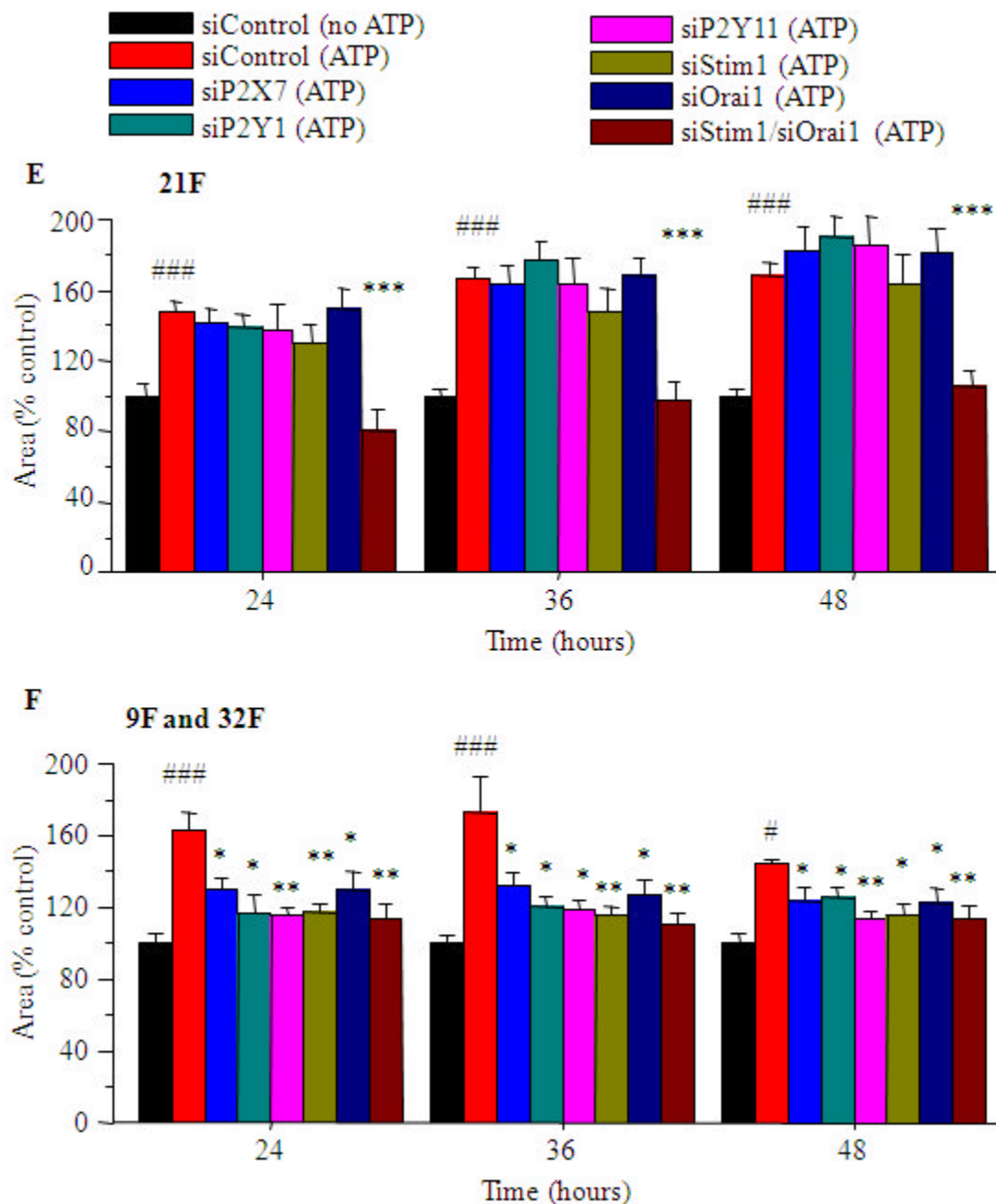


Figure 6.2 Effects of transfection with siRNA for P2X7, P2Y1, P2Y11, Stim1 and Orai1 on ATP-induced increase in hDP-MSC migration.

(A) Reduction in the wound width or cell migration for siControl-transfected control cells (P4, 9F) without exposure to ATP or cells transfected with siControl or siRNA for P2X7, P2Y1, P2Y11, Stim1, Orai1 and Stim1/Orai1 and exposed to ATP (30 μ M). (B) Summary of the migration areas at 24, 36 or 48 hours for cells (9F). (C-F) Summary of the cell migration expressed as percentage of that for matched control cells at 24, 36 or 48 hours: (C) 9F, P4, N = 4 wells; (D) 32F, P4, N = 4 wells; (E) 21F, P4, N = 4 wells; (F) 9F and 32F, n/N = 2/8. #, $p < 0.05$; ##, $p < 0.01$; ###, $p < 0.001$; compared to siControl without ATP. *, $p < 0.05$; **, $p < 0.01$; ***, $p < 0.001$; compared to siControl with ATP.

6.2.2 The role in osteogenic differentiation of hDP-MSCs

6.2.2.1 Effects of inhibitors for P2 receptors and SOC channels

In order to investigate the potential role of the P2X7 receptor, P2Y receptors, and Stim1/Orai SOC channels in the down-regulation by extracellular ATP of osteogenic differentiation, hDP-MSCs were cultured for 14 days in BM and ODM containing ATP or ATP together with the inhibitors for P2 receptors and SOC channels: 0.1 μ M CGS15943, 1 μ M AZ11645373, 10 μ M PPADS and 5 μ M 2-APB. The effects of such inhibitors on osteogenic differentiation of hDP-MSCs were determined using the ALP activity assays. Figure 6.3A shows the ALP activity under the above conditions. Figure 6.3B-E show the ALP activity expressed as percentage of that in control cells. As described in section 3.2.4 of chapter 3, ATP alone significantly down-regulated the ALP activity or osteogenic differentiation of hDP-MSCs in BM or ODM (Figure 6.3E). For cells cultured in BM, PPADS significantly inhibited ATP-induced decrease in the ALP activity but CGS15943 and AZ11645373 had no effect (Figure 6.3E). Similarly, ATP-induced decrease in osteogenic differentiation in ODM was significantly inhibited by PPADS, but not CGS15943 or AZ11645373. These results suggest that the P2Y receptors are involved in ATP-induced inhibition of osteogenic differentiation of hDP-MSCs, but the adenosine receptors and P2X7 receptor have no major role.

6.2.2.2 Effects of transfection with siRNAs on ATP-induced inhibition of osteogenic differentiation

In order to further investigate the role of the P2X7, P2Y1, P2Y11, Stim1 and Orai1 in extracellular ATP-induced inhibition of osteogenic differentiation, hDP-MSCs transfected with siRNAs were examined. Figure 6.4A shows the ALP activity in cells after transfection with siControl and siRNA for P2X7, P2Y1, P2Y11, Stim1, Orai1 and Stim1/Orai1 expressed as percentage of the ALP activity for siControl-transfected and untreated cells (Figure 6.4B-E).

As described in untransfected cells in chapter 3 (section 3.2.4) and Figure 6.3E, ATP significantly reduced the ALP activities in cells transfected with siControl in BM and ODM (Figure 6.4E). Transfection with siP2Y1, siP2Y11, siStim1, siOrai1, or co-transfection with siStim1/siOrai1, but not with siP2X7, significantly increased of the ALP activity in ATP-treated cells as compared to that in cells transfected with siControl. In addition, ATP-induced inhibition of the osteogenic differentiation in ODM was significantly attenuated by transfection with siP2Y1, siP2Y11, siOrai1 alone or co-transfection with siStim1/siOrai1, but not with siP2X7 and siStim1 alone. These results indicate that the P2Y1 and P2Y11 receptors and particularly Stim1/Orai1 SOC channels contribute to ATP-induced inhibition of the osteogenic differentiation of hDP-MSCs.

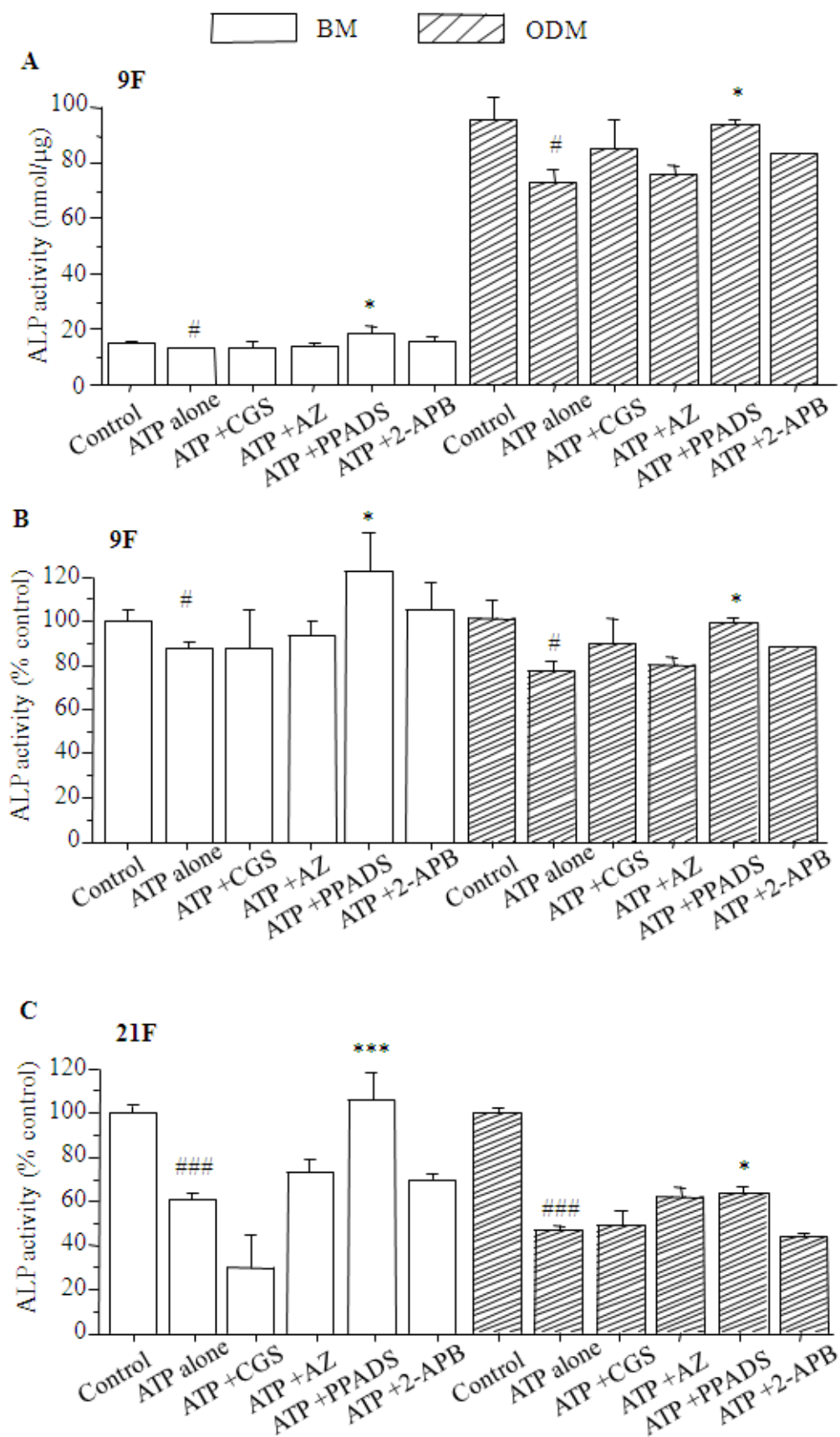


(Figure 6.3)

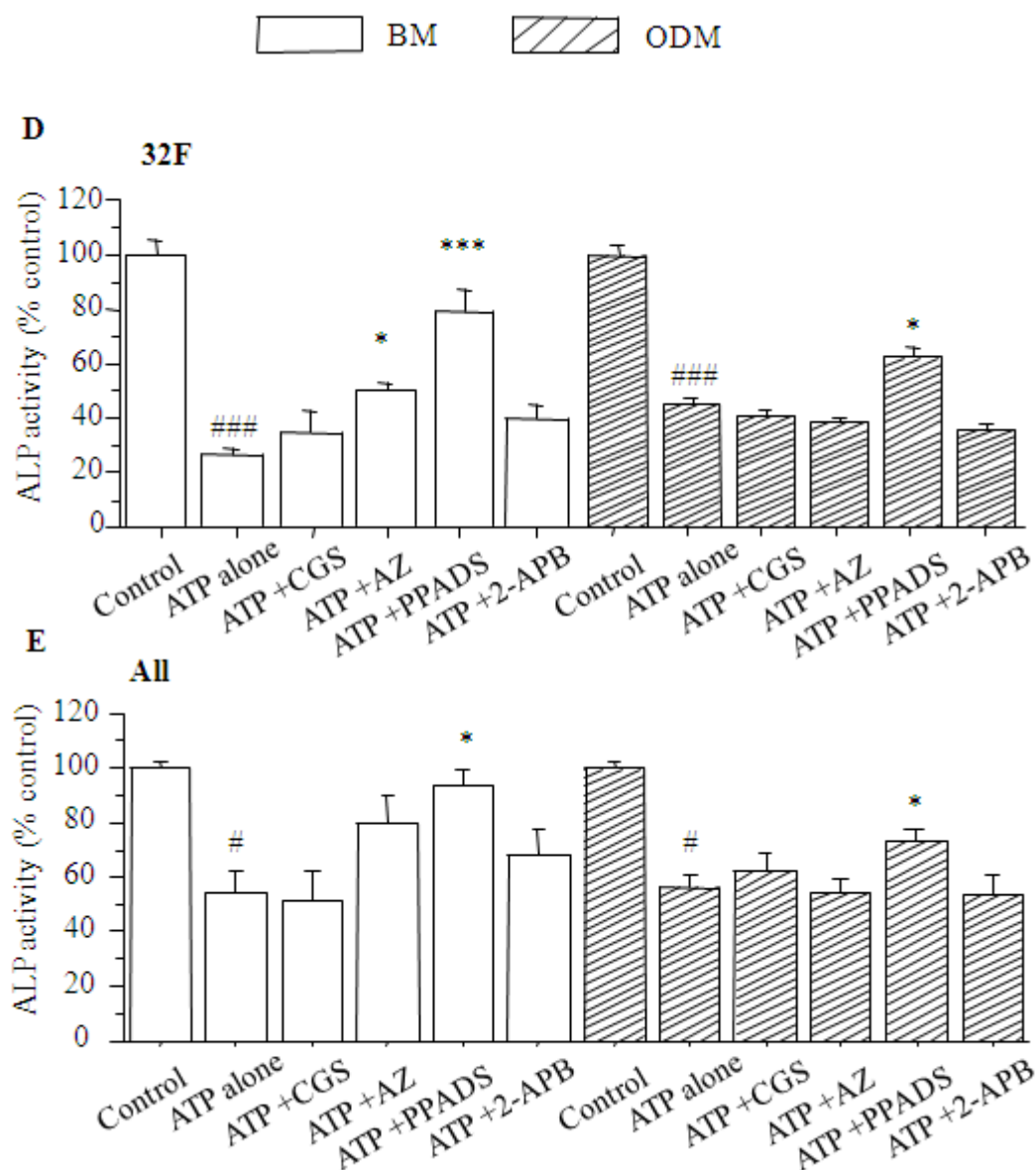
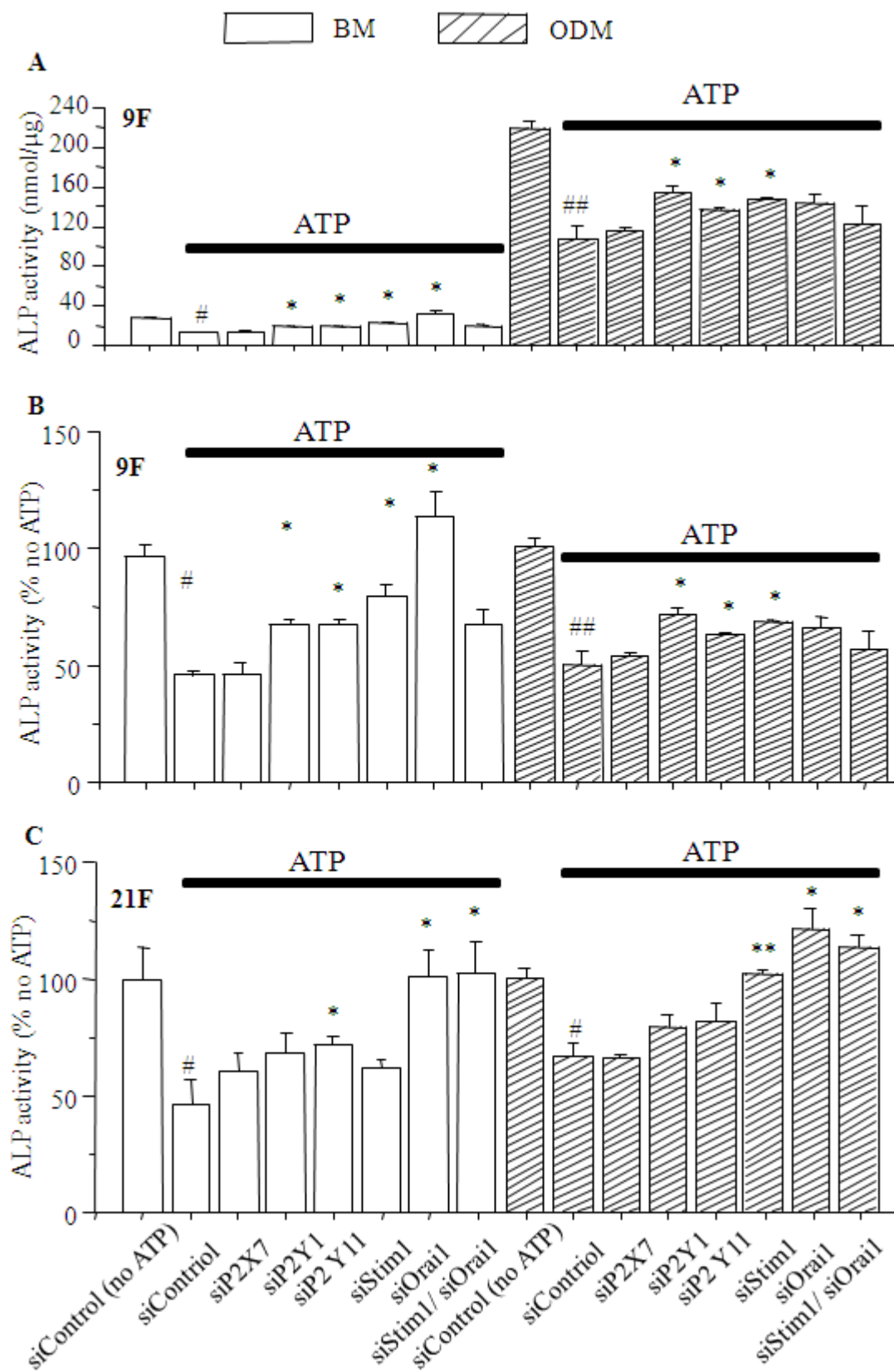


Figure 6.3 Effects of inhibitors on osteogenic differentiation in ATP-treated hDP-MSCs.

(A) The ALP activity in control cells (P4, 9F) or cells treated with 30 μ M ATP alone or together with CGS15943 at 0.1 μ M, AZ11645373 at 1 μ M, PPADS at 10 μ M and 2-APB at 5 μ M. Cells were cultured in BM and ODM for 14 days. (B-E) Summary of the ALP activity in treated cells as percentage of that in control or untreated cells: (B) 9F, P4, N = 4 wells; (C) 21F, P4, N = 4 wells; (D) 32F, P4, N = 4 wells; (E) 9F, 21F and 32F, n/N = 3/12. Cells were cultured in BM (open bars) and ODM (hatched bars). #, $p < 0.05$; ##, $p < 0.01$; ###, $p < 0.001$; compared to control without ATP. *, $p < 0.05$; **, $p < 0.01$; ***, $p < 0.001$; compared to ATP alone.



(Figure 6.4)

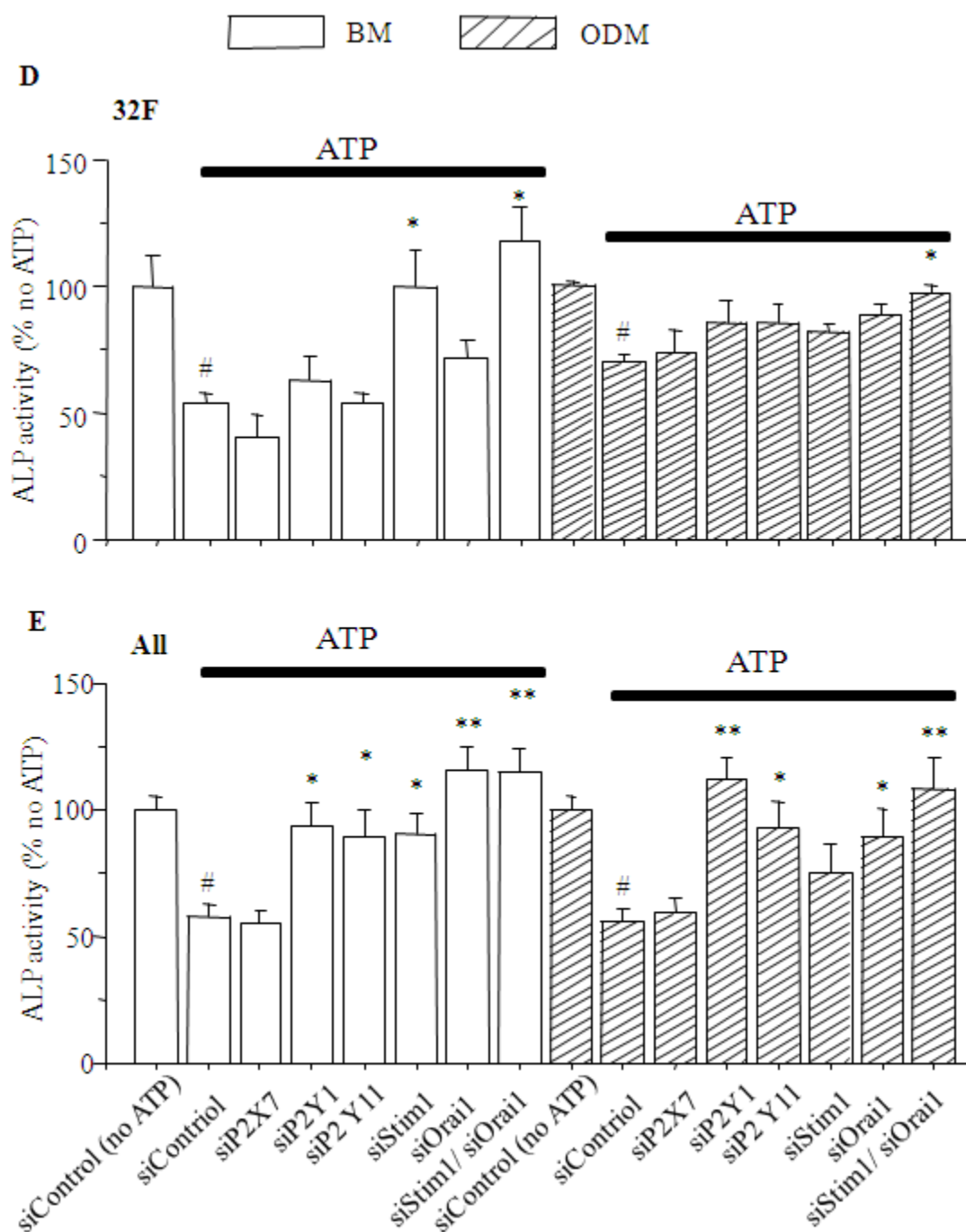


Figure 6.4 Effects of siRNAs on osteogenic differentiation in ATP-treated hDP-MSCs.

(A) The ALP activities in siControl-transfected and untreated cells (P4, 9F) and cells transfected with siControl or specific siRNA for P2X7, P2Y1, P2Y11 Stim1, Orail and Stim1/Orail and treated with ATP (30 μ M) in BM and ODM. Cells were cultured in BM and ODM for 14 days. (B-E) Summary of the ALP activity as percentage of that in matched control cells: (B) 9F, P4, N = 4 wells; (C) 21F, P4, N = 4 wells; (D) 32, P4, N = 4 wells; (E) 9F, 21F and 32F, n/N = 3/12. #, $p < 0.05$; ##, $p < 0.01$; ###, $p < 0.001$; compared to siControl without ATP. *, $p < 0.05$; **, $p < 0.01$; ***, $p < 0.001$; compared to siControl with ATP.

6.2.3 The role in adipogenic differentiation of hDP-MSCs

6.2.3.1 Effects of inhibitors for P2 receptors and SOC channels

The potential role of the P2X7 receptor, P2Y1 and P2Y11 receptors, and Stim1/Orai SOC channels in the up-regulation by extracellular ATP of adipogenic differentiation of hDP-MSC were investigated by determining the OD₅₁₀/DNA to quantify the Oil red O staining of cells treated with ATP alone or together with various inhibitors of the P2 receptors and SOC channels, including 0.1 μM CGS15943, 1 μM AZ11645373, 10 μM PPADS and 5 μM 2-APB. The DNA content was not significantly altered by these inhibitors (Figure 6.5A). Figure 6.5B shows the OD₅₁₀/DNA. Figure 6.5C-F show adipogenesis of cells treated with ATP alone or together with indicated inhibitors, expressed as percentage of that in control cells.

As described above in section 3.2.5 of chapter 3, ATP significantly improved adipogenic differentiation of hDP-MSCs cultured in ADM (Figure 6.5F). ATP-induced increase in adipogenic differentiation of hDP-MSCs in ADM was significantly inhibited by PPADS and 2-APB, but not AZ1164537, suggesting that the P2Y receptors and SOC channels, but not P2X7 receptor, are critically involved in ATP-induced facilitation of adipogenic differentiation (Figure 6.5 F). There was no significant effect by CGS15943 (Figure 6.5F), indicating no major role for the adenosine receptors.

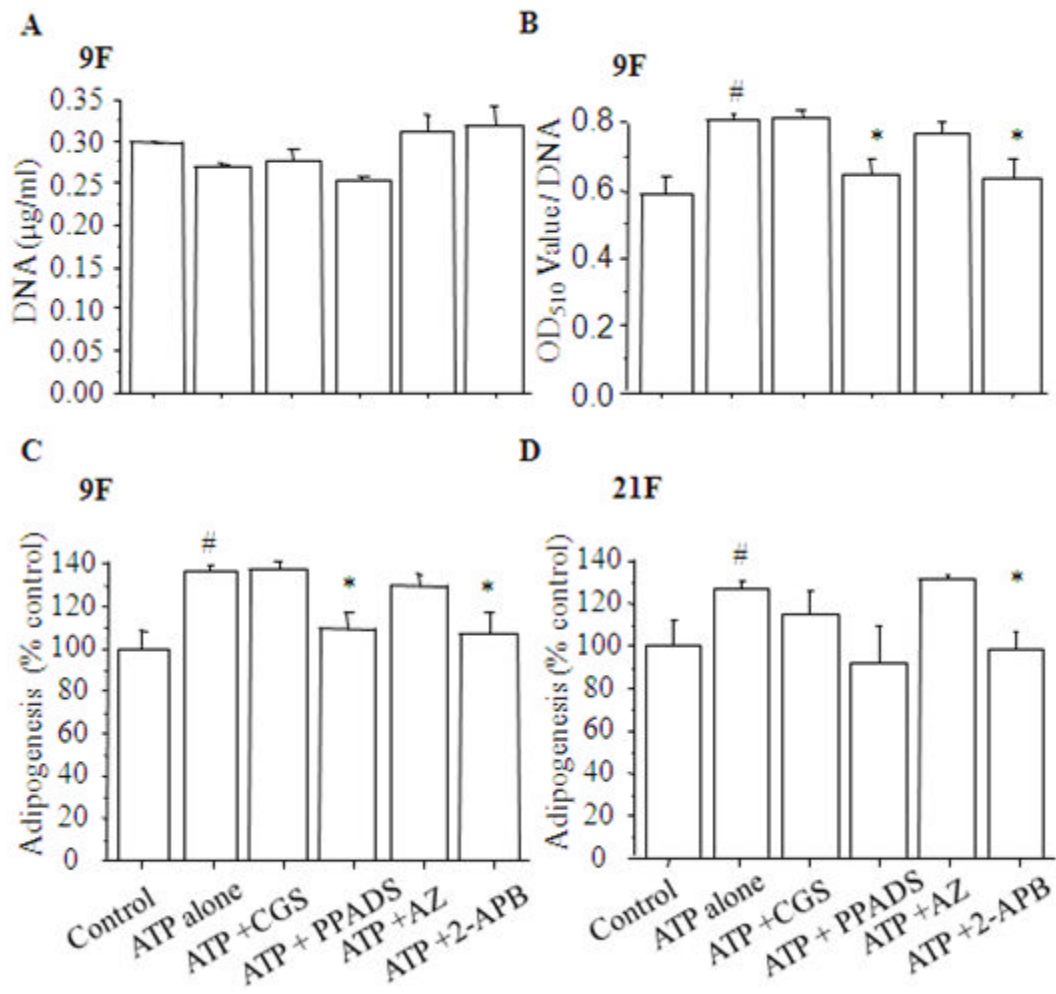


(Figure 6.5)

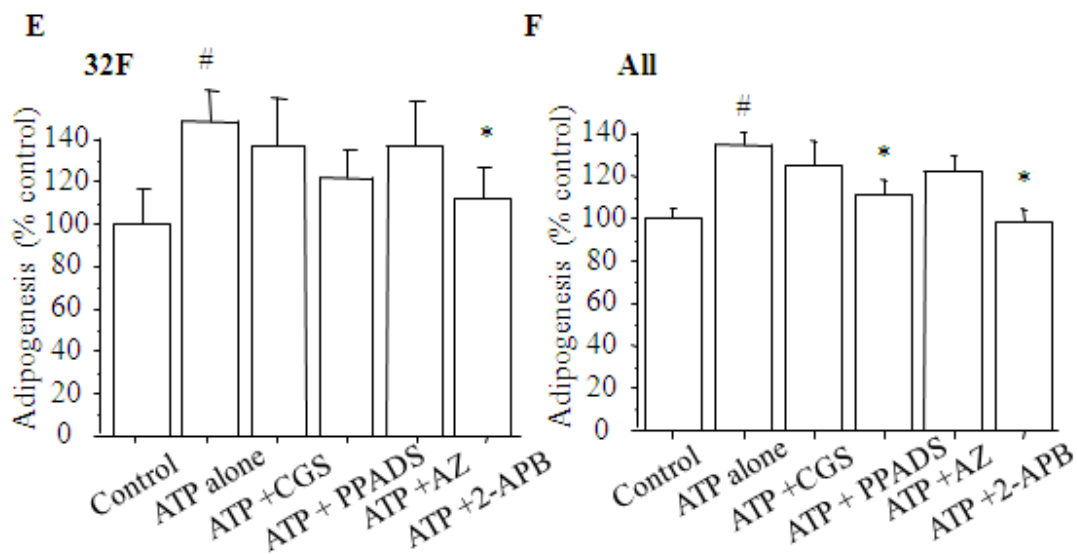


Figure 6.5 Effects of inhibitors on ATP-induced increase in adipogenic differentiation of hDP-MSCs.

(A) Summary of the DNA content in control cells or cells (P4, 9F, N = 4 wells) treated with ATP alone or together with CGS15943 at 0.1 μ M, AZ11645373 at 1 μ M, PPADS at 10 μ M and 2-APB at 5 μ M. Cells were cultured in ADM for 21 days. (B) Summary of the Oil Red staining determined by the OD₅₁₀ value per DNA (μ g/ml) in cells under the conditions shown in (A). (C-F) Summary of the adipogenesis in treated cells as percentage of that in control cells: (C) 9F, P4, N = 4 wells; (D) 21F, P4, N = 4 wells; (E) 32F, P4, N = 4 wells; (F) 9F, 21F and 32F, n/N = 3/12. #, $p < 0.05$; ##, $p < 0.01$; ###, $p < 0.001$; compared to control without ATP. *, $p < 0.05$; **, $p < 0.01$; ***, $p < 0.001$; compared to ATP alone.

6.2.3.2 Effects of transfection with siRNAs on osteogenic differentiation

In order to further investigate the role of P2X7, P2Y1, P2Y11, Stim1 and Orai1 in extracellular ATP-induced increase in adipogenic differentiation, hDP-MSCs transfected with siRNAs were examined.

The effects of transfection with siRNA on ATP-induced increase in adipogenic differentiation are shown in Figure 6.6A-C. Transfection with siP2Y1 and siP2Y11 significantly inhibited, whereas transfection with siP2X7 did not significantly alter, ATP-induced increase in adipogenic differentiation from all these donors (Figure 6.6D), indicating that the P2Y1 and P2Y11 receptors contribute to ATP-induced facilitation of adipogenic differentiation. However, transfection of siStim1 and siOrai1, and even co-transfection with siStim1 and siOrai1 did not significantly affect ATP-induced increase in adipogenic differentiation. The role of Orai3 was studied by transfection with siOrai3 (Figure 6.6A-C). Transfection with siOrai3 significantly reduced ATP-induced increase in adipogenic differentiation (Figure 6.6D). These results suggest that the Orai3 channel is involved in the up-regulation by extracellular ATP of adipogenic differentiation of hDP-MSCs.

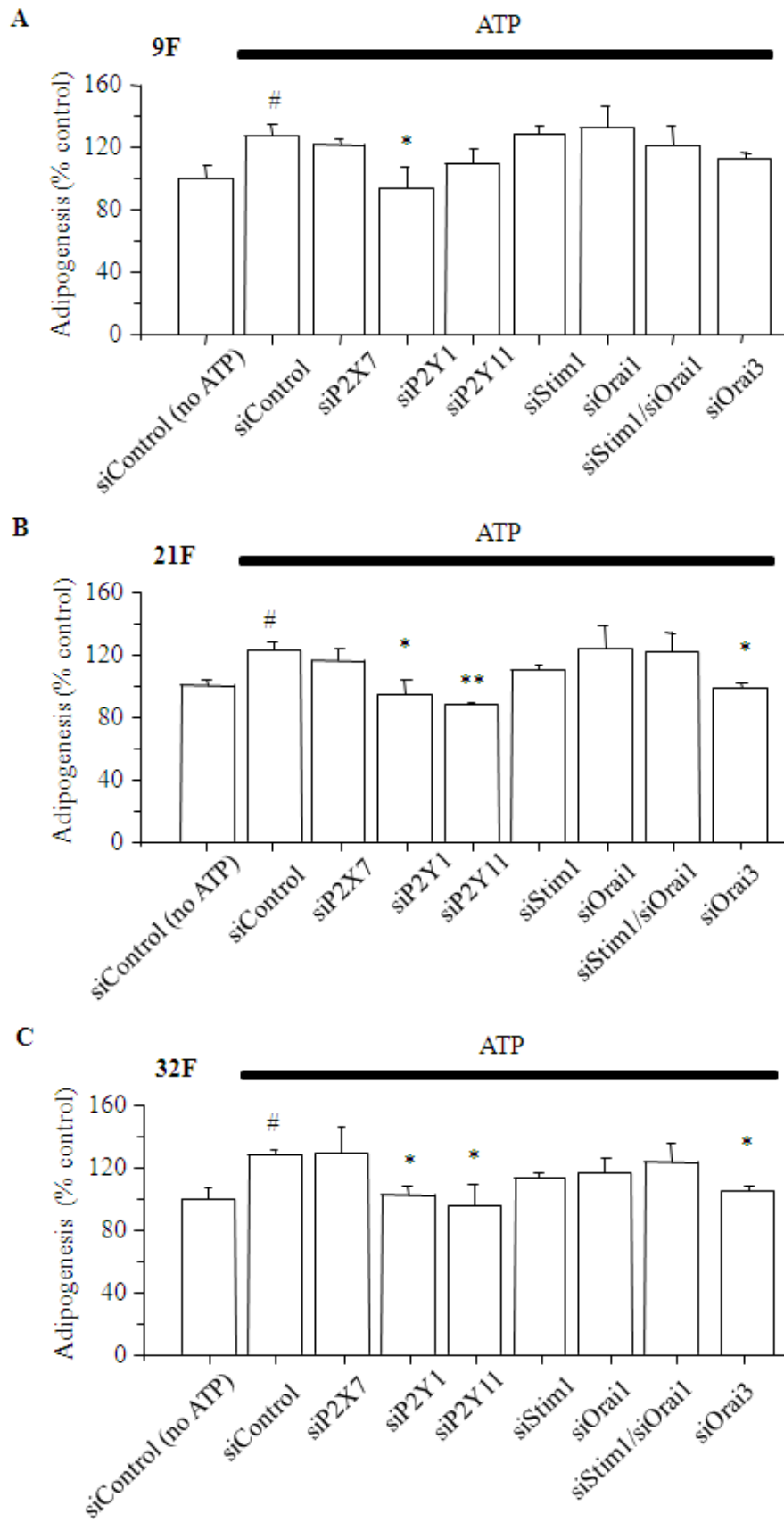


(Figure 6.6)

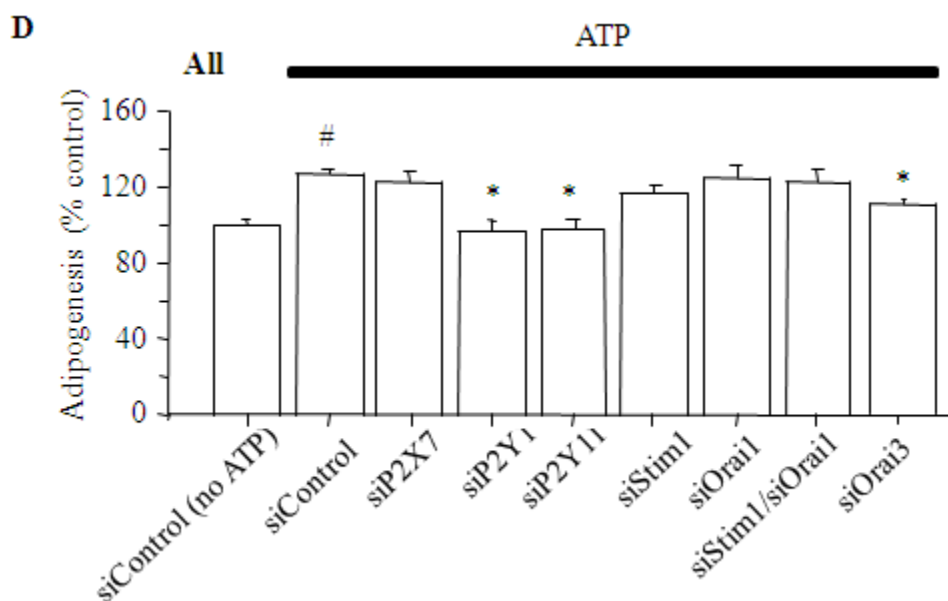


Figure 6.6 Effects of transfection with siRNA on adipogenic differentiation in ATP-treated hDP-MSCs.

(A-D) Summary of adipogenic differentiation of ATP-treated (30 μ M) hDP-MSCs (P4, 9F) transfected with siControl or siRNA for P2X7, P2Y1, P2Y11, Stim1, Orai1, Stim1/Orai1 and Orai3, presented as percentage of adipogenesis in siControl-transfected control cells untreated with ATP: (A) 9F, P4, N = 4 wells; (B) 21F, P4, N = 4 wells; (C) 32F, P4, N = 4 wells; (D) 9F, 21F and 32F, n/N = 3/12. Cells were cultured in ADM for 21 days. Adipogenesis was determined by the OD₅₁₀ value (Oil red staining) per μ g DNA. #, $p < 0.05$; ##, $p < 0.01$; ###, $p < 0.001$; compared to siControl without ATP. *, $p < 0.05$; **, $p < 0.01$; ***, $p < 0.001$; compared to siControl with ATP.

6.3 Discussion

The study in this chapter provides evidence to show that the P2X7, P2Y1, P2Y11, Stim1, Orai1 and Orai3 have differential roles in ATP-induced effects on hDP-MSCs functions. Specifically, the P2X7, P2Y1 and P2Y11 receptors and Stim1/Orai1 are involved in ATP-induced stimulation of cell migration. The P2Y1 and P2Y11 receptors and Stim1/Orai1 are engaged in ATP-induced inhibition of osteogenic differentiation. Finally, the P2Y1 and P2Y11 receptors and Orai3 are important in ATP-evoked increase in adipogenic differentiation.

ATP stimulated hDP-MSC migration. Such an effect was inhibited by PPADS, but not by CGS15943, indicating a critical role for the P2 receptors and no or a very minor role for the adenosine receptors (Figure 6.1F). ATP-induced effect on cell migration was slightly but significantly inhibited by AZ11645373 (Figure 6.1F) to inhibit the P2X7 receptor function and siRNA to reduce the P2X7 receptor expression level (Figure 6.2F), supporting a role for the P2X7 receptor. ATP-induced stimulation of cell migration was strongly blocked by down-regulation of the P2Y1 and P2Y11 receptor expression with siRNA (Figure 6.2F), and by 2-APB (Figure 6.1F) and down-regulation of Stim1, Orai1 expression level with siRNA (Figure 6.2F). Taken together, these results consistently show a significant role for the P2Y1 and P2Y11 receptors that are coupled to the Stim1/Orai1 SOC channels in ATP-induced increase in hDP-MSC migration. It was reported that ATP increased hBM-MSC migration using a transwell assay (Ferrari, Gulinelli et al. 2011). Ca^{2+} signalling was considered to play an important role in hBM-MSC migration (Ding, Zhang et al. 2012). The P2Y11 receptor has been shown to contribute to hBM-MSC migration stimulated by extracellular NAD^+ (Fruscione, Scarfi et al. 2011). The P2Y2 receptor is reported to be involved in ATP-enhanced cell migration in hepatocellular carcinoma cells (Xie, Xu et al. 2014) and UTP-enhanced cell migration in $CD34^+$ HSCs (Lemoli, Ferrari et al. 2004). However, the P2Y2 expression was not consistently observed in hDP-MSCs

(see section 4.2.2). Stim1 in hepatocellular carcinoma cells was involved in ATP-induced increase of cell migration (Xie, Xu et al. 2014). Additionally, the Stim1 and Orai1 expression levels and cell migration in breast cancer cells (MCF-7) are up-regulated by silencing Oct4 with siRNA, although the causative relationship between the Stim1/Orai1 expression and cell migration is unclear (Hu, Qin et al. 2011).

The present study shows that the ALP expression and activity in hDP-MSCs cultured in BM and ODM were reduced by ATP. The ATP-induced effect on the ALP activity in cells cultured in BM was significantly inhibited by PPADS, but not CGS15943 (Figure 6.3E). Treatment with 2-APB appeared to inhibit the decrease in the ALP activity in ATP-treated cells cultured in BM, but the inhibition was not statistically significant. ATP-induced inhibition of the ALP activity was not affected by AZ11645373 to inhibit the P2X7 receptor function or using siP2X7 to reduce the receptor expression, suggest no major role for the P2X7 receptor. Treatment with siP2Y1, siP2Y11, siStim1, siOrai1 and siStim1/siOrai1 almost completely blocked ATP-induced decrease in the ALP activity in cells cultured in BM (Figure 6.4E). These results indicate that ATP inhibits the osteogenic differentiation potential of hDP-MSCs via activating the P2Y1 and P2Y11 receptors and downstream Stim1/Orai1 SOC channels.

The present study also shows that ATP can down-regulate the ALP expression and activity or osteogenesis of hDP-MSCs cultured in ODM. Such an effect was also attenuated by PPADS (Figure 6.3E). CGS15943 (Figure 6.3E) and AZ11645373 or transfection of cells with siP2X7 failed to result in any effect. These observations are not consistent with that reported in a recent study of hBM-MSCs (Sun, Junger et al. 2013). In the previous study, the P2X7 receptor was shown to be involved in ATP-induced increase in osteogenic differentiation of hBM-MSCs. The difference

may be due to the fact that different cell preparations and the duration of treatment with ATP were different; hDP-MSCs were exposed to ATP during the osteogenic differentiation in the present study, whereas hBM-MSCs were treated with ATP for 5 minutes before introduction of osteogenic differentiation in the previous study (Sun, Junger et al. 2013). Treatment with siP2Y1, siP2Y11, siOrai1 and siStim1/siOrai1, largely reversed the reduction by ATP in the osteogenesis of hDP-MSCs cultured in ODM (Figure 6.4E). These results suggest that activation of the P2Y1 and P2Y11 receptors and Stim1/Orai1 SOC channels are significantly involved in the down-regulation by ATP of hDP-MSC osteogenesis. It was also reported that the expression level of the P2Y1 receptor was down-regulated during osteogenic differentiation of AT-MSCs, although the causative relationship between the P2Y1 receptor expression and osteogenic differentiation is unclear (Zippel, Limbach et al. 2012; Scarfi 2014). In contrast with using siRNA to reduce the SOC channel expression, there was no effect by 2-APB to block the SOC channels (Figure 6.4E). The exact reason for such a discrepancy is still unclear. It is possible that inhibition of the SOC channels by 2-APB was inefficient in preventing the action of osteogenesis-inducing molecules present in ODM, by inducing additional effects on other signalling molecules as it is well-known that 2-APB can activate and inhibit the functions of a number of other proteins, including TRP channels (Jiang, Yang et al. 2010).

In contrast to the inhibition or negative modulation of osteogenic differentiation, ATP facilitated the adipogenic differentiation of hDP-MSCs. Such an effect was significantly inhibited by PPADS, but not CGS15943, again supporting the role of the P2 receptors rather than the adenosine receptors (Figure 6.5E). Inhibition of the P2X7 receptor function using AZ1164537 or reduction of the P2X7 receptor expression failed to block ATP-induced facilitation of adipogenic differentiation, largely excluding a significant role for the P2X7 receptor. Transfection with siRNA for the P2Y1 or P2Y11 receptor strongly blocked ATP-induced effect on adipogenesis

(Figure 6.6D). These results suggest a significant role for the P2Y1 and P2Y11 receptors. Intriguingly, treatment with siStim1, siOrai1 and siStim1/siOrai1, which can mitigate ATP-induced inhibition of osteogenic differentiation, had no effect on ATP-induced facilitation of adipogenic differentiation. ATP-induced increase in adipogenic differentiation was slightly inhibited by using siOrai3 to reduce the Orai3 expression (Figure 6.6D). The expression level of Orai3 showed much higher than Stim1 and Orai1 in hDP-MSCs from all three donors (Figure 5.2 and 5.8). But, how the Orai3 channel was indirectly activated by ATP through downstream signalling pathways following activation of the P2Y1 and/or P2Y11 receptor is unclear and further studies are required. To date, it has been reported that ATP by activating the P2Y1 receptor up-regulates adipogenic differentiation of hBM-MSCs (Ciciarello, Zini et al. 2013). It was also reported that the expression level of the P2Y11 receptor was significantly up-regulated in adipogenic differentiation of hAT-MSCs, although the causative relationships between the P2Y11 receptor expression and adipogenic differentiation are unclear (Zippel, Limbach et al. 2012; Scarfi 2014).

In summary, the results from this chapter have demonstrated that the P2X7, P2Y1, P2Y11 receptors and Stim1/Orai1 SOC channels in hDP-MSCs contribute in ATP-induced increase in hDP-MSC migration. The P2Y1 and P2Y11 receptors and Stim1/Orai1 SOC channels also have a significant role in the down-regulation by ATP of osteogenic differentiation, whereas the P2Y1 and P2Y11 receptors and Orai3 are critically engaged in ATP-induced facilitation of adipogenic differentiation in hDP-MSCs.

Chapter 7

General Discussion

MSCs found in several tissues and organs (Figliuzzi, Bonandrini et al. 2014) exhibit the capacity of differentiating into multiple lineages, including osteoblasts, adipocytes, chondrocytes, myocytes, and neural precursors (Jiang, Jahagirdar et al. 2002; Phinney 2007; Bonfield, Nolan Koloze et al. 2010). Due to their easy accessibility, regenerative potential, potent immunoregulatory functions, and lack of ethical issues (Lee, Lim et al. 2014; Wuchter, Bieback et al. 2014), MSCs provide promising approaches of regeneration medicines, including tissue engineering (Abdallah and Kassem 2008; Farini, Sitzia et al. 2014). So far, on one hand, there is a large body of evidence supporting the therapeutic potential of hMSCs for cell therapy and tissue engineering. On the other hand, there is little understanding of the intrinsic signalling mechanisms that determine or regulate the proliferation, migration and differentiation potentials of hMSCs, although such properties of MSCs are known to be strongly influenced by the local microenvironments (Shi and Li 2008; Biver, Wang et al. 2013; Biver, Thouverey et al. 2014). A better understanding of the signalling mechanisms underlying such functions in hMSCs is expected to facilitate applications of hMSCs.

There is emergent evidence to suggest extracellular ATP plays a significant role in a diversity of cell functions, including proliferation, migration and differentiation of stem cells, including ESCs, HSCs, NSCs and BM-MSCs (Burnstock and Ulrich 2011; Scarfi 2014). In previous studies, extracellular ATP was shown to promote cell migration, osteogenesis and adipogenesis in hBM-MSCs (Ferrari, Gulinelli et al. 2011) (Ciciarello, Zini et al. 2013; Sun, Junger et al. 2013). However, our understanding of the intrinsic signalling mechanisms responding to extracellular ATP is still contentious. Therefore, the study presented in this thesis aimed to investigate the

effects of extracellular ATP on the proliferation, migration and differentiation of hDP-MSCs and the intrinsic signalling mechanisms activated by ATP.

In this study, hMSCs were isolated from dental pulp tissues from four donors with different age and gender (Figure 3.1-3.3; Table 3.1). The hDP-MSCs expressed STRO-1 (a MSC marker), a high level of CD105, CD90 and CD73, and a very low level of CD45, CD34 and CD14 (Table 3.1). Although the CD105 expression was slightly low and the CD14 expression was slightly high, hDP-MSCs in the present study displayed a potential of multipotent differentiation including osteocytes, adipocytes and chondrocytes (Figure 3.3).

Results from the XTT assay and cell counting methods indicate that treatment with extracellular ATP has no significant effect on cell proliferation in hDP-MSCs (Figure 3.4 and 3.5). In contrast, scratch wound assays demonstrated that ATP enhanced cell migration in hDP-MSCs (Figure 3.6 and 3.7). In addition, the ALP activity assay showed that ATP inhibited osteogenic differentiation of hDP-MSCs (Figure 3.8) and, by contrast, Oil red O staining revealed that ATP promoted adipogenic differentiation of hDP-MSCs (Figure 3.9).

The results from single cell Ca^{2+} imaging showed that ATP induced increases in the $[\text{Ca}^{2+}]_i$ in the extracellular Ca^{2+} -containing or Ca^{2+} -free solutions (Figure 4.1G). Furthermore, results from real-time RT-PCR and effects of selective inhibitors and siRNA knockdown on ATP-induced Ca^{2+} responses demonstrated functional expression of the ATP-sensitive P2X7, P2Y1 and P2Y11 receptors in hDP-MSCs (see chapter 4). Stim1/Orai SOC channels also contributed to extracellular ATP-induced Ca^{2+} signalling in hDP-MSCs (see chapter 5). The present study using inhibitors and transfection with siRNAs (see chapter 6) provided evidence to demonstrate that the P2X7 receptor is involved in ATP-induced increase in hDP-MSC migration, but not

in ATP-induced effects on osteogenic and adipogenic differentiation. Moreover, the P2Y1 and P2Y11 receptors are involved in mediating ATP-induced modulation of hDP-MSC migration, osteogenic and adipogenic differentiation. Stim1/Orai1 SOC channels are also involved in ATP-induced effect on hDP-MSC migration and osteogenic differentiation, while Orai3 is engaged in ATP-induced modulation of adipogenic differentiation. The final chapter aims to provide an integral discussion of the main findings described in this thesis.

7.1 Expression and function of the P2X7 receptor in hDP-MSCs

The results from real-time RT-PCR showed mRNA expression of P2X4, P2X6 and P2X7, but not P2X1, P2X2, P2X3 and P2X5 in hDP-MSCs (Figure 4.2). This finding is not completely consistent with a previous study reporting mRNA expression of all P2X receptors except P2X2 in hBM-MSCs (Ferrari, Gulinelli et al. 2011). Thus, both studies support the mRNA expression of P2X4, P2X6 and P2X7 but are different in terms of the mRNA expression for P2X1, P2X3 and P2X5. The present study has not examined the protein expression of P2X4, P2X6 and P2X7, but determined the effects of selective P2X antagonists on ATP-evoked Ca^{2+} responses in the extracellular Ca^{2+} -containing solutions. ATP-induced Ca^{2+} responses were insensitive to 5-BDBD, a P2X4 selective antagonist (Figure 4.6), suggesting lack or a very low level of functional expression of the P2X4 receptor. It is generally thought that the P2X6 protein does not form functional receptor on its own but can interact with the P2X2 or P2X4 protein to form heteromeric receptors (Khakh, Proctor et al. 1999; Schwindt, Trujillo et al. 2011). It is unlikely that P2X4 and P2X6 form a heteromeric receptor in hDP-MSCs although the present study could not rule out such a possibility.

However, there is clear evidence to support that hDP-MSCs express functional P2X7 receptors. First of all, both ATP and BzATP evoked robust Ca^{2+} responses in the

extracellular Ca^{2+} -containing solutions. BzATP-induced Ca^{2+} responses were consistently greater than those by ATP in hDP-MSCs from three donors (Figure 4.4D-F), and thus BzATP was more potent than ATP, a pharmacological property of the P2X7 receptor (see section 1.3.2.7). Secondly, ATP-induced Ca^{2+} responses were significantly inhibited by AZ11645373, a hP2X7 receptor selective antagonist (Figure 4.7). Finally the Ca^{2+} responses induced by ATP and BzATP were strongly attenuated using siRNA to reduce the P2X7 receptor expression (Figure 4.10). Taken together, these observations strongly support the expression of functional P2X7 receptor in hDP-MSCs. Consistent with this finding, previous studies showed protein and functional expression of the P2X7 receptor in hBM-MSCs (Riddle, Taylor et al. 2007; Ferrari, Gulinelli et al. 2011). The present study further investigated the potential of the P2X7 receptor in ATP-induced effect on hDP-MSC migration and differentiation. Inhibition of the P2X7 receptor with AZ11645373, or reduction of the P2X7 receptor expression with siP2X7, attenuated ATP-induced stimulation of cell migration (Figure 6.1F and Figure 6.2F), providing consistent evidence to suggest a significant role for the P2X7 receptor. In contrast, such pharmacological and genetic interventions failed to prevent ATP-induced inhibition of osteogenesis (Figure 6.3E and Figure 6.4E) and stimulation of adipogenesis of hDP-MSCs (Figure 6.5F and Figure 6.6D), suggesting no major role for the P2X7 receptor in ATP-induced regulation of osteogenic and adipogenic differentiation of hDP-MSCs. A recent study has shown that ATP released by shockwave or pretreatment with ATP for 5 minutes before osteogenic differentiation increased the osteogenic differentiation of hBM-MSCs and such ATP-induced stimulation was attenuated by using siP2X7 to reduce the P2X7 receptor expression and using selective P2X7 receptor antagonist KN62 to inhibit the P2X7 receptor function (Sun, Junger et al. 2013). The exact reasons for such discrepancies are unclear. The different concentrations of ATP and exposure duration used in the previous and present studies may contribute to such differences in ATP-induced effect on osteogenesis and the role of the P2X7 receptor.

In summary, the present study shows that the P2X7 receptor is functionally expressed in hDP-MSCs and plays a role in ATP-induced increase in cell migration, but not in ATP-induced effects on osteogenic and adipogenic differentiation.

7.2 Expression and function of the P2Y1 and P2Y11 receptors in hDP-MSCs

In addition to the P2X receptors, extracellular ATP can activate the P2Y1, P2Y2 and P2Y11 receptors that are coupled to the PLC-IP₃ signalling pathways to leading to intracellular Ca²⁺ release from the ER and subsequent activation of the SOC channels mediating extracellular Ca²⁺ entry (see section 1.3.3). The results from RT-PCR in this study showed the mRNA expression of P2Y1 and P2Y11 receptors in hDP-MSCs. The P2Y2 mRNA expression was not consistently detected in hDP-MSCs isolated from all three donors and the expression level in the 9F donor was very low (Figure 4.2). ATP induced Ca²⁺ release in hDP-MSCs in the extracellular Ca²⁺-free solution (Figure 4.8). ADP, an agonist at the P2Y1 receptor, and BzATP, an agonist at the P2Y11 receptor, also evoked Ca²⁺ release in the extracellular Ca²⁺-free solution (Figure 4.8). ATP-evoked Ca²⁺ responses in the extracellular Ca²⁺-containing solutions were inhibited by PPADS (Figure 4.3). Furthermore, transfection with siP2Y1 significantly decreased ATP- and ADP-evoked Ca²⁺ responses (Figure 4.11), while transfection with siP2Y11 reduced ATP-evoked Ca²⁺ responses (Figure 4.12). These results provide clear evidence to indicate functional expression of the P2Y1 and P2Y11 in ATP-induced Ca²⁺ signalling in hDP-MSCs. Consistent with the present study, previous studies detected the mRNA expression of the P2Y1 and P2Y11 receptors in hBM-MSCs (Ferrari, Gulinelli et al. 2011) and hAT-MSCs (Zippel, Limbach et al. 2012; Scarfi 2014). The protein expression of P2Y1 and P2Y11 receptors were further observed in hBM-MSCs by the immunostaining and Western blotting (Ichikawa and Gamba 2009).

The role of the P2Y1 and P2Y11 receptors in ATP-induced regulation of stimulation of hDP-MSC migration and differentiation was investigated in the present study. ATP-induced increase in cell migration was strongly blocked by PPADS (Figure 6.1F) and siRNAs to reduce the P2Y1 or P2Y11 receptor expression (Figure 6.2F). The ATP-induced decrease in osteogenesis and increase in adipogenesis of hDP-MSCs were also blocked by PPADS (Figure 6.3E and Figure 6.5F) and siP2Y1 or siP2Y11 (Figure 6.4E, and Figure 6.6D). These results show a significant role for the P2Y1 and P2Y11 receptors in mediating ATP-induced modulation of cell migration osteogenesis and adipogenesis. Consistently with the present study, the P2Y11 receptor has been shown be involved in hBM-MSC migration induced by extracellular NAD^+ (Fruscione, Scarfi et al. 2011), and the P2Y1 receptor is involved in ATP-induced promotion of adipogenic differentiation of hBM-MSCs (Ciciarello, Zini et al. 2013).

7.3 Expression and function of Stim1/Orai SOC channels in hDP-MSCs

The results from single cell Ca^{2+} imaging (Figure 5.1C-D) and FLEXstation (Figure 5.4A-B) showed that depletion of the ER Ca^{2+} store using TG induced a robust increase in the $[\text{Ca}^{2+}]_i$ in hDP-MSCs upon addition of extracellular Ca^{2+} into the extracellular Ca^{2+} -free solutions (Figure 5.1C-D and Figure 5.4A-B), supporting expression of the SOC channels in hDP-MSCs. Inhibition of the SOC channels using 2-APB or Synta66 significantly blocked TG-induced Ca^{2+} entry without altering the basal $[\text{Ca}^{2+}]_i$ and Ca^{2+} entry through the constitutively active Ca^{2+} conductance (Figure 5.3 and Figure 5.4), further supporting that the functional expression of the SOC channels in hDP-MSCs. The functional expression of the SOC channels was also reported in hBM-MSCs, but the molecular identity was completely unknown

(Kawano, Shoji et al. 2002). The present study using RT-PCR for the first time showed the mRNA expression of Stim1, Stim2, Orai1, Orai2 and Orai3 in hDP-MSCs (Figure 5.2). Reducing the expression level of all three Orai and Stim1 but not Stim2 (Figure 5.9F and Figure 5.11F) significantly inhibited TG-induced Ca^{2+} entry. The results from the FLEXstation experiments revealed that ATP-induced Ca^{2+} responses were also attenuated by 2-APB and Synta66 (Figure 5.5E and Figure 5.6E). Furthermore, ATP-induced Ca^{2+} responses were significantly reduced by transfection with siRNA for Stim1 and each of three Orai (Figure 5.10E), and co-transfection with siStim1/siOrai (Figure 5.12E), but not transfection with siStim2 alone (Figure 5.10E). Taken together, these results suggest that Stim1 and Orai contribute to formation of the SOC channels and mediate ATP-induced Ca^{2+} signalling in hDP-MSCs.

In a previous study, treatment with siRNA to reduce the Stim1 expression level inhibited ATP-induced increase of cell migration in hepatocellular carcinoma cells (Xie, Xu et al. 2014). Consistently, the present study has shown that the Stim1/Orai SOC channels play a role in ATP-induced regulation of hDP-MSC migration. Inhibition of the SOC channels with 2-APB (Figure 6.1F) or reduction in the expression of Stim1 and Orai1 using siStim1, siOrai1 and in combination strongly blocked ATP-induced increase of cell migration (Figure 6.2F). Such treatments also blocked ATP-induced decreases in osteogenesis in BM (Figure 6.3E and Figure 6.4E). Treatment with siOrai1 and siStim1/siOrai1 but not with siStim1 or 2-APB prevented ATP-induced reduction in osteogenesis of hDP-MSCs in ODM (Figure 6.3E and Figure 6.4E). However, there was no effect of treatment with siStim1, siOrai1 and siStim1/siOrai1 on ATP-induced stimulation of adipogenesis (Figure 6.6D). Treatment with 2-APB and siOrai3 slightly inhibited ATP-modulated increase of adipogenesis (Figure 6.5F and Figure 6.6D).

Taken together, these results show a significant role for the Stim1/Orai1 SOC

channels in ATP-induced increase in cell migration and osteogenesis of ATP-treated hDP-MSCs in BM or ODM, while Orai3 is importantly involved in ATP-modulated facilitation of adipogenic differentiation in ADM.

7.4 Future studies

This present study has provided clear evidence to show that extracellular ATP as an extrinsic signal regulates migration and differentiation of hDP-MSCs through the purinergic P2 receptors, particularly those involved in intracellular Ca^{2+} signalling. Further studies on the following aspects are required to help to gain a better and more mechanistic understanding.

In this study, the mRNA expression of P2Y2 was only detected in hDP-MSCs from one donor (9F), but not detected in hDP-MSCs from other two donors (21F and 32F), possibly due to the age-dependent change in gene expression. Moreover, the results in this study were obtained from three female donors. Therefore, future studies on the expression of P2 purinergic receptors in donors (males and females) from different age groups, would help to improve the understanding of genetic influences on aging.

This study has shown that ATP improves cell migration of hDP-MSCs using the IncuCyte real-time imaging system. More studies are needed to investigate that how ATP-induced Ca^{2+} signalling leads to enhanced cell migration.

Furthermore, this study has shown that ATP down-regulates osteogenic differentiation potential of hDP-MSCs using the ALP activity assay and up-regulates adipogenic differentiation using oil red O staining. In the future, studies on the gene expression and histochemical analysis of osteoblast-related (e.g., Runx2, osteocalcin) or

adipocyte-related differentiation markers (e.g., PPAR γ 2) would help to better understand the molecular mechanism of cell differentiation regulated by ATP in hDP-MSCs. It would be also important to investigate that how cell differentiation was mediated by ATP-induced Ca²⁺ signalling, which would enable a deeper insight into the signalling mechanisms that mediate cell differentiation.

In the present study, cells were cultured in 2-dimensional (2D) plastic or glass surfaces. However, cells *in vivo* primarily exist and operate in a three-dimensional (3D) extracellular environment that contains multiple extracellular matrix (ECM) components. Moreover, the results presented in this thesis have shown that extracellular ATP significantly stimulates cell migration and regulates osteogenic and adipogenic differentiation potential of hDP-MSCs. Therefore, future studies should use a 3D-scaffold to culture hDP-MSCs with the treatment of ATP to corroborate the findings made based 2D culture.

7.5 Conclusion

In conclusion, the study described in this thesis shows that exposure to extracellular ATP results in significant increase in cell migration and adipogenic differentiation and inhibition of osteogenic differentiation of hDP-MSCs. The study provides pharmacological and genetic evidence to indicate that the P2X7, P2Y1 and P2Y11 receptors, and Stim1/Orai SOC channels are functionally expressed as intrinsic mechanisms activated by extracellular ATP in hDP-MSCs. These signalling molecules play a differential role in ATP-induced regulation of hDP-MSC migration and differentiation. As summarized in Figure 7.1, the P2X7, P2Y1 and P2Y11 receptors all contribute in ATP-induced stimulation of cell migration. The P2Y1 and P2Y11 receptors, not the P2X7 receptor, are involved in ATP-induced inhibition of osteogenesis and stimulation of adipogenesis. The Stim1/Orai1 SOC channels have a

role in mediating ATP-induced stimulation of cell migration and inhibition of osteogenesis, but not ATP-induced stimulation of adipogenesis. The Orai3 protein is engaged in ATP-enhanced adipogenesis. These findings will provide a substantial insight into the intrinsic mechanisms underlying the regulation of MSC functions by extracellular ATP. Such information will facilitate developing better MSC-based cell therapies and regenerative medicines.

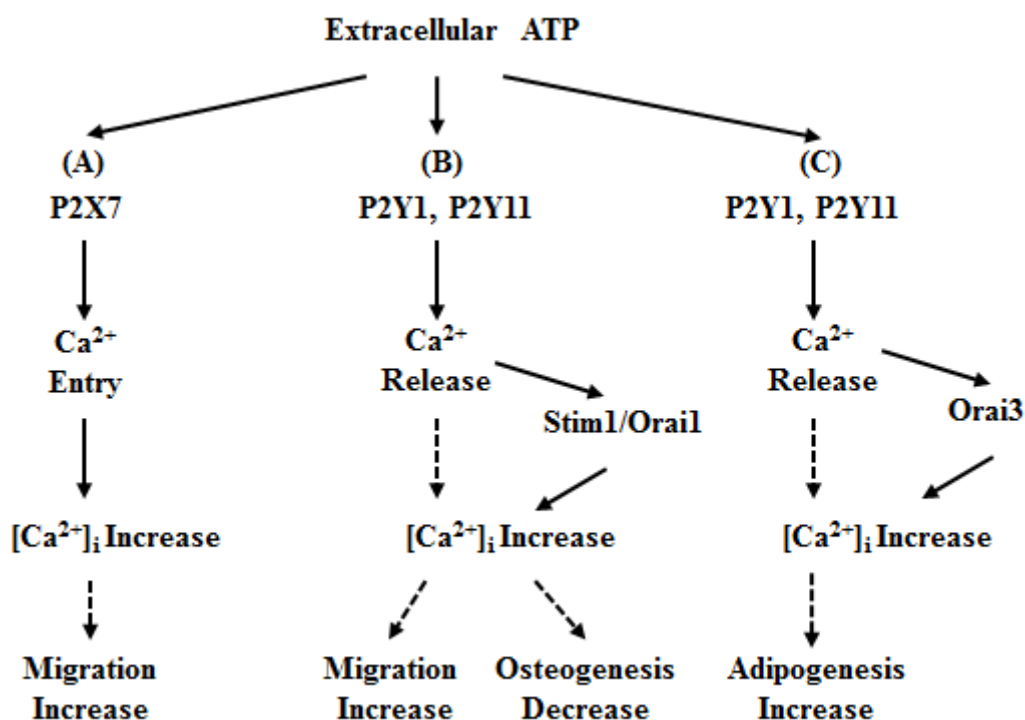


Figure 7.1 Schematic summary of ATP-induced Ca²⁺ signalling mechanism in migration and differentiation of hDP-MSCs.

(A) Extracellular ATP induces Ca²⁺ entry through the P2X7 receptor to increase the [Ca²⁺]_i, which contributes to the increase of cell migration. (B) Extracellular ATP induces Ca²⁺ release through the P2Y1 or P2Y11 receptor to activate the Stim1/Orai1 channel and subsequently increase the [Ca²⁺]_i, which contributes to the increase of cell migration and the decrease of cell osteogenesis. (C) Extracellular ATP induces Ca²⁺ release through the P2Y1 or P2Y11 receptor to activate the Orai3 channel and subsequently increase the [Ca²⁺]_i, which contributes to the increase of cell adipogenesis.

References

- Abdallah, B. M. and M. Kassem (2008). "Human mesenchymal stem cells: from basic biology to clinical applications." Gene Ther **15**(2): 109-116.
- Alvarez, C. V., M. Garcia-Lavandeira, et al. (2012). "Defining stem cell types: understanding the therapeutic potential of ESCs, ASCs, and iPS cells." J Mol Endocrinol **49**(2): 89-111.
- Ambudkar, I. S., H. L. Ong, et al. (2007). "TRPC1: the link between functionally distinct store-operated calcium channels." Cell Calcium **42**(2): 213-223.
- Ashour, F., M. Atterbury-Thomas, et al. (2006). "An evaluation of antibody detection of the P2X1 receptor subunit in the CNS of wild type and P2X1-knockout mice." Neurosci Lett **397**(1-2): 120-125.
- Augello, A. and C. De Bari (2010). "The regulation of differentiation in mesenchymal stem cells." Hum Gene Ther **21**(10): 1226-1238.
- Aurich, H., M. Sgodda, et al. (2009). "Hepatocyte differentiation of mesenchymal stem cells from human adipose tissue in vitro promotes hepatic integration in vivo." Gut **58**(4): 570-581.
- Baer, P. C. and H. Geiger (2012). "Adipose-derived mesenchymal stromal/stem cells: tissue localization, characterization, and heterogeneity." Stem Cells Int **2012**: 812693.
- Baer, P. C., S. Kuci, et al. (2013). "Comprehensive phenotypic characterization of human adipose-derived stromal/stem cells and their subsets by a high throughput technology." Stem Cells Dev **22**(2): 330-339.
- Bai, Q., R. Desprat, et al. (2013). "Embryonic stem cells or induced pluripotent stem cells? A DNA integrity perspective." Curr Gene Ther **13**(2): 93-98.
- Banas, A., T. Teratani, et al. (2009). "Rapid hepatic fate specification of adipose-derived stem cells and their therapeutic potential for liver failure." J Gastroenterol Hepatol **24**(1): 70-77.
- Banas, A., T. Teratani, et al. (2007). "Adipose tissue-derived mesenchymal stem cells as a source of human hepatocytes." Hepatology **46**(1): 219-228.
- Baqi, Y., R. Hausmann, et al. (2011). "Discovery of potent competitive antagonists and positive modulators of the P2X2 receptor." J Med Chem **54**(3): 817-830.
- Baroja-Mazo, A., M. Barbera-Cremades, et al. (2013). "The participation of plasma membrane hemichannels to purinergic signaling." Biochim Biophys Acta **1828**(1): 79-93.
- Barragan-Iglesias, P., J. B. Pineda-Farias, et al. (2014). "Role of spinal P2Y6 and P2Y11 receptors in neuropathic pain in rats: possible involvement of glial cells." Mol Pain **10**: 29.
- Basseri, S., S. Lhotak, et al. (2009). "The chemical chaperone 4-phenylbutyrate inhibits adipogenesis by modulating the unfolded protein response." J Lipid Res **50**(12): 2486-2501.

- Batouli, S., M. Miura, et al. (2003). "Comparison of stem-cell-mediated osteogenesis and dentinogenesis." J Dent Res **82**(12): 976-981.
- Berridge, M. J. (1993). "Inositol trisphosphate and calcium signalling." Nature **361**(6410): 315-325.
- Berridge, M. J., M. D. Bootman, et al. (2003). "Calcium signalling: dynamics, homeostasis and remodelling." Nat Rev Mol Cell Biol **4**(7): 517-529.
- Besada, P., D. H. Shin, et al. (2006). "Structure-activity relationships of uridine 5'-diphosphate analogues at the human P2Y6 receptor." J Med Chem **49**(18): 5532-5543.
- Bianchi, B. R., K. J. Lynch, et al. (1999). "Pharmacological characterization of recombinant human and rat P2X receptor subtypes." Eur J Pharmacol **376**(1-2): 127-138.
- Bianco, F., S. Ceruti, et al. (2006). "A role for P2X7 in microglial proliferation." J Neurochem **99**(3): 745-758.
- Biver, E., C. Thouverey, et al. (2014). "Crosstalk between tyrosine kinase receptors, GSK3 and BMP2 signaling during osteoblastic differentiation of human mesenchymal stem cells." Mol Cell Endocrinol **382**(1): 120-130.
- Biver, G., N. Wang, et al. (2013). "Role of the P2Y13 receptor in the differentiation of bone marrow stromal cells into osteoblasts and adipocytes." Stem Cells **31**(12): 2747-2758.
- Bo, X., M. Kim, et al. (2003). "Tissue distribution of P2X4 receptors studied with an ectodomain antibody." Cell Tissue Res **313**(2): 159-165.
- Bodor, E. T., G. L. Waldo, et al. (2004). "Delineation of ligand binding and receptor signaling activities of purified P2Y receptors reconstituted with heterotrimeric G proteins." Purinergic Signal **1**(1): 43-49.
- Bonab, M. M., K. Alimoghaddam, et al. (2006). "Aging of mesenchymal stem cell in vitro." BMC Cell Biol **7**: 14.
- Bonaguidi, M. A., M. A. Wheeler, et al. (2011). "In vivo clonal analysis reveals self-renewing and multipotent adult neural stem cell characteristics." Cell **145**(7): 1142-1155.
- Bonfield, T. L., M. T. Nolan Koloze, et al. (2010). "Defining human mesenchymal stem cell efficacy in vivo." J Inflamm (Lond) **7**: 51.
- Boquest, A. C., A. Shahdadfar, et al. (2006). "Isolation of stromal stem cells from human adipose tissue." Methods Mol Biol **325**: 35-46.
- Bourin, P., M. Gadelorge, et al. (2008). "Mesenchymal Progenitor Cells: Tissue Origin, Isolation and Culture." Transfus Med Hemother **35**(3): 160-167.
- Bradbury, E. J., G. Burnstock, et al. (1998). "The expression of P2X3 purinoreceptors in sensory neurons: effects of axotomy and glial-derived neurotrophic factor." Mol Cell Neurosci **12**(4-5): 256-268.
- Brotherton-Pleiss, C. E., M. P. Dillon, et al. (2010). "Discovery and optimization of RO-85, a novel drug-like, potent, and selective P2X3 receptor antagonist." Bioorg Med Chem Lett **20**(3): 1031-1036.

- Brzoska, M., H. Geiger, et al. (2005). "Epithelial differentiation of human adipose tissue-derived adult stem cells." Biochem Biophys Res Commun **330**(1): 142-150.
- Buckley, K. A., S. L. Golding, et al. (2003). "Release and interconversion of P2 receptor agonists by human osteoblast-like cells." FASEB J **17**(11): 1401-1410.
- Burke, Z. D. and D. Tosh (2012). "Ontogenesis of hepatic and pancreatic stem cells." Stem Cell Rev **8**(2): 586-596.
- Burnstock, G. (1972). "Purinergetic nerves." Pharmacol Rev **24**(3): 509-581.
- Burnstock, G. (2006). "Historical review: ATP as a neurotransmitter." Trends Pharmacol Sci **27**(3): 166-176.
- Burnstock, G. (2009). "Purinergetic signalling: past, present and future." Braz J Med Biol Res **42**(1): 3-8.
- Burnstock, G. (2011). "Introductory overview of purinergetic signalling." Front Biosci (Elite Ed) **3**: 896-900.
- Burnstock, G. (2013). "Introduction and perspective, historical note." Front Cell Neurosci **7**: 227.
- Burnstock, G. (2014). "Purinergetic signalling: from discovery to current developments." Exp Physiol **99**(1): 16-34.
- Burnstock, G., B. B. Fredholm, et al. (2010). "The birth and postnatal development of purinergetic signalling." Acta Physiol (Oxf) **199**(2): 93-147.
- Burnstock, G. and C. Kennedy (1985). "Is there a basis for distinguishing two types of P2-purinoceptor?" Gen Pharmacol **16**(5): 433-440.
- Burnstock, G. and G. E. Knight (2004). "Cellular distribution and functions of P2 receptor subtypes in different systems." Int Rev Cytol **240**: 31-304.
- Burnstock, G. and H. Ulrich (2011). "Purinergetic signaling in embryonic and stem cell development." Cell Mol Life Sci **68**(8): 1369-1394.
- Burnstock, G. and H. Wong (1978). "Comparison of the effects of ultraviolet light and purinergetic nerve stimulation on the guinea-pig taenia coli." Br J Pharmacol **62**(2): 293-302.
- Cao, Y., Z. Sun, et al. (2005). "Human adipose tissue-derived stem cells differentiate into endothelial cells in vitro and improve postnatal neovascularization in vivo." Biochem Biophys Res Commun **332**(2): 370-379.
- Casati, A., M. Frascoli, et al. (2011). "Cell-autonomous regulation of hematopoietic stem cell cycling activity by ATP." Cell Death Differ **18**(3): 396-404.
- Castinetti, F., S. W. Davis, et al. (2011). "Pituitary stem cell update and potential implications for treating hypopituitarism." Endocr Rev **32**(4): 453-471.
- Chadet, S., B. Jelassi, et al. (2014). "The activation of P2Y2 receptors increases MCF-7 breast cancer cells migration through the MEK-ERK1/2 signalling pathway." Carcinogenesis **35**(6): 1238-1247.
- Chang, C. M., C. L. Kao, et al. (2007). "Placenta-derived multipotent stem cells induced to differentiate into insulin-positive cells." Biochem Biophys Res Commun **357**(2): 414-420.

- Chen, C. C., A. N. Akopian, et al. (1995). "A P2X purinoceptor expressed by a subset of sensory neurons." Nature **377**(6548): 428-431.
- Chen, Q., Z. Yang, et al. (2010). "Adipose-derived stem cells modified genetically in vivo promote reconstruction of bone defects." Cytotherapy **12**(6): 831-840.
- Cheng, K. T., X. Liu, et al. (2008). "Functional requirement for Orai1 in store-operated TRPC1-STIM1 channels." J Biol Chem **283**(19): 12935-12940.
- Chessell, I. P., J. P. Hatcher, et al. (2005). "Disruption of the P2X7 purinoceptor gene abolishes chronic inflammatory and neuropathic pain." Pain **114**(3): 386-396.
- Chessell, I. P., A. D. Michel, et al. (1997). "Functional evidence for multiple purinoceptor subtypes in the rat medial vestibular nucleus." Neuroscience **77**(3): 783-791.
- Cheung, T. H., N. L. Quach, et al. (2012). "Maintenance of muscle stem-cell quiescence by microRNA-489." Nature **482**(7386): 524-528.
- Chhatiwala, M., R. G. Ravi, et al. (2004). "Induction of novel agonist selectivity for the ADP-activated P2Y1 receptor versus the ADP-activated P2Y12 and P2Y13 receptors by conformational constraint of an ADP analog." J Pharmacol Exp Ther **311**(3): 1038-1043.
- Ciciarello, M., R. Zini, et al. (2013). "Extracellular purines promote the differentiation of human bone marrow-derived mesenchymal stem cells to the osteogenic and adipogenic lineages." Stem Cells Dev **22**(7): 1097-1111.
- Coddou, C., Z. Yan, et al. (2011). "Activation and regulation of purinergic P2X receptor channels." Pharmacol Rev **63**(3): 641-683.
- Collo, G., S. Neidhart, et al. (1997). "Tissue distribution of the P2X7 receptor." Neuropharmacology **36**(9): 1277-1283.
- Communi, D., B. Robaye, et al. (1999). "Pharmacological characterization of the human P2Y11 receptor." Br J Pharmacol **128**(6): 1199-1206.
- Compan, V., L. Ulmann, et al. (2012). "P2X2 and P2X5 subunits define a new heteromeric receptor with P2X7-like properties." J Neurosci **32**(12): 4284-4296.
- Coppi, E., A. M. Pugliese, et al. (2007). "ATP modulates cell proliferation and elicits two different electrophysiological responses in human mesenchymal stem cells." Stem Cells **25**(7): 1840-1849.
- Coull, J. A., S. Beggs, et al. (2005). "BDNF from microglia causes the shift in neuronal anion gradient underlying neuropathic pain." Nature **438**(7070): 1017-1021.
- D'Amario, D., C. Fiorini, et al. (2011). "Functionally competent cardiac stem cells can be isolated from endomyocardial biopsies of patients with advanced cardiomyopathies." Circ Res **108**(7): 857-861.
- d'Aquino, R., A. Graziano, et al. (2007). "Human postnatal dental pulp cells co-differentiate into osteoblasts and endotheliocytes: a pivotal synergy leading to adult bone tissue formation." Cell Death Differ **14**(6): 1162-1171.
- Das, A., H. Ko, et al. (2010). "Human P2Y(14) receptor agonists: truncation of the hexose moiety of uridine-5'-diphosphoglucose and its replacement with alkyl and aryl groups." J Med Chem **53**(1): 471-480.

- De Bari, C., F. Dell'Accio, et al. (2001). "Multipotent mesenchymal stem cells from adult human synovial membrane." Arthritis Rheum **44**(8): 1928-1942.
- DeHaven, W. I., B. F. Jones, et al. (2009). "TRPC channels function independently of STIM1 and Orai1." J Physiol **587**(Pt 10): 2275-2298.
- DeHaven, W. I., J. T. Smyth, et al. (2008). "Complex actions of 2-aminoethyldiphenyl borate on store-operated calcium entry." J Biol Chem **283**(28): 19265-19273.
- Deng, X. L., H. Y. Sun, et al. (2006). "Properties of ion channels in rabbit mesenchymal stem cells from bone marrow." Biochem Biophys Res Commun **348**(1): 301-309.
- Ding, F., G. Zhang, et al. (2012). "Involvement of cationic channels in proliferation and migration of human mesenchymal stem cells." Tissue Cell **44**(6): 358-364.
- Dominici, M., K. Le Blanc, et al. (2006). "Minimal criteria for defining multipotent mesenchymal stromal cells. The International Society for Cellular Therapy position statement." Cytotherapy **8**(4): 315-317.
- Dominici, M., K. Le Blanc, et al. (2006). "Minimal criteria for defining multipotent mesenchymal stromal cells. The International Society for Cellular Therapy position statement." Cytotherapy **8**(4): 315-317.
- Douglass, J. G., J. B. deCamp, et al. (2008). "Adenosine analogues as inhibitors of P2Y12 receptor mediated platelet aggregation." Bioorg Med Chem Lett **18**(6): 2167-2171.
- Dragoni, S., U. Laforenza, et al. (2014). "Enhanced expression of Stim, Orai, and TRPC transcripts and proteins in endothelial progenitor cells isolated from patients with primary myelofibrosis." PLoS One **9**(3): e91099.
- Dunn, P. M., Y. Zhong, et al. (2001). "P2X receptors in peripheral neurons." Prog Neurobiol **65**(2): 107-134.
- Dziadek, M. A. and L. S. Johnstone (2007). "Biochemical properties and cellular localisation of STIM proteins." Cell Calcium **42**(2): 123-132.
- Edwards, F. A., A. J. Gibb, et al. (1992). "ATP receptor-mediated synaptic currents in the central nervous system." Nature **359**(6391): 144-147.
- El-Backly, R. M., A. G. Massoud, et al. (2008). "Regeneration of dentine/pulp-like tissue using a dental pulp stem cell/poly(lactic-co-glycolic) acid scaffold construct in New Zealand white rabbits." Aust Endod J **34**(2): 52-67.
- El-Tayeb, A., A. Qi, et al. (2006). "Synthesis and structure-activity relationships of uracil nucleotide derivatives and analogues as agonists at human P2Y2, P2Y4, and P2Y6 receptors." J Med Chem **49**(24): 7076-7087.
- Elsby, R., L. Fox, et al. (2011). "In vitro risk assessment of AZD9056 perpetrating a transporter-mediated drug-drug interaction with methotrexate." Eur J Pharm Sci **43**(1-2): 41-49.
- Evans, R. J., C. Lewis, et al. (1995). "Pharmacological characterization of heterologously expressed ATP-gated cation channels (P2x purinoceptors)." Mol Pharmacol **48**(2): 178-183.
- Fahrner, M., M. Muik, et al. (2009). "Mechanistic view on domains mediating STIM1-Orai coupling." Immunol Rev **231**(1): 99-112.

- Farini, A., C. Sitzia, et al. (2014). "Clinical applications of mesenchymal stem cells in chronic diseases." Stem Cells Int **2014**: 306573.
- Fernandez Vallone, V. B., M. A. Romaniuk, et al. (2013). "Mesenchymal stem cells and their use in therapy: what has been achieved?" Differentiation **85**(1-2): 1-10.
- Ferrari, D., S. Gulinelli, et al. (2011). "Purinergic stimulation of human mesenchymal stem cells potentiates their chemotactic response to CXCL12 and increases the homing capacity and production of proinflammatory cytokines." Exp Hematol **39**(3): 360-374, 374 e361-365.
- Ferro, F., R. Spelat, et al. (2012). "Acellular bone colonization and aggregate culture conditions diversely influence murine periosteum mesenchymal stem cell differentiation potential in long-term in vitro osteoinductive conditions." Tissue Eng Part A **18**(13-14): 1509-1519.
- Feske, S., Y. Gwack, et al. (2006). "A mutation in Orai1 causes immune deficiency by abrogating CRAC channel function." Nature **441**(7090): 179-185.
- Feske, S., M. Prakriya, et al. (2005). "A severe defect in CRAC Ca²⁺ channel activation and altered K⁺ channel gating in T cells from immunodeficient patients." J Exp Med **202**(5): 651-662.
- Figliuzzi, M., B. Bonandrini, et al. (2014). "Mesenchymal stem cells help pancreatic islet transplantation to control type 1 diabetes." World J Stem Cells **6**(2): 163-172.
- Ford, A. P. (2012). "In pursuit of P2X3 antagonists: novel therapeutics for chronic pain and afferent sensitization." Purinergic Signal **8**(Suppl 1): 3-26.
- Ford, A. P., J. R. Gever, et al. (2006). "Purinceptors as therapeutic targets for lower urinary tract dysfunction." Br J Pharmacol **147** Suppl 2: S132-143.
- Ford, A. P. and B. J. Udem (2013). "The therapeutic promise of ATP antagonism at P2X3 receptors in respiratory and urological disorders." Front Cell Neurosci **7**: 267.
- Formeister, E. J., A. L. Sionas, et al. (2009). "Distinct SOX9 levels differentially mark stem/progenitor populations and enteroendocrine cells of the small intestine epithelium." Am J Physiol Gastrointest Liver Physiol **296**(5): G1108-1118.
- Fricks, I. P., S. Maddileti, et al. (2008). "UDP is a competitive antagonist at the human P2Y14 receptor." J Pharmacol Exp Ther **325**(2): 588-594.
- Friedenstein, A. J., R. K. Chailakhjan, et al. (1970). "The development of fibroblast colonies in monolayer cultures of guinea-pig bone marrow and spleen cells." Cell Tissue Kinet **3**(4): 393-403.
- Friedlander, L. T., M. P. Cullinan, et al. (2009). "Dental stem cells and their potential role in apexogenesis and apexification." Int Endod J **42**(11): 955-962.
- Fruscione, F., S. Scarfi, et al. (2011). "Regulation of human mesenchymal stem cell functions by an autocrine loop involving NAD⁺ release and P2Y11-mediated signaling." Stem Cells Dev **20**(7): 1183-1198.
- Fuchs, E. and V. Horsley (2011). "Ferretting out stem cells from their niches." Nat Cell Biol **13**(5): 513-518.

- Galler, K. M., H. Schweikl, et al. (2011). "TEGDMA reduces mineralization in dental pulp cells." J Dent Res **90**(2): 257-262.
- Garcia-Guzman, M., F. Soto, et al. (1997). "Characterization of recombinant human P2X4 receptor reveals pharmacological differences to the rat homologue." Mol Pharmacol **51**(1): 109-118.
- Gargett, C. E. and J. S. Wiley (1997). "The isoquinoline derivative KN-62 a potent antagonist of the P2Z-receptor of human lymphocytes." Br J Pharmacol **120**(8): 1483-1490.
- Gever, J. R., D. A. Cockayne, et al. (2006). "Pharmacology of P2X channels." Pflugers Arch **452**(5): 513-537.
- Gever, J. R., R. Soto, et al. (2010). "AF-353, a novel, potent and orally bioavailable P2X3/P2X2/3 receptor antagonist." Br J Pharmacol **160**(6): 1387-1398.
- Ghai, G., J. E. Francis, et al. (1987). "Pharmacological characterization of CGS 15943A: a novel nonxanthine adenosine antagonist." J Pharmacol Exp Ther **242**(3): 784-790.
- Gimble, J. M., F. Guilak, et al. (2008). "In vitro Differentiation Potential of Mesenchymal Stem Cells." Transfus Med Hemother **35**(3): 228-238.
- Glaser, T., A. R. Cappellari, et al. (2012). "Perspectives of purinergic signaling in stem cell differentiation and tissue regeneration." Purinergic Signal **8**(3): 523-537.
- Glaser, T., S. L. de Oliveira, et al. (2014). "Modulation of mouse embryonic stem cell proliferation and neural differentiation by the P2X7 receptor." PLoS One **9**(5): e96281.
- Goto, J., A. Z. Suzuki, et al. (2010). "Two novel 2-aminoethyl diphenylborinate (2-APB) analogues differentially activate and inhibit store-operated Ca²⁺ entry via STIM proteins." Cell Calcium **47**(1): 1-10.
- Greig, A. V., S. E. James, et al. (2003). "Purinergic receptor expression in the regeneration epidermis in a rat model of normal and delayed wound healing." Exp Dermatol **12**(6): 860-871.
- Gronthos, S., J. Brahim, et al. (2002). "Stem cell properties of human dental pulp stem cells." J Dent Res **81**(8): 531-535.
- Gronthos, S., M. Mankani, et al. (2000). "Postnatal human dental pulp stem cells (DPSCs) in vitro and in vivo." Proc Natl Acad Sci U S A **97**(25): 13625-13630.
- Guile, S. D., L. Alcaraz, et al. (2009). "Antagonists of the P2X(7) receptor. From lead identification to drug development." J Med Chem **52**(10): 3123-3141.
- Gum, R. J., B. Wakefield, et al. (2012). "P2X receptor antagonists for pain management: examination of binding and physicochemical properties." Purinergic Signal **8**(Suppl 1): 41-56.
- Hernandez-Olmos, V., A. Abdelrahman, et al. (2012). "N-substituted phenoxazine and acridone derivatives: structure-activity relationships of potent P2X4 receptor antagonists." J Med Chem **55**(22): 9576-9588.
- Hoebertz, A., T. R. Arnett, et al. (2003). "Regulation of bone resorption and formation by purines and pyrimidines." Trends Pharmacol Sci **24**(6): 290-297.

- Holton, F. A. and P. Holton (1954). "The capillary dilator substances in dry powders of spinal roots; a possible role of adenosine triphosphate in chemical transmission from nerve endings." J Physiol **126**(1): 124-140.
- Holton, P. (1959). "The liberation of adenosine triphosphate on antidromic stimulation of sensory nerves." J Physiol **145**(3): 494-504.
- Hoth, M. and R. Penner (1992). "Depletion of intracellular calcium stores activates a calcium current in mast cells." Nature **355**(6358): 353-356.
- Hoth, M. and R. Penner (1993). "Calcium release-activated calcium current in rat mast cells." J Physiol **465**: 359-386.
- Hou, M., T. K. Harden, et al. (2002). "UDP acts as a growth factor for vascular smooth muscle cells by activation of P2Y(6) receptors." Am J Physiol Heart Circ Physiol **282**(2): H784-792.
- Hu, J., K. Qin, et al. (2011). "Downregulation of transcription factor Oct4 induces an epithelial-to-mesenchymal transition via enhancement of Ca²⁺ influx in breast cancer cells." Biochem Biophys Res Commun **411**(4): 786-791.
- Huang, G. T., S. Gronthos, et al. (2009). "Mesenchymal stem cells derived from dental tissues vs. those from other sources: their biology and role in regenerative medicine." J Dent Res **88**(9): 792-806.
- Huynh, K. W., M. R. Cohen, et al. (2014). "Application of Amphipols for Structure-Functional Analysis of TRP Channels." J Membr Biol.
- Ichikawa, J. and H. Gemba (2009). "Cell density-dependent changes in intracellular Ca²⁺ mobilization via the P2Y2 receptor in rat bone marrow stromal cells." J Cell Physiol **219**(2): 372-381.
- Ichikawa, J. and H. Gemba (2009). "Cell Density-Dependent Changes in Intracellular Ca²⁺ Mobilization Via the P2y(2) Receptor in Rat Bone Marrow Stromal Cells." Journal of Physiological Sciences **59**: 243-243.
- Ivanov, A. A., H. Ko, et al. (2007). "Molecular modeling of the human P2Y2 receptor and design of a selective agonist, 2'-amino-2'-deoxy-2-thiouridine 5'-triphosphate." J Med Chem **50**(6): 1166-1176.
- Jacobson, K. A., R. Balasubramanian, et al. (2012). "G protein-coupled adenosine (P1) and P2Y receptors: ligand design and receptor interactions." Purinergic Signal **8**(3): 419-436.
- Jacobson, K. A. and J. M. Boeynaems (2010). "P2Y nucleotide receptors: promise of therapeutic applications." Drug Discov Today **15**(13-14): 570-578.
- Jacobson, K. A., S. Costanzi, et al. (2004). "Molecular recognition at purine and pyrimidine nucleotide (P2) receptors." Curr Top Med Chem **4**(8): 805-819.
- Jacobson, K. A., Y. C. Kim, et al. (1998). "A pyridoxine cyclic phosphate and its 6-azoaryl derivative selectively potentiate and antagonize activation of P2X1 receptors." J Med Chem **41**(13): 2201-2206.
- Jahangir, A., M. Alam, et al. (2009). "Identification and SAR of novel diaminopyrimidines. Part 2: The discovery of RO-51, a potent and selective, dual P2X(3)/P2X(2/3) antagonist for the treatment of pain." Bioorg Med Chem Lett **19**(6): 1632-1635.

- Jaime-Figueroa, S., R. Greenhouse, et al. (2005). "Discovery and synthesis of a novel and selective drug-like P2X(1) antagonist." Bioorg Med Chem Lett **15**(13): 3292-3295.
- Jarvis, M. F., E. C. Burgard, et al. (2002). "A-317491, a novel potent and selective non-nucleotide antagonist of P2X3 and P2X2/3 receptors, reduces chronic inflammatory and neuropathic pain in the rat." Proc Natl Acad Sci U S A **99**(26): 17179-17184.
- Jarvis, M. F. and B. S. Khakh (2009). "ATP-gated P2X cation-channels." Neuropharmacology **56**(1): 208-215.
- Jiang, L.-H. (2012). "P2X receptor-mediated ATP purinergic signaling in health and disease." Cell Health and Cytoskeleton **4**: 83-101.
- Jiang, L. H., M. Kim, et al. (2003). "Subunit arrangement in P2X receptors." J Neurosci **23**(26): 8903-8910.
- Jiang, L. H., A. B. Mackenzie, et al. (2000). "Brilliant blue G selectively blocks ATP-gated rat P2X(7) receptors." Mol Pharmacol **58**(1): 82-88.
- Jiang, L. H., W. Yang, et al. (2010). "TRPM2 channel properties, functions and therapeutic potentials." Expert Opin Ther Targets **14**(9): 973-988.
- Jiang, Y., B. N. Jahagirdar, et al. (2002). "Pluripotency of mesenchymal stem cells derived from adult marrow." Nature **418**(6893): 41-49.
- Kaan, T. K., P. K. Yip, et al. (2010). "Endogenous purinergic control of bladder activity via presynaptic P2X3 and P2X2/3 receptors in the spinal cord." J Neurosci **30**(12): 4503-4507.
- Kajiyama, H., T. S. Hamazaki, et al. (2010). "Pdx1-transfected adipose tissue-derived stem cells differentiate into insulin-producing cells in vivo and reduce hyperglycemia in diabetic mice." Int J Dev Biol **54**(4): 699-705.
- Kajstura, J., M. Rota, et al. (2011). "Evidence for human lung stem cells." N Engl J Med **364**(19): 1795-1806.
- Karaoz, E., B. N. Dogan, et al. (2010). "Isolation and in vitro characterisation of dental pulp stem cells from natal teeth." Histochem Cell Biol **133**(1): 95-112.
- Kassack, M. U., K. Braun, et al. (2004). "Structure-activity relationships of analogues of NF449 confirm NF449 as the most potent and selective known P2X1 receptor antagonist." Eur J Med Chem **39**(4): 345-357.
- Kawano, S., K. Otsu, et al. (2006). "ATP autocrine/paracrine signaling induces calcium oscillations and NFAT activation in human mesenchymal stem cells." Cell Calcium **39**(4): 313-324.
- Kawano, S., K. Otsu, et al. (2003). "Ca²⁺ oscillations regulated by Na⁺-Ca²⁺ exchanger and plasma membrane Ca²⁺ pump induce fluctuations of membrane currents and potentials in human mesenchymal stem cells." Cell Calcium **34**(2): 145-156.
- Kawano, S., S. Shoji, et al. (2002). "Characterization of Ca²⁺ signaling pathways in human mesenchymal stem cells." Cell Calcium **32**(4): 165-174.
- Ke, H. Z., H. Qi, et al. (2003). "Deletion of the P2X7 nucleotide receptor reveals its regulatory roles in bone formation and resorption." Mol Endocrinol **17**(7): 1356-1367.

- Keystone, E. C., M. M. Wang, et al. (2012). "Clinical evaluation of the efficacy of the P2X7 purinergic receptor antagonist AZD9056 on the signs and symptoms of rheumatoid arthritis in patients with active disease despite treatment with methotrexate or sulphasalazine." Ann Rheum Dis **71**(10): 1630-1635.
- Khakh, B. S., G. Burnstock, et al. (2001). "International union of pharmacology. XXIV. Current status of the nomenclature and properties of P2X receptors and their subunits." Pharmacol Rev **53**(1): 107-118.
- Khakh, B. S., D. Gittermann, et al. (2003). "ATP modulation of excitatory synapses onto interneurons." J Neurosci **23**(19): 7426-7437.
- Khakh, B. S. and R. A. North (2006). "P2X receptors as cell-surface ATP sensors in health and disease." Nature **442**(7102): 527-532.
- Khakh, B. S. and R. A. North (2012). "Neuromodulation by extracellular ATP and P2X receptors in the CNS." Neuron **76**(1): 51-69.
- Khakh, B. S., W. R. Proctor, et al. (1999). "Allosteric control of gating and kinetics at P2X(4) receptor channels." J Neurosci **19**(17): 7289-7299.
- Kiel, M. J., O. H. Yilmaz, et al. (2005). "SLAM family receptors distinguish hematopoietic stem and progenitor cells and reveal endothelial niches for stem cells." Cell **121**(7): 1109-1121.
- Kim, H. S., M. Ohno, et al. (2003). "2-Substitution of adenine nucleotide analogues containing a bicyclo[3.1.0]hexane ring system locked in a northern conformation: enhanced potency as P2Y1 receptor antagonists." J Med Chem **46**(23): 4974-4987.
- Kim, Y. C., J. S. Lee, et al. (2005). "Synthesis of pyridoxal phosphate derivatives with antagonist activity at the P2Y13 receptor." Biochem Pharmacol **70**(2): 266-274.
- King, B. F., M. Liu, et al. (1999). "Diinosine pentaphosphate (IP5I) is a potent antagonist at recombinant rat P2X1 receptors." Br J Pharmacol **128**(5): 981-988.
- King, B. F. and A. Townsend-Nicholson (2008). "Involvement of P2Y1 and P2Y11 purinoceptors in parasympathetic inhibition of colonic smooth muscle." J Pharmacol Exp Ther **324**(3): 1055-1063.
- King, M., G. D. Housley, et al. (1998). "Expression of ATP-gated ion channels by Reissner's membrane epithelial cells." Neuroreport **9**(11): 2467-2474.
- Klapperstuck, M., C. Buttner, et al. (2000). "Antagonism by the suramin analogue NF279 on human P2X(1) and P2X(7) receptors." Eur J Pharmacol **387**(3): 245-252.
- Ko, H., R. L. Carter, et al. (2008). "Synthesis and potency of novel uracil nucleotides and derivatives as P2Y2 and P2Y6 receptor agonists." Bioorg Med Chem **16**(12): 6319-6332.
- Ko, H., I. Fricks, et al. (2007). "Structure-activity relationship of uridine 5'-diphosphoglucose analogues as agonists of the human P2Y14 receptor." J Med Chem **50**(9): 2030-2039.
- Kobayashi, K., H. Yamanaka, et al. (2013). "Expression of ATP receptors in the rat dorsal root ganglion and spinal cord." Anat Sci Int **88**(1): 10-16.

- Kobayashi, K., H. Yamanaka, et al. (2012). "Multiple P2Y subtypes in spinal microglia are involved in neuropathic pain after peripheral nerve injury." *Glia* **60**(10): 1529-1539.
- Korcok, J., L. N. Raimundo, et al. (2005). "P2Y6 nucleotide receptors activate NF-kappaB and increase survival of osteoclasts." *J Biol Chem* **280**(17): 16909-16915.
- Korcok, J., L. N. Raimundo, et al. (2004). "Extracellular nucleotides act through P2X7 receptors to activate NF-kappaB in osteoclasts." *J Bone Miner Res* **19**(4): 642-651.
- Koyama, N., Y. Okubo, et al. (2009). "Evaluation of pluripotency in human dental pulp cells." *J Oral Maxillofac Surg* **67**(3): 501-506.
- Kumabe, S., M. Nakatsuka, et al. (2006). "Human dental pulp cell culture and cell transplantation with an alginate scaffold." *Okajimas Folia Anat Jpn* **82**(4): 147-155.
- Kuo, T. F., H. C. Lin, et al. (2011). "Bone marrow combined with dental bud cells promotes tooth regeneration in miniature pig model." *Artif Organs* **35**(2): 113-121.
- Laino, G., R. d'Aquino, et al. (2005). "A new population of human adult dental pulp stem cells: a useful source of living autologous fibrous bone tissue (LAB)." *J Bone Miner Res* **20**(8): 1394-1402.
- Lambrecht, G., J. Rettinger, et al. (2000). "The novel pyridoxal-5'-phosphate derivative PPNDS potently antagonizes activation of P2X(1) receptors." *Eur J Pharmacol* **387**(3): R19-21.
- Latorre, R., C. Zaelzer, et al. (2009). "Structure-functional intimacies of transient receptor potential channels." *Q Rev Biophys* **42**(3): 201-246.
- Lee, B. C., T. Cheng, et al. (2003). "P2Y-like receptor, GPR105 (P2Y14), identifies and mediates chemotaxis of bone-marrow hematopoietic stem cells." *Genes Dev* **17**(13): 1592-1604.
- Lee, H. J., B. H. Choi, et al. (2006). "Low-intensity ultrasound stimulation enhances chondrogenic differentiation in alginate culture of mesenchymal stem cells." *Artif Organs* **30**(9): 707-715.
- Lee, H. K., S. H. Lim, et al. (2014). "Preclinical efficacy and mechanisms of mesenchymal stem cells in animal models of autoimmune diseases." *Immune Netw* **14**(2): 81-88.
- Lee, K. P., J. P. Yuan, et al. (2010). "An endoplasmic reticulum/plasma membrane junction: STIM1/Orai1/TRPCs." *FEBS Lett* **584**(10): 2022-2027.
- Lee, O. K., T. K. Kuo, et al. (2004). "Isolation of multipotent mesenchymal stem cells from umbilical cord blood." *Blood* **103**(5): 1669-1675.
- Lemoli, R. M., D. Ferrari, et al. (2004). "Extracellular nucleotides are potent stimulators of human hematopoietic stem cells in vitro and in vivo." *Blood* **104**(6): 1662-1670.
- Lewis, C., S. Neidhart, et al. (1995). "Coexpression of P2X2 and P2X3 receptor subunits can account for ATP-gated currents in sensory neurons." *Nature* **377**(6548): 432-435.

- Lewis, R. S. (2011). "Store-operated calcium channels: new perspectives on mechanism and function." Cold Spring Harb Perspect Biol **3**(12).
- Lewis, R. S. and M. D. Cahalan (1989). "Mitogen-induced oscillations of cytosolic Ca^{2+} and transmembrane Ca^{2+} current in human leukemic T cells." Cell Regul **1**(1): 99-112.
- Li, G. R., X. L. Deng, et al. (2006). "Ion channels in mesenchymal stem cells from rat bone marrow." Stem Cells **24**(6): 1519-1528.
- Li, H. J., F. Reinhardt, et al. (2012). "Cancer-stimulated mesenchymal stem cells create a carcinoma stem cell niche via prostaglandin E2 signaling." Cancer Discov **2**(9): 840-855.
- Li, J., R. M. Cubbon, et al. (2011). "Orai1 and CRAC channel dependence of VEGF-activated Ca^{2+} entry and endothelial tube formation." Circ Res **108**(10): 1190-1198.
- Li, J., L. McKeown, et al. (2011). "Nanomolar potency and selectivity of a Ca^{2+} release-activated Ca^{2+} channel inhibitor against store-operated Ca^{2+} entry and migration of vascular smooth muscle cells." Br J Pharmacol **164**(2): 382-393.
- Li, J., R. Meyer, et al. (2009). "P2X7 nucleotide receptor plays an important role in callus remodeling during fracture repair." Calcif Tissue Int **84**(5): 405-412.
- Li, K., Q. Han, et al. (2010). "Not a process of simple vicariousness, the differentiation of human adipose-derived mesenchymal stem cells to renal tubular epithelial cells plays an important role in acute kidney injury repairing." Stem Cells Dev **19**(8): 1267-1275.
- Li, M., C. Chen, et al. (2012). "A TRPC1-mediated increase in store-operated Ca^{2+} entry is required for the proliferation of adult hippocampal neural progenitor cells." Cell Calcium **51**(6): 486-496.
- Liao, Y., C. Erxleben, et al. (2008). "Functional interactions among Orai1, TRPCs, and STIM1 suggest a STIM-regulated heteromeric Orai/TRPC model for SOCE/Icrac channels." Proc Natl Acad Sci U S A **105**(8): 2895-2900.
- Lim, J. C. and C. H. Mitchell (2012). "Inflammation, pain, and pressure--purinergic signaling in oral tissues." J Dent Res **91**(12): 1103-1109.
- Lin, Z., J. S. Wang, et al. (2014). "Effects of BMP2 and VEGF165 on the osteogenic differentiation of rat bone marrow-derived mesenchymal stem cells." Exp Ther Med **7**(3): 625-629.
- Liou, J., M. L. Kim, et al. (2005). "STIM is a Ca^{2+} sensor essential for Ca^{2+} -store-depletion-triggered Ca^{2+} influx." Curr Biol **15**(13): 1235-1241.
- Lis, A., C. Peinelt, et al. (2007). "CRACM1, CRACM2, and CRACM3 are store-operated Ca^{2+} channels with distinct functional properties." Curr Biol **17**(9): 794-800.
- Livak, K. J. and T. D. Schmittgen (2001). "Analysis of relative gene expression data using real-time quantitative PCR and the 2(-Delta Delta C(T)) Method." Methods **25**(4): 402-408.
- Lynch, K. J., E. Touma, et al. (1999). "Molecular and functional characterization of human P2X(2) receptors." Mol Pharmacol **56**(6): 1171-1181.

- Ma, H. T., Z. Peng, et al. (2008). "Canonical transient receptor potential 5 channel in conjunction with Orai1 and STIM1 allows Sr^{2+} entry, optimal influx of Ca^{2+} , and degranulation in a rat mast cell line." J Immunol **180**(4): 2233-2239.
- Mafi, R., S. Hindocha, et al. (2011). "Sources of adult mesenchymal stem cells applicable for musculoskeletal applications - a systematic review of the literature." Open Orthop J **5 Suppl 2**: 242-248.
- Mamedova, L. K., B. V. Joshi, et al. (2004). "Diisothiocyanate derivatives as potent, insurmountable antagonists of P2Y6 nucleotide receptors." Biochem Pharmacol **67**(9): 1763-1770.
- Mark, P., M. Kleinsorge, et al. (2013). "Human Mesenchymal Stem Cells Display Reduced Expression of CD105 after Culture in Serum-Free Medium." Stem Cells Int **2013**: 698076.
- McGarraughty, S., C. T. Wismer, et al. (2003). "Effects of A-317491, a novel and selective P2X3/P2X2/3 receptor antagonist, on neuropathic, inflammatory and chemogenic nociception following intrathecal and intraplantar administration." Br J Pharmacol **140**(8): 1381-1388.
- McHale, N. G., M. A. Hollywood, et al. (2006). "Organization and function of ICC in the urinary tract." J Physiol **576**(Pt 3): 689-694.
- Mehlhorn, A. T., J. Zwingmann, et al. (2009). "Chondrogenesis of adipose-derived adult stem cells in a poly-lactide-co-glycolide scaffold." Tissue Eng Part A **15**(5): 1159-1167.
- Meis, S., A. Hamacher, et al. (2010). "NF546 [4,4'-(carbonylbis(imino-3,1-phenylene-carbonylimino-3,1-(4-methyl-phenylene)-carbonylimino))-bis(1,3-xylene-alpha,alpha'-diphosphonic acid) tetrasodium salt] is a non-nucleotide P2Y11 agonist and stimulates release of interleukin-8 from human monocyte-derived dendritic cells." J Pharmacol Exp Ther **332**(1): 238-247.
- Miura, M., S. Gronthos, et al. (2003). "SHED: stem cells from human exfoliated deciduous teeth." Proc Natl Acad Sci U S A **100**(10): 5807-5812.
- Miyashita, S., N. E. Ahmed, et al. (2014). "Mechanical forces induce odontoblastic differentiation of mesenchymal stem cells on three-dimensional biomimetic scaffolds." J Tissue Eng Regen Med.
- Monif, M., C. A. Reid, et al. (2009). "The P2X7 receptor drives microglial activation and proliferation: a trophic role for P2X7R pore." J Neurosci **29**(12): 3781-3791.
- Moore, D. J., P. R. Murdock, et al. (2003). "GPR105, a novel Gi/o-coupled UDP-glucose receptor expressed on brain glia and peripheral immune cells, is regulated by immunologic challenge: possible role in neuroimmune function." Brain Res Mol Brain Res **118**(1-2): 10-23.
- Motiani, R. K., X. Zhang, et al. (2013). "Orai3 is an estrogen receptor alpha-regulated Ca^{2+} channel that promotes tumorigenesis." FASEB J **27**(1): 63-75.
- Nandan, E., E. Camaioni, et al. (1999). "Structure-activity relationships of bisphosphate nucleotide derivatives as P2Y1 receptor antagonists and partial agonists." J Med Chem **42**(9): 1625-1638.

- Nawazish-i-Husain Syed and C. Kennedy (2012). "Pharmacology of P2X receptors." WIREs Membrane Transport and Signaling **1**: 16-30.
- Neelands, T. R., E. C. Burgard, et al. (2003). "2', 3'-O-(2,4,6-trinitrophenyl)-ATP and A-317491 are competitive antagonists at a slowly desensitizing chimeric human P2X3 receptor." Br J Pharmacol **140**(1): 202-210.
- Nicholas, R. A., E. R. Lazarowski, et al. (1996). "Pharmacological and second messenger signalling selectivities of cloned P2Y receptors." J Auton Pharmacol **16**(6): 319-323.
- North, R. A. (2002). "Molecular physiology of P2X receptors." Physiol Rev **82**(4): 1013-1067.
- North, R. A. and M. F. Jarvis (2013). "P2X receptors as drug targets." Mol Pharmacol **83**(4): 759-769.
- North, R. A. and A. Surprenant (2000). "Pharmacology of cloned P2X receptors." Annu Rev Pharmacol Toxicol **40**: 563-580.
- Novak, I. (2011). "Purinergic signalling in epithelial ion transport: regulation of secretion and absorption." Acta Physiol (Oxf) **202**(3): 501-522.
- Ochoa-Cortes, F., A. Linan-Rico, et al. (2014). "Potential for developing purinergic drugs for gastrointestinal diseases." Inflamm Bowel Dis **20**(7): 1259-1287.
- Ohga, K., R. Takezawa, et al. (2008). "Characterization of YM-58483/BTP2, a novel store-operated Ca²⁺ entry blocker, on T cell-mediated immune responses in vivo." Int Immunopharmacol **8**(13-14): 1787-1792.
- Ohta, A. and M. Sitkovsky (2009). "The adenosinergic immunomodulatory drugs." Curr Opin Pharmacol **9**(4): 501-506.
- Orriss, I. R., G. Burnstock, et al. (2010). "Purinergic signalling and bone remodelling." Curr Opin Pharmacol **10**(3): 322-330.
- Osathanon, T., N. Nowwarote, et al. (2011). "Basic Fibroblast Growth Factor Inhibits Mineralization but Induces Neuronal Differentiation by Human Dental Pulp Stem Cells Through a FGFR and PLC gamma Signaling Pathway." Journal of Cellular Biochemistry **112**(7): 1807-1816.
- Otaki, S., S. Ueshima, et al. (2007). "Mesenchymal progenitor cells in adult human dental pulp and their ability to form bone when transplanted into immunocompromised mice." Cell Biol Int **31**(10): 1191-1197.
- Oury, C., M. J. Kuijpers, et al. (2003). "Overexpression of the platelet P2X1 ion channel in transgenic mice generates a novel prothrombotic phenotype." Blood **101**(10): 3969-3976.
- Panupinthu, N., J. T. Rogers, et al. (2008). "P2X7 receptors on osteoblasts couple to production of lysophosphatidic acid: a signaling axis promoting osteogenesis." J Cell Biol **181**(5): 859-871.
- Parekh, A. B. and J. W. Putney, Jr. (2005). "Store-operated calcium channels." Physiol Rev **85**(2): 757-810.
- Park, C. Y., P. J. Hoover, et al. (2009). "STIM1 clusters and activates CRAC channels via direct binding of a cytosolic domain to Orai1." Cell **136**(5): 876-890.
- Pedata, F., A. Melani, et al. (2007). "The role of ATP and adenosine in the brain under normoxic and ischemic conditions." Purinergic Signal **3**(4): 299-310.

- Peinelt, C., A. Lis, et al. (2008). "2-Aminoethoxydiphenyl borate directly facilitates and indirectly inhibits STIM1-dependent gating of CRAC channels." J Physiol **586**(13): 3061-3073.
- Perry, B. C., D. Zhou, et al. (2008). "Collection, cryopreservation, and characterization of human dental pulp-derived mesenchymal stem cells for banking and clinical use." Tissue Eng Part C Methods **14**(2): 149-156.
- Petersen, O. H., M. Michalak, et al. (2005). "Calcium signalling: past, present and future." Cell Calcium **38**(3-4): 161-169.
- Phinney, D. G. (2007). "Biochemical heterogeneity of mesenchymal stem cell populations: clues to their therapeutic efficacy." Cell Cycle **6**(23): 2884-2889.
- Pilz, G. A., J. Braun, et al. (2011). "Human mesenchymal stromal cells express CD14 cross-reactive epitopes." Cytometry A **79**(8): 635-645.
- Pittenger, M. F., A. M. Mackay, et al. (1999). "Multilineage potential of adult human mesenchymal stem cells." Science **284**(5411): 143-147.
- Premkumar, L. S. (2014). "Transient Receptor Potential Channels as Targets for Phytochemicals." ACS Chem Neurosci.
- Puthussery, T. and E. L. Fletcher (2006). "P2X2 receptors on ganglion and amacrine cells in cone pathways of the rat retina." J Comp Neurol **496**(5): 595-609.
- Putney, J. W. (2010). "Pharmacology of store-operated calcium channels." Mol Interv **10**(4): 209-218.
- Qureshi, O. S., A. Paramasivam, et al. (2007). "Regulation of P2X4 receptors by lysosomal targeting, glycan protection and exocytosis." J Cell Sci **120**(Pt 21): 3838-3849.
- Raffaghello, L., P. Chiozzi, et al. (2006). "The P2X7 receptor sustains the growth of human neuroblastoma cells through a substance P-dependent mechanism." Cancer Res **66**(2): 907-914.
- Ramsey, I. S., M. Delling, et al. (2006). "An introduction to TRP channels." Annu Rev Physiol **68**: 619-647.
- Ranganathan, K. and V. Lakshminarayanan (2012). "Stem cells of the dental pulp." Indian J Dent Res **23**(4): 558.
- Resende, R. R., L. R. Britto, et al. (2008). "Pharmacological properties of purinergic receptors and their effects on proliferation and induction of neuronal differentiation of P19 embryonal carcinoma cells." Int J Dev Neurosci **26**(7): 763-777.
- Resende, R. R., P. Majumder, et al. (2007). "P19 embryonal carcinoma cells as in vitro model for studying purinergic receptor expression and modulation of N-methyl-D-aspartate-glutamate and acetylcholine receptors during neuronal differentiation." Neuroscience **146**(3): 1169-1181.
- Rettinger, J., K. Braun, et al. (2005). "Profiling at recombinant homomeric and heteromeric rat P2X receptors identifies the suramin analogue NF449 as a highly potent P2X1 receptor antagonist." Neuropharmacology **48**(3): 461-468.
- Rettinger, J., G. Schmalzing, et al. (2000). "The suramin analogue NF279 is a novel and potent antagonist selective for the P2X(1) receptor." Neuropharmacology **39**(11): 2044-2053.

- Reya, T., S. J. Morrison, et al. (2001). "Stem cells, cancer, and cancer stem cells." Nature **414**(6859): 105-111.
- Riddle, R. C., A. F. Taylor, et al. (2007). "ATP release mediates fluid flow-induced proliferation of human bone marrow stromal cells." J Bone Miner Res **22**(4): 589-600.
- Robaye, B., E. Ghanem, et al. (2003). "Loss of nucleotide regulation of epithelial chloride transport in the jejunum of P2Y4-null mice." Mol Pharmacol **63**(4): 777-783.
- Romagnoli, C. and M. L. Brandi (2014). "Adipose mesenchymal stem cells in the field of bone tissue engineering." World J Stem Cells **6**(2): 144-152.
- Rong, W., A. V. Gourine, et al. (2003). "Pivotal role of nucleotide P2X2 receptor subunit of the ATP-gated ion channel mediating ventilatory responses to hypoxia." J Neurosci **23**(36): 11315-11321.
- Rubio, D., J. Garcia-Castro, et al. (2005). "Spontaneous human adult stem cell transformation." Cancer Res **65**(8): 3035-3039.
- Ryten, M., P. M. Dunn, et al. (2002). "ATP regulates the differentiation of mammalian skeletal muscle by activation of a P2X5 receptor on satellite cells." J Cell Biol **158**(2): 345-355.
- Safford, K. M., K. C. Hicok, et al. (2002). "Neurogenic differentiation of murine and human adipose-derived stromal cells." Biochem Biophys Res Commun **294**(2): 371-379.
- Sainz, B., Jr. and C. Heeschen (2013). "Standing out from the crowd: cancer stem cells in hepatocellular carcinoma." Cancer Cell **23**(4): 431-433.
- Sakaki, H., M. Tsukimoto, et al. (2013). "Autocrine regulation of macrophage activation via exocytosis of ATP and activation of P2Y11 receptor." PLoS One **8**(4): e59778.
- Sansum, A. J., I. P. Chessell, et al. (1998). "Evidence that P2X purinoceptors mediate the excitatory effects of alphanbetamethylene-ADP in rat locus coeruleus neurones." Neuropharmacology **37**(7): 875-885.
- Santiago, L. Y., J. Clavijo-Alvarez, et al. (2009). "Delivery of adipose-derived precursor cells for peripheral nerve repair." Cell Transplant **18**(2): 145-158.
- Sanz, J. M., P. Chiozzi, et al. (2009). "Activation of microglia by amyloid {beta} requires P2X7 receptor expression." J Immunol **182**(7): 4378-4385.
- Scarfi, S. (2014). "Purinergic receptors and nucleotide processing ectoenzymes: Their roles in regulating mesenchymal stem cell functions." World J Stem Cells **6**(2): 153-162.
- Schenke-Layland, K., B. M. Strem, et al. (2009). "Adipose tissue-derived cells improve cardiac function following myocardial infarction." J Surg Res **153**(2): 217-223.
- Schindl, R., J. Bergsmann, et al. (2008). "2-aminoethoxydiphenyl borate alters selectivity of Orai3 channels by increasing their pore size." J Biol Chem **283**(29): 20261-20267.

- Schwindt, T. T., C. A. Trujillo, et al. (2011). "Directed differentiation of neural progenitors into neurons is accompanied by altered expression of P2X purinergic receptors." J Mol Neurosci **44**(3): 141-146.
- Sharon, E., S. A. Levesque, et al. (2006). "Fluorescent N2,N3-epsilon-adenine nucleoside and nucleotide probes: synthesis, spectroscopic properties, and biochemical evaluation." Chembiochem **7**(9): 1361-1374.
- Shi, R. Z. and Q. P. Li (2008). "Improving outcome of transplanted mesenchymal stem cells for ischemic heart disease." Biochem Biophys Res Commun **376**(2): 247-250.
- Shi, S., P. M. Bartold, et al. (2005). "The efficacy of mesenchymal stem cells to regenerate and repair dental structures." Orthod Craniofac Res **8**(3): 191-199.
- Shin, H. Y., Y. H. Hong, et al. (2010). "A role of canonical transient receptor potential 5 channel in neuronal differentiation from A2B5 neural progenitor cells." PLoS One **5**(5): e10359.
- Sim, J. A., M. T. Young, et al. (2004). "Reanalysis of P2X7 receptor expression in rodent brain." J Neurosci **24**(28): 6307-6314.
- Solle, M., J. Labasi, et al. (2001). "Altered cytokine production in mice lacking P2X(7) receptors." J Biol Chem **276**(1): 125-132.
- Soto, F., G. Lambrecht, et al. (1999). "Antagonistic properties of the suramin analogue NF023 at heterologously expressed P2X receptors." Neuropharmacology **38**(1): 141-149.
- Sours-Brothers, S., M. Ding, et al. (2009). "Interaction between TRPC1/TRPC4 assembly and STIM1 contributes to store-operated Ca²⁺ entry in mesangial cells." Exp Biol Med (Maywood) **234**(6): 673-682.
- Springthorpe, B., A. Bailey, et al. (2007). "From ATP to AZD6140: the discovery of an orally active reversible P2Y12 receptor antagonist for the prevention of thrombosis." Bioorg Med Chem Lett **17**(21): 6013-6018.
- Stock, T. C., B. J. Bloom, et al. (2012). "Efficacy and safety of CE-224,535, an antagonist of P2X7 receptor, in treatment of patients with rheumatoid arthritis inadequately controlled by methotrexate." J Rheumatol **39**(4): 720-727.
- Stokes, L., L. H. Jiang, et al. (2006). "Characterization of a selective and potent antagonist of human P2X(7) receptors, AZ11645373." Br J Pharmacol **149**(7): 880-887.
- Strubing, C., G. Krapivinsky, et al. (2003). "Formation of novel TRPC channels by complex subunit interactions in embryonic brain." J Biol Chem **278**(40): 39014-39019.
- Studený, S., A. Torabi, et al. (2005). "P2X2 and P2X3 receptor expression in postnatal and adult rat urinary bladder and lumbosacral spinal cord." Am J Physiol Regul Integr Comp Physiol **289**(4): R1155-1168.
- Sun, D., W. G. Junger, et al. (2013). "Shockwaves induce osteogenic differentiation of human mesenchymal stem cells through ATP release and activation of P2X7 receptors." Stem Cells **31**(6): 1170-1180.
- Surprenant, A. and R. A. North (2009). "Signaling at purinergic P2X receptors." Annu Rev Physiol **71**: 333-359.

- Surprenant, A., D. A. Schneider, et al. (2000). "Functional properties of heteromeric P2X(1/5) receptors expressed in HEK cells and excitatory junction potentials in guinea-pig submucosal arterioles." J Auton Nerv Syst **81**(1-3): 249-263.
- Takahashi, K., K. Okita, et al. (2007). "Induction of pluripotent stem cells from fibroblast cultures." Nat Protoc **2**(12): 3081-3089.
- Takahashi, K. and S. Yamanaka (2006). "Induction of pluripotent stem cells from mouse embryonic and adult fibroblast cultures by defined factors." Cell **126**(4): 663-676.
- Tanaka, T., Y. Tamba, et al. (2002). "La³⁺ and Gd³⁺ induce shape change of giant unilamellar vesicles of phosphatidylcholine." Biochim Biophys Acta **1564**(1): 173-182.
- Tao, R., C. P. Lau, et al. (2007). "Functional ion channels in mouse bone marrow mesenchymal stem cells." Am J Physiol Cell Physiol **293**(5): C1561-1567.
- Tao, R., C. P. Lau, et al. (2008). "Regulation of cell proliferation by intermediate-conductance Ca²⁺-activated potassium and volume-sensitive chloride channels in mouse mesenchymal stem cells." Am J Physiol Cell Physiol **295**(5): C1409-1416.
- Tao, R., H. Y. Sun, et al. (2011). "Cyclic ADP ribose is a novel regulator of intracellular Ca²⁺ oscillations in human bone marrow mesenchymal stem cells." J Cell Mol Med **15**(12): 2684-2696.
- Thomson, J. A., J. Itskovitz-Eldor, et al. (1998). "Embryonic stem cell lines derived from human blastocysts." Science **282**(5391): 1145-1147.
- Tobita, M. and H. Mizuno (2013). "Adipose-derived stem cells and periodontal tissue engineering." Int J Oral Maxillofac Implants **28**(6): e487-493.
- Tokalov, S. V., S. Gruner, et al. (2007). "Age-related changes in the frequency of mesenchymal stem cells in the bone marrow of rats." Stem Cells Dev **16**(3): 439-446.
- Torres, B., A. C. Zambon, et al. (2002). "P2Y11 receptors activate adenylyl cyclase and contribute to nucleotide-promoted cAMP formation in MDCK-D(1) cells. A mechanism for nucleotide-mediated autocrine-paracrine regulation." J Biol Chem **277**(10): 7761-7765.
- Trebak, M., W. Zhang, et al. (2013). "What role for store-operated Ca²⁺ entry in muscle?" Microcirculation **20**(4): 330-336.
- Ullmann, H., S. Meis, et al. (2005). "Synthesis and structure-activity relationships of suramin-derived P2Y11 receptor antagonists with nanomolar potency." J Med Chem **48**(22): 7040-7048.
- Ulrich, H., M. P. Abbracchio, et al. (2012). "Extrinsic purinergic regulation of neural stem/progenitor cells: implications for CNS development and repair." Stem Cell Rev **8**(3): 755-767.
- van Kruchten, R., A. Braun, et al. (2012). "Antithrombotic potential of blockers of store-operated calcium channels in platelets." Arterioscler Thromb Vasc Biol **32**(7): 1717-1723.
- Vaughan, K. R., L. Stokes, et al. (2007). "Inhibition of neutrophil apoptosis by ATP is mediated by the P2Y11 receptor." J Immunol **179**(12): 8544-8553.

- Vemuri, M. C., L. G. Chase, et al. (2011). "Mesenchymal stem cell assays and applications." Methods Mol Biol **698**: 3-8.
- Venkatachalam, K. and C. Montell (2007). "TRP channels." Annu Rev Biochem **76**: 387-417.
- von Kugelgen, I. (2006). "Pharmacological profiles of cloned mammalian P2Y-receptor subtypes." Pharmacol Ther **110**(3): 415-432.
- von Kugelgen, I. and T. K. Harden (2011). "Molecular pharmacology, physiology, and structure of the P2Y receptors." Adv Pharmacol **61**: 373-415.
- Wagers, A. J. and I. L. Weissman (2004). "Plasticity of adult stem cells." Cell **116**(5): 639-648.
- Wagner, W. and A. D. Ho (2007). "Mesenchymal stem cell preparations--comparing apples and oranges." Stem Cell Rev **3**(4): 239-248.
- Wang, N., R. M. Rumney, et al. (2013). "The P2Y₁₃ receptor regulates extracellular ATP metabolism and the osteogenic response to mechanical loading." J Bone Miner Res **28**(6): 1446-1456.
- Webb, T. E., J. Simon, et al. (1994). "Transient expression of the recombinant chick brain P2y₁ purinoceptor and localization of the corresponding mRNA." Cell Mol Biol (Noisy-le-grand) **40**(3): 437-442.
- Wildman, S. S., S. G. Brown, et al. (1999). "Selectivity of diadenosine polyphosphates for rat P2X receptor subunits." Eur J Pharmacol **367**(1): 119-123.
- Wilmut, I. (2002). "Cloning and stem cells." Cloning Stem Cells **4**(2): 103-104.
- Wolf, C., C. Rosefort, et al. (2011). "Molecular determinants of potent P2X₂ antagonism identified by functional analysis, mutagenesis, and homology docking." Mol Pharmacol **79**(4): 649-661.
- Wu, P. Y., Y. C. Lin, et al. (2009). "Functional decreases in P2X₇ receptors are associated with retinoic acid-induced neuronal differentiation of Neuro-2a neuroblastoma cells." Cell Signal **21**(6): 881-891.
- Wuchter, P., K. Bieback, et al. (2014). "Standardization of Good Manufacturing Practice-compliant production of bone marrow-derived human mesenchymal stromal cells for immunotherapeutic applications." Cytotherapy.
- Xie, R., J. Xu, et al. (2014). "The P2Y₂ nucleotide receptor mediates the proliferation and migration of human hepatocellular carcinoma cells induced by ATP." J Biol Chem **289**(27): 19137-19149.
- Xu, S., A. De Becker, et al. (2010). "An improved harvest and in vitro expansion protocol for murine bone marrow-derived mesenchymal stem cells." J Biomed Biotechnol **2010**: 105940.
- Yanagida, E., S. Shoji, et al. (2004). "Functional expression of Ca²⁺ signaling pathways in mouse embryonic stem cells." Cell Calcium **36**(2): 135-146.
- Yang, S., J. J. Zhang, et al. (2009). "Orai1 and STIM1 are critical for breast tumor cell migration and metastasis." Cancer Cell **15**(2): 124-134.
- Ye, H., C. Chen, et al. (2008). "Carba-nucleosides as potent antagonists of the adenosine 5'-diphosphate (ADP) purinergic receptor (P2Y₁₂ on human platelets." ChemMedChem **3**(5): 732-736.

- Yen, A. H. and P. T. Sharpe (2006). "Regeneration of teeth using stem cell-based tissue engineering." Expert Opin Biol Ther **6**(1): 9-16.
- Yeromin, A. V., S. L. Zhang, et al. (2006). "Molecular identification of the CRAC channel by altered ion selectivity in a mutant of Orai." Nature **443**(7108): 226-229.
- Yoon, M. J., H. J. Lee, et al. (2007). "Extracellular ATP is involved in the induction of apoptosis in murine hematopoietic cells." Biol Pharm Bull **30**(4): 671-676.
- Yu, V., M. Damek-Poprawa, et al. (2009). "Dynamic hydrostatic pressure promotes differentiation of human dental pulp stem cells." Biochem Biophys Res Commun **386**(4): 661-665.
- Yuahasi, K. K., M. A. Demasi, et al. (2012). "Regulation of neurogenesis and gliogenesis of retinoic acid-induced P19 embryonal carcinoma cells by P2X2 and P2X7 receptors studied by RNA interference." Int J Dev Neurosci **30**(2): 91-97.
- Yuan, J. P., M. S. Kim, et al. (2009). "TRPC channels as STIM1-regulated SOCs." Channels (Austin) **3**(4): 221-225.
- Yuan, J. P., K. P. Lee, et al. (2012). "The closing and opening of TRPC channels by Homer1 and STIM1." Acta Physiol (Oxf) **204**(2): 238-247.
- Yuan, J. P., W. Zeng, et al. (2007). "STIM1 heteromultimerizes TRPC channels to determine their function as store-operated channels." Nat Cell Biol **9**(6): 636-645.
- Zapata, A. G., D. Alfaro, et al. (2012). "Biology of stem cells: the role of microenvironments." Adv Exp Med Biol **741**: 135-151.
- Zeng, W., J. P. Yuan, et al. (2008). "STIM1 gates TRPC channels, but not Orai1, by electrostatic interaction." Mol Cell **32**(3): 439-448.
- Zhang, C., J. Chang, et al. (2008). "Inhibition of human dental pulp stem cell differentiation by Notch signaling." J Dent Res **87**(3): 250-255.
- Zhang, S. L., J. A. Kozak, et al. (2008). "Store-dependent and -independent modes regulating Ca²⁺ release-activated Ca²⁺ channel activity of human Orai1 and Orai3." J Biol Chem **283**(25): 17662-17671.
- Zhang, S. L., Y. Yu, et al. (2005). "STIM1 is a Ca²⁺ sensor that activates CRAC channels and migrates from the Ca²⁺ store to the plasma membrane." Nature **437**(7060): 902-905.
- Zippel, N., C. A. Limbach, et al. (2012). "Purinergic receptors influence the differentiation of human mesenchymal stem cells." Stem Cells Dev **21**(6): 884-900.
- Zitt, C., B. Strauss, et al. (2004). "Potent inhibition of Ca²⁺ release-activated Ca²⁺ channels and T-lymphocyte activation by the pyrazole derivative BTP2." J Biol Chem **279**(13): 12427-12437.
- Zuk, P. A., M. Zhu, et al. (2002). "Human adipose tissue is a source of multipotent stem cells." Mol Biol Cell **13**(12): 4279-4295.
- Zuk, P. A., M. Zhu, et al. (2001). "Multilineage cells from human adipose tissue: implications for cell-based therapies." Tissue Eng **7**(2): 211-228.

Zweifach, A. and R. S. Lewis (1993). "Mitogen-regulated Ca^{2+} current of T lymphocytes is activated by depletion of intracellular Ca^{2+} stores." Proc Natl Acad Sci U S A **90**(13): 6295-6299.